UNIVERSITAT DE
BARCELONA

Synthesis of biaryl bicyclic peptides for recognition of protein surfaces

Júlia Garcia Pindado

Synthesis of biaryl bicyclic peptides for recognition of protein surfaces

Júlia Garcia Pindado

Tesi doctoral dirigida per:

Prof. Ernest Giralt Lledó

Universitat de Barcelona

Facultat de Química

Departament de Química Orgànica

Barcelona, 2017

A los que están luchando

Als meus pares, la meva familia i, especialment, a l'Alexy.

ACKNOWLEDGEMENTS

Para mí, esta parte de la tesis es, indudablemente, una de las mejores. La tesis es algo más que los buenos, o malos, resultados obtenidos a lo largo de estos años. Mi tesis no es más que un reflejo de lo que ha sido mi vida desde el 12 de septiembre de 2011, cuando me incorporé al 300. Y está claro que no hubiera llegado a este punto sin un puñado de personas maravillosas que me han acompañado, dentro y/o fuera del lab a andar este camino, así que no me queda más remedio que daros las GRACIAS, por haberme ayudado tanto en el trabajo como a ser feliz durante ésta, no corta, etapa de mi vida.

Así que vamos a ello… Hará ya unos cuatro años y medio que, terminando química orgánica en el IQS decidí pisar el IRB por primera vez. Todo ello gracias a tres compañeros de mi misma facultad a quienes no voy a olvidar mencionar más adelante. Todavía recuerdo esa primera entrevista con Ernest, la ilusión de que todo en el proyecto era nuevo y distinto a lo que había hecho hasta entonces. Y, como no pudo ser de otro modo, decidí encantada embarcarme en esta aventura. Estos años han estado repletos de muchos momentos, todo empezó bastante bien, nuevos péptidos que salían, ensayos que apuntaban que eran buenos candidatos…hasta que decidimos atacar con p53. La lucha con las proteínas no fue fácil, casi dos años expresando para tener nuestro NMR bidimensional, se me saltan las lágrimas de recordar ese momento. Pero la guerra no había terminado, quedaban muchas cosas que abordar. Una colaboración con Bélgica después de un congreso, me hizo retomar la motivación con la síntesis, un poco perdida por las agónicas purificaciones de esos crudos que parecían las montañas de Montserrat. Con la ayuda de un nuevo postdoc y también amigo pudimos sacar más proteína y lanzarnos al desenfrenado estudio final por dicroísmo y, como bien dijo el jefe "alguna vez tenía que salir algo a la primera". La lástima de todo ello son los experimentos que se quedan en el tintero, ese proyecto de triptófanos que tuve que abandonar, entre otros. Finalmente, escribir. Aunque no se puede decir que fuera finalmente, la escritura empezó en simultáneo con los últimos experimentos, a una no le gustaba la idea de que "le pillara el toro". Así que el proceso fue duro, muchas horas, mucho café, pero eso no quitó el placer de disfrutar al máximo de todo lo que se iba aprendiendo. Y así ha salido la "pequeña", con mucho mimo y mucha ilusión, quizás un poco distinta (y más pesada) a lo que esperaba en un inicio pero puedo decir que, me gusta.

Sin más dilación toca empezar a homenajear a todas esas personas que han estado a mi lado durante este tiempo.

No podia començar de cap altre manera que pel nostre capità, l'**Ernest**, gràcies per aceptar-me al teu laboratori, per deixar-me sempre proposar idees i portar-les a terme, per tenir sempre "5 minuts" i, com no, per totes les converses, perquè mai aprèn un tant com escoltant a qui sap.

I tampoc hi ha una altra manera de seguir que no sigui donant les gràcies a la **Txell**, per fer que tot continui endavant i ajudar-me a creure en mi. Pels cafès que ho curen tot. Per tota la feina que t'he portat. Pel teu gran suport.

A **Sol**, mi mentora, la que se peleó desde el momento cero con estos biciclos, gracias por todo lo que me enseñaste.

A Jesús G., por tu ayuda, tus conocimientos, gracias por los experimentos que hiciste y forman parte de la tesis.

Thinking about collaborations I cannot forget to mention Prof. Steven and Tom Willemse. Thank you very much Steven for the opportunity to use the tryptophans and explore new compounds. And, of course, thanks a lot Tom for preparing the products and sending more amounts when needed.

I ara sí, cap al lab 300. Gràcies a tots els companys, els que ja no hi són i els que encara estàn. Obligadament he de començar per la meva **Cris G.**, per masses coses. Perquè conèixe't ha sigut de les millors coses que he viscut aquests anys, no sabia el que era tenir una germana. Gràcies per haver-me soportat de veïna de taula, per animar-me sempre, per les nostres confesions i sobretot per cuidar-me, fins i tot, sense que jo me n'adonés. I, com no, gràcies per haver portat en Guiro a les nostres vides. I segueixo amb les Cristines, gràcies per ser com sou, per a fet de la nostra illa un ambient formidable per treballar. **Fustera**, tot i que em vas acabar enganxant això de renegar (cal dir que ho he superat) se't va trobar a faltar mentre eres al Japó, no canviïs mai, especialment les teves ganes de somriure, que sempre es contagien. Gràcies per totes les pomes al forn! **Cris D.**, per suportar les meves anades d'olla a la nostra illa, tu que ets tan tranquil·la, jaja, i aguantar els pampas i les suzukis amb aquelles màquines de soroll infernal, però sobretot per estar sempre disponible per ajudar i no fer mai una mala cara. Sobretot quan m'han fet falta els teus "truquillos". Tu, juntament amb la **Sonia** i en **Pol**, heu sigut uns grans companys per abordar el simposi. Gràcies a tots tres per haver-me fet un cop de mà sempre que us ho he demanat. En especial t'he d'agrair a tu, Sonia, la paciència per guiar-me amb tot el paperam pre-tesis. Anem al sector valencià. Gràcies **Salvata**, per mantenir viu el mot de "La Roberts", pels beers4science, pels ànims i per donar vidilla al lab…ara molta força que ja no et queda res. A en **Pep**, el meu secret santa paellero, merci per tots els consells, per compartir les penúries de la FPU i per estar present quan em tocava treballar amb cèl·lules, ets molt gran, merci per haver-me escoltat sempre. I ara voldria pasar amb els amyloids. Per començar, agraïr-te **Natàlia** tots els comentaris durant els meetings, haver pogut aprendre de la teva forma de treballar, encara que fos indirectament i pel teu entusiame, que sempre se m'ha contagiat. A l'**Aurelio**, el "manitas" del lab, gràcies per obrir-me aquell matràs d'1L i evitar que perdés el producte (ho havia de dir) però sobretot gràcies per donar ànims i haver-me ajudat quan t'ho demanat. Al **Martí**, perquè et vaig molestar força amb el FPLC, merci per ser sempre tan amable i pel teu bon rotllo. A l'**Edu**, perquè no et queixes mai quan et demano canviar els dissolvents, i mira que sóc pesada, gràcies per la teva paciència. A la **Sílvia**, una de les responsables de que estigui aquí, gràcies per animar-me a visitar l'IRB i per totes les activitats que vas organitzar. A la **Montserrat**, perquè també vas patir mil preguntes sobre el FPLC, gràcies per la teva ajuda i també per les receptes que em vas passar. I canviant cap al grup de la BBB…merci **Benji** per liar-me a venir al lab i, juntament, amb la Sílvia rebrem ja fa un temps a l'IRB, gràcies pels consells i, no me'n descuido, pel balls. Gracias **Macarena**, por ser la alegría de la huerta, por tu siempre valuosa ayuda, por animar las horas de la comida y, también, por animarme a mí. Merci **Adam**, qui diría que ens tornaríem a retrobar després de la carrera, et desitjo la millor sort del món i que no perdis mai la teva actitut tan positiva. I ara voldria mencionar al postdocs que em falten, **Mark,** thanks a lot for your constant smile, for making time to help me (specially your corrections) and for the funny moments talking about English-catalan situations. **Daniela,** thanks for the nice talks, for helping me understand that at the end of the thesis everything would work and, specially, I'll always remember your "res de res"

A les persones meravelloses que la salsa m'ha portat, gràcies per ajudar-me a desconnectar amb el ball.

A la meva familia, la que està lluny però estimo igualment. Gracias por adoptarme y por vuestro apoyo desde el otro lado del charco. Gracias **Ale** y, sobretodo, gracias **Cira**, por ser una segunda madre. A la familia que tengo más cerca, gracias a mis tías y sobrinas, porque no es fácil verse pero siempre puedo contar con vosotros.

A mis padres, **Julia** y **Xavier**, porque soy lo que soy por vosotros, gracias por ese apoyo y amor que mueve montañas, os quiero.

A mi todo, **Alexy**, simplemente GRACIAS. Si hiciera una lista no terminaría, gracias por tu apoyo, comprensión y amor sin límites. Gracias por creer en mí y ayudarme a creer. Gracias por ser mi luz. Te amo.

"If your dreams don't scare you,

they aren't big enough"

Muhammad Ali

"El fracaso es parte de la vida; si no fracasas,

no aprendes y si no aprendes, no cambias"

Paulo Coelho

"Don't count the days,

make the days count"

Muhammad Ali

ABBREVIATIONS

AA	amino acids
ACC	adrenocortical carcinoma
ACE	angiontesin-converting enzyme
ACH	α-cyano-4-hydroxycinnamic acid
Alloc	allyloxycarbonyl
APS	ammonium persulfate
BBB	blood-brain barrier
BBMEC	bovine brain microvessel endothelial cells
BBPs	bridged bicyclic peptides
BCECs	brain capillary endothelial cells
BCSFB	blood-cerebrospinal fluid barrier
Boc	*tert*-butyloxycarbonyl
CATEX	cation exchange chromatography
CD	circular dichroism
CNS	central nervous system
CSA	cyclosporine A
CSF	cerebrospinal fluid
CT	*C*-terminal
CTC	chlorotrityl resin
DCM	dichloromethane
DIEA	diisopropylethylamine
DIPCDI	diisopropylcarbodiimide
DKP	diketopiperazine
DMF	dimethylformamide
DMSO	dimethyl sulfoxide
DNA	deoxyribonucleic acid
DPPA	diphenylphosphoryl azide

DSC	differential scanning calorimetry
DMEM	Dulbecco's modified Eagle's medium
EDT	1,2-ethanedithiol
ESI-MS	electrospray ionization-mass spectroscopy
FDA	dood and drug administration activities
FP	fluorescence polarization
Fmoc	9-fluorenylmethoxycarbonyl
FPLC	fast protein liquid chromatography
f_u	unfolded fraction
GLP	glucagon-like peptide
HeLa	cell line derived from cervical cancer (taken from Henrietta Lacks, 1951)
HOAt	1-hydroxy-7-azabenzotriazole
HPLC	high performance liquid chromatography
HR-MS	high resolution mass spectroscopy
HSQC	heteronuclear single-quantum coherence spectroscopy
HTS	high throughput screening
IPTG	isopropyl β-D-1-thiogalactopyranoside
J	coupling constant
K_{av}	partition coefficient
logP	partition coefficient (solubility water/solubility 1-octanol)
L-CLP	left-handed circularly polarized light
LFS	Li-Fraumeni syndrome
LFLS	Li-Fraumeni-like syndromes
LTQ-FTMS	linear quadrupole ion trap Fourier transform mass spectrometer
MALDI-TOF MS	matrix-assisted laser desorption/ionization-time of flying mass spectrometry
MD	molecular dynamics
MDCK	Madin Darby canine kidney cells

MDM2	murine double minute protein
MES	2-(*N*-morpholino)ethanesulfonic acid
MeCN	acetronitrile
MTBE	methyl-*tert*-butyl ether
MTT	3-(4,5-dimethylthiazol-2-yl)-2,5-diphenyltetrazolium bromidefor
mRNA	messenger ribonucleic acid
m/z	mass/charge
NCE	new chemical entity
NMR	nuclear magnetic resonance
OTf	triflates
PAMPA	parallel artificial membrane permeability assay
Pbf	2,2,4,6,7-pentamethyldihydrobenzofuran-5-sulfonyl
PBMEC	porcine brain microvessel endothelial cells
P_e	effective permeability
PBLE	porcine brain lipid extract
PDB	protein data bank
PG	protecting group
Pd	palladium
*p*NZ	*para*-nitrobenzyloxycarbonyl
PPI	Protein-protein interactions
pKa	-logarithm of the acid dissociation constant
PRR	proline-rich region
PTP1B	protein tyrosine phosphatase 1B
PyBOP	1H-benzotriazol-1-yloxytris(pyrrolidino)phosphoniumhexafluorophosphate
p53	gene codifying p53
p53-tesS	protein p53
p53TD	protein p53 tetramerization domain

RBMEC	rat brain microvascular endothelial cells
R-CLP	right-handed circularly polarized light
Reagent K	TFA:H_2O:thioanisole:ethanedithiol:phenol, 85:5:5:2.5:2.5
RMSd	root mean square deviation
RNA	ribonucleic acid
RP	reversed phase
SAR	structure activity relationship
SDS-PAGE	sodium dodecyl sulfate polyacrylamide gel electrophoresis
SEC	size exclusion chromatography
SM	Suzuki-Miyaura
SPPS	solid-Phase Peptide Synthesis
T (4%)	transport after 4h
TAD	transcription activation domain
*t*Bu	*tert*-butyl
T_{05}	half unfolding transition temperature
TEMED	*N,N,N',N'*-tetramethylethylenediamine
TET	tetramerization domain
TFA	trifluoroacetic acid
TD	tetramerization domain
TIS	triisopropylsilane
TLC	thin layer chromatohgraphy
TJs	tight junctions
TP53	tumor suppressor gene p53
Trt	trityl
UPLC	ultra high performance liquid chromatography
UV	ultraviolet
V_c	column volume

V_e	elution volume
V_o	void volumen
XTT	2,3-bis-(2-methoxy-4-nitro-5-sulfophenyl)-2H-tetrazolium-5-carboxanilide
θ	molar ellipticity
$θ_{MR}$	mean residue ellipticity
ε	molar extinction coefficient
δ	chemical shift

CONTENTS

x

xi

Proteinogenic amino acids

A
Ala
L-Alanine
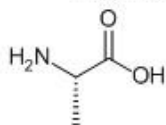
C
Cis
L-Cisteine
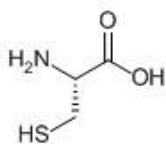
D
Asp
L-Aspartate
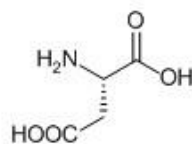
E
Glu
L-Glutamate
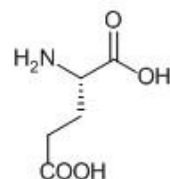
F
Phe
L-Phenylalanine
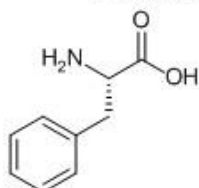
G
Gly
L-Glycine
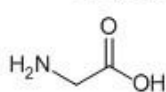
H
His
L-Histidine
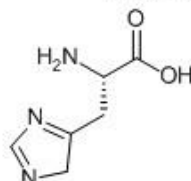
I
Ile
L-Isoleucine
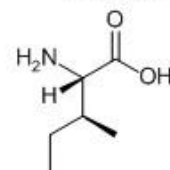
K
Lys
L-Lysine
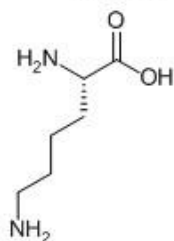
L
Leu
L-Leucine
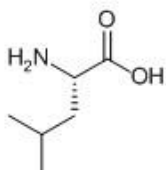
M
Met
L-Methionine
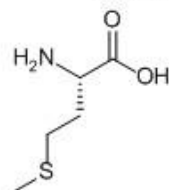
N
Asn
L-Asparagine
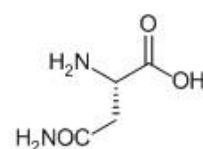
P
Pro
L-Proline
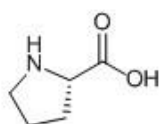
Q
Gln
L-Glutamine
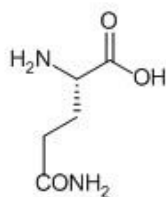
R
Arg
L-Arginine
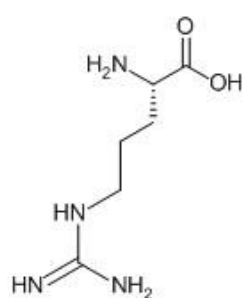
S
Ser
L-Serine
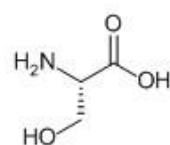
T
Thr
L-Threonine
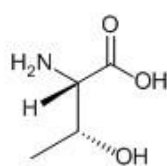
V
Val
L-Valine
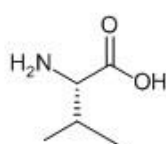
W
Trp
L-Tryptophan
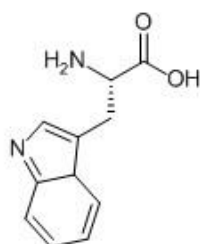
Y
Tyr
L-Tyrosine
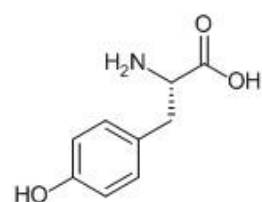
Protecting groups
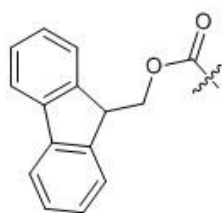
9-fluorenylmethoxycarbonyl
(Fmoc)

tert-butyl
(*t*Bu)
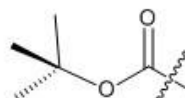
tert-butoxycarbonyl
(Boc)
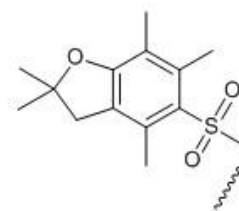
2,2,4,5,7-pentamethyl-
dihydrobenzofurane-5-sulfonyl
(Pbf)
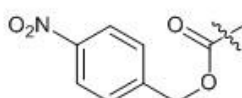
para-nitrobenzyloxycarbonyl
(*p*NZ)
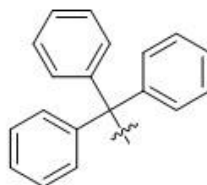
Trityl
(Trt)
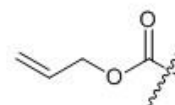
Allyloxycarbonyl
(Alloc)

Coupling reagents and additives
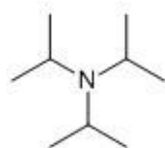
N, *N*-diisopropylethylamine
(DIEA)
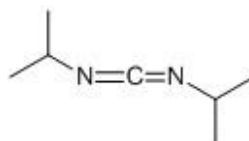
diisopropylcarbodiimide
(DIC)
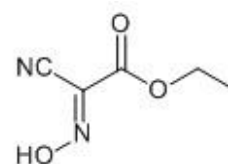
ethyl cyano-glyoxylate-
2-oxime
(Oxyma)
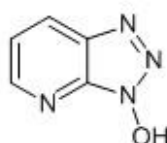
1-hydroxy-7-azabenzotriazole
(HOAt)
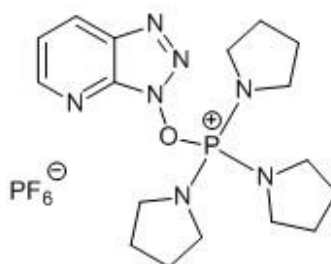
1H-benzotriazol-1-yloxytris
(pyrrolidino)phosphonium
hexafluorophosphate
(PyBOP)
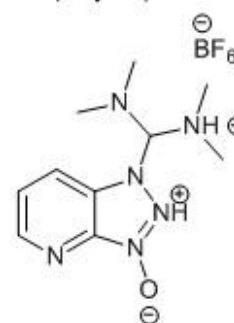
O-(benzotriazol-1-yl)-1,1,3,3-
tetramethyluronium
tetrafluoroborate
(TBTU)

Resins
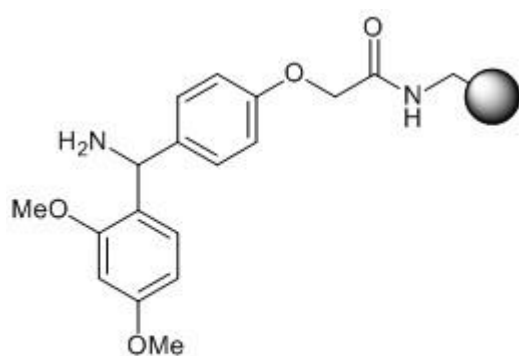
RinkAmide Chemmatrix resin
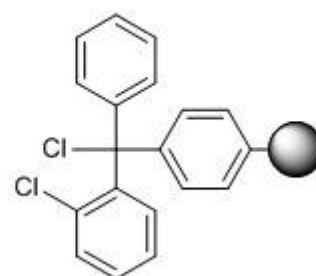
2-chlorotrityl resin
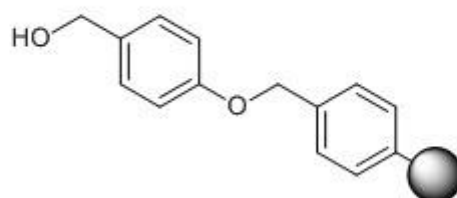
Wang resin

INTRODUCTION

Protein comes from the Greek word "proteis" whose meaning is "of primary importance". Protein name was coined in 1838 by the Dutch chemist Gerardus Muller. At that time, the relevance of these biomolecules was scarcely known in comparison with current understanding. Nowadays, proteins continue being in the middle of scientific and industrial research progress and they have thoroughly won their name. More than 7000 naturally occurring peptides have been identified, mostly of them playing important roles in human physiology[1,2,3,4]

Proteins and peptides are the responsible of many physical and chemical processes that take place in biological organism which means that these biomolecules are essential in life. There are four biological types of macromolecules each one in charge of their own functionalities. Nucleic acids are *the storage of the genetic information* and have the ability to manipulate it. Carbohydrates are *the source of the energy*. Lipids have the relevant role of structurally constitute biological membranes. Proteins and peptides are *the agents of action*[5] in cells. Most activities are developed due to these biomolecules, responsible of the catalysis, motility, physiological regulation, transport, structural composition and defense.

Proteins and peptides are linear polymers structurally constituted by amino acids. The difference between them is kind of arbitrary since short amino acid sequences that contain less than forty residues are known as peptides while larger sequences are referred as proteins.

Peptides in medicinal chemistry: overview and future directions

During the last decades, the use of peptides has significantly increased year by year. Just one century ago, the first peptide was synthesized by Emil Fischer[6]. At that time, peptides were prepared on solution being a difficult and time-consuming task. The real breakthrough was the development of the Solid-Phase Peptide Synthesis (SPPS) by B. Merrifield[7] in 1963. Having optimized the strategy to prepare them in a straightforward manner, the role of peptides could be greater than expected due to the possibility of gaining access even to very difficult sequences in an acceptable period of time. Furthermore, the development of a new purification method based on high-performance liquid chromatography (HPLC) also allowed separation of incredibly complex mixtures of products. From that moment, peptides were considered as the drugs of the future and several companies decided to invest in their development. However, the low bioavailability of these products, which is their main drawback, led to the failure of some of them during the late state of clinical phases. Therefore, the new concept of peptidomimetic was coined and enabled to overcome this important issue. Over the following years, some peptides with interesting pharmacological properties have been obtained and together with the improvement of SPPS, as well as proper peptide modifications, has made possible to have more than 500 peptides as potential drug candidates and already more than 60 in the market[8].

In 2011, around 500 peptides were in pre-clinical phases[9].T he following year, 5 and 6 peptides reached the market in Europe and USA, respectively, being the highest number of approvals ever achieved in a year[10]. Comparing these values with conventional small molecules, the successful rate to reach the market is higher for peptides in front of small molecules (2:1). In addition, the number of peptides entering clinical trials was 1 in the year 1970 and it has already increased up to 20[9].

One of the most promising areas of research for peptides rely on G Protein-coupled receptor binding peptides, such as those for treating type 2 diabetes approved in 2012[11]. Furthermore, the frightening advent of increasing resistance towards conventional antibiotics has led to the search for new alternatives such as antimicrobial peptides. Moreover, peptides as vaccines are in on-going trials in

different phases of clinical development. In Table 0.1 are summarized the key peptides being used, classified by different medical conditions[12].

Table 0.1. Marketed peptides used by medical condition.

Oncology	Zoladex
	Velcade
	Lupron/Enantone/Eligard
Cardiovascular	Angiomax
	Integrilin
Central Nervous System	Copaxone
Metabolic disorders	Victoza
	Byetta
Infection	Incivek
	Victrelis
Hematological disorders	Firazyr
	Kalbitor
Gastrointestinal disorders	Gattex
	Linzess
Repiratory disorders	Acromegaly
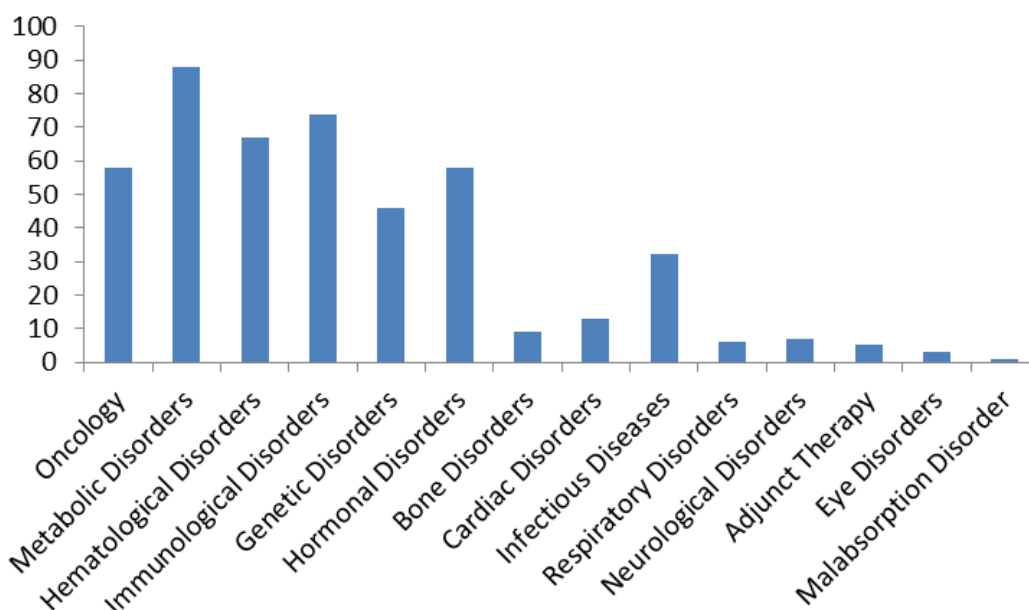
Figure 0.1. Comparative number of proteins and peptides used, classified by medical conditions.

Analyzing these numbers is possible to observe that peptides and proteins are present in the different medical conditions from cancer to genetic or cardiac disorders, which implies a high potential in any research area. Futhermore, the number of therapeutic peptides and proteins in some diseases such as cancer and metabolic, hematological, immunological, genetic and hormonal disorders are quite relevant, validating the utility of these drugs (THPdb source).

Over the 20th century, drug development was mostly focused on the use of traditional small molecules. This category comprises chemically synthesized drugs with a molecular weight less than 500 Daltons. In this era, drug candidates were obtained or inspired by natural products[13] either by screening or rational design including ligand-based, mechanism-based or receptor-based design. During this period a large number of new chemical entities (NCEs) were discovered leading to the satisfactory treatment of an important number of diseases. The golden era of these products is no longer present and the number of 20 NCEs has remained constant over the years despite the increasing number of discovered drug targets. Taking into account the properties that the successful candidates have in common, some generalizations were assumed being

the most relevant, the so-called rule-of-five. Lipinski found that poor oral absorption is likely when molecular weight is higher than 500, logP higher than 5 and if there are more than 5H-bond donors and/or 10-H bond acceptors present in a drug molecule[14]. Therefore, in order to have a favourable oral bioavailability the molecular weight should be below 500Da. This simple property is enough to exclude peptides as good drug candidates since this value is easy overcome with just five amino acids.

Despite the fact that this approximation could imply a dead point for peptide drugs, the latter part of the 20th century redefined the use of small molecules drugs and allow the entrance of a new kind of pharmaceuticals. The small size of conventional small molecules may imply a reduced target selectivity which leads to human side effects. This was the main reason to explore new possibilities. Proteins can offer high potency and selectivity for their molecular target, which can be translated into fewer (off-target) side effects. These new type of protein-based drugs were referred to as "biologics" and comprises molecules such as insulin, antibodies or growth factors. Considering the previously mentioned rule-of-five it is no surprise that they cannot be orally delivered since they present higher molecular weight than 500 Da. Biologics are administered by injection or intranasally. They have demonstrated their potential in the treatment of several diseases such as cancer, rheumatoid arthritis or multiple sclerosis among others.

Halfway between the two previously mentioned different categoriess, small molecules and biologics, a group constituted by chemically synthesized peptides can be found. In Figure 0.2 the advantages and disadvantages of each category are summarized.
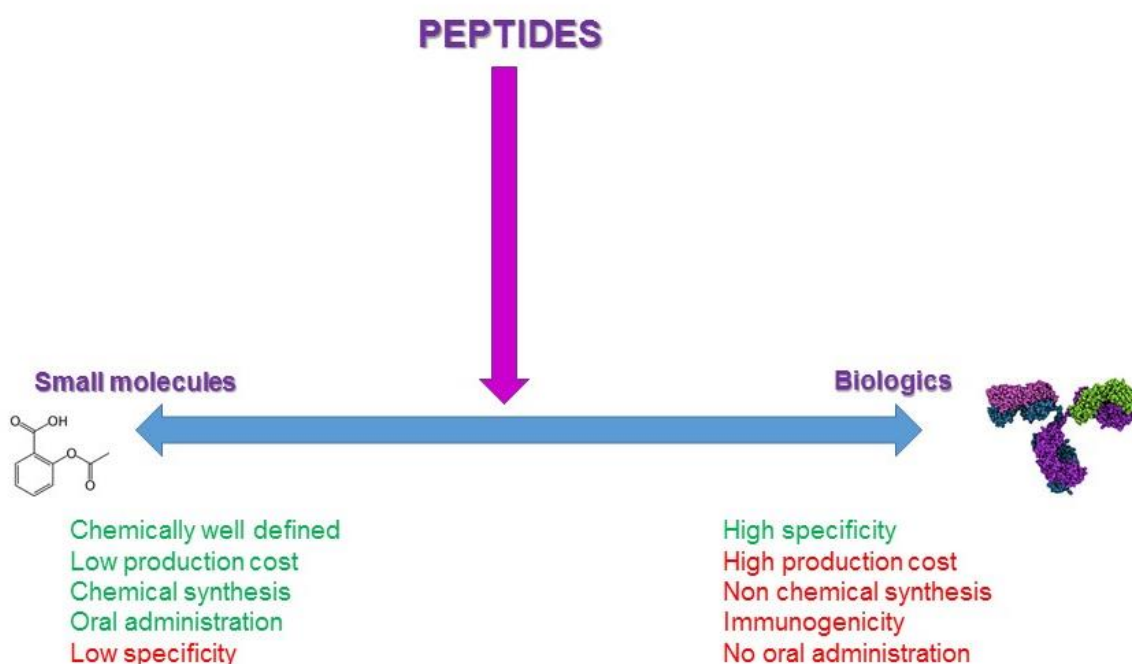
Figure 0.2. Illustrative comparison between small molecules and biologics types of drugs, advantages and disadvantages and the place that synthetic peptides occupy.

Peptides have similar properties to proteins in the sense of exquisite specificity for their targets which result in high potency and few side effects. Peptides have been fine-tuned so as to interact with good specificity with their biological targets which make them interesting candidates in biomedicine. Nevertheless, chemically synthesized peptides are limited by their low biostability, high clearance, poor membrane permeability and solubility and the difficulty of being orally administered. Despite the different disadvantages that peptides may present as drug candidates, more than 100 peptidic drugs have already reached the market, a market which is growing much faster than other pharmaceuticals. More than 40$ billion per year are invested in protein and peptide-based drug candidates. Some examples of successful drugs are listed in Table 0.2[13].

Noteworthy, the peptidic-based drugs range from 3 to 39 amino acids, meaning that the size of the peptides does not limit their potential future, as it could be though

considering Lipinski rule-of-five. In fact, in Figure 0.3, the number of amino acids for FDA approved peptides and proteins are listed.

Table 0.2. Marketed peptide drugs derived from natural sources. Table extracted from Craik *et al.*[13]

Drug	Size (aa)	Target disease	Pharmacological mechanism	Registration year
Captopril (Capoten)	3	Hypertension	ACE inhibitor	1982
Tirofiban (Aggrastat)	3	Anticoagulant	Platelet inhibitor	1996
Epifibatide (Integrilin)	7	Acute coronary syndrome, unstable angina	Anticoagulant	1996
Bivalirudinrub (Angiomax)	20	Unstable angina	Anticoagulant	2000
Ziconotide (Prialt)	26	Neuropathic pain	*N*-type Ca channel blocker	2004
Exenatide (Byetta)	39	Type 2 diabetes	GLP-1 receptor antagonist	2006

Table 0.3. Number of discovered and registered peptides and proteins with biological applications classified according to the number of residues of their sequences.

Size range	Number of peptides/proteins	Examples
1-30	13	Oxytocin, Vasopressin
31-60	20	Insulin (regular, lispro, glargine, porcine, aspart, determir, glulisine, isophane), Aprotinin
61-100	5	Insulin (pork, beef), Preotact
101-200	25	Epoetin alfa, Interferon α-2a recombinant
201-400	42	Cetuximab, Antihemophilic factor
401-800	40	Human serum albumin, Hyaluronidase
801-1500	12	Botulinium toxin type A, Pancrelipase
More than 1500	1	Alemtuzumab

Despite having only one available protein as therapeutic agent for more than 1500 residues, ranging from 100 up to 800, a significant number of protein drugs are found, again proving the high potential of these kind of therapeutics.

Taking a closer look to the Table 0.3, it can be realize that these examples are derived from animal venoms or plants extracts. In fact, peptides from natural sources can be mined and detected in a direct or indirect manner. Natural products are an unyielding source of bioactive molecules whose structure may present particular features. The well-known example of cyclosporine A (CSA) is interesting to be discussed as a proof of concept. This natural peptide offers oral bioavailability and it is used as immunosuppressant and in organ transplant therapy. CSA is an undecapeptide with three key structural features for their biopharmaceutical properties (Figure 0.3). First, its cyclic backbone which protects the peptide to be proteolytically degradated and together with its hydrophobic side-chains hidden in the interior of the molecule the polars groups. In addition, seven *N*-methylated residues reduce hydrogen bonding for water solvation due to the lack of their amide hydrogen bond donors.
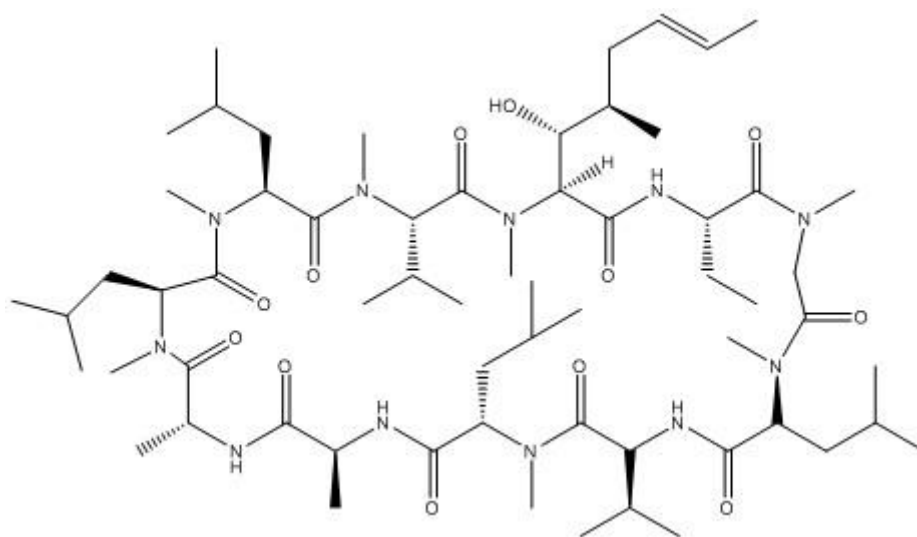
Figure 0.3. Structure of the macrocyclic peptide cyclosporine A.

After having taken a look to these interesting motifs one can realize about some important properties that should be considered once designing peptidic scaffolds.

Macrocyclization, as well as, the presence of non-natural amino acids can protect from peptide degradation at the same time that enables the access to molecules with the ability to permeate across biological barriers or increase the transport of cargoes through them. As a matter of fact, regarding permeability across biological barriers, peptidic sequences should incorporate amino acids that allow achieving the equilibrium between the hydrophobicity and hydrophilicity also avoiding membrane retention.

However, not only the size of the peptide candidates is important to be considered but also the structure that they present. B-strands have demonstrated to be important structural features recognized by enzymes such as proteases and by other strands that form sheets (like amyloids). These structural elements can be also mimicked in an efficient way by short constrained peptides. Helices have also been mimicked mainly by the presence of heterocycles[15] and stapling between amino acids chains[16]. Furthermore, biological activities of the peptides can be reached by stabilizing the above mentioned secondary structures.

Protein-protein interactions: the design of peptidomimetics to target PPIs

Having reached this point, it could be interesting to revisit the definition of peptidomimetics. Literature is inconsistent since it ranges from definitions that simply cover scaffolds replacing the peptide backbone to other that include sequences with modifications that result in improved biological properties. In the present thesis, peptidomimetics will be referred as molecules that are design to improve the biopharmaceutical properties but mimicking the binding properties of the precursors.

Almost all biological functions require communication between proteins. Protein-protein interactions (PPIs) are involved in most cellular processes and participate in enzymatic activity, subcellular localization, as well as, binding properties. The network that these interactions create is huge and by mapping the interactions, cellular behaviour can be better understood. For this reason, over the years the search for modulators of these important and challenging targets has increased. Modulations of PPIs would allow improving the current knowledge of PPIs network which at the same time facilitates the understanding of the pathogenic mechanisms involved in diseases enabling the possible development of therapeutic agents, as well as, the diagnosis. Targeting PPIs is extremely difficult due to the large surface area (around 1500-2000 $Å^2$) involved. In general, PPIs can be classified as mediated by the interaction of two protein domains (domain-domain) or by the interaction between a domain and a linear sequence of residues of the other partner (peptide-domain). However, in many cases additional weak contacts distant to the defined interaction area are also contributing to the binding, which make more difficult to predict the whole PPI. 60% of PPIs are domain-domain mediated. Protein-protein interfaces are usually flat and they lack of particular features such as pockets or grooves which are commonly present in the surfaces of proteins that bind small sequences[17].

It has been reported in different examples the failure of small molecule scaffolds, commonly used in standard drug discovery, to obtain active and selective PPI inhibitors. These discoveries have stimulated the search of new kind of molecules to be used for this purpose.

The potential of peptides as PPIs modulators lies on the many advantages they present. (i) Flexible peptides can allow better adaptability to the surfaces, (ii) modularity would imply higher structural diversity and at the end the increasement in selectivity and potency, (iii) their reduced size prevents from tissue accumulation, (iv) low toxicity in humans due to their biocompatibility[18]. The last two characteristics are very remarkable since most of the therapeutic peptides are hindered by the usual disadvantages. However, one cannot forget about the most important consideration which is the fact that peptides can tackle the limitation of the big surface area since they can perfectly mimic the main features of proteins with improved properties and an easier obtaining strategy.

Turn mimetics

Many PPIs are mediated by small peptides with a specific secondary structure that adapts to interact with the surface. One may wonder why not using short protein sequences with the same aim. The explanation lies on the high flexibility that they would display and the loss of the three-dimensional structure stability as a consequence of the isolation from the entire protein. For this reason, chemical modification should be introduced to solve the problem.

Macrocyclization   *N*-Methylation   Turn inducing amino acids
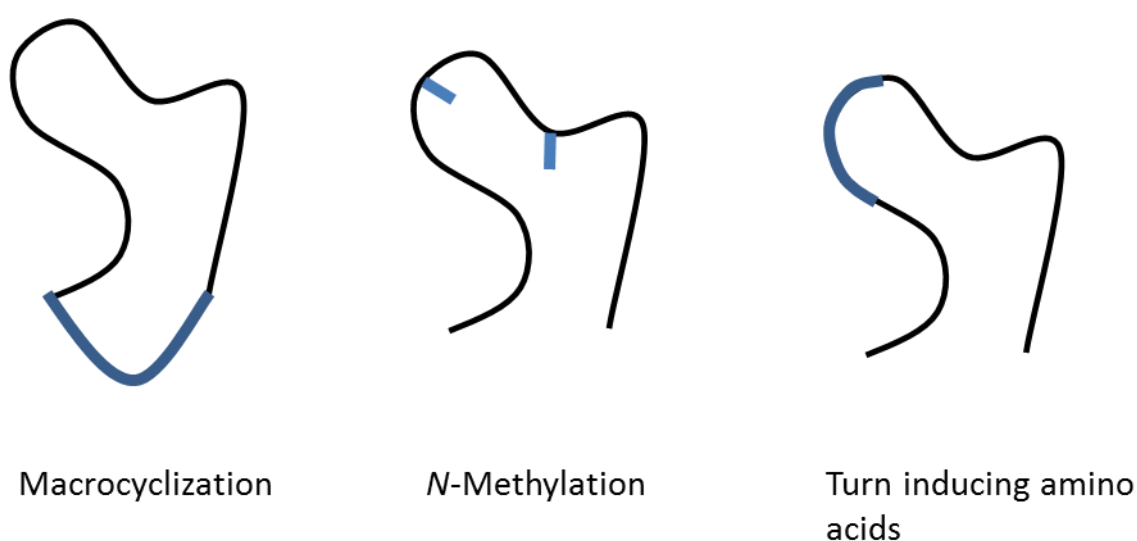
Figure 0.4. General strategies for turn stabilization and mimicry, adapted from Pelay *et al.*[19]

There are different possibilities to prepare peptidomimetics. One option is based on mimicking structures, for instance, secondary structures. Turns are irregular secondary structure elements whose difference lies on the dihedral angles of the backbones. These regions, which go from helices to β-sheets, enabling the folding of the chain. Turns are classified according to the hydrogen-bond pattern formed between the backbone carbonyl group of the residue at position i and the backbone amide proton at position i+n[20]. There are four families of γ-, β-, α- and π-turns with three to six amino acids in length and n=2-5.

A reverse hydrogen-bonding pattern is observed between the main chain amide proton at position i and the carbonyl group at position i+n for δ- and ε-turns with n=1,2. Open turns correspond to the lack of hydrogen-bonding but the display of a specific $C^{\alpha i}$- $C^{\alpha i+n}$. Within a family subgroups types are defined according to backbone conformations and the dihedral angles involved Φ, ψ. Nine types of β-turns have been described: type I, I', II, II', VIa1, VIa2, VIb, VIII and IV[21]. In addition to single turn conformations, there are so-called turn motifs which consider overlapping turn structures[22] and are often present in structured protein domains, mainly loop regions which have high relevance in the field of protein-protein interactions.

Single turn mimetics can be achieved by taking advantage of cyclization strategies. Macrocyclization is a common strategy used as a constraint in turn structures and frequently displayed in natural proteins and peptides in the form of disulfide, thioether[23], biaryl or biaryl ether bridges[24]. High numbers of cyclization strategies have been described over the last decades, including head-to-tail, side chain-to-side chain and side chain-to-backbone[25].
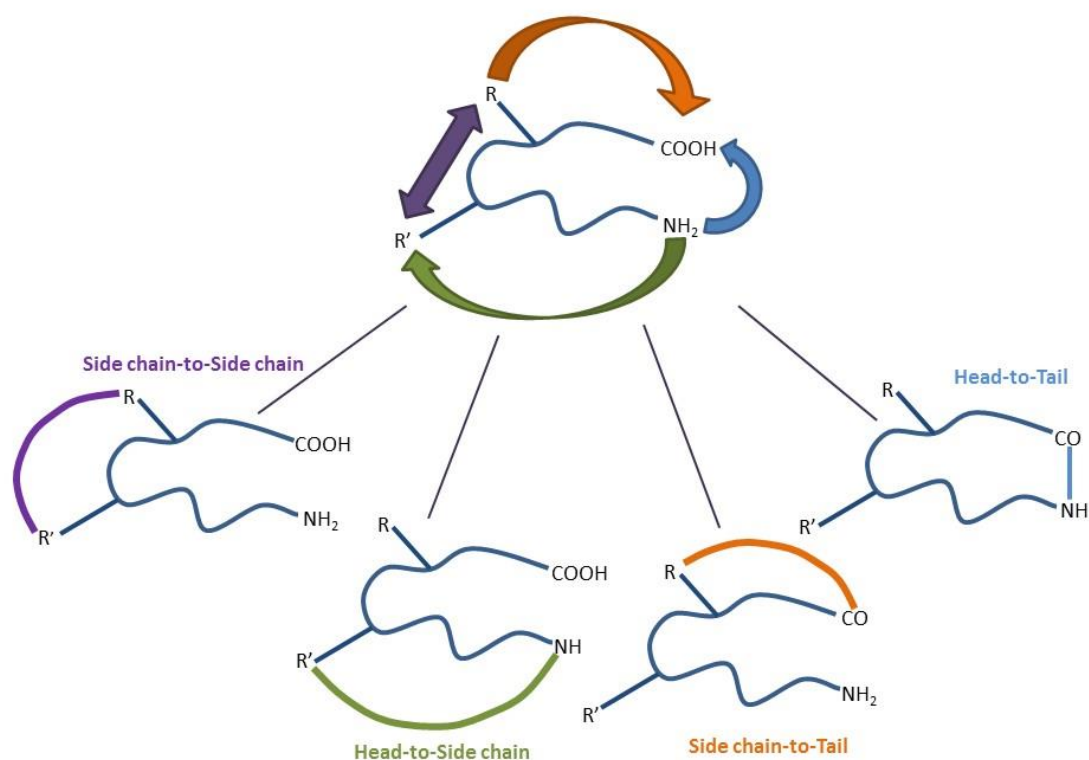
Figure 0.5. General macrocyclization strategies, adapted from White *et al.*[25]

Kessler and co-workers were pioneers in working with head-to-tail cyclic peptides and investigating their structure-activity relationship (SAR) by NMR spectroscopy. Natural disulfide bridges were also substituted by hydrocarbon crosslinkers by Grubbs and co-workers. In addition, binding motifs can also be introduced in the sequence as in the case of the cysteine-ladders, being another possible alternative to disulfide bonds. Lasso peptides are peculiar and complex structures which consist on the passing of their *C*-terminal tail through the ring[26]. Bicyclic peptides have also been explored, mainly by crosslinking thiol-containing natural or non-natural amino acids[27,28].

Despite the fact that cyclic peptides offer a more rigid scaffold than their linear and flexible analogs, one cyclization in the sequence may not be enough to ensure a single conformation of the molecules meaning that further constraining elements should also be introduced in the design. Some amino acids such as Pro, Gly, Asn and Asp are overpopulated in β-turns[29]. In fact, proline plays a unique role in protein folding, which is not a surprise taking into account their peculiar structure which includes a secondary

backbone amine in the ring involving backbone, being the only proteinogenic amino acid with these characteristics. In this case, hydrogen-bonding cannot exist due to the absence of the amide proton and the reduced conformational flexibility. The other relevant feature of proline is the existing equilibrium between *cis-trans* state.

Stapled peptides

An alternative and interesting strategy to prepare peptidomimetics is found in the synthesis of stapled peptides. Although the use of stapled peptides is mostly focused in fixing a particular peptide conformation for instance, α-helix, for improving pharmacologic parameters, it can also be applied on triggering biological activities[24,19,30]. It has also been shown that the incorporation of the staple could be an interesting tool to increase cell permeability[31]. A recent paper published by Verdine and co-workers[16] described that hydrocarbon-stapled-α-helical peptides permeate across cell membrane more efficiently that their unstapled versions and even better than well-characterized cell penetrating peptides such as penetratin. They suggested a dose-dependent accumulation of the stapled peptides in cells which takes place by a clathrin- and caveolin-independent, energy-dependent endocytosis pathway.

Linus Pauling[32] was the first one who described α-helixes. This structural motif is a major component of protein-protein interfaces[33] but due to their lack of stability as an isolated feature, it is limited in the therapeutic field. This important motif has proved to be stabilized by the incorporation of a single stapling between two amino acids present in the sequence. The all-hydrocarbon staple strategy has been extensively studied[31,34]. Stapled peptides can be obtained by SPPS and using C-C bond-forming catalyzed reactions. This staple combines two different stabilization strategies to induce α-helical structure, namely α,α-disubstitution and macrocyclization[35]. The introduction of this motif increases the level of α-helical content, as well as, the target affinity prevents from proteolytic degradation extending the half-life time also *in vivo* and enhances cell permeability. The latter can be achieved due to the avoidance of extra heteroatoms in the macrocyclic bridge, which could hinder cell permeation.

Crosslinking can be performed by Grubbs catalyzed reaction between i, i+3; i, i+4 or i, i+7 in order to achieve the desired α-helical conformation[31].

Structural mimetics: β-strands, β-sheets and β-hairpins

Protein recognition mediated by peptides is not only limited to α-helices. Other secondary structures have also their role, such as β-hairpin. This structure is constituted by two antiparallel β-strands linked by a turn or a loop sequence. The efforts devoted to prepare this type of peptidomimetics are based on the use of a constrained template by performing head-to-tail cyclization or via the linkage between the strands by disulfide bridges[36]. Inspired by the structure of antibodies, a new kind of highly efficient binding peptides was obtained from stabilized β-hairpins, aptides.

Chemical modification of peptides has mainly been applied with the aim of avoiding proteolytic degradation but maintaining the binding which usually relates with the folding of the peptidomimetic. A successful example of this approach relays on β–peptides, oligomers of β-amino acids, a type of foldamers with the ability to well adopt secondary structures that are able to target certain PPIs. Also oligomers of *N*-alkyl glycine where the side-chain is attached to backbone nitrogen instead of the C^{α}, called peptoids, adopt predictable conformations and are resistant to protease degradation.

Macrocyclization

The low permeability and stability of linear peptides together with the weak and no selectivity binding owing to their flexibility reinforces the theory that more rigid scaffolds could be useful in order to address PPIs. Different innovative technologies have been developed in order to obtain cyclic peptide in an individual or combinatorial manner.

Rigidification of linear peptides have been achieved using different strategies, the most used cyclization[37] since the entropic penalty due to rigidification is balanced by the

preorganization of the scaffold. At the same time, this strategy may also involve the enhancement of serum stability[38], as well as, target selectivity.

Head-to-tail cyclization was one of the first approaches studied to avoid denaturation and enzymatic degradation of peptides[25]. From amide bond formation to other less classic methodologies such as imine-induced Ser/Thr ligation[39], enzymatic reactions[40] or lactam bridges[41] have been applied. Nonetheless, head-to-tail cyclization is still a challenging reaction depending on the sequence to react and the amino acids involved in the amide bond formation. Sometimes, this reaction is not possible to be carried out and requires and alternative approach to attempt the cyclization of the molecule.

In this context, Bartoloni *et al.*[37] proposed a new strategy to expand the chemical space of bioactive peptides by introducing extra branching points in peptidic sequences enabling the synthesis of bridged bicyclic peptides (BBPs).

Nevertheless, a major limitation of peptides is their general lack of permeability to cellular membranes, which can hinder their accessibility to intracellular targets. Despite the fact that hydrogen bonds[42] and/or N^{α}-methylation of the backbone[43] can lead to an improvement of the penetration, other strategies have also been studied[44]. Lian *et al.*[44] proposed bicyclic fusion peptides which are formed by a target-binding peptide and a cell permeable peptidic sequence with the desired activity for the molecule (which in the example is the PTP1B inhibition). These bifunctional bicyclic sequences overcome the permeation issue at the same time that display the expected activity.

Regarding the different techniques that have been applied for the isolation of potential PPIs candidates, the most widely used has been the screening towards large combinatorial libraries[45]. The first one is phage display, in which a gene encoding a peptide is inserted into a phage causing the display of this peptide in its surface and allowing its screening towards the protein of interest. This methodology has been applied to bicyclic peptides[46] due to the size and constraining structure that these molecules possess which makes them able to bind with high affinity and selectivity to protein targets. In fact, general bicyclic peptides inhibitors have been discovered by HTS of phage display libraries and mRNA display[47].

Miniproteins and photoswitchable peptides

In this context, selectivity can be enhanced by the use of miniproteins owing to the potential exploration of larger surfaces. Nature has a clear example that can be found in plants, cyclotides. These disulfide rich miniproteins have been used as scaffolds for the incorporation of epitopes with biological activities, obtaining a new class of molecules named "grafted" peptides[48].

Extra rigid elements can be added to the general scaffold, leading to the formation of bicyclic peptides. On the other side, there is also the possibility to introduce a motif that not only represents a decrease in the flexibility but also the control of the structure. Light regulation of the activity of the peptides can be achieved by the introduction of a photoswitchable crosslinker[49].

Flexible or rigid ligands?

When designing molecules for their use in molecular recognition, the rigidity or flexibility of the scaffold is an important parameter to be concerned about[50].

In 1894, Emil Fisher proposed the mechanistic explanation for molecular recognition of the lock-and-key model. This early model postulated that in enzymatic catalysis both the involved enzyme and the substrate have specific complementary geometry shapes that perfectly fit. Enzyme specificity can be easily understood but the model fails when explaining the stabilization of the transition state that enzyme achieves.

Some modification of this model where suggested by Daniel Koshland in 1958. After considering the inherent flexibility that enzymes possess, it was hypothesized that permanent reshaped of the active site takes place due to the interactions with the substrate. This implies that the substrate does not simply bind to a rigid active site since the amino acid side-chains are flexible. Once the substrate is bound to the active site a final conformation of the enzyme is adopted. This model is called induced fit and it has been compared to a hand-in-glove model.

Nowadays, scientists are aware about the flexibility that proteins possess which may involve the use of ligands with a scaffold flexible enough to be adapted to the active site of the proteins. Nonetheless, as mentioned above, the finding of new strategies to introduce constrains in peptidomimetics is constantly increasing. As a matter of fact, ridigification of peptides is related to an overall increasement on the speficity, affinity, oral activity, as well as, stability. What may seem controversial at this point is the enhancement in the affinity binding. However, better activity can only be gained when fixing the preferential conformation of the peptides. For this reason, the relevance of the proper design is reinforced. Some studies have revealed a general approach to obtain successful results[51]. The first step must involve the selection of a defined minimal sequence with the ability to bind the receptor, which can be performed either by testing different synthesized analogs of the peptide candidate or by screening of a peptidic library. The next step is to incorporate the constraining motif in the sequence of interest and evaluate whether the rigidification of the peptide provides the desired results. As expected, the final step involves the optimization process to further restrict the conformational freedom and improve the fit with the receptor[52].

Biaryl motif: inspiration and introduction in peptidomimetics

As it has been previously mentioned, biaryl bond are present in several natural products, including peptides, alkaloids, flavonoids, polyketides, tannins, terpenes, coumarins and lignans, which indicates the relevance of this structural motif constituting a site for protein surfaces recognition mainly due to the influence of the phenyls in π-cation interactions[53].
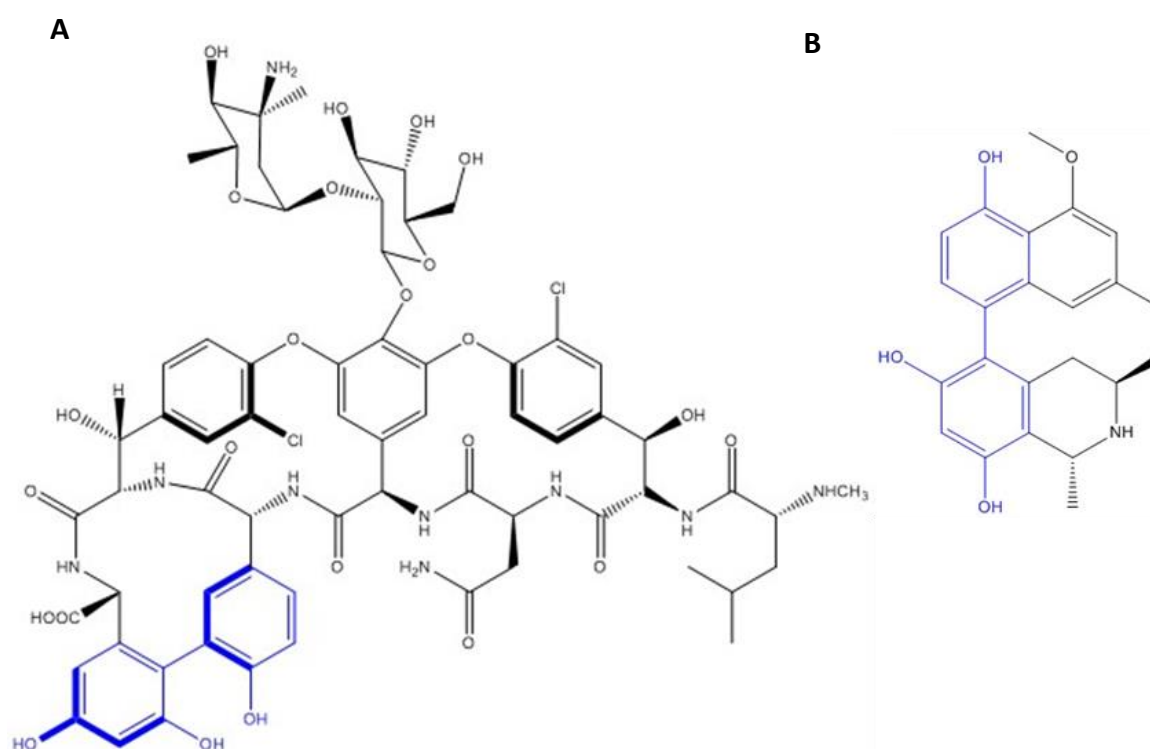
Figure 0.6. Structures of vancomycin (A) and korupensamide A (B).

One classic and well-known example of a natural product containing a biphenyl bond is vancomycin. This antibiotic was sold for the first time in 1954 but it is still used for the treatment of a relevant number of bacterial infections being the more relevant the treatment of resistant bacterial pathogens. Owing to the efficacy of this drug, several research groups have extensively studied the activity of this molecule, trying to achieve better antibiotics derived from structure activity results (SAR). From the complex structure that the molecule presents, there are some more relevant features such the aglycone part and biaryl subunit, known as actinoidinic acid. SAR results from

Rodriguez *et al.*[54] demonstrated that the presence of biphenyl render a substantial improvement on the activity of the analogues in different bacterial strains while a third aromatic ring does not translate into better activities. All this data pointed out the role of biaryl motif in the field of molecular recognition. Nonetheless, biphenyl presence has also a non neglectable effect in the overall structure of the molecule in which is incorporated as it will be further explained when later revisiting the concept of atropoisomerism.

The incorporation of this feature in peptidomimetics has already been pointed out since it is a conformational constrain that also can increase biostability, selectivity and activity of the modified sequences[24,44,46,50,53].

En route towards biaryl formation

Biaryl formation can be accomplished by taking advantage of palladium catalyzed cross-coupling reactions, which have become the main strategy in organic synthesis for carbon-carbon bond formation. These reactions are compatible with a wide range of functional groups. The scheme found in Figure 0.6 is summarized as the coupling of two catalytic cycles, the aryl boronic compound obtained from Miyaura borylation reaction acts as a partner for the transmetalation in Suzuki cross-coupling catalytic cycle to render the desired product. Nonetheless, these reactions are not only performed in tandem since the aryl boronic product obtained in Miyaura borylation is stable under certain conditions[55].

Miyaura catalytic cycle is based on the oxidative addition of the catalyst to the aryl halide, followed by a transmetalation with the boronic reagent to render an aryl palladium intermediate that evolves by reductive elimination as the boronic ester or acid (depending on medium conditions) to be used in the subsequent catalytic cycle. Suzuki cross-coupling is also initiated by an oxidative addition of the catalyst to the aryl halide, followed by a transmetalation which in this case, renders a diaryl palladium intermediate, the last step is the reductive elimination which finally yields the biaryl products and the palladium (0) catalyst regenerated to be used again in the cycle.
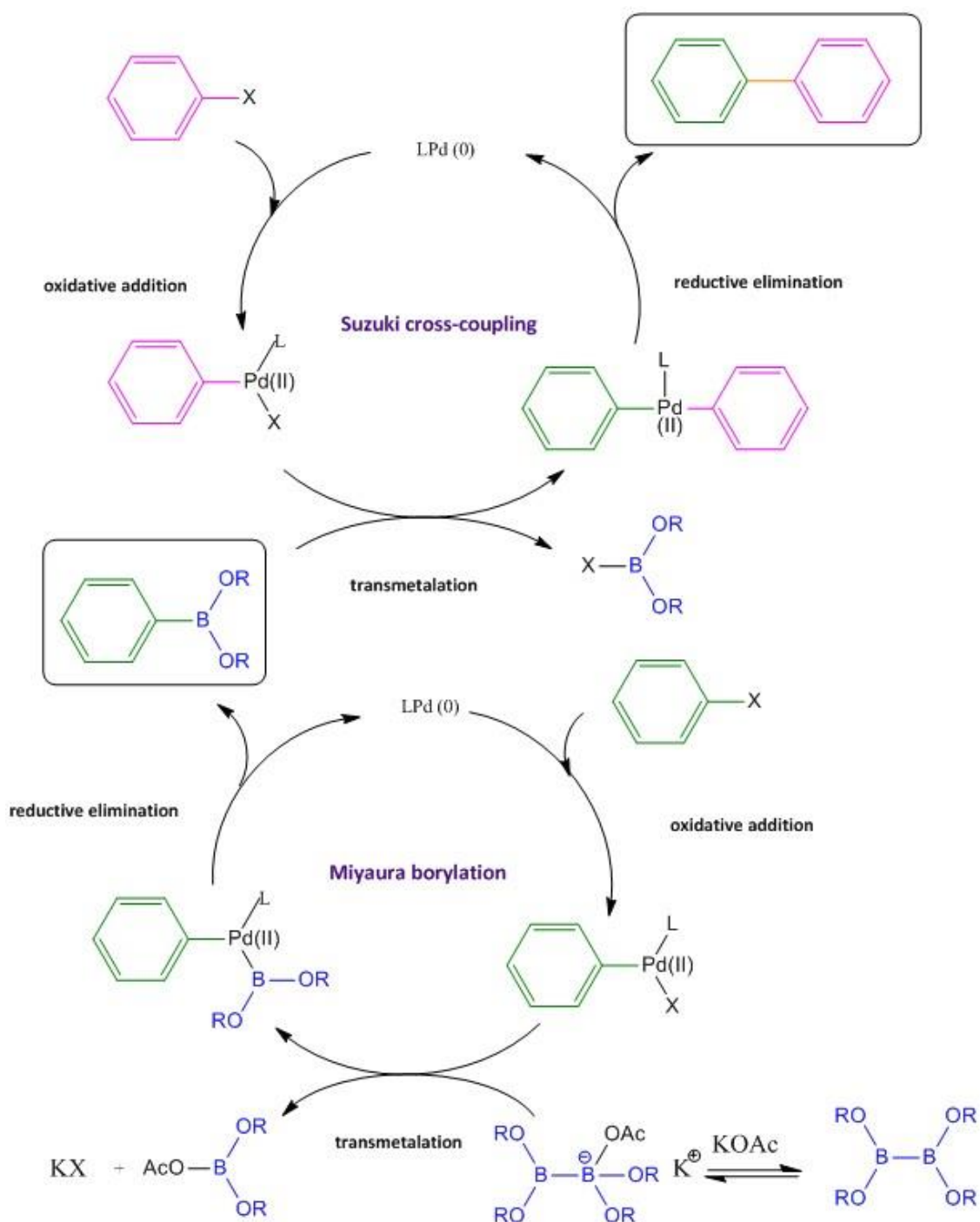
Figure 0.7. Catalytic cycle of Miyaura borylation and Suzuki cross-coupling reaction. The obtained products in each catalytic cycle are remarked, as well as, the final C-C bond formed coloured in orange.

In addition to Suzuki cross-coupling, there are other catalyzed reactions that can be perfomed to obtain C-C bonds.

Stille coupling[56] enables C-C bond formation by the reaction of an aryl halide or triflate with an arylstannane also enabling phenols as substrates. Suzuki coupling[55], one of the most widespread methods, is based on the reaction of an arylboronic acid or their derivates (such as arylboronates) and aryl halides. The main advantages of this strategy are the tolerance with more functionalities and the applicability even in sterically crowded aromatic systems.

The metal-catalyzed selected reaction in the present thesis is Suzuki-Miyaura due to the previously described virtues that offer. The use of this reaction has been extended recently to SPPS[24,53,57,58,59,60] enabling the discovery of some interesting products[61]. Suzuki-Miyaura (SM) allow the C-C bond construction in mild conditions and a safe environment gaining access to drug-like molecules which can mimic the natural biaryl bond. In order to perform Suzuki cross-coupling on solid-phase, previous borylation also on resin should be also carried out, which has been scarcely reported[24,53]. The application of this reaction on SPPS constitutes a relevant tool for the generation of combinatorial libraries including the biaryl feature.

Moreover, the interest in this reaction is such that a patent to prepare self-assembled peptides embedded with complex organic electronic subunits was filed by J.D. Tovar and A. M. Sanders describing the application of them on SPPS.

Nevertheless, Suzuki-Miyaura is not the only cross-coupled reactions to consider when addressing the formation of C-C bonds. Another commonly used palladium-catalyzed reaction is Sonogashira[62]. Sonogashira reaction is the condensation of aryl halides with terminal alkynes with Cu(I) and Pd(0) catalysts.

In early 1998, Dyatkin *et al.*[63] described the synthesis of complex propargylamines by taking advantage of Sonogashira reaction on solid-phase. More recent studies[64] presented the application of this metal-catalyzed reaction microwaved-assisted.

However, Sonogashira reaction introduces a triple bond connector between the two aromatic residues, which have a very important impact in the molecular recognition but an even greater effect in the conformation of the final molecule.

At this point, it is worth revisiting the concept of atropoisomerism[50]. It corresponds to a type of stereoisomerism that can be present in systems where free rotation about a

single covalent bond is enoughly hindered to enable the isolation of the arising stereoisomers[65]. This effect is commonly observed in biaryls with substituents restricting free rotation about the sp2-sp2 C-C bond. Atropoisomerism has been vastly studied in the case of biaryls[66,67].

Due to the relevance that vancomycin has as antibiotic and the present interest in the context of this thesis, it is worth emphasizing the impact of the biphenyl in the atropoisomerism of the molecule. The biaryl bond is a key crosslinker responsible of the structure since the thermodynamic biaryl atropoisomer is governed by the global architecture of the molecule rather than stereochemical effect close to the biaryl axis.

Furthermore, biphenyl motifs have their interest not only due to the π-cation interactions and the rigidification of the molecules but also owing to the potential recognition that allow. Some groups have demonstrated the fact that biphenyl incorporation in particular molecules can enable recognition by carbohydrates[68]. In the sugar recognition field, biphenyls have been commonly used as building blocks for macrocyclic receptors[69]. The relevance of these studies intrinsically lies on the role of carbohydrates in human body. Gaining access to synthetic carbohydrate receptors would imply the discovery of new therapeutic agents to be used in diseases such as diabetes. In fact, those receptors can display different modes of action like targeting cell types, as synthetic antibodies or behaving as shuttles that can transport saccharides or related pharmaceuticals across cell membranes. In addition, they can also be used as carbohydrate sensors which are required for diagnosis, among other applications[70].

Biaryl building blocks are also applied as chiral reagents for chromatography or liquid crystals, as well as, in laser-dyes or conducting polymers[71].

The relevance of tryptophan amino acid

The relevance of tryptophan amino acid is well known in the field of natural products. Furthermore, this key building block is also an important biosynthetic precursor in different bioactive compounds, mainly alkaloids[72].

Statistical analyses of membrane proteins have demonstrated[73] that a common feature of membrane-spanning proteins is their preference for aromatic amino acids such as tyrosine or trypthopan at the interfacial lipid headgroup region[74]. Aromatic or charged amino acids may act as an anchor for this type of proteins, while in the studies with small membrane adsorbed model peptides and model transmembrane helical proteins, they seem to be related to distinct interfacial interaction[75]. Amphiphatic or dipolar interactions were discarded to be the main kind of interaction when introducing this amino acid thanks to the results obtained in the studies carried out between tryptophan analogs and phosphatidylcholine membranes. In fact, these studies reveal that the interfacial preference is based on the flat rigid paddle-like structure of tryptophan associated with the aromacity of the indole π-electron cloud[76].

The indole group present in tryptophan, as we early described regarding biaryl bonds, can display π-cation interactions that are known to be important in biological systems and have an increasing interest in medicinal chemistry. In fact, several groups have devoted great efforts to predict π-cation interactions in new systems[77] and understand the real effect that this interaction has in biological systems[73].

Different types of interactions play their own role in the scenario of molecular recognition. Nonetheless, π-cation interactions are considered one of the driving forces in biological systems since they are present if 65% of the interfaces[78]. In fact, they have been compared to electrostatic interactions such as Van der Waals and hydrogen bonding[79]. This interaction is dominated by the electrostatic attraction of positive cation charge toward the quadrupole resulting by the π-electron distribution of the aromatic ring[80]. Some relevant contributions of π-cation interactions have also been related with the folding and stability of proteins[81], as well as, in specific drug-receptor interactions[82]. The most appropriate amino acid for establish π-cation

interactions is considered to be tryptophan while histidine is the worst one[77] even if its heteroatom could participate in π-cation interactions.

However, in this context, we should not forget about the relevance of salt-bridge interactions, even if they are not the center of discussion[83].

Over the last years, π-cation interactions have been studied in proteins, protein-protein and protein-DNA systems.

In the landscape of protein systems, these interactions are crucial for execution of function such as ion channels[84], G-protein-coupled receptors[85], transporters[86] and enzymes[78]. Regarding to protein recognition, positively charged amino acids such as lysine or arginine may play an interesting role by interacting with the aromatic rings that tryptophan, as well as, tyrosine or phenylalanine contain. The biological relevance of this interaction may be understood as a result of the additive potentials coming from the polarized nature of charge ions and the out-of-plane distributions in the aromatic ring[87]. Furthermore, π-cation pairs can also be responsible for the binding in which strong influence of electrostatic forces can be found[77]. The role of π-cation interactions have also been studied in protein-RNA interfaces[88] being sequence and structure specific.

Macrocyclization strategies

Synthetic macrocyclic peptides are of great interest for chemists having found applications in a wide variety of fields from medicinal chemistry to nanomaterials. As it was previously mentioned for cyclosporine A, cyclic peptides were used as therapeutic agents for the treatment of different diseases. Some examples include nisin, polymixin, colistin, calcitonin, among others.

The remarkable properties of macrocyclic peptides and the potential fine-tuning of their functions make them excellent candidates to be explored.

Despite of the increasing interest in this kind of molecules, an exponential growth is still expected to be experienced[89]. Large macrocyclic molecules may present molecular weight ranging from 600 to 1.500 Da and spite of the early belief that such molecule may never be good drug candidates, it has been demonstrated their potential application in PPIs.

Nonetheless, the difficulty of cyclization is strongly dependent on the linear precursor sequence. So, new methodologies were developed[25] in order to successfully address their synthesis also beyond the conventional amide bond formation.

Some important concerns to achieve head-to-tail cyclization strictly depend on the size of the ring, as well as, the amino acids involved in the bond formation. Regarding small-to-medium-sized rings, the main difficulty is the ground-state *E* geometry of the peptide bond which hinders a ring-like conformation to proceed towards cyclization. This problem is not present in larger ring sizes since they can accommodate *E* peptide bonds although there synthesis of them is also complex since intermolecular reactivity should be prevented. In fact, cyclization of large peptides with more than seven amino acids is not as problematic as it was commonly thought and the synthesis is actually straightforward. On the other hand, smaller peptides tend to be more troublesome and, in some cases, even impossible to cyclize as it was clearly demonstrated in some studies of small peptide cyclizations[90]. In addition, epimerization of the *C*-terminus should also be prevented to maintain the desired stereochemistry of interest. Taking into account all these consideration, ring disconnection must be chosen carefully[91].

This can also implies the introduction of turn-inducing structural elements embedded midway in the linear precursor to yield a more efficient macrocyclization.

From the different methods used to cyclize peptides the most common reaction is lactamization[92], lactonization[93] or disulfide bridge formation. A common precaution is the high dilution, around submillimolar concentrations, to minimized undesired intermolecular reactions such as oligo- and polymerizations.

An alternative strategy is based on solid-phase cyclizations, in which the solid support creates a pseudodilution effect that prevents intermolecular processes[94]. The work-up of these cyclizations is reduced to the wash and filtration of the resin, which facilitates the procedure. Cyclization on resin requires the anchoring of the first amino acid through the side-chain and typically evolves a more complex methodology which involves three dimensions of orthogonality to obtain the final product.

To summarize, the success or failure of macrocyclization lies on the ability of the linear precursor to be preorganize in the space in a conformation in which the reactive ends are close enough to render ring closure. This prearrangament avoids the undesired intermolecular processes and favours the intramolecular reaction by a high effective molarity. Many strategies have been explored[95] to gain access to the conformational preorganization for performing macrocyclizations. There are two different categories: the first one, based on the internal conformational elements which can be introduced in the linear precursor and the second one, external conformational elements, involving the use of molecular scaffolds that are non-covalently attached to the molecules and not consumed during the reaction, which will be classified as a templated-mediated macrocyclization. Due to the interest of macrocyclization in the present thesis, it is worth to go in depth in each one of the two possible mechanisms to better understand them.

Ring-closure of peptidic sequences is favoured when the angular requirements for the *N-* and the *C-* termini in the transition reaction state can be accommodated with a minor energetic penalty. Some studies developed in this direction[96] showed that the loop-closure kinetics in longer peptides depends on intramolecular hydrogen bonding and transient β-sheet structure, which accelerated the finding between the residues

even distant in the sequence[97]. The rate constants of this state are in the scale of 20-100 nanoseconds for peptides having more than ten residues. The role of hydrogen bonds present between residues of the same sequence is based on lowering the free energy required for the closure of the long sequences. This observation allows the understanding of more intrinsically difficulties to cyclize shorter sequence due to the lack on intrapeptide hydrogen bonds. To overcome this drawback, strategies to adopt secondary structures can be used. The presence of proline, as well as, D-amino acids into all-L peptides have turn-inducing effects that can be exploited[98].

The same effect that proline displays can be mimicked by *N*-methylated amino acids. They have the potential to introduce *cis*-amide bonds into peptide sequences and induce suitable β-turns[99].

Pseudoprolines have also been extensively studied. They were first introduced as structure-disrupting building blocks to prevent aggregation and self-association of peptides during SPPS[100]. Pseudoprolines are modified heterocyclic amino acids that can be obtained from acid-catalysed cyclocondensation of serine, threonine or cysteine with an aldehyde or a ketone. They mostly induce *cisoid* conformation of the amide bond preceding them when incorporated into a peptide chain, type-VI β-turn structure[101]. In addition, their cleavage can be performed after cyclization under acidic conditions yielding the desired product. Regarding to the disadvantages, the main drawback is that NH pseudoprolines are difficult to acylated due to their steric hindrance.

On the other side, external elements used for assisting macrocyclization are based on the site isolation mechanism. Those templates provide cavities in which only one linear precursor can fit and cyclize. Incorporation of these scaffolds translates into reduced probability of cyclooligomerization. Difficult products that cannot be obtained by traditional methodologies have been synthesized using this strategy[102].

For instance, the synthesis of complex and potent antimicrobial compounds can be achieved taken advantage of chemoenzymatic approaches[103]. Taken a close look to some macrocyclic peptides in nature one can realize that they are formed by non-

ribosomal biosynthases, which are known to tether the activated linear intermediates via thioester linkages being analogue to what is used in SPPS[104]. Another well-described strategy is the use of metal ions to conformationally preorganize the linear precursors[105]. Some possible ions are lithium or silver salts. Of course, sulfur-mediated cyclization has also its role. Direct aminolysis of thioesters using imidazole can be carried out[106], the discovery of this reaction was inspired by the role that imidazole has in the catalysis of the hydrolysis and transfer of activated acyl groups acting as a nucleophilic catalyst. In the same context, Sanger's reagent has its application via generation of a reactive thioester. Sulfur is the most common element to perform side chain-to-side chain macrocyclization via disulfide formation. Intramolecular disulfide bridges are constraining motifs commonly assessed by reaction between two cysteine thiol groups present in the sequence. The important concern in this case is when attempting to perform multiple disulfide bridges, since a convenient orthogonal strategy should be designed to allow proper pointing of the residues involved. However, cysteines can also be used for a thiol-ene reaction which is better resulting on SPPS but can also be carried out in solution at low concentrations (millimolar)[107]. *N*-terminal cysteines contain 1,2-aminothiol group that can be applied into different types of macrocyclization strategies. This functionality can react with an aldehyde rendering a thiazolidine ring or an amide bond via a tricyclic intramolecular rearrangement when using *C*-terminal glyceric ester as the aldehyde. Ligation strategies also lies on this functionality such as the native chemical ligation[108,109], based on *S*-to-*N* acyl migration of the *C*-terminal thioester reacting with an unprotected *N*-terminal cysteine, driven by the thermodynamic strength of the amide bond over the thioester link. Despite of its effectiveness, the major drawback is the requirement of a cysteine at the *N*-terminus. Nonetheless, great efforts have been put to mimic the side-chain of this amino acid and have allowed the wider the range of macrocyclizations that can be performed[110]. An even more recent results demonstrated the application of native chemical ligation in a cysteine-free peptide[111] by a final desulfurization reaction that eliminates the sulfur using nickel Raney. Macrolactamization amenable for unprotected peptides is also possible by taking advantage of Staudinger ligation[112] in which a phosphine tethered to a thioester at the

C-terminus of the peptide reacts with an azide at the *N*-terminus, forcing intramolecular cyclization and a cyclic iminophosphorane final product.
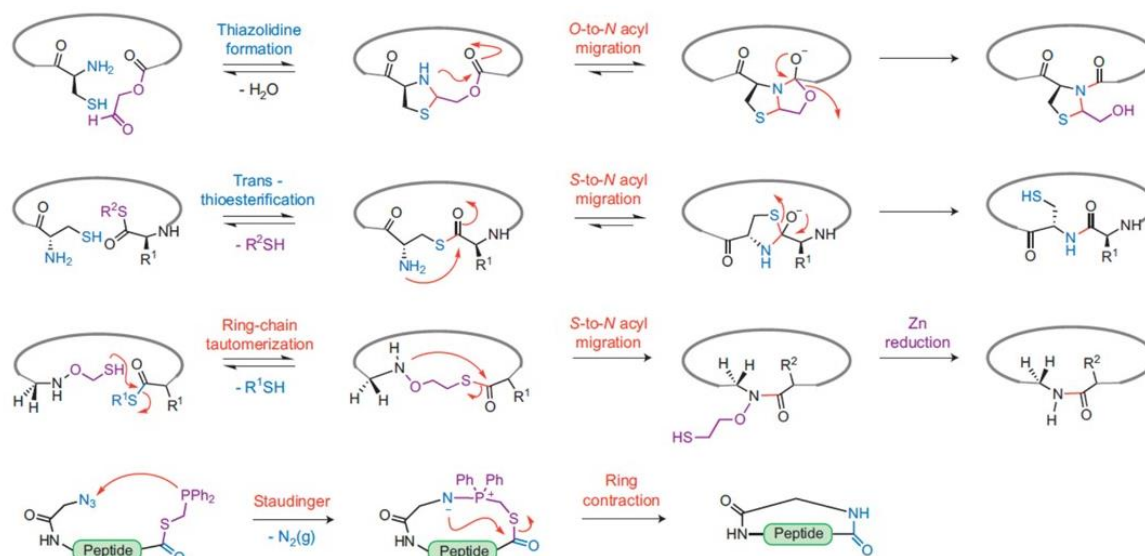
Figure 0.8. Peptide macrocyclization strategies based on the used of sulfur-containing auxiliaries (extracted from White *et al.*[25])

Considering the fact that the entropic penalty that should be paid to perform macrocyclization is directly responsible for the difficulty to carry out this reaction, some strategies were focused on alleviating the energetic cost required. Ring contraction is based on the formation of a larger and more flexible macrocycle in a first step and followed by the contraction of this ring yielding the final desired product. Different examples of ring contraction based on an *O*-to-*N* acyl migration[113] have been performed even in difficult sequences also involving macrolactamization[114] enabling the synthesis of homodiketopiperazines[115].

Click-chemistry is an alternative way to gain access to macrocyclization compounds. Some peptides synthesized by this methodology incorporates heterocyclic rings such as 1,2,3-triazole. The real interest of them can be found in marine natural peptides with relevant biological activities[116]. Azide-alkyne cooper-catalysed cycloadditions can also be applied on SPPS[117].

Catalysis by ruthenium can also be applied to perform ring-closing metathesis of olefins, forming carbon-carbon bonds as described above[118].

To finish with the different external elements, multicomponent reactions must also be presented. The most commonly used is the Ugi four-component reaction, used as a tool for peptoid-based framework synthesis[119]. The main drawback is undesired dimerization when the sequences contain less than six amino acids. To prevent this side reaction, electrostatically controlled macrocyclizations can be useful. Since short peptides adopt preferently random coil structures in aqueous medium by the disruption of intramolecular hydrogen bonds, polar organic solvents can substitute water. Ion pairing between the *C-* and *N-*termini results in circular conformation of the linear peptides, rendering to electrostatically induced pre cyclization conformers[120]. No epimerization occurs in this high chemo- and stereoselective reaction; cyclo- or oligomerization is neither detected. Furthermore, high yields are obtained in reduced reaction times.

Targeting p53 tetramerization domain

The tumor suppressor protein p53 is a transcription factor of genes which control the cell cycle and preserve the genomic integrity of the organism[121,122]. Therefore, talking about this protein is talking about cancer, since nearly 60% of human tumours display alterations in its pathway. There are several factors which can trigger the activation of p53 mainly DNA damage or cellular stress situations. Regarding its response, it presents a huge variety of ways, including cell-cycle arrest and DNA repair or apoptosis[123,124].

Due to its high relevance in life (so-called "genome guardian"), p53 is extensively studied mainly related to cancer therapy.
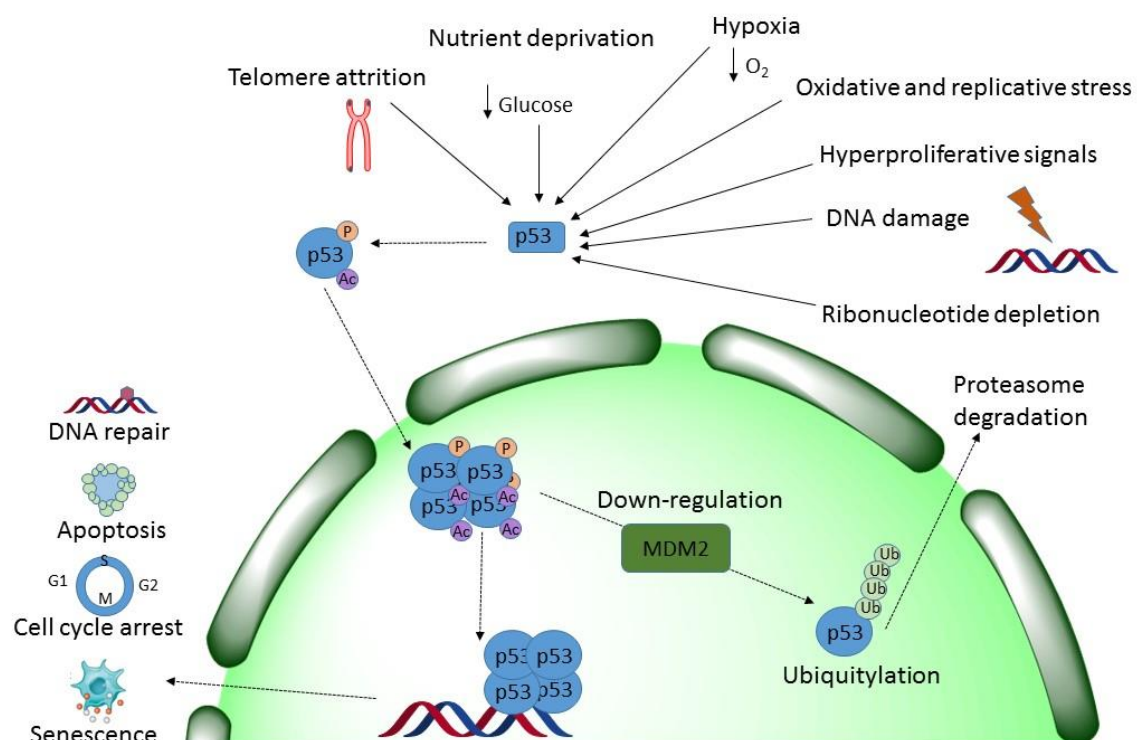
Figure 0.9. p53 activation mechanisms and cellular responses.

From a structural point, the active form of p53 is a homotetramer whose monomer contain 393 residues each one[125]. There are five main domains in this protein (three folded domains and two disordered ones): residues 1-93 form the intrinsically disordered *N*-terminal domain (TAD) containing a proline-rich region (PRR) 61-93; 94-292 corresponds to the folded core domain (p53C); 293-324 constitute a disordered linker; 325-353 is the folded tetramerization domain (TET); and 354-393 is the *C*-terminal disordered domain (CT)[125,126,127].

The large size of the protein, as well as, the presence of disordered regions has prevented the crystallization of the full-length protein. Nonetheless, the tetramerization and the DNA-binding domain have both been crystallized. In addition, selective labelling of the protein gave acces to the NMR characterization of the full-length protein and DNA complex[127].

Despite the fact that the most important domain is the central DNA binding domain, in the present thesis we focused on the region between the 326 and 357 residues, which contains the tetramerization domain, mainly due to its structural function.
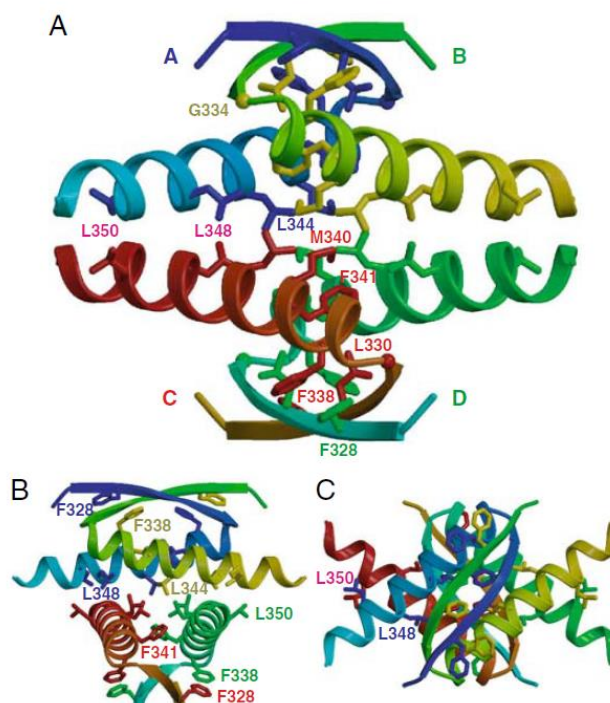
Figure 0.10. Three-dimensional structure of p53 tetramerization domain. The four subunits are labelled as A, B, C and D. Side-chains of hydrophobic residues that mediate important inter-subunit interactions are shown. Figures A, B and C represent different views. Extracted from Stavridi *et al.*[128]

The tetramerization domain is a dimer of dimers with D2 symmetry in which the four monomers possess identical conformations. Each subunit is formed by a β-strand (327-333) and an α-helix (335-355) displaying a V-like shape. Antiparallel arrangement of the β-strands stabilizes the dimers while their interface is constituted by large hydrophobic areas at the orthogonal intersection of α-helices[129]. Hydrophobic interactions are vastly observed between the four subunits[128].

The activity of this protein is regulated by numerous mechanisms which control expression levels, degradation rate, structure, etc. The most common impairment is the direct mutation of p53 gene, which directly affects the DNA binding region in 95% of the cases[130,131,132,133,134]. Single missense mutations can also compromise its structure or modify key residues either involved in the interaction with other biomolecules or required for post-translational modifications. Loss-of-function is not the only result of these mutations, since they can also produce undesired oncogenic activity by promoting the transcription of oncogenes[135,136].

The failure in the pathway is related with the partners of this protein, in a relevant 10% of p53-associated tumours, being one of the most vastly studied MDM2[133].

During the last years, several studies have been focused in the reconstruction of the p53 tumor suppressor pathway and it has been a relevant increase in the number of p53-targeting strategies proposed, being the main target p53-MDM2 interaction[137,138,139].

Regarding the mutation of p53 gene, last efforts have been devoted on the rescue of the non-functional protein by small binding molecules. Since the mutations mainly affect the DNA-binding domain, very little attention has been paid to the other regions, in spite of having been found in human cancer[137,138,139]. For instance, taking the tetramerization domain as an example, successful attempts of improving its stability have been reported, although they require synthetic or genetic modification of the protein sequence.

Mutant R337H

Mutation of arginine 337 to histidine is the most frequent mutation in the tetramerization domain, as well as, for the p53 gene[140,141,142].

This inherited mutation is mainly related with the atypically frequent cases of pediatric adrenocortical carcinoma (ACC) in southern Brazil[143,144,145]. ACC has been possibly associated with Li-Fraumeni syndrome (LFS) and Li-Fraumeni-like syndromes (LFLS). High incidence (97%) of ACC harbours the R337H point mutation in children from southern Brazil who were developing tumors in the adrenal gland[146]. The pediatric ACC has only been observed in patients with this genotype despite the fact that several different types of cancer types, also including ACC, has often been associated with inherited p53 mutations. The most relevant fact is that the function of this particular point mutation is indistinguishable from the function of the wild-type protein[146,147]. Taking into account the development of the pediatric ACC further studies were carried out to unveil the real influence[148]. Previous studies has pointed out that both proteins are structurally similar although the mutation R337H is less stable and pH-dependent. The extraordinary pH sensitivity of R337H mutant was responsible for the tissue-specificity tumor development[149]. The elevated pH within adrenals cells destabilizes the tetramerization domain of R337H mutant causing the loss of tumor suppression function. Nevertheless, normal functioning occurs in intracellular enviroments closer to pH 7.0. Described disfunction in adrenal cells can allow the outgrowth of abnormal cells, which would by controlled and eliminated by p53 wild-type, to develop into tumors.
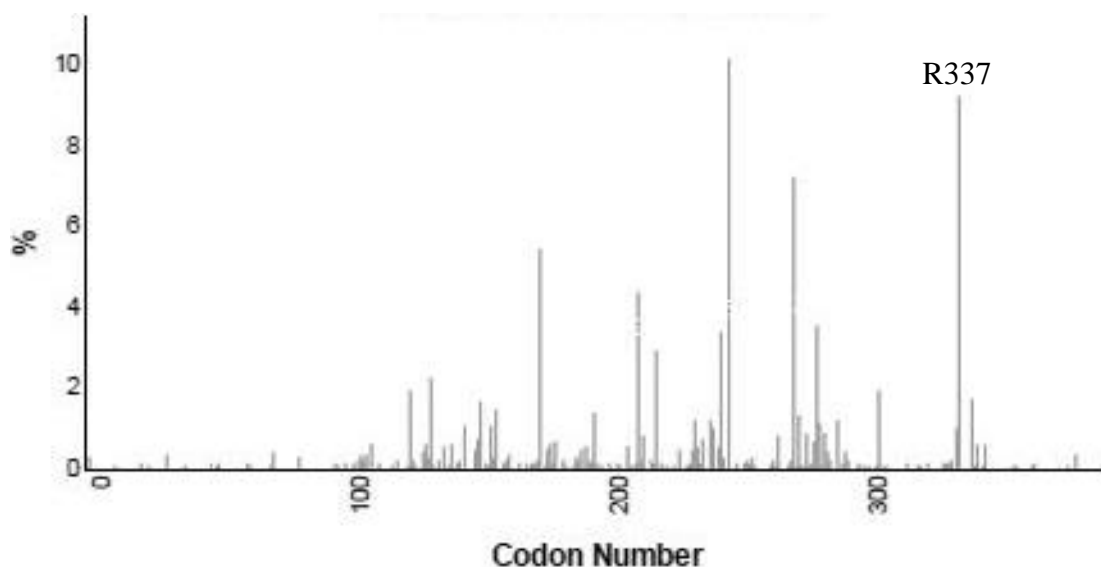
Figure 0.11. Frequency and distribution of p53 mutations along the sequence. From the IARC TP53 Database, release 18 ,April 2016 (N=1509).

The tetramerization domain of mutant R337H has the ability to adopt a native-like structure although it should be taken into account the lesser stability that it presents. In fact, it is highly sensitive to physiological range pH (6.5-8), due to the protonation of H337[150]. Nonetheless, at high concentrations (such as the commonly used for nuclear magnetic resonance experiments or circular dichroism) the mutated protein also adopts a tetramerization state.

In the wild-type sequence, the guanidinium moiety from R337 side-chain is involved into a salt bridge and a hydrogen bond with the carboxylate group from the D352 side-chain[151,152] The formed ionic pairing plus some hydrophobic interactions between the methylene groups from the arginine and other residues present in the sequence, have a relevant contribution to the whole tetramer stability[153].

The single-mutation affects both non-polar and charge characteristics of the side-chain. On one side, the histidine side-chain is shorter and less hydrophobic than the arginine and, on the other hand, its imidazole ring can only be protonated under relatively acidic conditions. The pKa for the H337 side-chain is 7.7, which is unusually high for this kind of residue; this fact supports the premise that the protonated state is stabilized by a favourable electrostatic interaction with the D352 side-chain[154].

So, the protonated H337 enables the tetrameric stable form of the protein and the same function that the wild-type p53 exerts. Nevertheless, neutralization of the salt bridge between H337 and D352 drives to an unusual tetramerization domain that is hardly folded under physiological conditions. Therefore, intracellular pH modulates the function of this mutant. The tissue specificity observed in ACC could be associated with the high pH of adrenal cells, around 7.9, under certain situations[155].

Previous studies in the lab[156] demonstrated that the use of calix[4]arenes are able to recover the self-assembly of mutated p53TD proteins, specifically mutants R337H, G334V and L334P.

Stabilizing self-assembly of mutated p53

Stabilization of protein structures is a potential therapeutic strategy. Although the efforts are mainly focused on protein-protein interactions inhibitors[157,158,159].

Stabilization of protein-protein interactions can prove to be even more effective than inhibition[144].

Some commercialized drugs such as rapamycin or taxol, which act by stabilizing pre-existing protein-protein systems, were discovered as inhibitors by hightroughput screening of natural products, since they inhibit the target protein by stabilizing other protein-protein interactions.

Regarding the discovered compounds at the beginning designed as stabilizers, only few have been reported to date and without reaching the market[156,160]. One of these examples was developed by Prof. de Mendoza at ICIQ and studied in collaboration with our laboratory by Dr. Susana Gordo. In that case, mutated p53 tetramerization domain proteins can be stabilized and the self-assembly of the wild-type recovered by the use of calix[4]enes[156].

Biophysical methods: taking advantage of circular dichroism

There are different biophysical methods that can be used to study protein-protein and protein-ligand interactions. Some of them are nuclear magnetic resonance (NMR), differential scanning calorimetry (DSC), fluorescence polarization (FP), mass spectrometry by electrospray ionization or circular dichroism (CD), among others.

In the current thesis, circular dichroism technique was used to study the protein-ligand interaction of some peptide with R337H, for this reason, understanding the basics of this technique enable to better understand the obtained results. Therefore, protein interactions and folding can be studied by this technique.

Circular dichroism phenomenon (Figure 0.12) is the difference in the absorption of left-handed circularly polarised light (L-CPL) and right-handed circularly polarised light (R-CPL) and takes place when the sample contains a molecule with chiral chromophores, which are light-absorbing groups.

A beam of polarized light has the two components, the left-handed and the right-handed, in a plane with the same phase and amplitude. Due to the different interaction of each component with the chiral centers, they are absorbed in a different manner. Once the light has passed through the sample, both components are still polarized but their phase and amplitude are not equal, meaning that the polarized light beam is elliptically distorted, θ.
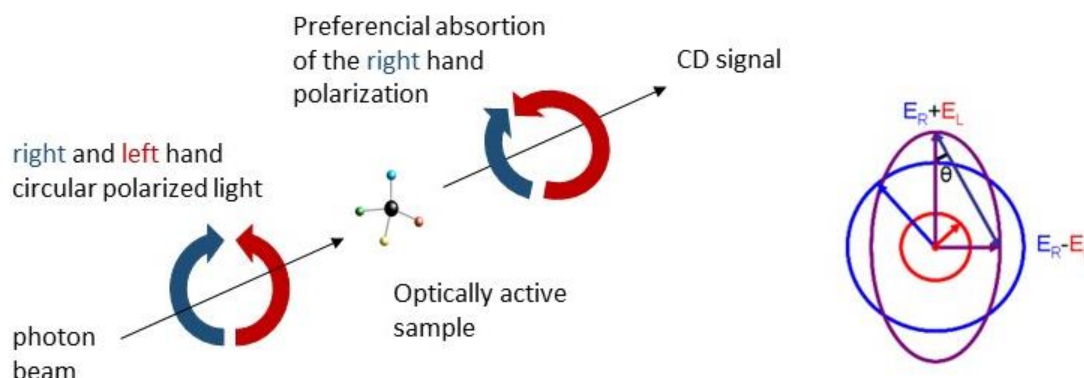
Figure 0.12. Illustration of the circular dichroism phenomenon. At the beginning, right-handed (in blue) and left-handed (in red) components of polarized light are equal phased and have the same amplitude. The resulting beam of light elliptically polarized is shown with a zoom on the right of the figure. Magnitude of CD is measured by the ellipticity, which is the theta angle (θ).

Except for glycine, all amino acids are chiral, containing at least one asymmetric carbon atom. In the conformation of a protein, the spatial arrangement and periodicity of the residues gives raise a characteristic CD spectrum.

In the far ultraviolet region, between 178-260 nm, CD bands correspond to amide bonds of the protein backbone (transition n-π* at 220nm and π-π* at 190 nm). Peptide bonds orientation within the protein structure can split optical transitions of the amide bond into multiple transitions, either increasing or decreasing the wavelengths as well as the intensity. Therefore, each secondary structure motif possesses a particular CD pattern as it is shown in Figure 0.12.
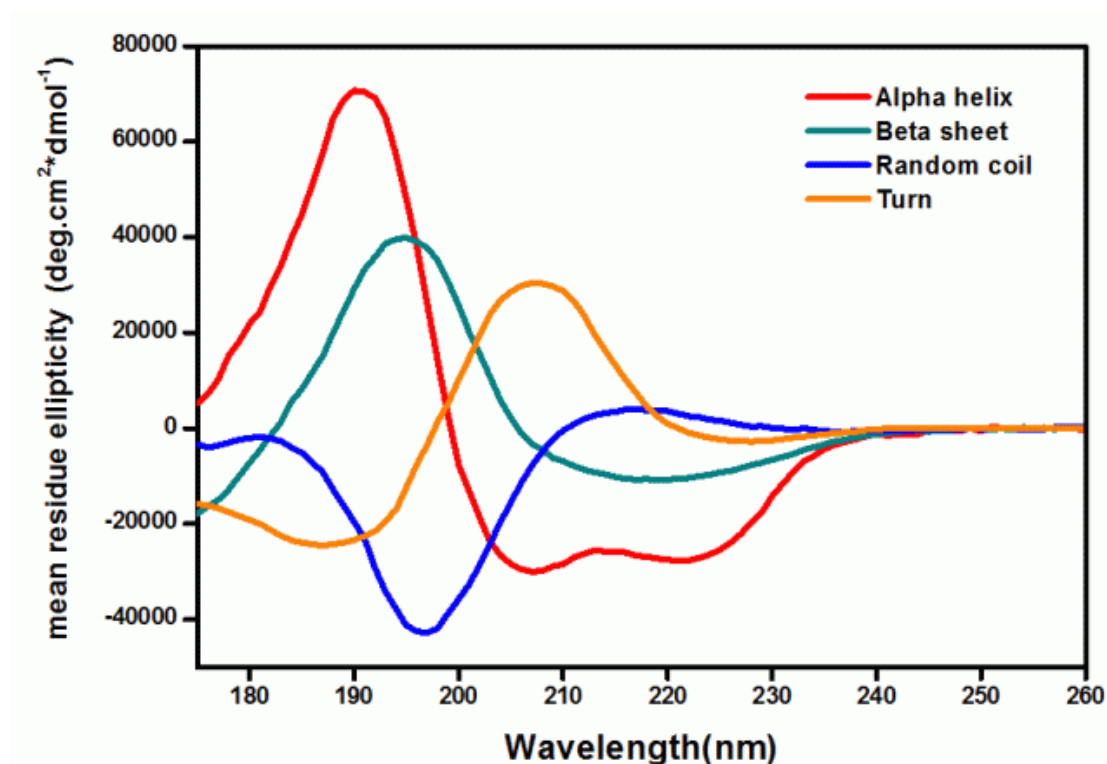
Figure 0.12. Circular dichroism spectra in the far UV range for proteins or peptides having all α-helix, β-sheet, β-turn or random coil conformation.

α-helices present two negative bands at 222nm and 208nm and a positive one at 190nm. β-sheets have two negative bands at 217nm and 180nm and a positive one at 195nm, being all of them less intense and sensible to relative orientations of the pattern. Each particular type of turn has its profile although one example can be found in the image. Random coil (disordered structures) only displays a negative band at 200nm.

Furthermore, in the near ultraviolet, 350-260nm, and visible region, some proteins have a particular CD spectrum due to the π-π* interactions, strongly dependent on the environment of the chromophores, which relates to the tertiary structure of the protein.

Analyzing the CD spectra of proteins can allow structural determination in a fast manner and with few amounts of protein. Thermodynamic and kinetic information can also be obtained when studying the effect of the temperature in the CD changes[156].

Protein-ligand interaction can also be studied, even in a quantitative manner, since the changes in the CD spectra are directly proportional to the amount of complex formed.

Thermal stabilization of the protein complexes by ligand introduction can be determined by monitoring the ellipticity when increasing the temperature.

The blood-brain barrier: challenging brain access

The p53 tummor suppressor gene (TP53) is the most frequently altered gene in human cancer ands it has been found to be mutated in several types of brain tumors[161]. Brain tumors with p53 wild-type and mutated p53 proteins may responde differently to radiotherapy applied. In addition to potential treatment by restoring p53 native functions, tumor genesis, diagnosis and prognosis can also be improved by targeting mutated p53 proteins in the brain. Therefore, strategies to access the brain should be considered in order to reach this target inside the central nervous system (CNS). In this field, gene therapy has been evaluated as a way to perform TP53 gene transfer[161]. A potential alternative is the delivery across the blood-brain barrier (BBB) of drugs targeting p53 mutated proteins.

Drug targeting to the brain has gained many relevance along the years owing to the large number of diseases which affect the CNS such as Alzheimer's and Parkinson's diseases, schizophrenia or epilepsy, among them. In this field, the role of peptides has gained importance, experimenting their golden era. Nevertheless, an existing problem shared by a vast majority of potential drug candidates is their difficulty to cross the blood-brain barrier. This barrier is essential for the normal function of the CNS and limits the influx of most compounds present in extracellular environment to prevent the potential damage of the CNS. This implies that not only toxic substances are impeded to enter but also many therapeutic agents.

This important limitation has emerged as a challenge to efficiently deliver substances inside the brain for therapeutic and diagnostic purposes.

This brain parenchyma protection is organized in three barriers. These are the blood-brain barrier (BBB), which is found in the capillaries; the blood-cerebrospinal fluid barrier (BCSFB), constituted by choroid plexus epithelium; and ependyma, which is placed on the interphase between the cerebrospinal fluid (CSF) and the brain.

The BBB is a physical and enzymatic barrier mainly formed by brain capillary endothelial cells (BCECs). However, other cell types also play some relevant role on regulating permeability of the BBB, like the astrocytes, pericytes and neurons.

Endothelial cells from the BBB differ from the ones in the rest of the body due to the absence of fenestrations, uniform thickness, the presence of the so-called tight junctions (TJs) which are more restrictive intercellular junctions[162], low pinocytotic activity, continues basement membrane and negative surface charge). TJs limit the paracellular flux of hydrophilic molecules across the BBB while small hydrophobic molecules such as O_2 or CO_2 diffuse across plasma membranes along their concentration gradient[163]. Besides this, the existence of efflux transporters and multidrug-resistance proteins present avoid the transcytosis of some compounds.

Drug delivery to the brain: mechanisms of transport

The brain is an energy intensive organ, requiring a high rate of glucose and other essential nutrients. Nevertheless, it is also one of the most protected organs. To reconcile this high energy demand with its exceedingly protective nature, effective transport mechanisms are required. Using one of these transport mechanisms is one of the existing strategies being explored for drug delivery to the brain.

Nutrients such as glucose and amino acids can reach brain via transporters, whereas receptor-mediated transcytosis is responsible for the uptake of larger molecules such as insulin, leptin and iron transferrin[163].

Passage of small molecules through the BBB basically relies on passive diffusion mechanism (free or facilitated) based on the physicochemical properties such as lipophilicity, ionisation and polarity. By changing these properties penetration can be enhanced[164,165,166].

Passive diffusion

Low molecular size molecules with high lipophilicity can penetrate the brain by passive diffusion. Permeability rate of uncharged molecules at the physiological pH is higher than for hydrophilic charged molecules which are distributed within blood unable to

cross the endothelial cells and frequently being excreted from brain parenchyma[167]. There are two mechanisms for passive the diffusion, free or facilitated diffusion.

Free diffusion takes places at downhill concentration gradient. Some compounds like sucrose can move freely paracellularly between cells to a limited extent and in the case of ethanol by transcytosis[168]. This mechanism is non-competitive and non-saturable.

Facilitated diffusion mechanism is a carrier mediated endocytosis which occurs downhill by the binding of the target compound to a specific membrane protein. Conformational changes of the membrane protein are responsible of the crossing of the molecules, typically amino acids, nucleosides, small peptides as glutathione and monocarboxylates[168].

Reaching the CNS: current strategies

Nowadays, there are three different approaches used to attempt the delivery of drug molecules into the brain, invasive, pharmacological and physiological.

Invasive approach

Different techniques such as intracerebro-ventricular infusion, convection-enhanced delivery and polymer or microchip systems are used to deliver drugs by mechanically breaching the BBB[169]. The main inconvenients of these strategies rely on the low diffusion of the drug in the brain parenchyma, the difficulty to saturate some areas of brain such as tissues surrounding a cavity, dependency on the distance of the injection to achieve successful diffusion and their high cost and displeasure of the patients. Furthermore, neurons may be damaged permanently from unwanted substances entering inside the brain.

Pharmacological approach

Molecular size, charge and lipohilicity are key parameter to define the permeability[14]. Some molecules may present relevant activites in front of a CNS target but their lack of

permeability prevents their use as drug candidates. Medicinal chemistry has been focused on improving the pharmacological properties of this kind of substances by reducing the number of polar groups or attaching them to other molecules that can act as a carrier. Pardridge *et al.*[170] reported the use of lipid carriers, which decreases polarity and enhances crossing through the BBB. Sawada *et al.*[171] proved that antioxidants with pyrrolopyrimidines possess higher brain permeability. Apart from the described examples, literature is full of other successful modification carried out to address this approach[172,173,174].

However, required modifications may result in loss of CNS activity.

Physiological approach

Some molecules are recognized by specific receptor or transporters and get into the brain. Mostly, these are essential nutrients for metabolism and survival like glucose or insulin. Modification of the drugs or conjugation to ligands recognized by BBB-expressed receptors can be performed to facilitate transcytosis.

Focusing on peptides which are constituted by amino acids, their similarity with these essential nutrients is considered to be used as a potential successful approach by transporter-mediated delivery.

One of the drawbacks to be considered is the impossibility to modify the native balance of the transport mechanism, as well as, the undesired competition with the natural ligand.

In vitro evaluation of BBB penetration

Evaluation of permeation across the BBB of drug candidates is required to predict the potential of the developed compounds. In vitro evaluation is performed before reaching *in vivo* assays.

Drug permeation across artificial membranes is mainly related to passive diffusion mechanism including paracellular and transcellular permeation. Assessing active transport across the BBB *in vitro* can be performed by different cell-based models

using bovine brain microvessel endothelial cells (BBMEC)[175],[176], porcine brain microvessel endothelial cells (PBMEC)[177,178], rat brain microvascular endothelial cells (RBMEC)[179] and Madin Darby canine kidney cells (MDCK)[180]. All these are cell-based assays requiring cell culture and being time-consuming. Furthermore, both passive and active mechanisms are involved, which impossibilities the use of them to measure passive diffusion exclusively. As an alternative, PAMPA, which stands for Parallel Artificial Membrane Permeability Assay[181] and consists on a 96-well microtiter plate, completely artificial, without pores nor active transporter systems. The filterplate that separes both compartments is coated with phospholipids. Depending on the phospholipid type, this assay can predict oral absorption, human skin permeation and BBB permeation.
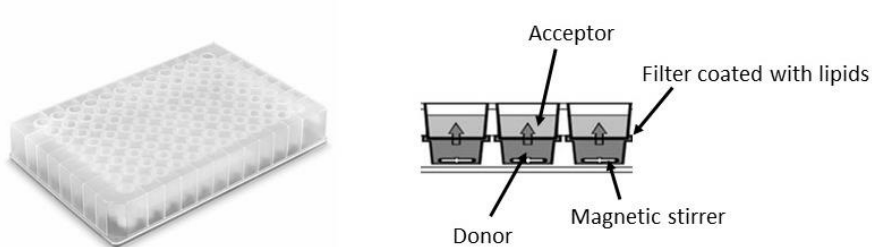
Figure 0.13. PAMPA plaques and explanation of the donor and acceptor compartments with the filter and stirrer required for the assay.

PAMPA technique allows high throuput screening due to its simplicity. The analysis method is generally based on the UV measurement by HPLC. The percentage of transport after 4h of assay and the effective permeability are calculated parameters.

BIBLIOGRAPHY

[1] A. Padhi, M. Sengupta, S. Sengupta, K. H. Roehm, A. Sonawane, Antimicrobials peptides and proteins in mycobacterial therapy: current status and future prospects, *Tuberculosis* **2014**, *94*, 363-373.

[2] H. Buchwald, R. B. Dorman, N. F. Rasmus, V. M. Michalek, N. M. Landvik, S. Ikramuddin, Effects on GLP-1, PYY, and leptin by direct stimulation of terminal ileum and cecum in humans: implications for ileal transposition, *Surgery for obesisty and related diseases* **2014** , *10*, 780-786.

[3] C. Giordano, M. Marchio, E. Timofeeva, G. Biagini, Neuroactive peptides as putative mediators of antiepileptic ketogenic diets, *Frontiers in neurology* **2014**, *5*, 1-14.

[4] S. D. Robinson, H. S. Hemani, L. D. McIntosh, A. W. Purcell, R. S. Norton, Diversity of conotoxin gene superfamilies in the venomous snail, *Conus Victoriae*, *PLOS ONE* **2014,** *9*, e87648.

[5] S. M. Hecht, Bioorganic chemistry: peptides and proteins, *Oxford University Press* **1998**.

[6] J. J. Nestor Jr., The medicinal chemistry of peptides, *Current medicinal chemistry* **2009** *16*, 4399-4418.

[7] R. B. Merrifield, Solid phase peptide synthesis. I. The synthesis of a tetrapeptide, *JACS* **1963**, *85*, 2149-2154.

[8] K. Fosgerau, T. Hoffman, Peptide therapeutics: current status and future directions, *Drug discovery today* **2015**, *20*, 122-128.

[9] R. Lax, The future of peptide development in the pharmaceutical industry, *PharManufacturing: Int. Peptide Rev.* **2013**, 10-15.

[10] A. A. Kaspar, J. M. Reichert, Future directions for peptide therapeutics, *Drug discovery today* **2013**, *18*, 807-817.

[11] T. Uhlig, T. Kyprianou, F. G. Martinelli, C. A. Oppici, D. Heilingers, D. Hills, X. R. Calvo, P. Verhaert, The emergence of peptides in the pharmaceutical business: from exploration to exploitation, *EuPa Open Proteomics* **2014**, *4*, 58-69.

[12] https://globenewswire.com/news-release/2016/09/12/871199/0/en/Peptide-Therapeutics-Market-Increasing-Demand-for-Peptide-Therapeutics-in-Cancer-and-Diabetes-Treatment-to-Boost-Sales-Global-Industry-Analysis-Size-Share-Growth-Trends-and-Forecas.html

[13] D. J. Craik, D. P. Fairlie, S. Liras, D. Price, The future of peptide-based drugs, *Chem Biol Drug Des* **2013**, *81*, 136-147.

[14] C. A. Lipinski, F. Lombardo, B. W. Dominy, P. J. Feeney, Experimental and computational approaches to estimate solubility and permeability in drug discovery and development settings, *Advanced drug delivery reviews* **1997**, *23*, 3-25.

[15] M. M. Madden, A. Muppidi, Z. Li, X. Li, J. Chen, Q. Lin, Synthesis of cell-permeable stapled peptide dual inhibitors of the p53-Mdm2/Mdmx interactions via photoinduced cycloaddition, *Bioorg Med Chem* **2011**, *21*, 1472-1475.

[16] Q. Chu, R. E. Moellering, G. J. Hilinski, Y.-W. Kim, T. N. Grossmann, J. T.-H. Yeh, G. L. Verdine, Towards understanding cell penetration by stapled peptides, *MedChemComm* **2015**, *6*, 111-119.

[17] J. A. Wells, C. L. McClendon, Reaching for high-hanging fruit in drug discovery at protein-protein interfaces, *Nature* **2007**, *450*, 1001-1009.

[18] A. P. Higueruelo, H. Jubb, T. L. Blundell, Protein-protein interactions as druggable targets: recent technological advances, *Curr. Opin. Pharmacol.* **2013**, *13*, 791-796.

[19] M. Pelay-Gimeno, A. Glas, O. Koch, T. M. Grossmann, Structure-based desing of inhibitors of protein-protein interactions: mimicking peptide binding epitopes, *Angewandte Reviews* **2015**, *54*, 8896-8927.

[20] K. –C. Chou, Prediction of tight turns and their type in proteins, *Anal Biochem.* **2000**, *286*, 1-16.

[21] E. G. Hutchinson, J. M. Thornton, A revised set of potentials for beta-turn formations in proteins, *Protein Science* **1994**, *3*, 2207-2216.

[22] C. Schellman, Protein Folding (Ed.: R. Jaenicke), Elsevier/North-Holland, New York, 1980, pp. 53 – 61.

[23] F. Siedler, D. Quarzago, S. Rudolph-Böhner, L. Moroder, Redox-active bis-cisteinyl peptides. II. Comparative study on the sequence-dependent tendency for disulfide loop formation, *Biopolymers* **1994**, *34*, 1563-1572.

[24] L. Feliu, M. Planas, Cyclic peptides containing biaryl and biaryl ether linkages, *Int. J. Pept. Res. Ther.* **2005**, *11*, 53-97.

[25] C. J. White, A. K. Yudin, Contemporary strategies for peptide macrocyclization, *Nature chemistry* **2011**, *3*, 509-524.

[26] R. Katahira, M. Yamasaki, Y. Matsuda, M. Yoshida, MS-271: a novel inhibitor of calmodulin-activated myosin light chain kinase from *Streptomyces* sp.-II. Solution structure of MS-271: characteristic features of the "lasso" structure, *Bioorganic & Medicinal chemistry* **1996**, *4*, 121.129.

[27] S. Chen, R. Gopalakrishnan, T. Schaer, F. Marger, R.Hovius, D. Bertrand, F. Pojer, C. Heinis, Dithiol amino acids can structurally shape and enhance the ligand-binding properties of polypeptides, *Nature chemistry* **2014**, *6*, 1009-1016.

[28] C. Heinis, T. Rutherford, S. Freund, G. Winter, Phage-encoded combinatorial chemical libraries based on bicyclic peptides, *Nature chemical biology* **2005**, *5*, 502-507.

[29] P. Y. Chou, G. D. Fasman, β-turns in proteins, *Journal of molecular biology* **1977**, *115*, 135-175.

[30] Y. S. Chang, B. Graves, V. Guerlavais, C. Tovar, K. Packman, K. Him, K. A. Olson, K. Kesavan, P. Gangurde, A. Mukherjee, T. Baker, K. Darlak, C. Elkin, Z. Filipovic, F. Z. Qureshi, H. Cai, P. Berry, E. Feyfant, X. E. Shi, D. A. Annis, A. M. Manning, N. Fotouhi, H. Nash, L. T. Vassilev, T. K. Sawyer, Stapled α-helical peptide drug development: A potent dual inhibitor of MDM2 and MDMX for p53-dependent cancer therapy, *PNAS*, **2013**, *110*, E3445.

[31] G. L. Verdine, G. J. Hilinski, All hydrocarbon stapled peptides as synthetic cell-accessible mini-proteins, *Drug discovery today: technologies*, **2012**, *9*, e41.

[32] L. Pauling, R. B. Corey, H. R. Branson, The structure of proteins; two hydrogen-bonded helical configurations of the polypeptide chain *Prot. Nat. Acad. Sci. USA* **1951**, *37*, 205-211.

[33] A. Jochim, P. S. Arora, Assessment of helical interfaces in protein-protein interactions, *Mol. Biosyst.* **2009**, *5*, 924-926.

[34] L. D. Walensky, G. H. Bird, Hydrocarbon-stapled peptides: principles, practice and progress, *Journal of medicinal chemistry* **2013**, *57*, 6275-6288.

[35] L. K. Henchey, A. L. Jochim, P. S. Arora, Contemporary strategies for the stabilization of peptides in the alpha-helical conformation, *Curr. Opin. Chem. Biol.* **2008**, *12*, 692-697.

[36] J. A. Robinson, β-hairpin peptidomimetics : design, structures and biological activities, *Acc. Chem. Res.* **2008**, *41*, 1278-1288.

[37] M. Bartoloni, X. Jin, M. J. Marcaida, J. Banha, I. Dibonaventura, S. Bongoni, K. Bartho, O. Gräbner, M. Sekflow, T. Darbre, J. –L. Reymond, Bridged bicyclic peptides as potential drug scaffolds: synthesis, structure, protein binding and stability, *Chem. Sci.* **2015**, *6*, 5473-5490.

[38] J. S. Davies, The cyclization of peptides and depsipeptides, *Journal of peptide science* **2003**, *9*, 471-501.

[39] C. T. Wong, H. Y. Lam, T. Song, G. Chen, X. Li, Realizing serine/threonine ligation: scope and limitations and mechanistic implication thereof, *Angewandte Chemie Int. Ed.* **2013**, *52*, 10212-10215.

[40] A. Tavassoli, Q. Lu, J. Gam, H. Pan, S. J. Benkovic, S. N. Cohen, Inhibition of HIV budding by a genetically selected cyclic peptide targeting the gag-TSG101 interaction, *ACS Chem. Biol.* **2008**, *3*, 757-764.

[41] A. M. Felix, E. P. Heimer, C. T. Wang, T. J. Lambros, A. Fournier, T. F. Mowles, S. Maines, R. M. Campbell, B. B. Wegrzynski, V. Toome, D. Fry, V. S. Madison, Synthesis, biological activity and conformational analysis of cyclic GRF analogs, *Int. J. Pep. Protein Res.* **1988**, *32*, 441-454.

[42] T. Rezai, J. E. Bock, M. V. Zhou, C. Kalyanaraman, R. S. Lokey, M. P. Jacobson, Conformational flexibility, internal hydrogen bonding, and passive membrane permeability: successful in silico prediction of the relatives permeabilities of cyclic peptides, *J. Am. Chem. Soc.* **2006**, *128*, 14073-14080.

[43] J. Chatterjee, C. Gilon, A. Hoffmann, H. Kessler, *N*-methylation of peptides: a new perspective in medicinal chemistry, *Acc. Chem. Res.* **2008**, *41*, 1331-1342.

[44] W. Lian, B. Jiang, Z. Qian, D. Pei, Cell-permeable bicyclic peptide inhibitors agains intracellular proteins, *J. Am. Chem. Soc.* **2014**, *136*, 9830-9833.

[45] G. P. Smith, Filamentous fusion phage: novel expression vectors that display cloned antigens on the virion surface, *Science* **1985**, *228*, 1315-1317.

[46] I. R. Rebollo, C. Heinis, Phage selection of bicyclic peptides, *Methods* **2013**, *60*, 46-54.

[47] L. Nevola, E. Giralt, *Modulating* protein-protein interactions: the potential of peptides, *ChemComm* **2015**, *51*, 3302-3315.

[48] J. B. Blanco-Canosa, B . Nardone, F. Albericio, P. E. Dawson, Chemical protein synthesis using a second-generation *N*-acylurea linker for the preparation of peptide-thioester precursors, *J. Am. Chem. Soc* **2015**, *137*, 7197-7209.

[49] L. Nevola, A. Martín-Quirós, K. Eckelt, N. Camarero, S. Tosi, A. Llobet, E. Giralt, P. Gorostiza, Light-regulated stapled peptides to inhibit protein-protein interactions involved in clathrin-mediated endocytosis, *Angewandte Chemie* **2013**, *52*, 7704-7708.

[50] P. Lloyd-Williams and E. Giralt, Atropisomerism, biphenyls and the Suzuki coupling: peptide antibiotics, *Chem. Soc. Rev.* **2001**, *30*, 145-147.

[51] S. Jackson, W. DeGraco, A. Dwivedi, A. Parthasarathy, A. Higley, J. Krywko, A. Rockwell, J. Markwalder, G. Wells, R. Wexler, S. Mousa, R. Harlow, Template-constrained cyclic peptides: design of high-affinity ligands for GPIIb/IIIa, *J. Am. Chem. Soc.* **1994**, *116*, 3220-3230.

[52] L. Alig, A. Edenhofer, P. Hadváry, M. Hürzeler, D. Knoop, M. Müller, B. Steiner, A. Trzeciak, T. Weller, Low molecular weight, non-peptide fibrinogen receptor antagonists, *J. Med. Chem.* **1992**, *35*, 4393-4407.

[53] A. Afonso, C. Rosés, M. Planas, L. Feliu, Biaryl peptides from 4-iodophenylalanine by solid-phase borylation and Suzuki-Miyaura cross-coupling, *Eur. J. Org. Chem* **2010**, 1461-1468.

[54] M. J. Rodriguez, N. J. Snyder, M. J. Zweifel, S. C. Wilkie, D. R. Stack, R. D. Cooper, T. I. Nicas, D. L. Mullen, T. F. Butler, R. C. Thompson, Novel glycopeptide antibiotics: *N*-alkyl derivatives active against vancomycin-resistant enterococci, *J. Antibiot. (Tokio)* **1998**, *51*, 560-569.

[55] N. Miyaura, A. Suzuki, Palladium-catalyzed cross-coupling reactions of organoboron compounds, *Chem. Rev.* **1995**, *95*, 2457-2483.

[56] J. K. Stille, The palladium-catalyzed cross-coupling reactions of organotic reagents with organic electrophiles, *Angewandte Chemie* **1986**, *26*, 508-524.

[57] B. E. Haug, W. Stensen, J. S. Svendsen, Application of the Suzuki-Miyaura cross-coupling to increase antimicrobial potency generates promising novel antibacterials, *Bioorg. Med. Chem. Lett.* **2007**, *17*, 2361-2364.

[58] A. Afonso, L. Feliu, M. Planas, Solid-phase synthesis of biaryl cyclic peptides by borylation and microwave-assisted intramolecular Suzuki-Miyaura reaction, *Tetrahedron* **2011**, *67*, 2238.

[59] V. Cerezo, M. Amblard, J. Martinez, P. Verdié, M. Planas, L. Feliu, Solid-phase synthesis of 5-arylhistidines via a microwave-assisted Suzuki-Miyaura cross-coupling, *Tetrahedron* **2008**, *64*, 10538-10545.

[60] A. Afonso, O. Cussó, L. Feliu, M. Planas, Solid-phase synthesis of biaryl cyclic peptides containing a 3-aryltyrosine, *EuroJOC* **2012**, *31*, 6204-6211.

[61] F. Alonso, I. P. Beletskaya, M. Yus, Non-conventional methodologies for transition metal-catalysed carbon-carbon coupling: a critical overwiev. Part 2: the Suzuki reaction, *Tetrahedron* **2008**, *64*, 3047-3101.

[62] K. Sonogashira, Y. Todha, N. Hagihara, A convenient synthesis of acetylenes: catalytic substitutions of acetylenic hydrogen with bromoalkenes, iodoarenes and bromopyridines, *Tetrahedron Letters* **1975**, *16*, 4467-4470.

[63] A. B. Dyatkin, R. A. Rivero, The solid phase synthesis of complex propargylamines using the combination of sonogashira and mannich reactions, *Tetrahedron Letters* **1998**, *39*, 3647-3650.

[64] M. Ederléyi, A. Gogoll, Rapid microwave promoted Sonogashira coupling reactions of solid phase, *J. Org. Chem* **2033**, *68*, 6431-6434.

[65] G. P. Moss, Basic terminology of stereochemistr *Pure Appl. Chem.* **1996**, *68*, 2193-2222.

[66] R. Adams, H. C. Yuan, The stereochemistry of diphenyls and analogous compounds, *Chem Rev.* **1933**, *12*, 261-338.

[67] O. Bastiansen, S. Samdal, Structure and barrier of internal rotation of biphenyl derivatives in the gaseous state: Part4.Barrier of internal rotation in biphenyl, perdeuterated biphenyl and seven non-*ortho*-subtituted halogen derivatives, *J. Mol. Struct.* **1985**, *128*, 115-125.

[68] M. Mazik, A. König, Recognition properties of an acyclic biphenyl-based receptor towards carbohydrates, *J. Org. Chem.* **2006**, *71*, 7854-7857.

[69] E. Klein, M. P. Crump, A. P. Davis, Carbohydrate recognition in water by a tricyclic polyamide receptor, *Angewandte Chemie* **2005**, *44*, 298-302.

[70] Y. Ferrand, M. P. Crump, A. P. Davis, A synthetic lectin analog for biomimetic disaccharide recognition, *Science*, **2007**, *318*, 619-622.

[71] S. Paul, J. H. Clark, A higly active and reusable heterogeneous catalyst for the Suzuki reaction: synthesis of biayrls and polyaryls, *Green chemistry* **2003**, *5*, 635-638.

[72] N. L. Segraves, P. Crews, Investigation of brominated tryptophan alkaloids from two thorectidae sponges: *Thorectandra* and *Smenospongia*, *J. Nat. Prod.* **2005**, *68*, 1484-1488.

[73] F. N. R. Petersen, M. O. Jensen, C. H. Nielsen, Interafacial tryptophan residues: a role for the cation-π effect?, *Biophysical Journal* **2005**, *89*, 3985-3996.

[74] M. Schiffer, C. –H. Chang, F. J. Stevens, The functions of tryptophan residues in membrane proteins, *Protein Eng.* **1992**, *5*, 213-214.

[75] W. –M. Yau, W. C. Wimley, K. Gawrish, S. H. White, The preference of tryptophan for membrane interfaces, *Biochemistry* **1998**, *37*, 14713-14718.

[76] H. C. Gaede, W. –M. Yau, K. Gawrish, Electrostatic contributions to indole-lipid interactions, *J. Phys. Chem.* **2005**, *109*, 13014-13023.

[77] S. Mecozzi, A. P. West, Jr., D. A. Dougherty, Cation-π interactions in aromatics and biological and medicinal interest: electrostatic potential surfaces as a useful qualitative guide, *Proc. Natl. Acad. Sci. USA* **1996**, *93*, 10566-10571.

[78] J. C. Ma, D. A. Dougherty, The cation-pi interaction, *Chem. Rev.* **1997**, *97*, 1303-1324.

[79] U. D. Priyakumar, M. Punnagai, G. P. K. Mohan, G. N. Sastry, A computational study of cation-π interactions in polycyclic systems: exploring the dependence of the curvature and electronic factors, *Tetrahedron* **2004**, *60*, 3037-3043.

[80] D. A. Dougherty, Cation-π interactions in chemistry and biology: a new view of benzene, Phe, Tyr, and Trp, *Science* **1996**, *271*, 163-168.

[81] M. M. Gromiha, Distinct roles of conventional non-covalent and cation-π interactions in protein stability, *Polymer* **2005**, *46*, 983-990.

[82] B. Yang, J. Wright, M. E. Eldefrawi, S. Pou, A. D. MacKerell Jr., Conformational, aqueous solvation, and pKa contributions to the binding and activity of cocaine, WIN 35 065-2, and the WIN vinyl analog, *J. Am. Chem. Soc.* **1994**, *116*, 8722-8732.

[83] M. P. Aliste, J. L. MacCallum, D. P. Tieleman, Molecular dynamic simulations of pentapeptides at interfaces: salt bridge and cation-π interactions, *Biochemistry* **2003**, *42*, 8976-8987.

[84] D. A. Dougherty, Cation-pi interactions involving aromatic amino acids, *J. Nutr.* **2007**, *137*, 1504-1517.

[85] G. J. Boks, J. P. Tollenaere, J. Kroon, Possible ligand-receptor interactions for NK1 antagonists as observed in their crystal structures , *Bioorg. Med. Chem.* **1997**, *5*, 535-547.

[86] S. C. R. Lummis, I. McGonigle, J. A. Ashby, D. A. Dougherty, Two amino acid residues contribute to a cation-π binding interaction in the binding site of an insect GABA receptor, *J. Neurosci.* **2011**, *31¸* 12371-12376.

[87] E. Cubero, F. J. Luque, M. Orozco, Is polarization important in the catión-π interactions?, *Proc. Natl. Acad. Sci. USA* **1998**, *95*, 5976-5980.

[88] H. Zhang, C. Li, F. Yang, J. Su, J. Tan, X. Zhang, C. Wang, Cation-π interactions at non-redundant protein-RNA interfaces, *Biochemistry* **2014,** *79*, 643-652.

[89] E. M. Driggers, S. P. Hale, J. Lee, N. K. Terrett, The exploration of macrocycles for drug discovery-an underexploited structural class, *Nature Rev. Drug Disc.* **2008**, *7*, 608-624.

[90] U. Schmidt, J. Langner, Cyclotetrapeptides and cyclopentapeptides: occurrence and synthesis, *J. Pep. Res.* **1997**, *49*, 67-73.

[91] J. M. Humphrey, A. R. Chamberlin, Chemical synthesis of natural products peptides: coupling methods for incorporation of noncoded amino acids into peptides, *Chem. Rev.* **1997**, *97*, 2243-2266.

[92] C. A. G. N. Montalbetti, V. Falque, Amide bond formation and peptide coupling, *Tetrahedron* **2005**, *61*, 10827-10852.

[93] A. Parenty, X. Moreau and J. –M. Campagne, Macrolactonizations in the total synthesis of natural products, *Chem. Rev.* **2006**, *106*, 911-939.

[94] L. T. Scott, J. Rebek, L. Ovsyanko, C. Sims, Organic chemistry on the solid phase. Site-site interactions of functionalized polysterene, *J. Am. Chem. Soc.* **1977**, *99*, 626-627.

[95] J. Blankenstein, J. Zhu, Conformation-directed macrocyclization reactions, *Eur. J. Org. Chem.* **2005**, 1949-1964.

[96] F. Cavelier-Frontin, G. Pèpe, J. Verducci, D. Siri, R. Jacquier, Prediction of the best linear precursor in the synthesis of cyclotetrapeptides by molecular mechanic calculations, *J. Am. Chem. Soc.* **1992**, *114*, 8885-8890.

[97] J. Smith, L. G. Pease, Reverse turns in peptides and proteins, *CRC Crit. Rev. Biochem.* **1980**, *8*, 315-399.

[98] H. Kessler, B. Haase, Cyclic hexapeptides derived from the human thympoietin II, *Int J. Peptide Protein Res.* **1992**, *39*, 36-40.

[99] Y. Takeuchi, G. R. Marshall, Conformation analysis of reverse-turns constraints by *N*-methylation and *N*-hydroxylation of amide bonds in peptides and non-peptide mimetics, *J. Am. Chem. Soc.* **1998**, *120*, 5363-5372.

[100] T. Wöhr, F. Wahl, A. Nefzi, B. Rohwedder, T. Sato, X. Sun, M. Mutter, Pseudo-prolines as a solubilizing, structure-disrupting protection technique in peptide synthesis, *J. Am. Chem. Soc.* **1996**, *118*, 9218-9227.

[101] P. Dumy, M. Keller, D. E. Ryan, B. Rohwedder, T. Wöhr, M. Mutter, Pseudo-prolines as a molecular hinge: reversible induction of *cis* amide bonds into peptide backbones, *J. Am. Chem. Soc.* **1997**, *119*, 918-925.

[102] L. Zhang, J. P. Tam, Synthesis and application of unprotected cyclic peptides as building blocks for peptide dendrimers, *J. Am. Chem. Soc.* **1997**, *119*, 2363-2370.

[103] R. M. Kohli, C. T. Walsh, M. D. Burkart, Biomimetic synthesis and optimization of cyclic peptide antibiotics, *Nature* **2002**, *418*, 658-661.

[104] E. A. Felnagle, E. E. Jackson, Y. A. Chan, A. M. Podevels, A. D. Berti, M. D. McMahon, M. G. Thomas, Nonribosomal peptide synthetases involved in the production of medically relevant natural products, *Mol. Pharm.* **2008**, *5*, 191-211.

[105] K. Haas, W. Ponikwar, H. Nöth, W. Beck, Facile synthesis of cyclic tetrapeptides from nonactivated peptide esters on metal centers, *Angewandte Chemie* **1998**, *37*, 1086-1089.

[106] Y. Li, A. Yongye, M. Giulianotti, K. Martinez-Mayorga, Y. Yu, R. A. Houghten, Synthesis of cyclic peptides through direct aminolysis of peptide tioesters catalyzed by imidazole in aqueous organic solutions, *J. Comb. Chem.* **2009**, *11*, 1066-1072.

[107] A. A. Aimetti, R. K. Shoemaker, C. –C. Lin, K. S. Anseth, On-resin peptide macrocyclization using thiol-ene click chemistry, *Chem. Commun.* **2010**, *46*, 4061-4063.

[108] P. E. Dawson, T. W. Muir, I. Clark-Lewis, S. B. H. Kent, Synthesis of proteins by native chemical ligation, *Science* **1994**, *266*, 776-779.

[109] J. Tulla-Puche, G. Barany, On-resin native chemical ligation for cyclic peptide synthesis, *J. Org. Chem.* **2004**, *69*, 4101-4107.

[110] Y. Shao, W. Lu, S. B. H. Kent, A novel method to synthesize cyclic peptides, *Tetrahedron Letters* **1998**, *39*, 3911-3914.

[111] L. Z. Yan, P. E. Dawson, Synthesis of peptides and proteins without cystein residues by native chemical ligation combined with desulfuration, *J. Am. Chem. Soc.* **2001**, *123*, 526-533.

[112] R. Kleineweischede, C. P. R. Hackenberger, Chemoselective peptide cyclization by traceless ligation, *Angewandte Chemie* **2008**, *47*, 5984-5988.

[113] C. Hyde, T. Johnson, D. Owell, M. Quibell, R. C. Sheppard, Some "difficult sequences" made easy, *Int. J. Peptide Protein Res.* **1994**, *43*, 431-440.

[114] H. Bieräugel, H. E. Schoemaker, H. Hiemstra, J. H. van Maarseveen, A pincer auxiliary to force difficult lactamisations, *Org. Biomol. Chem.* **2003**, *1*, 1830-1832.

[115] J. Springer, T. P. Jansen, S. Ingemann, H. Hiemstra, J. H. van Maarseveen, Improved auxiliary to the synthesis of medium-sized bis(lactams), *Eur. J. Org. Chem.* **2008**, 361-367.

[116] V. D. Bock, R. Perciaccante, T. P. Jansen, H. Hiemstra, J. H. van Maarseveen, Click chemistry as a route to cyclic tetrapeptide analogues: synthesis of *cyclo*-[Pro-Val-ψ(triazole)-Pro-Tyr], *Org. Lett.* **2006**, *8*, 919-922.

[117] R. A. Turner, A. G. Oliver, R. S. Lokey, Click chemistry as a macrocyclization tool in the solid-phase synthesis of small cyclic peptides, *Org. Lett.* **2007**, *9*, 5011-5014.

[118] J. S. Miller, H. E. Blackwell, R. H. Grubbs, Application of ring-closing metathesis to the synthesis of rigidified amino acids and peptides, *J. Am. Chem. Soc.* **1996**, *118*, 9606-9614.

[119] O. E. Vercillo, C. K. Z. Andrade, L. A. Wessjohan, Design and synthesis of cyclic RGD pentapeptoids by consecutive Ugi reactions, *Org. Lett.* **2008**, *10*, 205-208.

[120] R. Hili, V. Rai, A. K. Yudi, Macrocyclization of linear peptides enabled by amphoteric molecules, *J. Am. Chem. Soc.* **2010**, *132*, 2889-2891.

[121] A. J. Levine, p53, the celular gatekeeper for growth and division, *Cell* **1997**, *88*, 323-331.

[122] D. P. Lane, Cancer. p53, guardian of the genome, *Nature* **1992**, *358*, 15-16.

[123] C. Prives, P. A. Hall, The p53 pathway, *J. Pathol.* **1999**, *187*, 112-126.

[124] A. J. Levine, W. Hu, Z. Feng, The p53 pathway: what questions remain to be explored?, *Cell Death Differ.* **2006**, *13*, 1027-1036.

[125] H. Tidow, R. Melero, E. Mylonas, S. M. V. Freund, J. G. Grossmann, J. M. Carazo, D. I. Svergun, M. Valle, A. R. Fehrst, Quaternary structures of tumor suppressor p53 and a specific p53 DNA complex, *Proc. Natl. Acad. Sci. USA* **2007**, *104*, 12324-12329.

[126] P. Wang, M. Reed, Y. Wang, G. Mayr, J. E. Stenger, M. E. Anderson, J. F. Schwedes, P. Tegtmeyer, p53 domains: structure, oligomerization, and transformation, *Mol. Cell. Biol.* **1994**, *14*, 5182-5191.

[127] M. Bista, S. M. Freund, A. R. Fehrst, Domain-domain interactions in full-length p53 and a specific DNA complex probed by methyl NMR spectroscopy, *Proc. Natl. Acad. Sci. USA* **2012**, *109*, 15752-15756.

[128] E. S. Stavridi, Y. Huyen, E. A. Sheston, T. D. Halazonetis, Chapter 2. The three-dimensional structure of p53, *The p53 tumor suppressor pathway and cancer,* edited by Zambetti, New York, **2005**.

[129] W. Lee, T. S. Harvey, Y. Yin, P. Yau, D. Litchfield, C. H. Arrowsmith, Solution structure of the tetrameric minimum transforming domain of p53, *Nat. Struc. Biol.* **1994, *1*, 877-890.**

[130] A. J. Levine, J. Momand, C. A. Finlay, The p53 tumor supresor gene, *Nature* **1991**, *351*, 453-456.

[131] M. S. Grenblatt, W. P. Bennett, M. Hollstein, C. C. Harris, Mutations in the p53 tumor suppressor gene: clues to cancer etiology and molecular pathogenesis, *Cancer Res.* **1994**, *54*, 4855-4878.

[132] A. Petitjean, E. Mathe, S. Kato, C. Ishioka, S. V. Tagtigian P. Hainaut, M. Olivier, Impact of mutant p53 functional properties on TP53 mutation patterns and tumor phenotype: lessons from recent developments in the IARC TP53 database, *Hum. Mutat.* **2007**, *28*, 622-629.

[133] C. Asker, K. G. Wiman, G. Selivanova, p53-induced apoptosis as a safeguard against cancer, *Biochem. Biphys. Res. Commun.* **1999**, *265*, 1-6.

[134] A. Sigal, V. Rotter, Oncogenic mutations of the p53 tumor suppressor: the demons of the guardian of the genome, *Cancer Res.* **2000**, *60*, 6788-6793.

[135] S. M. Picksley, J. F. Spicer, D. M. Barnes, D. P. Lane, The p53-MDM2 interaction in a cancer-prone family, and the identification of a novel therapeutic agent, *Acta Oncol.* **1996**, *35*, 429-434.

[136] D. I. Zheleva, D. P. Lane, P. M. Fischer, The p53-Mdm2 pathway: targets for the development of new anticancer therapeutics, *Mini. Rev. Med. Chem.* **2003**, *3*, 257-270.

[137] B. A. Foster, H. A. Coffey, M. J. Morin, F. Rastinejad, Pharmacological rescue of mutant p53 conformation and function, *Science* **1999**, *286*, 2507-2510.

[138] D. Maurici, P. Monti, P. Campomenosi, S. North, T. Frebourg, G. Fronza, P. Hainaut, Amifostine (WR2721) restores transcriptional activity of specific p53 mutant proteins in yeast functional assay, *Onocogene* **2001**, *20*, 3533-3540.

[139] N. Issaeva, A. Friedler, P. Bozko, K. G. Wiman, A. R. Fehrst, G. Selivanova, Rescue of mutants of the tumor suppressor p53 in cancer cells by a designed peptide, *Proc. Natl. Acad. Sci. USA* **2003**, *100*, 13303-13307.

[140] R. Zutshi, M. Brickner, J. Chmielewski, Inhibiting the assembly of protein-protein interfaces. *Curr. Opin. Chem. Biol.* **1998**, *2*, 62-66.

[141] A. G. Cochran, Protein-protein interfaces: mimics and inhibitors, *Curr. Opin. Chem. Biol.* **2001**, *5*, 654-659.

[142] K. V. Kishan, Structural biology, protein conformations and drug designing, *Cuur. Protein Peptide Sci.* **2007**, *8*, 376-380.

[143] D. C. Fry, L. T. Vassilev, Targeting protein-protein interactions for cancer therapy, *J. Mol. Med.* **2005**, *83*, 955-963.

[144] P. Block, N. Weskamp, A. Wolf, G. Klebe, Strategies to search and design stabilizers of protein-protein interactions: a feasibility study, *Proteins* **2007**, *68*, 170-186.

[145] M. R. Arkin, J. A. Wells, Small-molecule inhibitors of protein-protein interactions: progressing towards the dream, *Nat. Rev. Drug. Discov.* **2004**, *3*, 301-317.

[146] R. C. Ribeiro, F. Sandrini, B. Figueiredo, G. P. Zambetti, E. Michalkiewicz, A. R. Lafferty, L. DeLacerda, M. Rabin, C. Cadwell, G. Sampaio, I. Cat, C. A. Stratakis, R. Sandrini, An inherited p53-mutation that contributes in a tissue-specific manner to pediatric adrenal cortical carcinoma, *Proc. Natl. Acad. Sci. USA* **2001**, *98*, 9330-9335.

[147] M. G. Mateu, A. R. Fehrst, Nine hydrophobic side chains are key determinants of the thermodynamic stability and oligomerization status of tumour suppressor p53 tetramerization domain, *EMBO J.* **1998**, *17*, 2748-2758.

[148] E. L. DiGiammarino, A. S. Lee, C. Cadwell, W. Zhang, B. Bothner, R. S. Ribeiro, G. Zambetti, R. W. Kriwacki, A novel mechanism of tumorigenesis involving pH-depedent destabilization of a mutant p53 tetramer, *Nat. Struc. Biol.* **2002**, *9*, 12-16.

[149] W. G. Cole, Collagen genes: mutations affecting collagen structure and expression, *Prog. Nucleic Acid Res. Mol. Biol.* **1994**, *47*, 29-80.

[150] Z. Huang, The chemical biology of apoptosis. Exploring protein-protein interactions and the life and death of cells with small molecules, *Chem. Biol.* **2002**, *9*, 1059-1072.

[151] H. J. Dyson, P. R. Wright, Intrinsically unstructured proteins and their functions, *Nat. Rev. Mol. Cell Biol.* **2005**, *6*, 197-208.

[152] Z. Huang, Structural chemistry and therapeutic intervention of protein-protein interactions in immune response, human immunodeficiency virus entry, and apoptosis, *Pharmacol. Ther.* **2000**, *86*, 201-215.

[153] P. E. Wright, H. J. Dyson, Intrinsically unstructured proteins: re-asessing the protein structure-function paradigm, *J. Mol. Biol.* **1999**, *293*, 321-331.

[154] R. Perez-Monfort, M. T. Gomez-Puyou, A. Gomez-Puyou, The interfaces of oligomeric proteins as targets for drug design against enzymes from parasites, *Curr. Top. Med. Chem.* **2002**, *2*, 457-470.

[155] W. Dall'Acqua, P. Carter, Antibody engineering, *Curr. Opin. Struct. Biol.* **1998**, *8*, 443-450.

[156] S. Gordo, V. Martos, E. Santos, M. Menéndez, C. Bo, E. Giralt, J. de Mendoza, Stability and structural recovery of the tetramerization domain of p53-R337H mutant induced by a design templating ligand, *Proc. Natl. Acad. Sci. USA* **2008**, *105*, 16426-16431.

[157] A. C. Braisted, J. A. Wells, Minimizing a binding domain from protein A, *Proc. Natl. Acad. Sci. USA* **1996**, *93*, 5688-5692.

[158] W. Cooper, M. L. Waters, Molecular recognition with designed peptides and proteins, *Curr. Opin. Chem. Biol.* **2005**, *9*, 627-631.

[159] L. O. Sillerud, R. S. Larson, Design and structure of peptide and peptidomimetic antagonists of protein-protein interaction, *Curr. Protein Peptide Sci.* **2005**, *6,* 151-169.

[160] J. F. Amara, T. Clackson, V. M. Rivera, T. Guo, T. Keenan, S. Natesan, R. Pollock, W. Yang, N. L. Courage, D. A. Holt, M. Gilman, A versatile dimerizer for the regulation of protein-protein interactions, *Proc. Natl. Acad. Sci. USA* **1997**, *94*, 10618-10623.

[161] G. Fulci, N. Ishii, E. G. Van Meir, p53 and brain tumours: from gene mutations to gene therapy, *Brain Pathology* **1998**, *8*, 599-613.

[162] F. L. Cardoso, D. Brites, M. A. Brito, Looking at the blood-brain barrier: molecular anatomy and possible investigation approaches, *Brain Res. Rev.* **2010**, *64*, 328-363.

[163] P. Ballabh, A. Braun, M. Nedergaard, The blood-brain barrier: an overwiev structure, regulation and clinical implications, *Neurobiology of Disease* **2004**, *16*, 1-13.

[164] A.G. de Boer, P. J. Gaillard, Drug targeting to the brain, *Annu. Rev. Pharmacol. Toxicol.* **2007**, *47*, 323-355.

[165] K. A. Witt, T. J. Gillespie, J. D. Huber, R. D. Egleton, T. P. Davis, Peptide drug modifications to enhance bioavailability and blood-brain barrier permeability, *Peptides* **2001**, *22*, 2329.

[166] R. D. Egleton, T. P. Davis, Bioavailability and transport of peptides and peptide drugs into the brain, *Peptides* **1997**, *18*, 1431.

[167] M. S. Alavijeh, M. Chishty, M. Z. Qaiser, A. M. Palmer, Drug metabolism and pharmacokinetics, the blood-brain barrier and central nervous system drug discovery, *Neurotherapeutics* **2005**, *2*, 554.

[168] M. I. Alam, S. Beg, A. Samad, S. Baboota, K. Kohli, J. Ali, a. Ahuja, M. Akbar, Strategy for effective drug delivery, *Eur. J. Pharm. Sci.* **2010**, *5*, 385-403.

[169] R. Gabathuler, Approaches to transport therapeutic drugs across the blood-brain barrier to treat brain diseases, *Neurobiology of Disease* **2010**, *37*, 48-57.

[170] W. M. Pardridge, Drug transport across the blood-brain barrier, *J. Cereb. Blood Flow Metab.* **2013**, *32*, 1959-1972.

[171] G. A. Sawada, L. R. Williams, B. S. Lutzke, T. J. Raub, Novel, higly lipophilic antioxidants readily diffuse across the blood-brain barrier and access intracellular sites, *J. Phamarcol. Exp. Ther.* **1999**, *288,* 1327-1333.

[172] N. Bodor, M. E. Brewster, Problems of delivery of drugs to the brain, *Pharmacology&Therapeutics* **1982**, *19*, 337-386.

[173] J. Temsamani, J. M. Scherrmann, A. R. Rees, M. Kaczorek, Brain drug delivery technologies: Novel approaches for transporting therapeutics, *Pharm. Sci. Technol. Today,* **2000**, *3*, 155.

[174] M. Teixidó, E. Zurita, M. Malakoutikhah, E. Giralt, Diketopiperazines as a tool for the study of transport across the blood-brain barrier (BBB) and their potential use as BBB-shuttles, *J. Am. Chem. Soc.* **2007**, *129*, 11802-11813.

[175] P. A. Sieber, A new acid-labile anchor group for the solid-phase synthesis of *C*-terminal peptide amides by the Fmoc method, *Tetrahedron Lett.* **1987**, *28*, 2107-2110.

[176] L. Di, E. H. Kerns, I. Bezar, S. L. Petuski, Y. Huang, Comparison of blood-brain barrier permeability assays: *in situ* brain perfusion, MDR1-MDCKII and PAMPA-BBB, *J. Pharm. Sci.* **2009**, *98*, 1980-1991.

[177] K. W. Otis, M. L. Avery, S. M. Broward-Partin, D. K. Hansen, H. W, Behlow Jr., D. O. Scottb, T. N. Thompson, Evaluation of the BBMEC model for screening the CNS permeability of drugs, *J. Pharmacol. Toxicol. Meth.* **2011**, *45*, 71-77.

[178] D. K. Hansen, D. O. Scott, K. W. Otis, S. M. Lunte, Comparison of *in vitro* BBMEC permeability and *in vivo* CNS uptake by microdialysis sampling, *J. Pharm. Biomed. Anal.* **2002**, *27*, 945-958.

[179] H. Frank, H. J. Galla, C. T. Beuckman, An improved low-permeability *in vitro*-model of the blood-brain barrier: transport studies on retinoids, sucrose, haloperidol, caffeine and mannitol, *Brain Res.* **1999**, *818*, 65-71.

[180] Y. Zhang, C. S. W. Li, Y. Ye, K. Johnson, J. Poe, S. Johnson, W. Brobowski, R. Garrido, C. Madhu, Porcine brain microvessel endothelial cells as an *in vitro* model to predict *in vivo* blood-brain barrier permeability, *Drug Metab. Dispos.* **2006**, *34*, 1935-1943.

[181] M. Kansy, F. Senner, K. Gubernator, Physicochemical high throughput screening: parallel artificial membrane permeation assay in the description of passive absorption processes*, J. Med. Chem.* **1998**, *41*, 1007.

OBJECTIVES

Introduction of a structural constraint in peptides is a promising strategy to prepare compounds with improved pharmacological properties and activity against their targets. In this context, peptidomimetics can be used to target protein-protein interactions, not only disrupting the undesired ones, but also stabilizing or recovering the correct folding state of the active protein.

The objectives for the present thesis are the following:

1. To synthesize different biaryl bicyclic peptides by expanding the previous methodology to amino acids with functionalized side-chains.

2. To study the effect of the biaryl motif in terms of permeability, biostability, cytotoxicity and immunogenicity risk.

3. To prepare new kind of biaryl bicyclic peptides with other staple motifs, Trp-Trp.

4. To evaluate the potential use of these compounds in the recovery of the self-assembly of mutated p53TD proteins (R337H mutant).

RESULTS AND DISCUSSION

CHAPTER 1

EN ROUTE TO BIKE PEPTIDES

Natural products are the source of a wealth of bioactive molecules with particular structural features. Among them, complex macrocyclic peptides displaying biaryl bridge motifs have shown biological relevant activities. These natural staples can be mimicked by taking advantage of Suzuki-Miyaura cross-coupling reactions.

Peptides have been used for different purposes, one of the most relevant for recognition of protein surfaces. In this context, linear peptides modulate interactions with proteins by entering inside particular cavities formed in those proteins.

Low biostability, high clearance, as well as, poor permeability across cell membranes are the main inconvenients for what these peptides should be properly modified. Over the years, the use of cyclic peptides has significantly increased, not only due to the more favoured pharmacological properties but also due to the fact that they can easily fit in the interface between different proteins involved in the interaction.

In some cases when reinforcing or stabilizing the interaction is the main goal, peptides with a particular three-dimensional volume and the ability to fit inside a cavity formed by the proteins are demanded. Bicyclic peptides display a three-dimensional volume in the space, being privileged scaffolds to be used for this purpose.

During her Posdoctoral research in our group, Dr. Soledad Royo started the development of a methodology based on Suzuki-Miyaura cross-coupling reactions on resin to prepare biaryl bicyclic pentapeptides. In the present chapter, this methodology was fine-tuned and expanded with the required orthogonality in order to introduce new amino acids that can contain different functionalities in their side-chains.

Furthermore, last step of head-to-tail cyclization in solution was extensively studied in order to characterize cyclodimerization byproducts, as well as, to open the gate to this new kind of structures.

1.1 Selection of the general peptide scaffold

Our peptide scaffold is constituted by a sequence of five amino acids; three of them are fixed, a D-proline and two L-phenyalanines while the remaining two residues will be modified giving some versatility to the general structure (Figure 1.1).
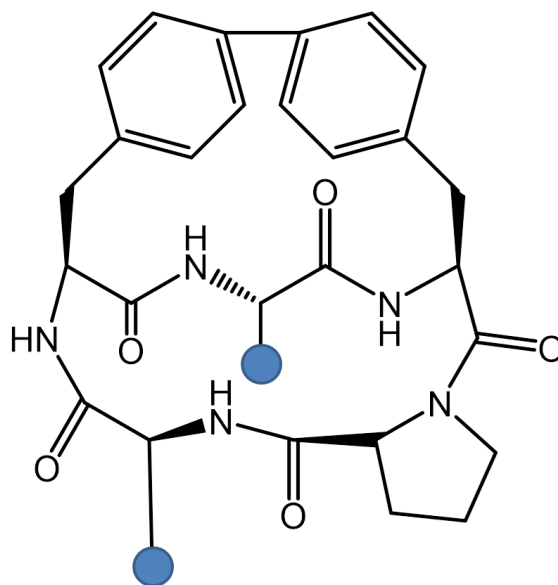
Figure 1.1. Structure of the general peptide scaffold with the staple between the L-phenyalanines in *para-para* positions of the aromatic ring. Blue spheres indicate the side-chains of the two amino acids that can be modified to introduce the previously mentioned versatily.

The peptide size was selected owing to the fact that cyclization of five amino acid rings can be achieved without further difficulties reaching reasonable yields and rendering molecules with some rigidity. Stapling of the scaffold was performed as a strategy to increase rigidity of the peptide and also enhance their pharmacological properties. Biaryl motif was used as staple constraint due to their common presence in natural products and the possibility to interact by π-cation interactions with protein surfaces in recognition processes.

D-Proline was selected as *C*-terminal amino acid on resin in order to favor cyclization in solution by inducing tight loops that generate the cyclization-prone conformation[182]. The two phenylalanines are required to carry out the biaryl stapling between the *meta*

or *para* positions of their side-chain aromatic ring. Suzuki-Miyaura cross-coupling reactions on resin were used for this purpose.

1.2 Initial methodology to prepare biaryl bicyclic pentapeptides

Biaryl bicyclic pentapeptides, named bike peptide, were prepared using properly modified Fmoc/*t*Bu SPPS.

The first model peptide to prove the possibility to successfully achieve the synthesis of this particular and complex sequences was cyclo(Ala-(4&)Phe-Ala-(4&)Phe-DPro)[183]. The amino acid alanine was selected due to the lack of a reacting group in the side-chain which avoids a more complex scheme of side-chain protecting groups and also avoids high steric hindrance. Alanine was used as a spacer between the two aromatic residues to allow their carbon-carbon stapling. One may wonder whether would be possible to explore the synthesis of these compounds by using the smallest natural amino acid, glycine. However, the reduced size of this residue together with the presence of two hydrogen substituents on the C^α tends to induce undesired flexibility in the peptide chain.

The synthetic route includes an on resin borylation, intramolecular solid-phase Suzuki-Miyaura reactions and in solution head-to-tail cyclization. Figure 1.2 shows the synthetic strategy followed for the obtention of the model peptide. This same strategy was also used to prepare the bicyclic peptide with *meta-meta* stapling, using 3I-phenylalanine derivatives.
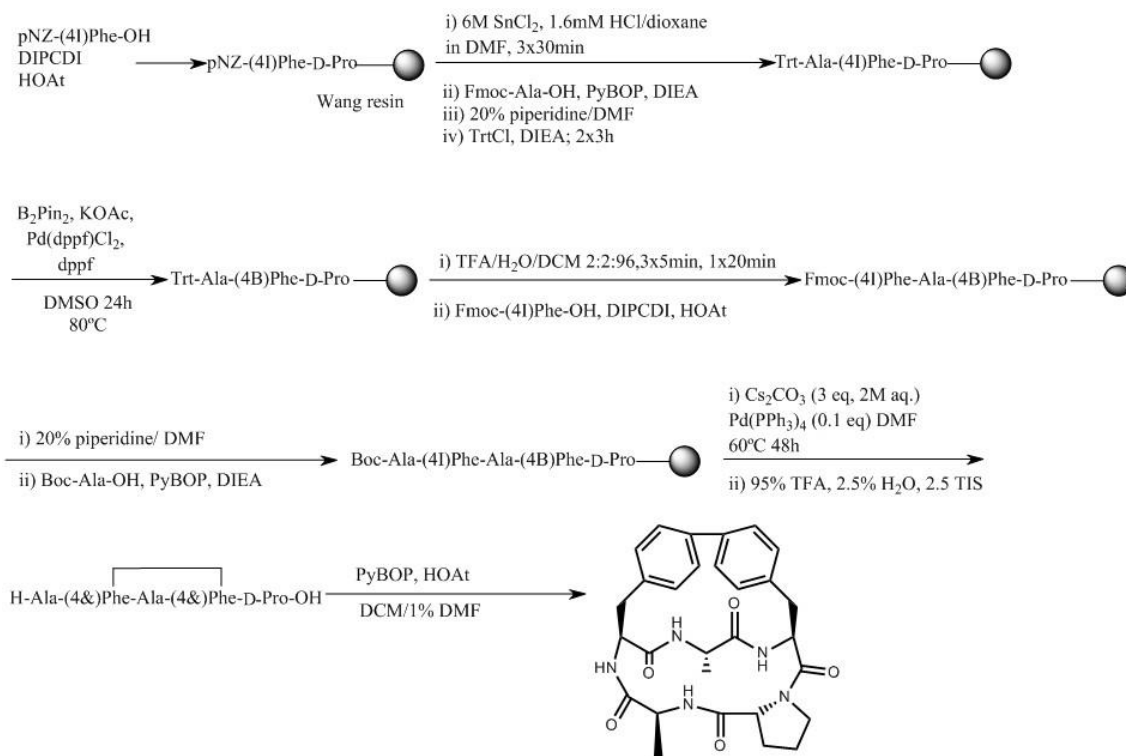
Figure 1.2. SPPS of the cyclo(Ala-(4&)Phe-Ala-(4&)Phe-D-Pro) and cyclo(Ala-(3&)Phe-Ala-(3&)Phe-D-Pro).

The peptide was synthesized on solid-phase using Fmoc/*t*Bu chemistry. It must be taken into account that this sequence is very diketopiperazine (DKP) prone. High risk of DKP formation exists when Pro is attached to the resin as the first amino acid and when the sequence of first and second amino acid is L-D or D-L in terms of configuration. Since both conditions were given in this peptide scaffold, formation of DKP was a big concern.[6] The second amino acid was therefore protected with *p*NZ to avoid DKP formation during coupling of the third residue, when the second residue had the *N*-terminus unprotected. Regarding the third residue, it was introduced with Trt protecting group. After this coupling, Miyaura reaction was performed on resin to carry out the borylation of the phenylalanine amino acid. Basic and palladium-catalyzed conditions of this reaction reduced the number of compatible protecting groups (PG) that could be used in the elongation of the main chain. Then, the remaining two or three amino acids were coupled using Fmoc/*t*Bu chemistry. However, last amino acid should be introduced with Boc protecting group so that it was stable under Suzuki reaction conditions. This reaction was performed on resin to

build the biaryl bridge between the two aromatic residues and when it was finished, cleavage from the resin was carried out. Head-to-tail cyclization was performed under high diluted conditions to hinder the intermolecular and favor the intramolecular reaction, since the interest was to obtain a bicyclic peptide and dimerization should be prevented.

The desired rigidity of the peptide was achieved with the biaryl bridge and also with the number of amino acids which constitute the cyclic peptide. The scheme of cyclization is highly important, as two different rings must be formed. With this in mind, we must consider the most appropiate order, to generate our desired compound.

That means, whether Suzuki should be performed before or after head-to-tail cyclization. It must be taken into account that after the first cycle has been formed, the conformational constrain is bigger and this could either hinder or facilitate the formation of the second cycle, but it is difficult to predict which one of them will be more complicated to be formed. Results obtained with different sequences performing cyclization on resin resulted in poor yields, deciding that Suzuki must be performed first on resin and the head-to-tail cyclization as the last step in solution. The synthetic protecting group scheme is shown in Figure 1.3.
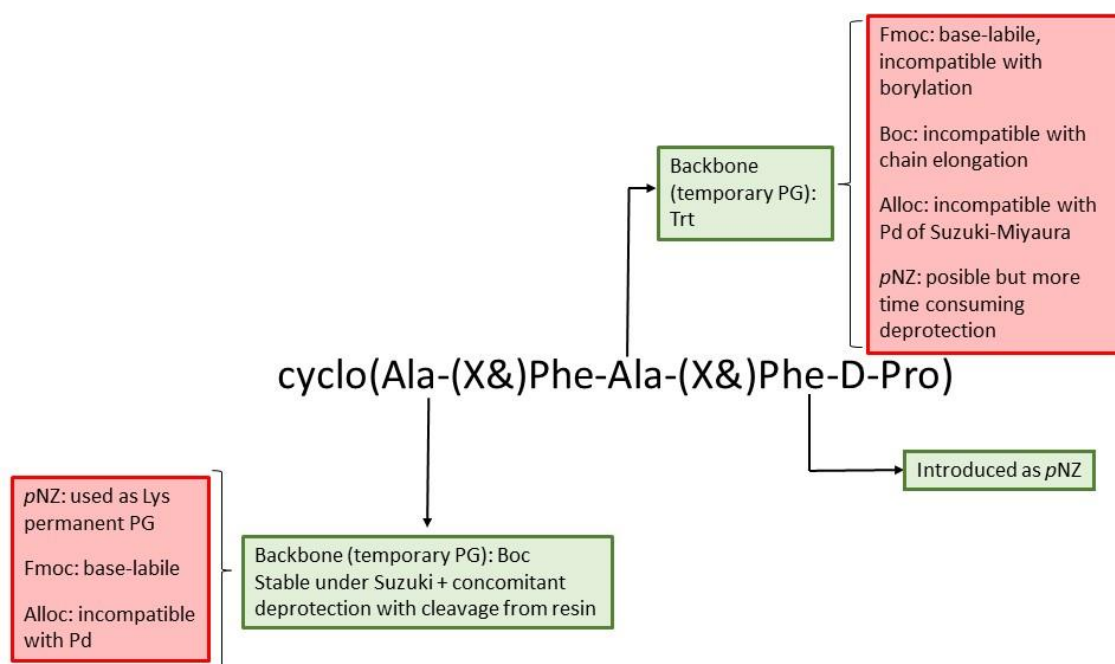
Figure 1.3. Protecting group scheme for the synthesis of cyclo(Ala-(4&)Phe-Ala-(4&)Phe-D-Pro) and cyclo(Ala-(3&)Phe-Ala-(3&)Phe-D-Pro).

Regarding the biaryl bond, as it was mentioned above, intramolecular Suzuki cross-coupling reaction was selected due to the compatibility that it offered with several functional groups and the possibility to be also performed on resin.

Suzuki is a palladium-catalyzed reaction (this should be taken into account to avoid undesired removal of PG that are labile to this reagent) of an aryl halide and a boronic acid or ester in basic conditions.

The boronic acid or ester should be previously obtained, prepared from an aryl halide by taking advantage of Miyaura borylation reaction. This reaction is also catalysed by the presence of palladium under similar conditions.

At the beginning of the synthetic strategy design, it was thought that the biaryl bond could be introduced as a biaryl bisamino acid, but this would mean having orthogonal protecting groups to differentiate between the two amino and the carboxylic groups (Figure 1.4).
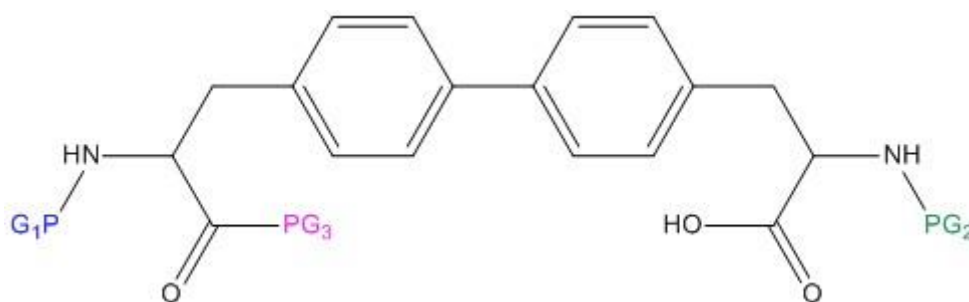
Figure 1.4. Biaryl bisamino acid that could have been directly introduced on resin. This strategy would have required three protecting groups at least (remarked in blue, green and purple). Protection of one carboxylic acid could be avoided, this would be the reactive group to be activated and attached to the *N*-teminus of the resin. Orthogonality of the remaining three protecting groups would be necessary for selective couplings.

A more adequate strategy was selected, based on the incorporation of the two aromatic residues with an halogenated side-chain; one of them being transformed into an arylboronic ester, prior to performing Suzuki reaction. Since a one-pot process would not differentiate between the two residues leading to complex mixtures, borylation was carried out on the first introduced aromatic residue and before coupling the second aromatic amino acid. Therefore, borylation was performed at the tripeptide level prior to the coupling of the fourth amino acid, which was the second iodinated phenyalanine. This was decided based on the fact that the dipeptide was difficult to be followed by HPLC-MS and steric hindrance from the resin could difficult the reaction.

Some important aspects such as the resin, the coupling reagents or the reaction conditions used are worth to be described in a more detailed manner. Wang resin was chosen as the best option, as this resin provided the linear peptide with a *C*-terminal carboxylic acid and it was stable under the required reaction conditions. Whereas 2-chlorotrytil resin would be labile during deprotection of the main chain protecting group after Miyaura borylation.

Mild coupling conditions were chosen in order to avoid side reactions. Therefore, couplings were performed with DIPCDI, even in the case of couplings onto secondary

amines. When the amino acid to be coupled was protected with Trt, phosphonium salts were used due to stronger conditions required for the coupling.

Another important point to consider was the pH of the medium before the couplings of the amino acids. After removing *p*NZ the medium was neutralized since deprotection took place in acid conditions. Nevertheless, it could be developed while performing the coupling with a base like DIEA, commonly used in tandem with other coupling agents like PyBOP.

Proper selection of the protecting groups was also influenced by the medium conditions, reagents and the resin used.

After having set up the methodology to synthesize this model sequence, another similar model peptide was prepared, cyclo(Ala-(3&)Phe-Ala-(3&)Phe-DPro). The difference with the parent peptide laid on the stapling position in the phenylalanines side-chain.

It is worth noting that different positions in an aromatic ring are not equally reactive nor accessible, for this reason, testing *meta* and *para* positions in different model sequences was required. The following synthetic strategy does not introduce any modification except for the iodine position in the introduced phenylalanine in the sequence.

Control of the synthesis intermediates

Although the methodology was set up to be a straightforward protocol for the synthesis of bicyclic pentapeptides, the difficulty that involves is not deniable.

Therefore, an exhaustive analysis of the crude intermediates prepared during the synthesis was carried out by performing minicleavages in high acidic conditions (Figure 1.5-1.10). The obtained information was especially valuable when performing Miyaura and Suzuki cross-couplings, since reaction times could be affected by different parameters. HPLC chromatograms were shown for the intermediates of the model

peptide cyclo(Ala-(4&)Phe-Ala-(4&)Phe-D-Pro) although similar results were obtained for the sequence cyclo(Ala-(3&)Phe-Ala-(3&)Phe-D-Pro).
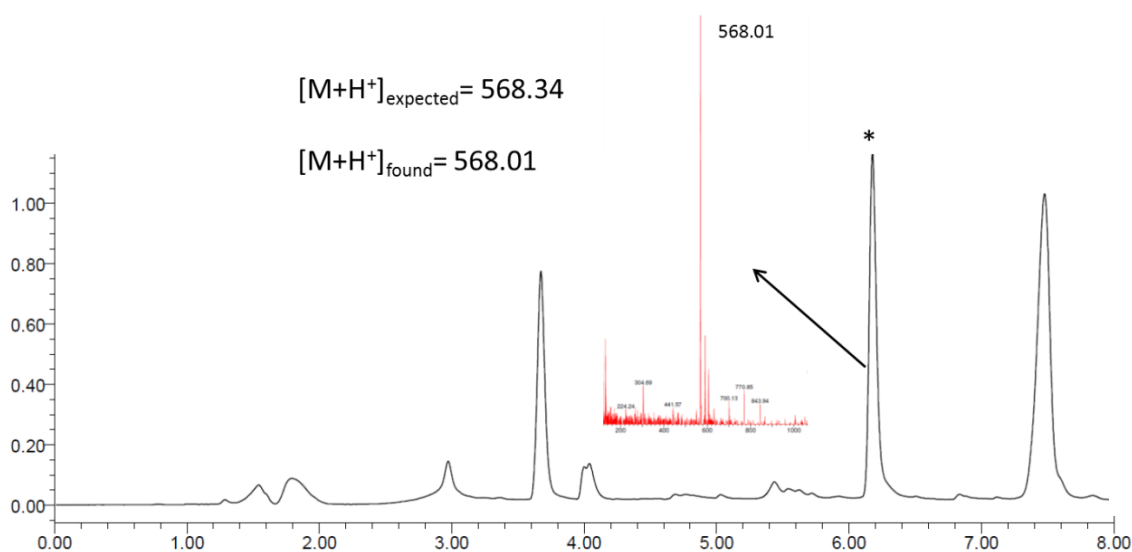
Figure 1.5. HPLC chromatogram of the crude peptide *pNZ*-(4I)Phe-D-Pro-OH in a 0-100% MeCN in 8 min gradient. Column SunFire C$_{18}$ 3.5μm, 4.6x100mm. t$_R$=6.20min. * denotes the desired product
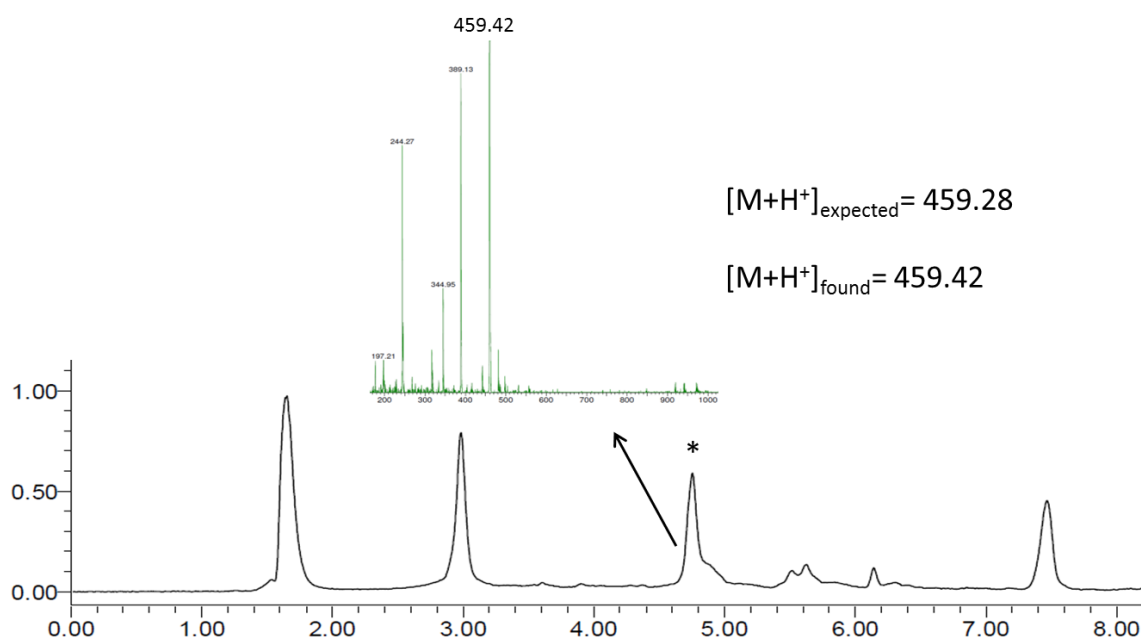
Figure 1.6. HPLC chromatogram of the crude peptide H-Ala-(4I)Phe-D-Pro-OH in a 0-100% MeCN in 8 min gradient. Column SunFire C$_{18}$ 3.5μm, 4.6x100mm. t$_R$=4.78min. * denotes the desired product

$[M+H^+]_{expected} = 378.20$

$[M+H^+]_{found} = 378.27$
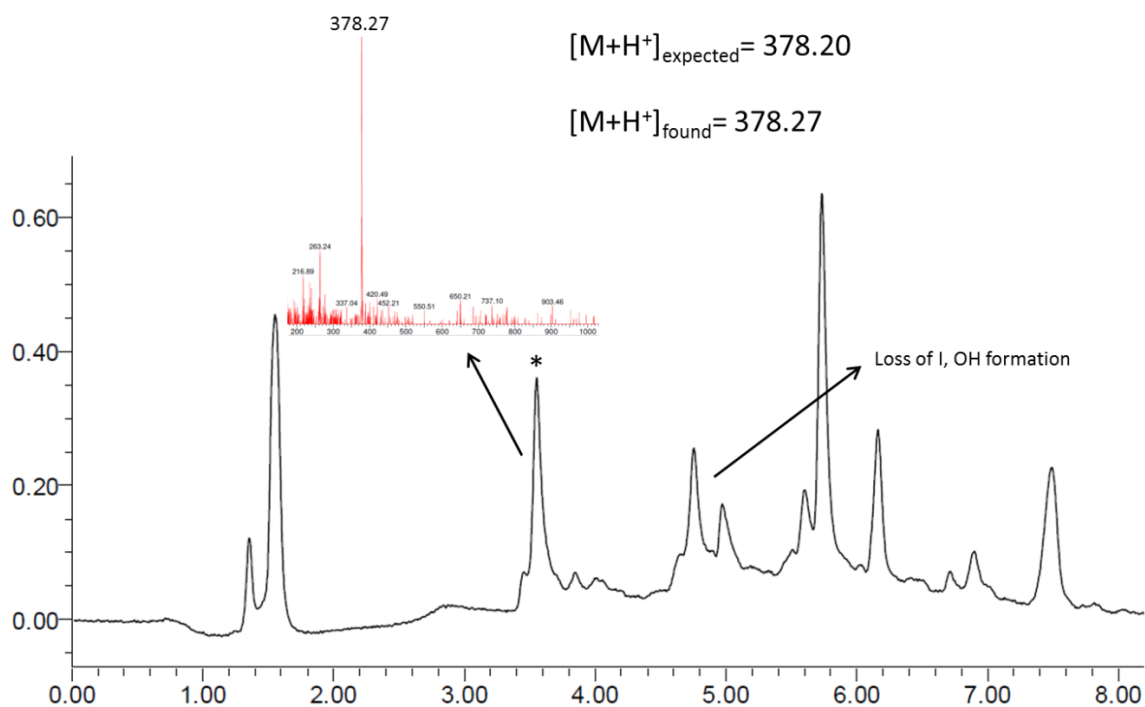
Figure 1.7. HPLC chromatogram of the crude peptide H-Ala-(4B)Phe-D-Pro-OH in a 0-100% MeCN in 8 min gradient. Column SunFire C$_{18}$ 3.5μm, 4.6x100mm. t$_R$=3.59min. * denotes the desired product

$[M+H^+]_{expected} = 651.28$

$[M+H^+]_{found} = 651.19$
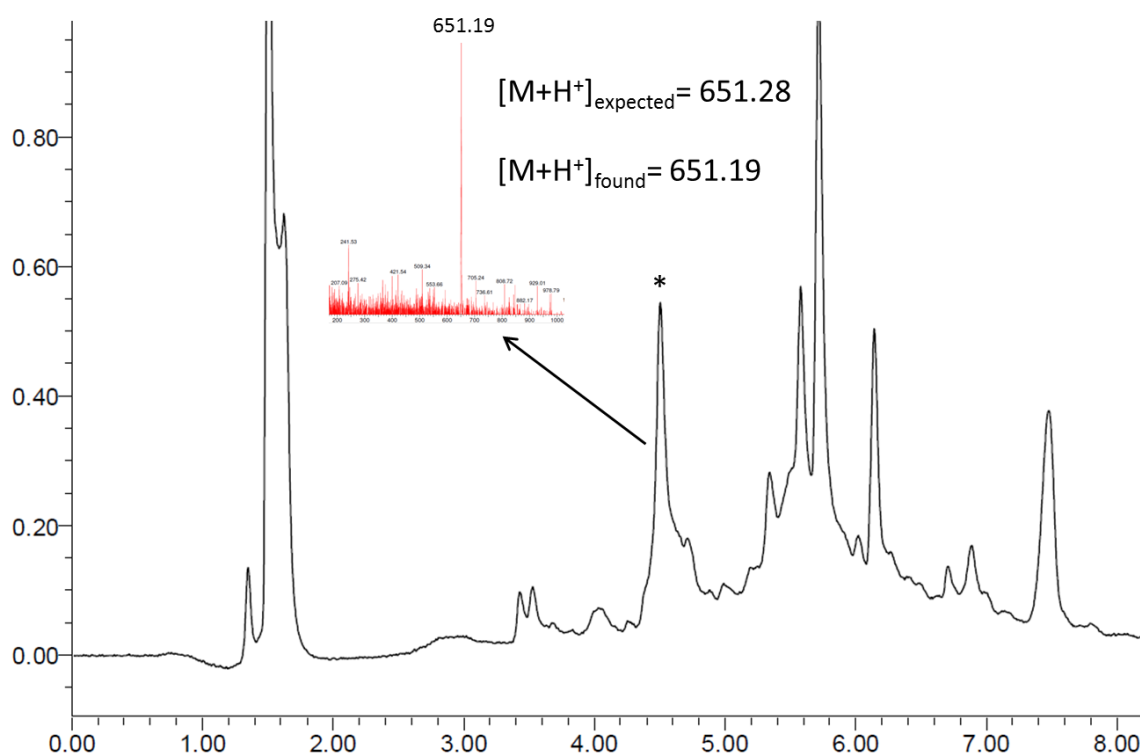
Figure 1.8. HPLC chromatogram of the crude peptide H-(4I)Phe-Ala-(4B)Phe-D-Pro-OH in a 0-100% MeCN in 8 min gradient. Column SunFire C$_{18}$ 3.5μm, 4.6x100mm. t$_R$=4.55min. * denotes the desired product
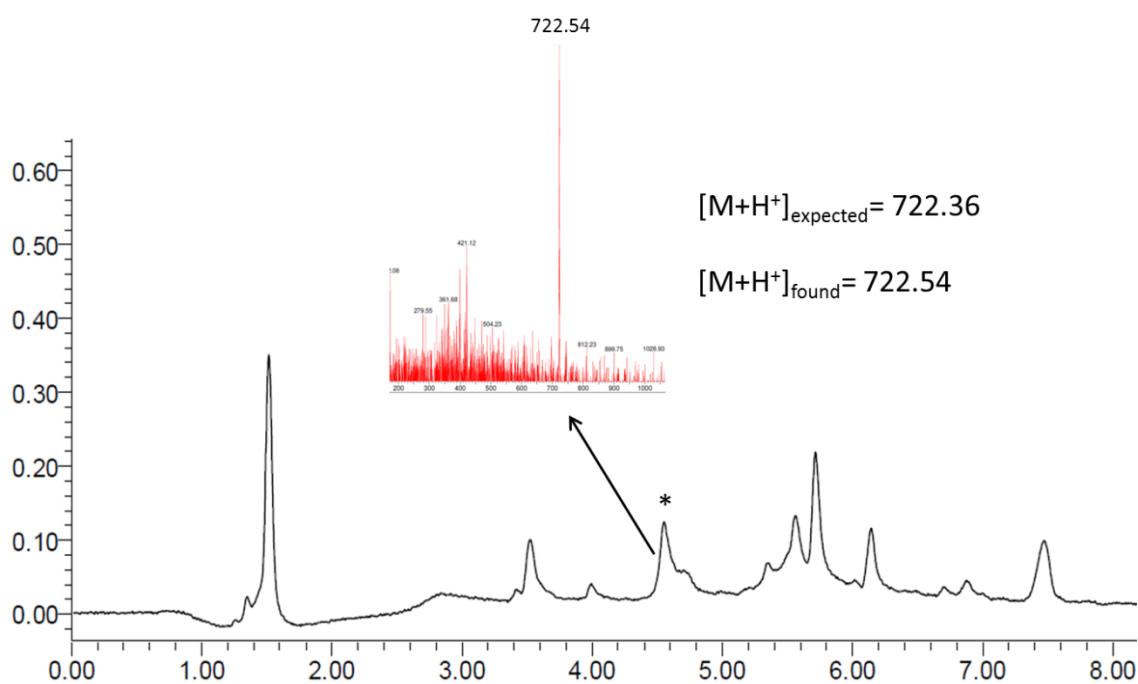
Figure 1.9. HPLC chromatogram of the crude peptide H-Ala-(4I)Phe-Ala-(4B)Phe-D-Pro-OH in a 0-100% MeCN in 8 min gradient. Column SunFire C₁₈ 3.5μm, 4.6x100mm. t_R=4.58min. * denotes the desired product
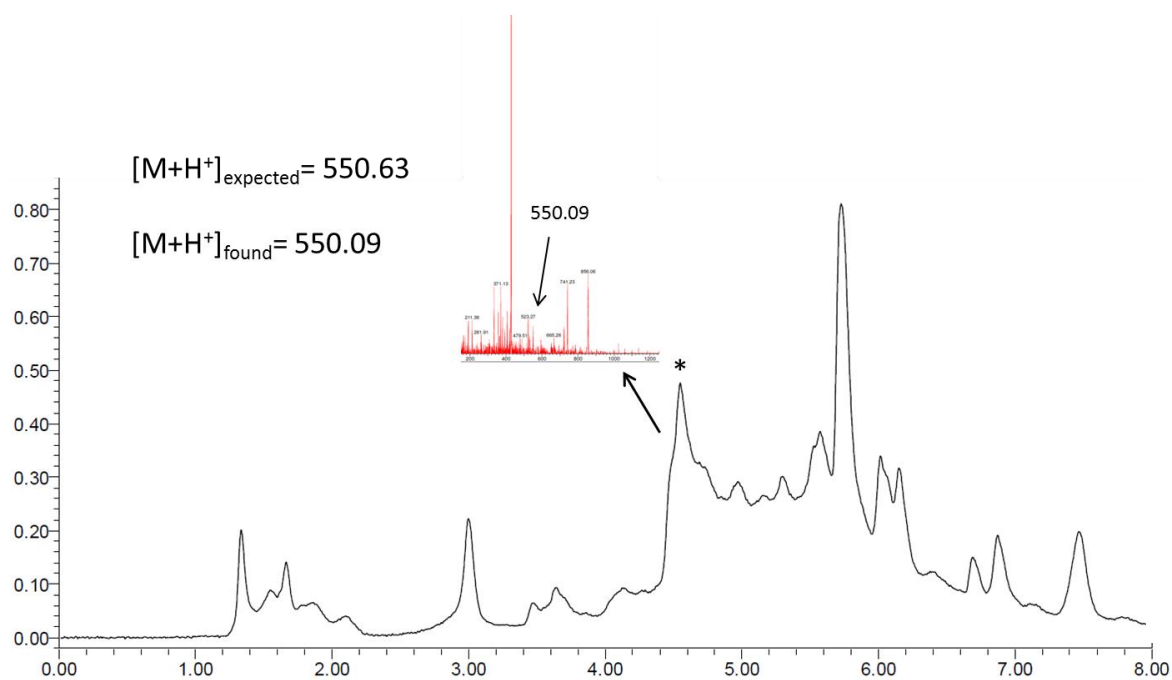
Figure 1.10. HPLC chromatogram of the crude peptide H-Ala-(4&)Phe-Ala-(4&)Phe-D-Pro-OH in a 0-100% MeCN in 8 min gradient. Column SunFire C₁₈ 3.5μm, 4.6x100mm. t_R=4.58min. * denotes the desired product

Two important byproducts of Miyaura borylation were the loss of iodine, protodeboronation, and the hydroxylation at iodine position of the aromatic ring of the phenylalanine. These byproducts were detected during the minicleavage (Figure 1.7).

Protodeboronation has been scarcely reported[184,185]. Under Miyaura borylation base-catalyzed conditions this side reaction is common. Since this byproduct is obtained from the borylated final compound once Miyaura borylation has finished, longer reaction times can increase its formation. When oxygen enters inside the catalytic system, a peroxide is formed, anaerobically generated, which is capable of oxidising the boronic acid giving rise to a hydroxyl at the position in the aromatic ring previously occupied by the reacting halide[186].

In order to avoid these side reactions, testing the reaction evolution at shorter times by minicleavage can be useful. Due to the fact that 100% conversion is not achieved, closer evaluation of the remaining starting material and byproduct formation is advised in order to gain access to a satisfactory yield. Formation of these byproducts is illustrated in Figure 1.11.

A
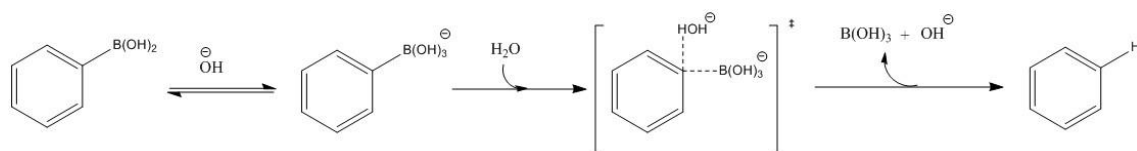
B
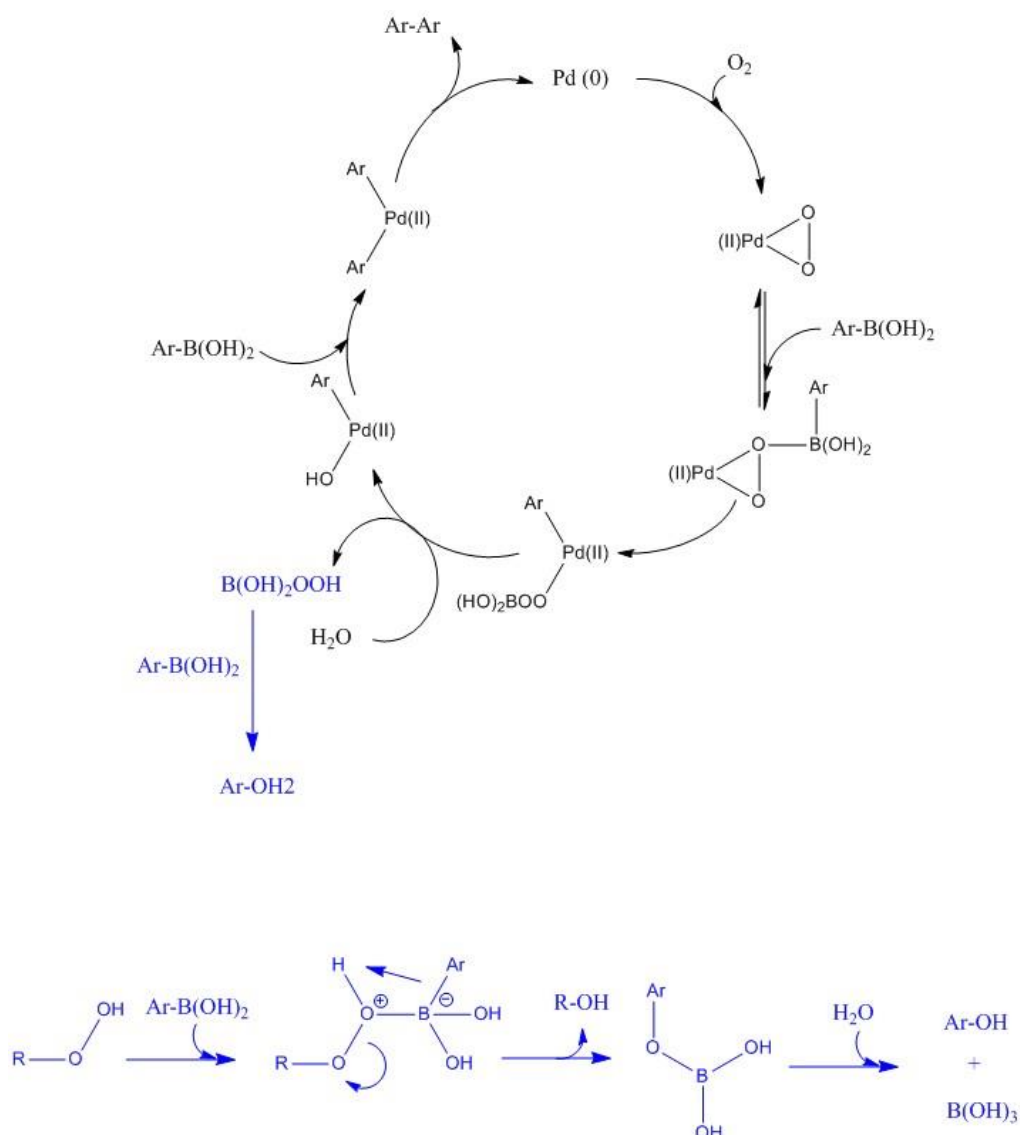
Figure 1.11. A) Protodeboronation mechanism B) Catalyitic side reaction when oxygen enters in the cycle and oxo-palladium most-likely pathway remarked in blue.

After Suzuki reaction, pentapeptide crude was difficult to characterize as it can be seen in Figure 1.10. One of the main problems was the presence of palladium introduced during Suzuki and Miyaura cross-coupling. Therefore, Porapak™ column was performed as a pre purification of the crude, reducing the number of impurities as it is shown in Figure 1.12.
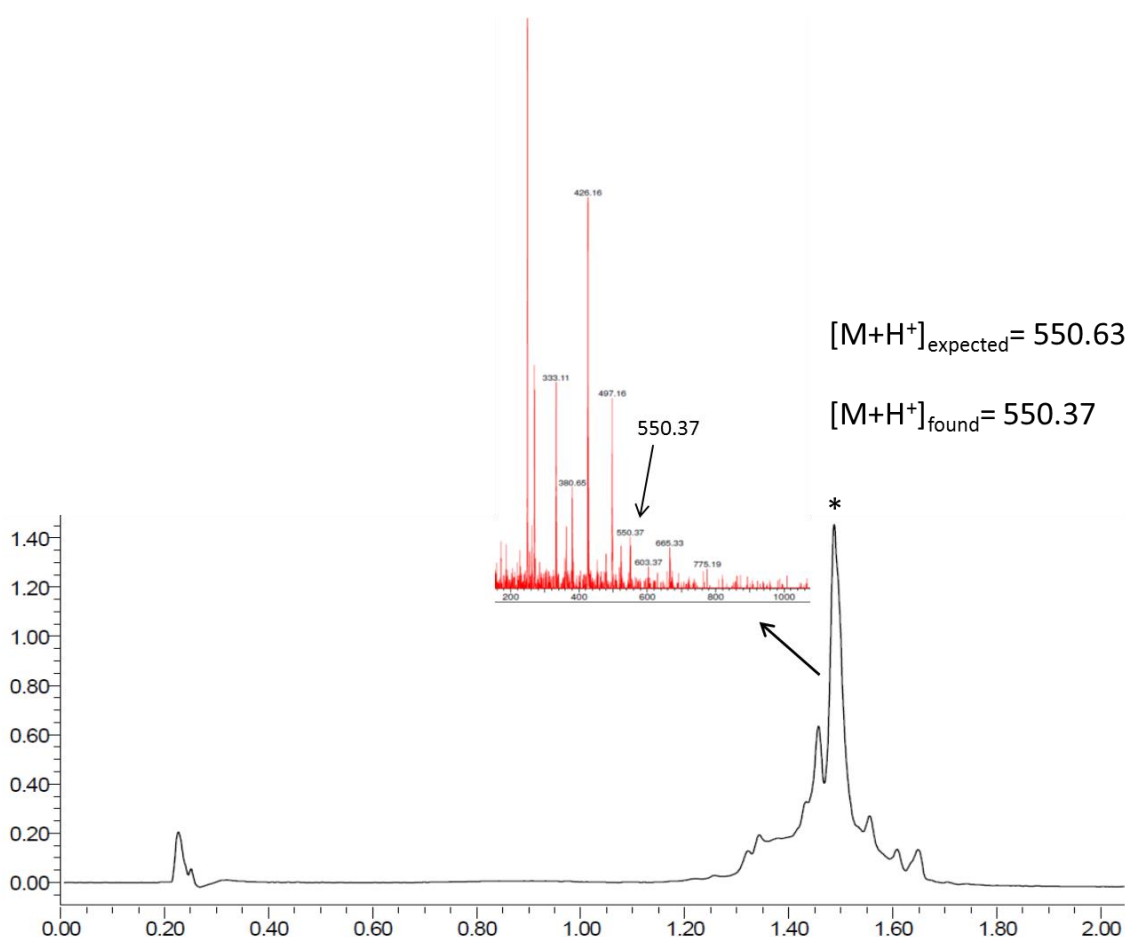
Figure 1.12. UPLC chromatogram of the crude peptide **H-Ala-(4&)Phe-Ala-(4&)Phe-D-Pro-OH** in a 0-100% MeCN in 2 min gradient. Column BEH C$_{18}$, 1.7 μm, 2.1x50mm. t$_R$=1.49min. * denotes the desired product

Full characterization of the linear precursor was performed before carrying out head-to-tail cyclization in solution, confirming the access to the desired product.
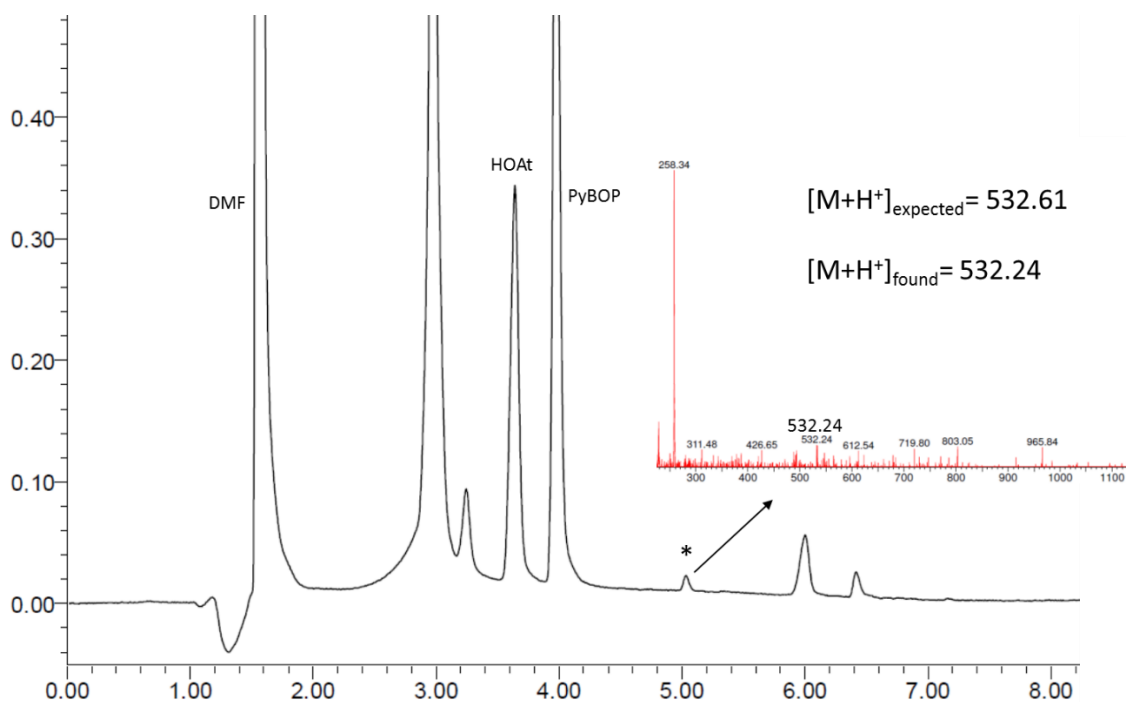
Figure 1.13. HPLC chromatogram of the final crude peptide cyclo(Ala-(4&)Phe-Ala-(4&)Phe-D-Pro) in a 0-100% MeCN in 8 min gradient. Column SunFire C$_{18}$ 3.5μm, 4.6x100mm. t$_R$=5.04min. * denotes the desired product

Cyclization in solution introduced several reagents that were removed by performing and appropriate work-up and followed by the purification by HPLC-semipreparative.
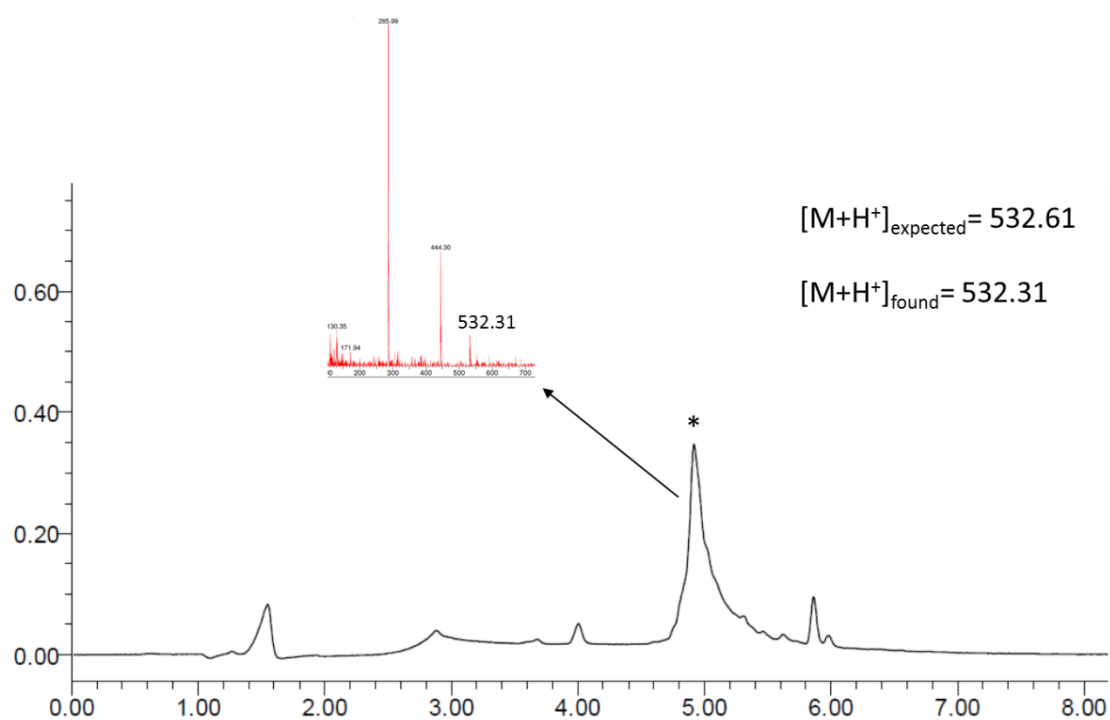
Figure 1.14. HPLC chromatogram of pure peptide after purification, cyclo(Ala-(4&)Phe-Ala-(4&)Phe-D-Pro), in a 0-100% MeCN in 8 min gradient. Column SunFire C$_{18}$, 3.5μm, 4.6x100mm. t$_R$=5.04min. * denotes the desired product

Control minicleavages were interesting not only to follow the reactions, but also to understand the amount of byproducts and their nature. Nevertheless, some protecting groups were removed under the minicleavage conditions and could not be detected, limiting the characterization of key intermediates such as the starting material of the Miyaura borylation, Trt-Ala-(4I)Phe-D-Pro-OH, or the Suzuki cross-coupling, Boc-Ala-(4I)Phe-Ala-(4B)Phe-D-Pro-OH.

Synthetic consideration remarks

Some synthetic precautions and considerations may be taken into account to successfully obtain the synthesis of the desired product. First, washes of the resin and the solvents used were very important. Especially, washes after borylation and Suzuki were very relevant to get rid of the excess of palladium catalyst, used base and the boronic reagent in the case of Miyaura reaction.

Temperature was a parameter that could influence more than expected. When *p*NZ deprotection was not completely achieved, the resin was transferred to a glass vial and heated with the deprotection cocktail. Orange solution was obtained when *p*NZ was being successfully removed.

After Porapak™ column, an extra pre purification step by HPLC-semipreparative was introduced to perform the cyclization with a cleaner crude that could also be purified afterwards.

Insolubility of the peptides should be carefully considered when dissolving them before performing HPLC purification. Higher amounts of acetonitrile difficult purification although sometimes were required to ensure product solubility. In this context, extraction work-up to remove high excess of salts was also important.

1.2.1 Computational studies

During the initial steps of the project together with the setting up of the methodology, we collaborated with Dr. Michella Candotti from Prof. M. Orozco research group at the IRB Barcelona, to perform structural studies of the model bicyclic peptides.

Short molecular dynamic simulations of 10 ns were run for each bicyclic peptide in order to estimate the rigidity level imposed by the presence of the biaryl staple.

For the *para-para* version, the simulation was run in DMSO, water and hydrophobic media. We observed no significant differences between each of the solvents. However, for the *meta-meta* bicyclic peptide, dynamic simulation was only studied in DMSO.

Simulations were done with implicit solvent (Born Solvent Model) in AMBER using 5 clusters to group the trajectories, each one with a representative structure.

High similarity between the clusters allows grouping them according to the occupancy and the average final structure.

(a) (b) (c)
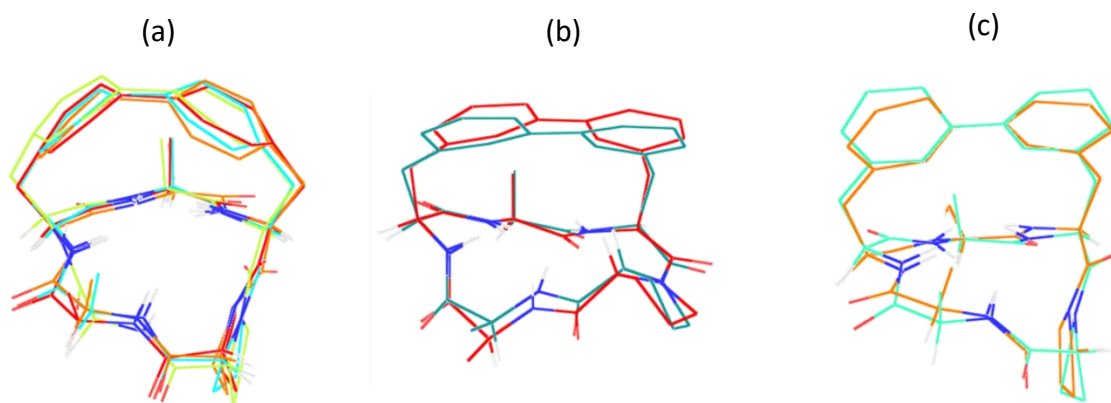
Figure 1.15. Representative structures in DMSO of (a) *para-para*: **cyclo(Ala-(4&)Phe-Ala-(4&)Phe-D-Pro). (total occupancy >95% (b,c)** *meta-meta*: **cyclo(Ala-(3&)Phe-Ala-(3&)Phe-D-Pro), total occupancy b) 55% c) 42%. Figures done by Dr. Michella Candotti.**

It is worth mentioning the short times of these dynamic simulation studies, since it is possible that longer times could have given more representation to one of the presented structures.

From these structural studies we can make the following conclusions. Firstly, m*eta-meta* biaryl bicyclic peptide proved to be less restricted than the *para-para* version. For the latter, only one major population structure was obtained due to the high ridigity. While for the *meta-meta* two almost equally populated structures were obtained demonstrating the higher flexibility of this peptide in front of the *para-para*. In both peptides, the most flexible part corresponded to D-Pro-Ala, being much more flexible for the *meta-meta* version. Simulations showed that the *para-para* biphenyl was rigid and remained almost static all the time, while the *meta-meta* biphenyl was quite flexible.

The computational data was confirmed experimentallly using a fluorescence based assay. The planar nature of the biphenyl motif proved to be fluorescent while the absorbance observed disappeared after head-to-tail cyclization. This confirms our previous conclusion that the biphenyl is under torsion and no longer planar (Figure 1.15 (a).

1.3 Cyclodimers

It is important to highlight that during the preparation of the two first model peptides, cyclo(Ala-(4&)Phe-Ala-(4&)Phe-D-Pro) and cyclo(Ala-(3&)Phe-Ala-(3&)Phe-D-Pro) we realized about the existence of cyclodimers. During the last step of head-to-tail cyclization in solution two units of the linear stapled peptide reacted forming the dimer, which is actually a tricyclic peptide (Figure 1.16).
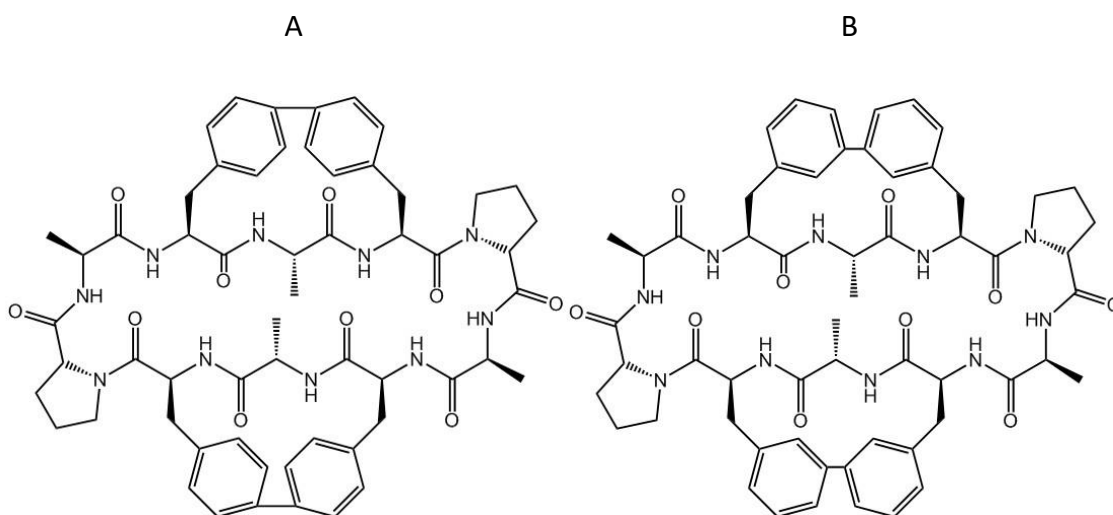
Figure 1.16. Structure of the cyclodimers formed for the two model peptides. A) cyclo(Ala-(4&1)Phe-Ala-(4&1)Phe-D-Pro-Ala-(4&2)Phe-Ala-(4&2)Phe-D-Pro), B) cyclo(Ala-(3&1)Phe-Ala-(3&1)Phe-D-Pro-Ala-(3&2)Phe-Ala-(3&2)Phe-D-Pro).

Performing minicleavage of the sequences once Suzuki reaction had been carried out on solid-phase unveiled that, at this level, the peptides were still monomeric sequences, which confirmed that dimerization did not take place during Suzuki reaction but in the head-to-tail cyclization in solution step.

Exact mass determination allows differentiating between the monomer and the dimer species due to the values of the mass/charge obtained. Dimerization was not an artefact during the exact mass analysis since it was present even when performing the measure under high diluted conditions in gas phase.
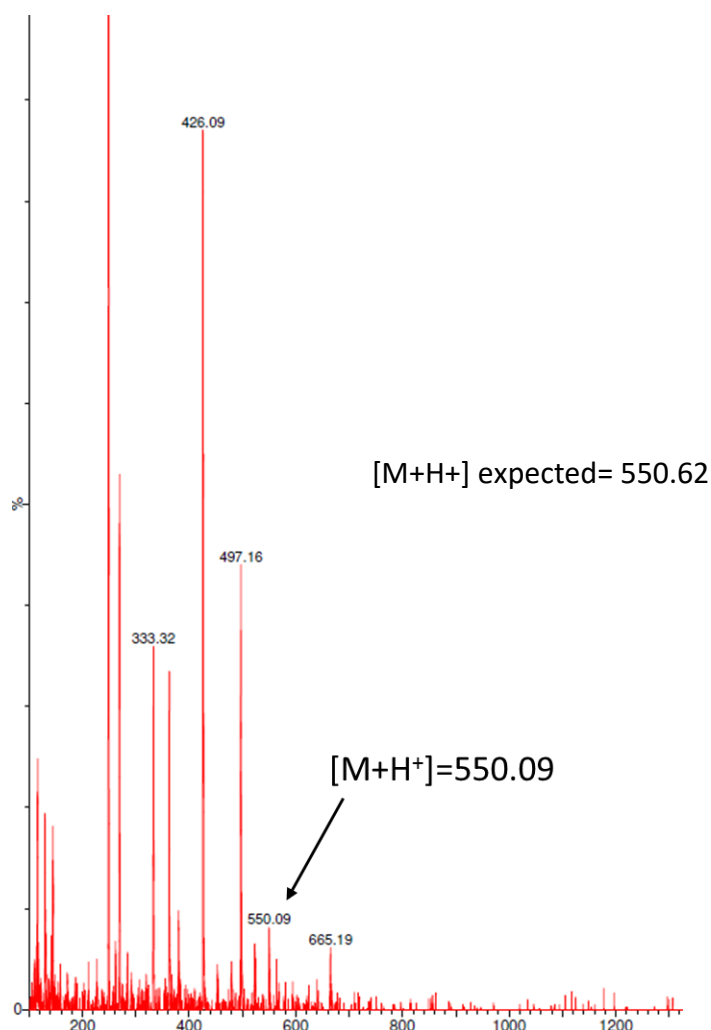
Figure 1.17. Mass spectrum of the monomeric H-Ala-(4&)Phe-Ala-(4&)Phe-D-Pro-OH before head-to-tail cyclization in solution in a 0-100% MeCN in 2min gradient, Column BEH C$_{18}$ 1.7µm, 2.1x50mm, t$_R$=1.22min, [M+H$^+$]expected=550.62, [M+H$^+$]found=550.09. Mass of the cyclodimer, [M+H$^+$]=1100.28, was not detected.

Exact mass determination of the final products proved that the corresponding mass of the cyclodimer (named in the experiment [2M+H$^+$]) correspond to a charge 1 specie, implying that the dimerization has taken place during the head-to-tail macrocyclization in solution. The exact mass determination experiments were done at 20µM and 200nM concentrations to avoid possible artefacts related to high concentration or aggregation process during the MS analysis. Both concentration experiments provided similar results (Figure 1.19).
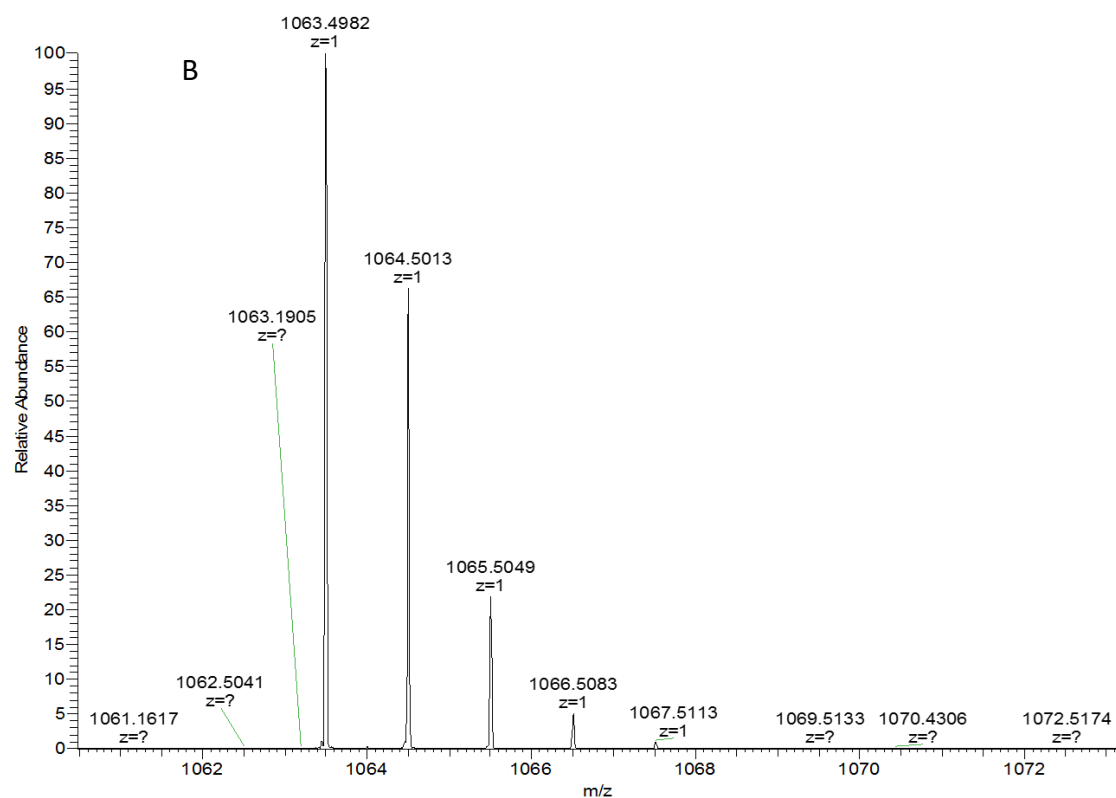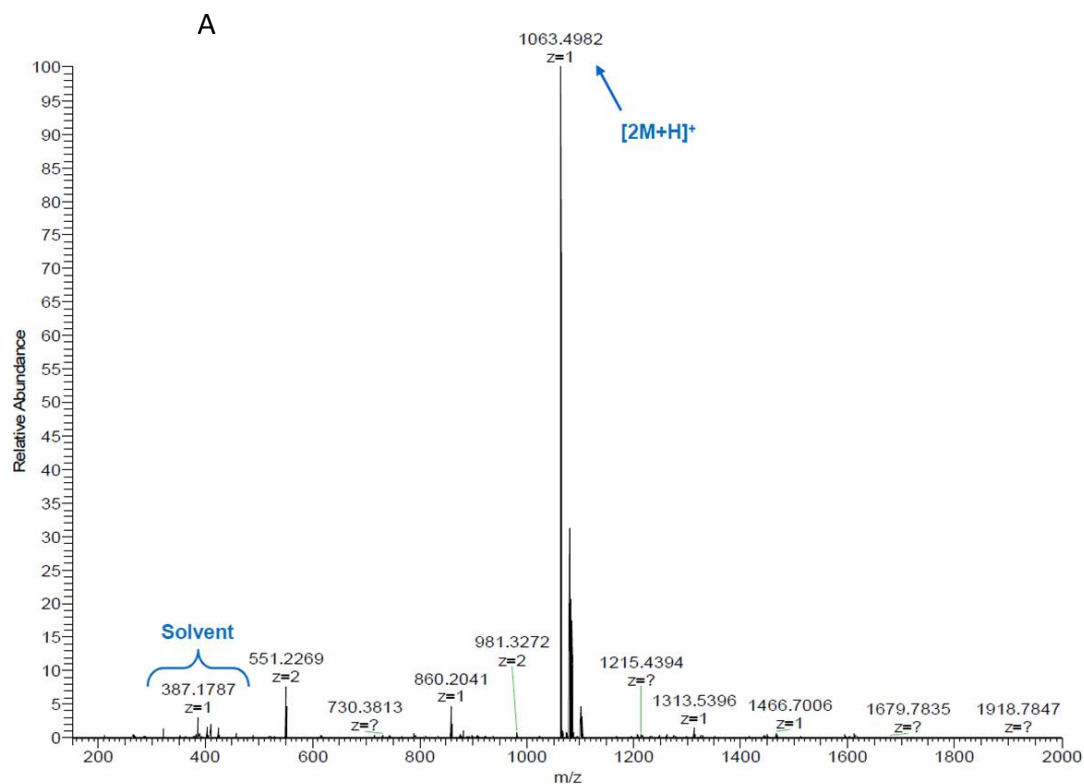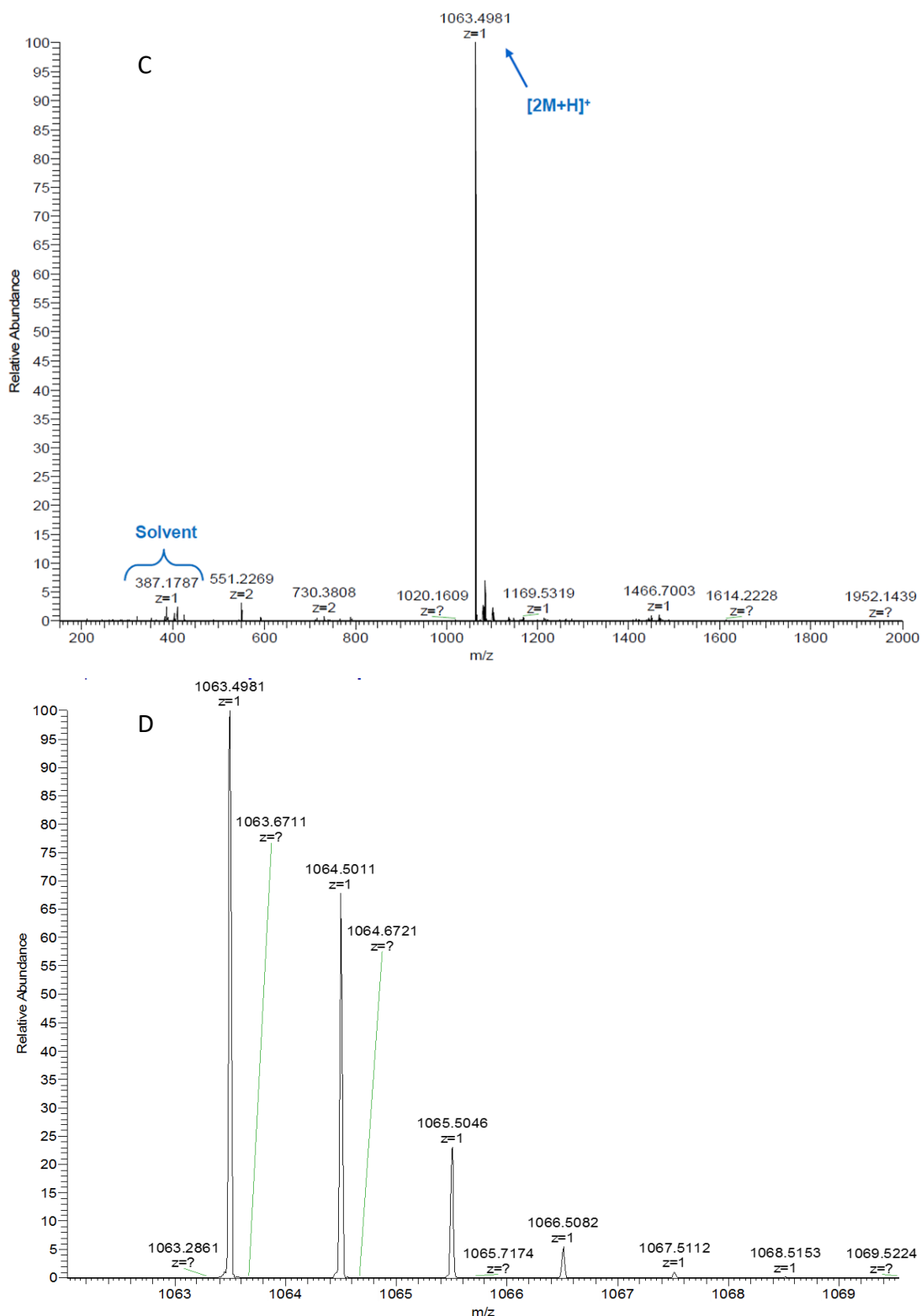
Figure 1.19. A) HRMS of the peptide cyclo(Ala-(3&$_1$)Phe-Ala-(3&$_1$)Phe-D-Pro-Ala-(3&$_2$)Phe-Ala-(3&$_2$)Phe-D-Pro) at 20μM, [M+H$^+$]expected=1063.5036; [M+H$^+$]found=1063.4982 B) zoom of the HRMS A, differences of 1Da between the isotopic peaks confirmed charge 1 specie C) HRMS of the peptide cyclo(Ala-(4&$_1$)Phe-Ala-(4&$_1$)Phe-D-Pro-Ala-(4&$_2$)Phe-Ala-(4&$_2$)Phe-D-Pro) at 20μM, [M+H$^+$]expected=1063.5036; [M+H$^+$]found=1063.4981 C) zoom of the HRMS B, differences of 1Da between the isotopic peaks confirmed charge 1 specie.

Once knowing the existence of these byproducts, we decided to study how to avoid them and also to consider this side reaction as an opportunity to have access to these new compounds. Therefore, it is mandatory to control the dimerization, in the sense of having a methodology to prepare the bicyclic monomers, as well as, the cyclodimers with a completely selective and efficient strategy.

For this reason, cyclization conditions were extensively studied to unveil the relevance of the reagents, the solvents, as well as, the concentration.

1.3.1 Studies of the head-to-tail cyclization

cyclo(Ala-(3&)Phe-Ala-(3&)Phe-D-Pro) and cyclo(Ala-(4&)Phe-Ala-(4&)Phe-D-Pro) stapled versions were synthesized in large scale to carry out the different cyclization trials. Studying the diverse parameters that can be changed, it was possible to establish the required conditions that favour the obtention of the bicyclic monomers, as well as, a method for the cyclodimers obtention.

On one side, the bicyclic monomeric peptides could be almost exclusively obtained when working with PyBOP/HOAt as cyclization reagents, DIEA as base and DCM/1% DMF as solvents (Table 1.1). In fact, even increasing concentration as it is shown in Table 1.2, only traces of the cyclodimers were formed. This study demonstrated that the important factor for cyclization was not only the concentration of the starting material but also the reagents and the solvents used to carry out this reaction. It is worth noting that the starting material was not fully converted into the bicyclic version although being the main product in the final crude.

Table 1.1. In solution Head-to-tail cyclization studies. Five different conditions were attempted at different concentrations, reagents, base and solvent for the starting material H-Ala-(4&)Phe-Ala-(4&)Phe-D-Pro-OH and H-Ala-(3&)Phe-Ala-(3&)Phe-D-Pro-OH.

	Cond.1	Cond.2	Cond.3	Cond.4	Cond.5
Concentration	5mM	50mM	1mM	0.5mM	100mM
Reagents	DPPA	DPPA	PyBOP/HOAt	PyBOP/HOAt	DPPA
Base	NaHCO$_3$	NaHCO$_3$	DIEA	DIEA	NaHCO$_3$
Solvent	DMF	DMF	DCM/1% DMF	DCM/1% DMF	DMF

Analyzing the different experiments, being conditions 1 the initial ones established by Dr. S. Royo, conditions 3 seemed to be the best option to obtain the biaryl bicyclic peptides in their monomeric form. Conditions 4 were difficult to be monitored due to the high dilution. Using conditions 3, starting material was still present, no cyclodimer was detected and the bicyclic peptide was found at a higher retention time than the linear precursor.

On the other side, conditions 2 and 5 were done to evaluate the effect of increasing the concentration working with the initial solvents and reagents, DPPA, NaHCO$_3$ and DMF. No trimers or larger products were detected. Nevertheless, in spite of working at really high concentration, 100mM, we could not force 100% formation of the cyclodimer. Conditons 2 and 5 yielded to similar results, 25% of the starting material was recovered, 25% corresponded to the cyclodimer while 50% was the bicyclic peptide. UPLC chromatogram at the end of the reaction time is shown in Figure 1.20 for conditions 2.
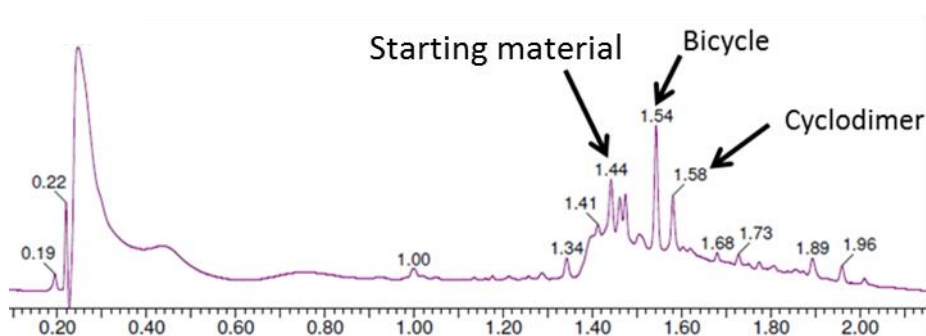
Figure 1.20. UPLC chromatogram for conditions 2.

Percentages of starting material, bicyclic monomer and cyclodimer are summarized for the different conditons in Table 1.2.

Table 1.2. Percentatges of starting material, bicyclic peptide and cyclodimer, calculated by integration and comparison of the peaks corresponding to each product.

	Starting material (t_R=1.44min)	Bicyclic peptide (t_R=1.54min)	Cyclodimer (t_R=1.58min)
Conditions1	23%	15%	62%
Conditions2	25%	50%	25%
Conditions3	53%	47%	NO
Conditions4	45%	55%	NO
Conditions5	25%	50%	25%

These results were similar for the tests run with cyclo(Ala-(3&)Phe-Ala-(3&)Phe-D-Pro) and cyclo(Ala-(4&)Phe-Ala-(4&)Phe-D-Pro) impliying that the different stapling position does not affect the head-to-tail cyclization condition results.

Using these conditions that demonstrated no dimerization, we run different experiments with increased concentrations, Table 1.3 to force the reaction by increasing the concentration of starting material and even with longer reaction times.

Table 1.3. In solution head-to-tail cyclization studies of the concentration effect using the same reagents, base and solvent in five different conditions.

	Cond.3	Cond.6	Cond.7	Cond.8	Cond.9
Concentration	1mM	5mM	10mM	50mM	100mM
Reagents	PyBOP/ HOAt	PyBOP/ HOAt	PyBOP/ HOAt	PyBOP/ HOAt	PyBOP/ HOAt
Base	DIEA	DIEA	DIEA	DIEA	DIEA
Solvent	DCM/1% DMF	DCM/1% DMF	DCM/1% DMF	DCM/1% DMF	DCM/1% DMF

As it was observed in the previous 5 experiments, starting material was detected after two days of reaction in all the experiments. The majoritary product was the bicyclic peptide, being detected the cyclodimer as traces only at high concentrations.

With these results in hand, we could conclude that concentration was an important factor when performing macrocyclizations, since the dimerization could appear although in minimal amount when increasing it, but there were other important parameters than could influence even more. In this case, DPPA/NaHCO$_3$/DMF conditions favour more cyclodimerization than PyBOP/HOAt/DIEA/DCM.

Biaryl biyciclic peptides could be obtained without risk of cyclodimerization when using the previously mentioned optimized conditions. Nevertheless, in order to gain access to the cyclodimers, the method was based on the purification of the crude that also contained the bicyclic monomer being the best optimal conditions 50-100mM DPPA/NaHCO$_3$/DMF.

The effect of the solvent was further studied performing the cyclizations at 1mM of DMF and using PyBOP/HOAt/DIEA. Similar results to the ones with DCM and PyBOP/HOAt/DIEA were obtained. No cyclodimer was detected while starting material was still present and the majoritary product was the bicyclic peptide.

Despite the fact that this chapter was devoted to the comparison between the bicyclic and cyclodimerization of the Ala containing peptides, it should be mentioned that for the other peptides prepared during the present thesis, dimerization to be considered and just minimal amounts were detected in some cases but easily isolated during the last step of purification.

1.3.2 SPPS of the cyclodimers

Due to the absence of conditions to exclusively prepare the cyclodimers and with the aim of setting up a methodology to achieve their straighforward synthesis as the only final product, we envisaged a SPPS based strategy (Figure 1.21).

pNZ-(XI)Phe-OH
DIPCDI
HOAt
——→ pNZ-(XI)Phe-D-Pro —⬤

Wang resin

i) 6M SnCl$_2$, 1.6mM HCl/dioxane
in DMF, 3x30min
——————————————————→ Trt-Ala-(XI)Phe-D-Pro —⬤
ii) Fmoc-Ala-OH, PyBOP, DIEA
iii) 20% piperidine/DMF
iv) TrtCl, DIEA; 2x3h

B$_2$Pin$_2$, KOAc,
Pd(dppf)Cl$_2$,
dppf
—————————→ Trt-Ala-(XB)Phe-D-Pro —⬤
DMSO 24h
80ºC

i) TFA/H$_2$O/DCM 2:2:96,3x5min, 1x20 min
————————————————————————→ Fmoc-(XI)Phe-Ala-(XB)Phe-D-Pro —⬤
ii) Fmoc-(XI)Phe-OH, DIPCDI, HOAt

i) 20% piperidine/ DMF
————————————————————→ Trt-Ala-(XI)Phe-Ala-(XB)Phe-D-Pro —⬤
ii) Fmoc-Ala-OH, PyBOP, DIEA
iii) 20% piperidine/DMF
iv) TrtCl, DIEA; 2x3h

Cs$_2$CO$_3$ (3 eq, 2M aq.)
Pd(PPh$_3$)$_4$ (0.1 eq) DMF
60ºC 48h
———————————————————→

Trt-Ala-(X&$_2$)Phe-Ala-(X&$_2$)Phe-D-Pro —⬤

i) TFA/H$_2$O/DCM 2:2:96,3x5min, 1x20min
ii) Fmoc-(XI)Phe-OH, DICPDI, HOAt
————————————————————————→
iii) 20% piperidine/DMF
iv) Fmoc-Ala-OH, PyBOP, DIEA

v) 20% piperidine/DMF
vi) TrtCl, DIEA 2x3h
———————————————→

Trt-Ala-(XI)Phe-DPro-Ala-(X&$_2$)Phe-Ala-(X&$_2$)Phe-D-Pro —⬤

B$_2$Pin$_2$, KOAc,
Pd(dppf)Cl$_2$,
dppf
———————————→ Trt-Ala-(XB)Phe-DPro-Ala-(X&$_2$)Phe-Ala-(X&$_2$)Phe-D-Pro —⬤
DMSO 24h
80ºC

i) TFA/H$_2$O/DCM 2:2:96,3x5min. 1x20 min
ii) Fmoc-(XI)Phe-OH, DIPCDI, HOAt
————————————————————————→
iii) 20% piperidine/DMF
iv) Boc-Ala-OH, PyBOP, DIEA

i) Cs$_2$CO$_3$ (3 eq, 2M aq.)
Pd(PPh$_3$)$_4$ (0.1 eq) DMF
60ºC 48h
————————————————→
ii) 95% TFA, 2.5% H$_2$O,
2.5% TIS

Figure 1.21. Proposed SPPS strategy for the cyclodimers cyclo(Ala-(3&$_1$)Phe-Ala-(3&$_1$)Phe-D-Pro-Ala-(3&$_2$)Phe-Ala-(3&$_2$)Phe-D-Pro) and cyclo(Ala-(4&$_1$)Phe-Ala-(4&$_1$)Phe-D-Pro-Ala-(4&$_2$)Phe-Ala-(4&$_2$)Phe-D-Pro).

The linear cyclodimer precursor could be obtained by SPPS, this decapeptide contains two byaril bridges formed by consecutive Suzuki-Miyaura reactions that could be performed on resin. Until the pentapeptide, the synthesis would be exactly the same described for the bicyclic peptides, considering that in this case Trt protecting group would be used for the fifth residue since further elongation of the peptide on the resin should be done. The remaining part of the sequence would be synthesized exactly as the first part. Miyaura and Suzuki reactions cannot be done in a single step for both staples since it would render to a mixture of products due to the impossibility to control the desired positions during C-C bond formation. After the cleavage of the

peptidyl resin a Porapak™ column would be used for removing palladium from the linear two-stapled pentapeptide crude. This pre purification would be carried out in order to obtain a more pure crude product to be used as starting material of the final head-to-tail cyclization in solution.

After several attempts, the synthesis of the cyclodimers failed when performing borylation at the octapeptide level. The precursor of the borylation was characterized and it is shown in the following figures (Figure 1.22 and 1.23), while after performing Miyaura reaction under the established conditions neither final product (borylated octapeptide) nor starting material (octapeptide) were detected. We hypothesize that the presence of palladium from the first borylation and the Suzuki reaction can affect the iodinated octapeptide, producing a secondary byproduct that can no longer react to form the borylated desired octapeptide.
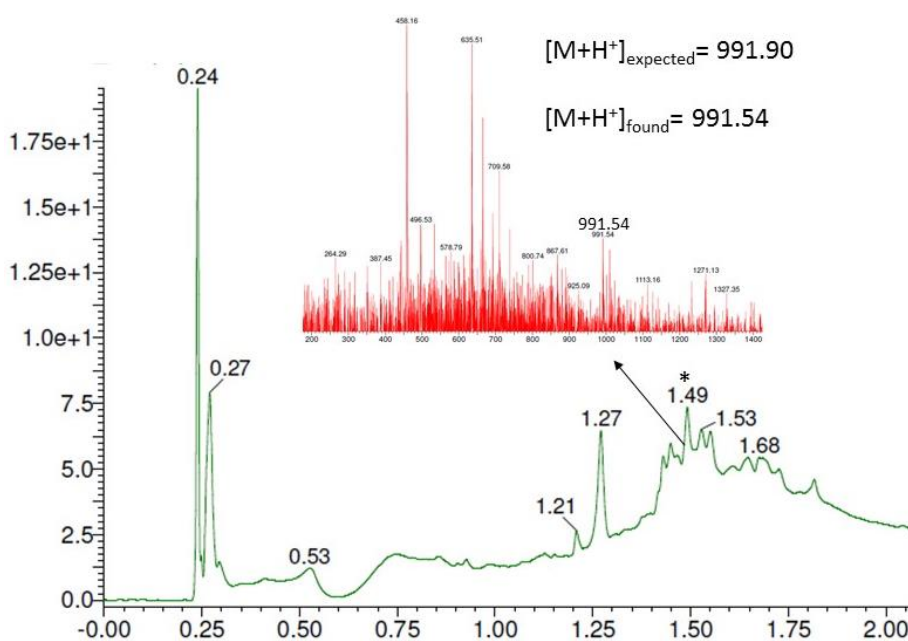
Figure 1.22. UPLC-MS chromatogram of the minicleavage done for the crude peptide H-Ala-(4I)Phe-D-Pro-Ala-(4&2)Phe-Ala-(4&2)Phe-D-Pro-OH in a 0-100% MeCN in 2min gradient, column BEH C$_{18}$ 1.7μm, 2.1x50mm, t$_R$=1.49min.
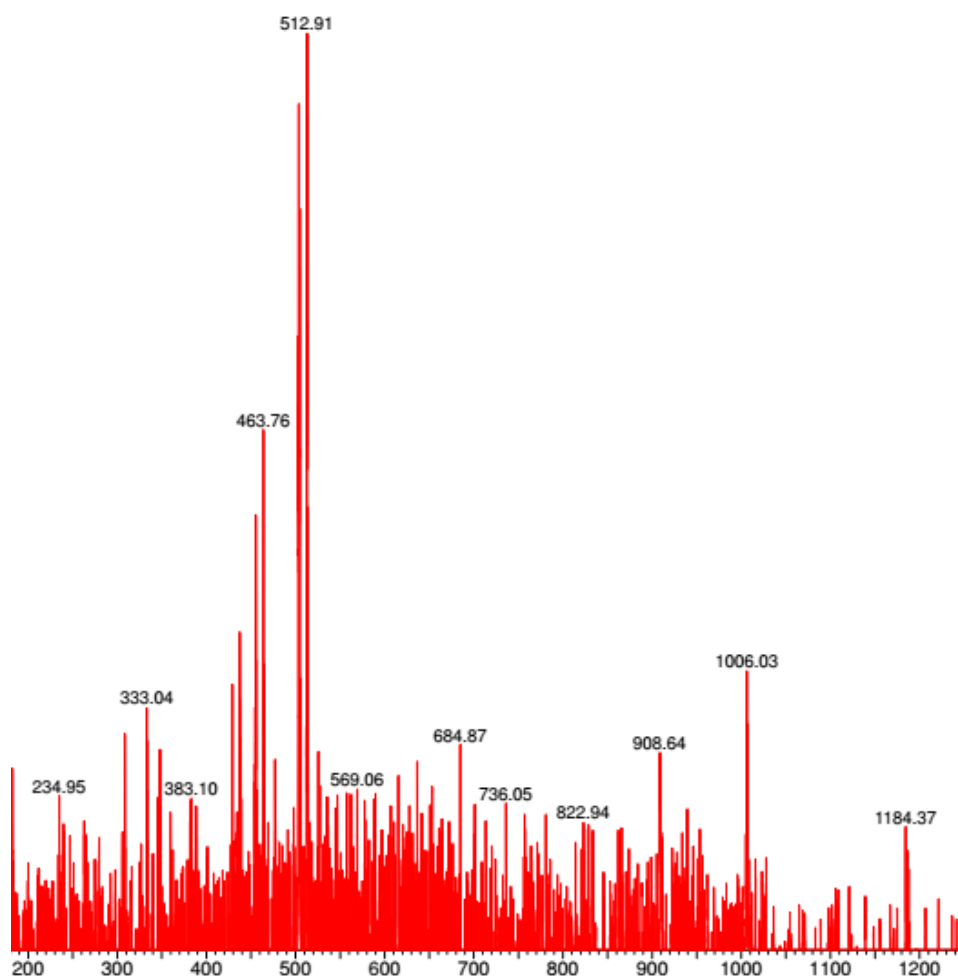
Figure 1.23. UPLC-MS of the minicleavage done for the crude peptide H-Ala-(4B)Phe-D-Pro-Ala-(4&2)Phe-Ala-(4&2)Phe-D-Pro-OH after 48h of Miyaura borylation in a 0-100% MeCN in 2min gradient, colum BEH C$_{18}$ 1.7μm, 2.1x50mm, t$_R$=1.51min; [M+H$^+$]expected= 909.42; this mass was not not found and the mainly observed mass 512.91 could not be assigned to any possible synthethic byproduct.

Although the mass corresponding to the product of interest, H-Ala-(4B)Phe-D-Pro-Ala-(4&)Phe-Ala-(4&)Phe-D-Pro-OH, [M+H$^+$]=909.42 was not found, in order to discard that this was due to detection problems of this product, the synthesis was continued. The following intermeadiates could not be found, confirming that the synthesis failed at the borylation reaction step.

The different intermediate products characterized during the synthesis by control minicleavages are shown in Table 1.4.

Table 1.4. Retention time (t_R) and molecular weight (MW) of the synthetic intermediates characterized by minicleavage during the attempted SPPS of cyclo(-Ala-(4&₁)Phe-Ala-(4&₁)Phe-DPro-Ala-(4&₂)Phe-Ala-(4&₂)Phe-DPro-).

	t_R (min)	MW
*p*NZ-(4I)Phe-D-Pro-CH	6.2	567.59
H-Ala-(4I)Phe-D-Pro-OH	4.8	459.70
H-Ala-(4B)Phe-D-Pro-OH	3.6	378.48
H-(4I)Phe-Ala-(4B)Phe-D-Pro-OH	4.6	651.19
H-Ala-(4I)Phe-Ala-(4B)Phe-D-Pro-OH	4.6	722.33
H-Ala-(4&)Phe-Ala-(4&)Phe-D-Pro-OH	4.4	550.09
H-DPro-Ala-(4&)Phe-Ala-(4&)Phe-D-Pro-OH	4.5	647.20
H-Ala-(4I)Phe-D-Pro-Ala-(4&)Phe-Ala-(4&)Phe-D-Pro-OH	5.6	991.54

1.3.3 NMR characterization

NMR studies of the cyclodimers were carried out by Dr. S. Royo and Dr. J. Garcia in order to characterize these novel compounds. Figures 1.24 and 1.25 show the ^{1}H-NMR spectra acquired for both products. For the seek of clarity, an expansion of the aromatic region is displayed in the upper part of both Figures. Significant differences were observed, as expected, between the two compounds due to the positions of the aromatic ring involved in the stapling.
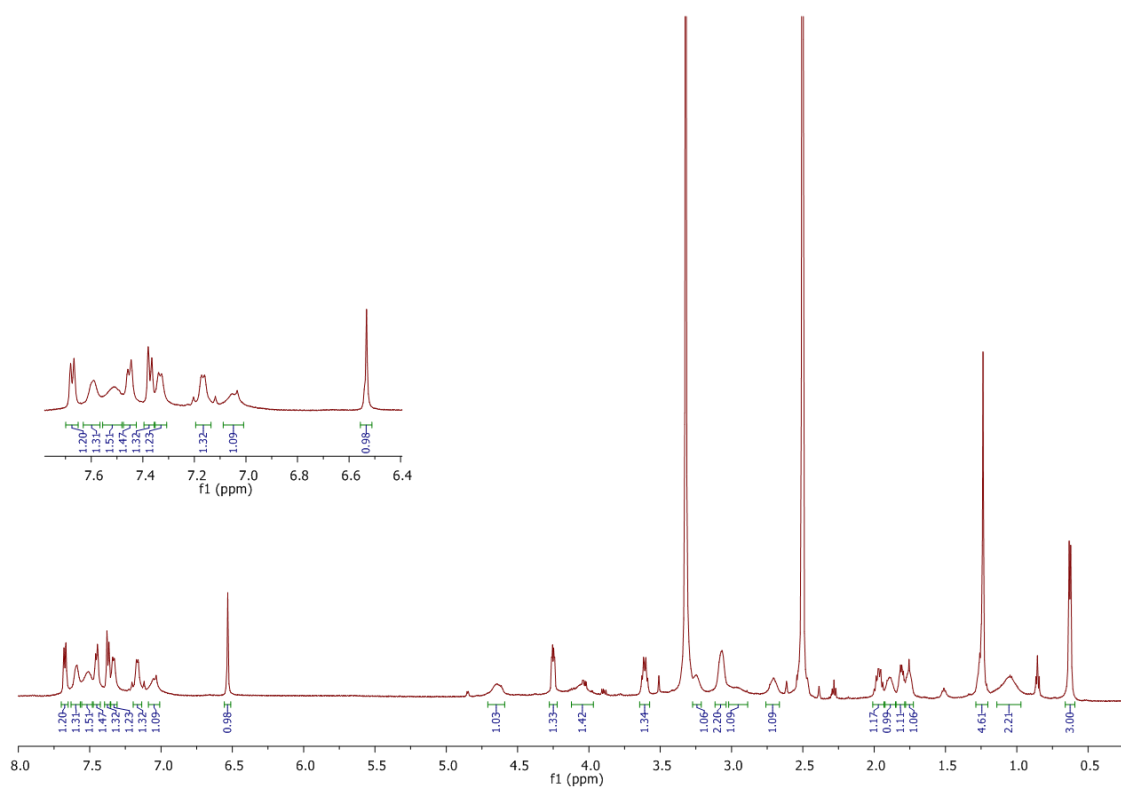
Figure 1.24. ^{1}H-NMR spectrum of cyclo(Ala-(4&$_1$)Phe-Ala-(4&$_1$)Phe-D-Pro-Ala-(4&$_2$)Phe-Ala-(4&$_2$)Phe-D-Pro) at 6mM in DMSO, 298K, 600MHz.
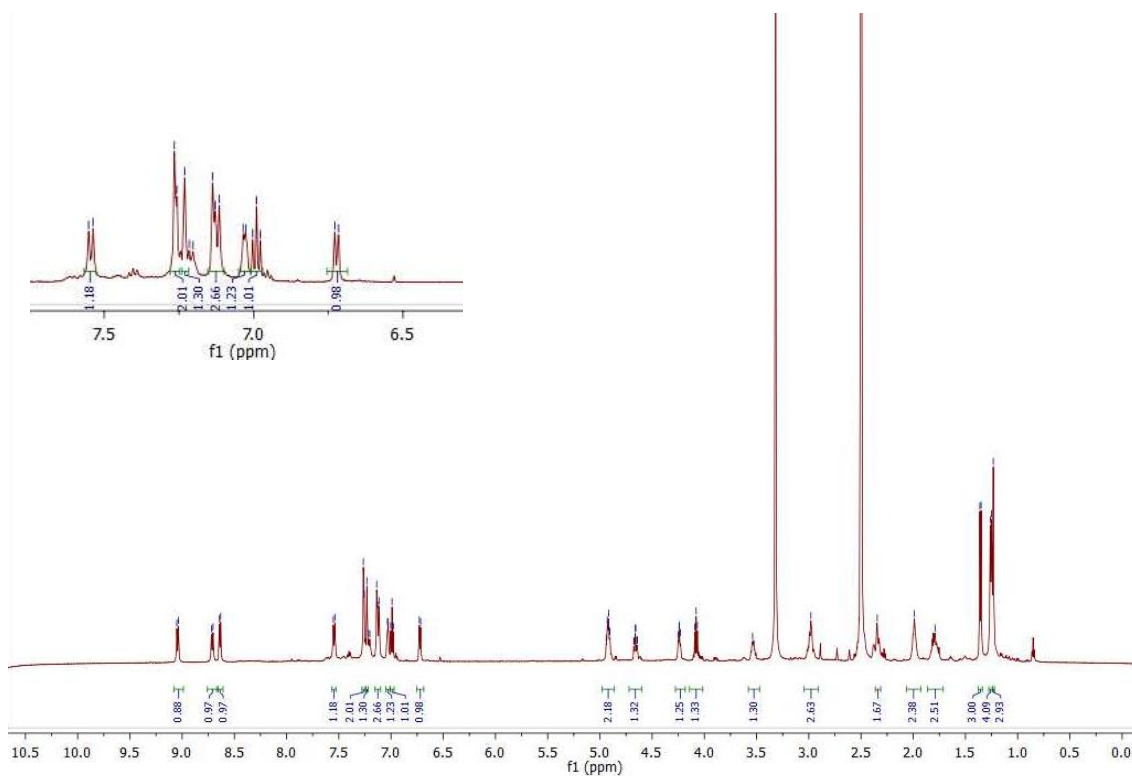
Figure 1.25. ^{1}H-NMR spectrum of cyclo(-Ala-(3&$_1$)Phe-Ala-(3&$_1$)Phe-D-Pro-Ala-(3&$_2$)Phe-Ala-(3&$_2$)Phe-D-Pro) at 6mM in DMSO, 298K, 600MHz.

1.3.4 Computational studies

After having realized about the existence of the cyclodimers, we were interested in studying the structural aspects of these new products as it was previously done with the bicyclic monomers.

Dr. F. Colizzi from Prof. M. Orozco research group at IRB Barcelona perfomed some molecular dynamics assays in order to determine the possible structure of the *meta-meta* and *para-para* cyclodimers, as well as, the differences between them.

In Figure 1.27, dynamic simulations of both cyclodimers peptides were illustrated. Structures were grouped in six clusters. Cluster population ratio showed that for the *para-para* version there was a majority structure, around 70% occupancy, which displays an interesting β-hairpin. Although, it should be mentioned that the second most populated structure, less than 20% occupancy, did not reveal this structure. These two major structures may correlate with the high rigidity that was also detected for the monomeric bicyclic *para-para* peptide.

Regarding the *meta-meta* version, the occupancy was more divided into the six different clusters being two major with around 50% and 20%. Therefore, more flexibility was observed for this peptide, as it was observed for the *meta-meta* version of the monomeric bicyclic one. Furthermore, four of the six clusters possessed structures with β-hairpin.

A   **B**
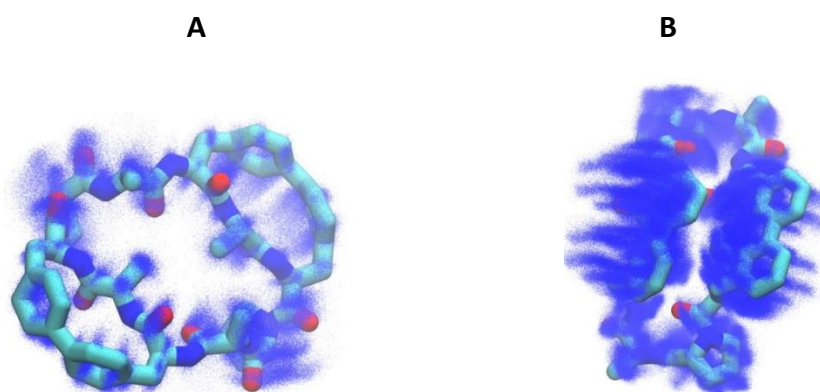
Figure 1.26. Snapshots of the simulation of cyclodimers A)*para-para* **B)***meta-meta.* **Orientation of the biaryl motif can flunctuate as displayed in these illustrations. Less population of the β-hairpin in the** *para-para* **peptide were observed also in equilibrium with more open conformations.**
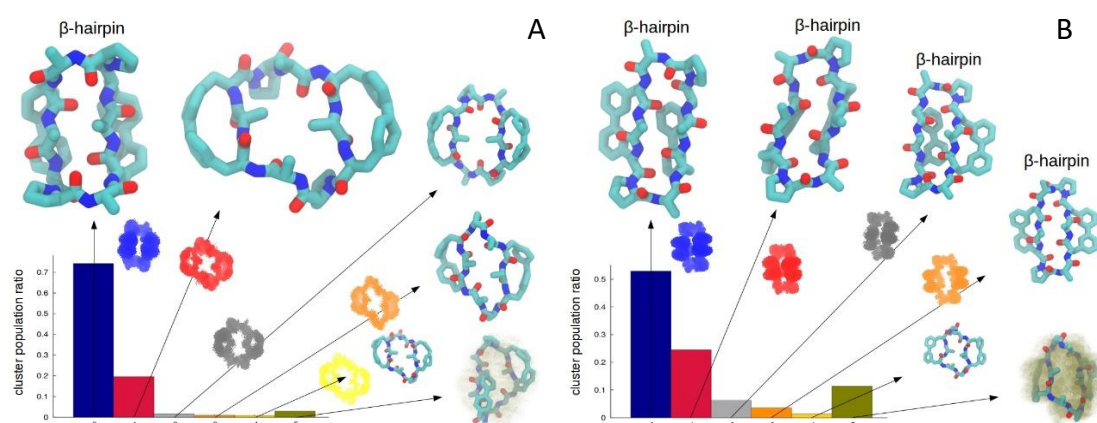
Figure 1.27. Cluster population ratios of the cyclodimers after simulation A) *para-para* B) *meta-meta*. β-hairpin scaffold was mainly present in the different obtained structures for *meta-meta* construct. For the *para-para* version, β-hairpin looked more distorted and, consequently, less stable and/or populated.

Despite of having different flexibilities, both versions *para-para* and *meta-meta*, were hypothesized to display β-hairpin structures. In this context, the presence of the two D-Pro may be responsible of the appearance of this secondary structure.

Moreover, the obtained results were consistent with the dihedral angle restraints ($^3J_{HH}$) obtained for the *meta-meta* version in the NMR experiment. Large coupling constants, J> 8Hz, are characteristic of a β–sheet conformation, validating the molecular dynamics performed (Table 1.5) . In Figure 1.28, the amino acids involved in the measurement of the constants are labelled.

Table 1.5. Calculated $^3J_{HH}$ (Hz) in NMR experiments for *meta-meta* version at 298K.

<div align="center">

$^3J_{HH}$ **(Hz)**

</div>

H^N Ala^A	H^N Phe^A	H^N Ala^B	H^N Phe^B
8.7	8.8	7.2	8.9
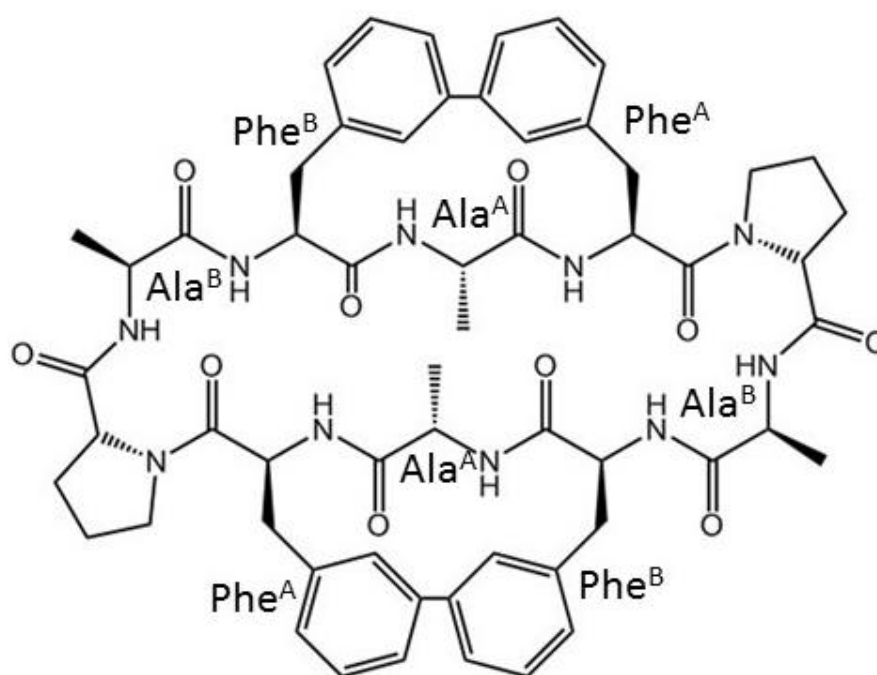
Figure 1.28. Assignement of the amino acids involved in the calculation of the coupling constants, $^3J_{HH}$.

1.3.5 Circular dichroism studies

Encouraged by the obtained results during simulations and the hypothesized secondary structure of the cyclodimers, circular dichroism characterization was carried out.

Circular dichroism was not performed in water due to the poor solubility of the cyclodimers. Estimated isoelectric point (pI) was ~7, therefore basic conditions were used as buffer, selecting 10mM ammonium carbonate pH 10. Improved solubility of the compounds was observed. We hypothesized that H-bonding interactions which could imply poor water solubility can be disrupted by the used buffer conditions.

Noteworthy, CD spectra of both peptides displayed bands corresponding to secondary structure although they were significantly different (Figure 1.29).

A
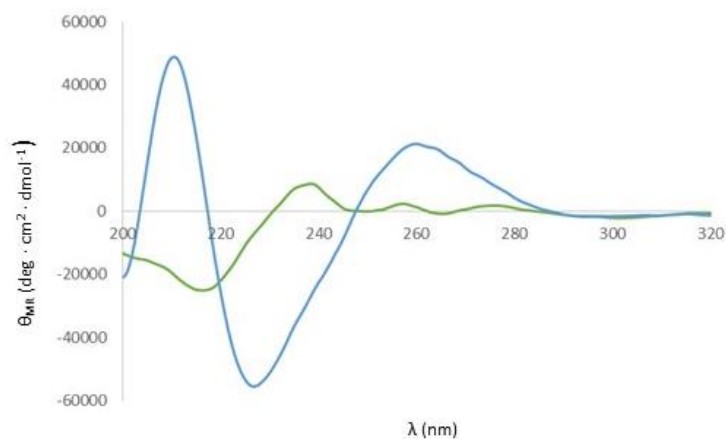
B
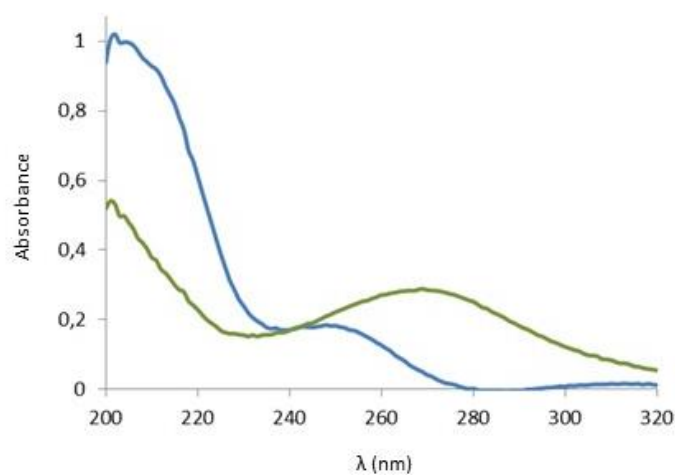
Figure 1.29. A) CD spectra of 30 µM concentration cyclodimers *meta-meta* in blue and *para-para* in green at 25°C in 10mM ammonium carbonate buffer pH 10, B) UV spectra of 30 µM concentration cyclodimers *meta-meta* in blue and *para-para* in green at 25°C in 10mM ammonium carbonate buffer pH 10.

Cyclodimer *meta-meta* displayed a negative band at 227nm and a positive band at 210nm. The spectrum could be assigned to a turn secondary structure, although a mixture of different conformations were present since the classical spectrum was not observed.

Regarding the *para-para* version, CD spectrum showed a negative band at 217nm, characteristic of β-secondary structure, such as the proposed β-hairpin.

In the light of these results and together with the NMR data, we could confirm the different conformation of the cyclodimers, being the stapling position the responsible of that.

Correlating these results with the simulations previously run we could hypothesized that the clearer secondary structure of the *para-para* version was related to the higher occupancy in the simulations of this structure, allowing a better defined secondary structured organization of the peptide. On the other side, despite the existence of β-hairpin structures in the differents clusters for the simulation of the *meta-meta* peptide, lower occupancy of them could lead to an equilibrium which translates into the turn-type CD spectrum.

CD spectra of the peptides were also performed at 5°C, since lowering temperature is a common strategy to stabilize β-conformations and could slow down the equilibrium.
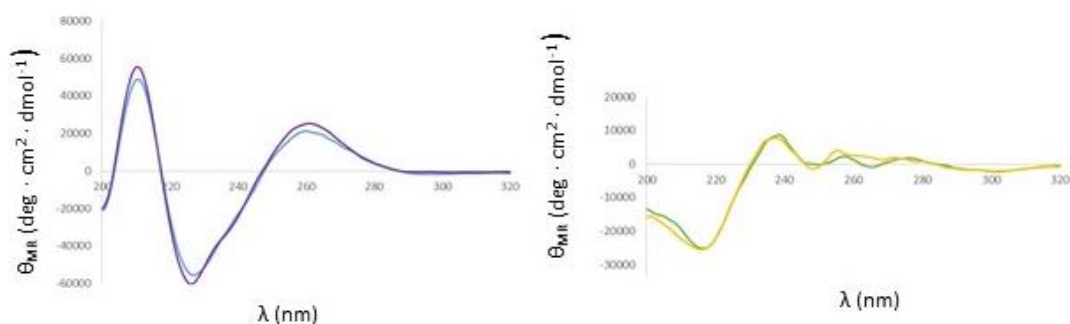
Figure 1.30. CD spectra of 30μM cyclodimers in 10mM ammonium carbonate pH 10. a) *meta-meta* **peptide in blue at 25°C, in purple 5°C b)** *para-para* **peptide in green 25°C, in purple 5°C.**

Overlap of both *meta-meta* and *para-para* peptides at different temperatures was observed in Figure 1.30 showing very similar results. Lowering temperature slightly changed the CD spectra. Therefore, we could hypothesize that fast equilibrium did not take place in these molecules.

1.4 Expanding the synthetic methodology to other functionalities

Once it was confirmed that the biaryl bicyclic pentapeptides could be synthesized, we aimed to expand the synthetic methodology to other families of compounds that could introduce other functional groups to the general scaffold. This versatility was very relevant when aiming to use these compounds for recognition of protein surfaces.

All the following sequences prepared and described were based on the *para-para* stapling model peptide. *Meta-meta* versions of these peptides should be accessible under a similar protocol since the synthesis of both scaffolds is analogous. Extra difficulties must only be considered when including additional substituents in the aromatic ring side-chain of the involved phenylalanines.

Para-para versions were selected mainly due to the higher rigidity of the scaffold seen by the molecular dynamic simulations.

The first requirement to achieve these novel compounds was the proper selection of the orthogonal protecting groups for the side-chain of the amino acids. Those permanent protecting groups must be stable under basic conditions, used to remove Fmoc (the temporary protecting group of some residues) and in the medium for Miyaura borylation and Suzuki cross-coupling reactions. Furthermore, stability in front of palladium was also mandatory to avoid undesired removal, since palladium was used as the catalyst for the previously mentioned reactions. In addition to this, the orthogonality with some temporary protecting groups such as Trt or Boc should be also taken into account, as well as, the resistance to cleavage conditions (95% TFA).

1.4.1 Lysine family

The first amino acids selected to be introduced in the general scaffold were lysines. This amino acid contains a positive charge and a hydrophobic side-chain that can

balance hydrophobicity and hydrophilicity enhancing solubility of the final bicyclic product.

Figure 1.31 shows the synthetic scheme for the synthesis of the sequence cyclo(Lys-(4&)Phe-Lys-(4&)Phe-D-Pro), which was based on the one described for the parent peptide cyclo(Ala-(4&)Phe-Ala-(4&)Phe-D-Pro) (Figure 1.2) but including the proper protecting groups for the side-chain of lysines, as well as, the final deprotection in solution.
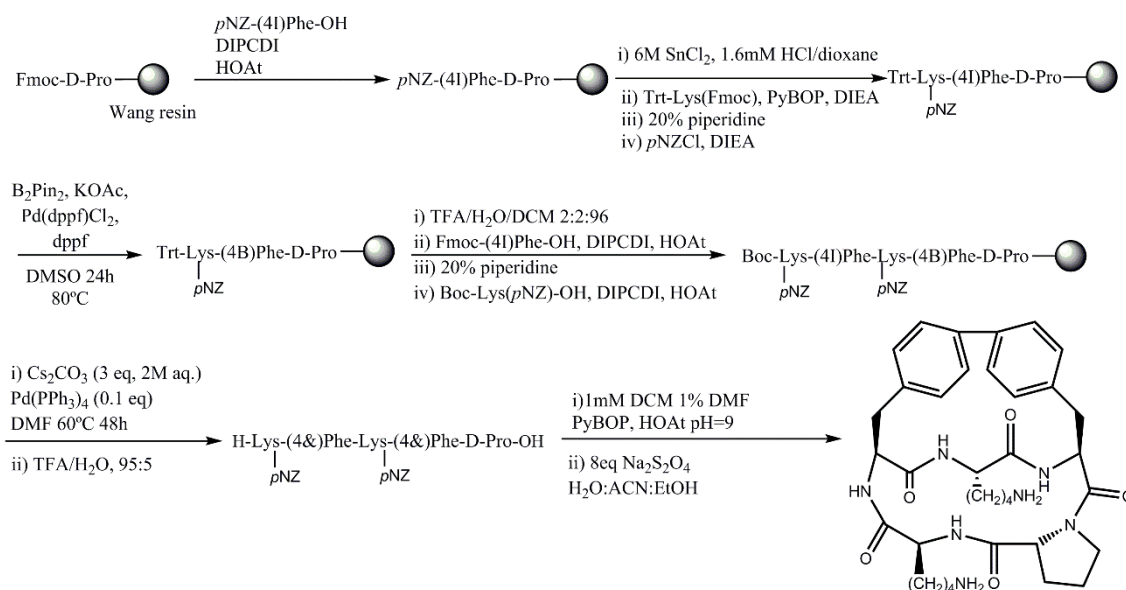
Figure 1.31. SPPS strategy of cyclo(Lys-(4&)Phe-Lys-(4&)Phe-D-Pro).

Regarding the introduction of the first lysine, the temporary protecting group was Trt, as in the general strategy while side-chain was protected with *p*NZ. Trt-Lys(Fmoc)-OH is commercially available, being this amino acid introduced in the sequence. Exchange of Fmoc for *p*NZ could be easily performed on resin. As it is described in Figure 1.32, this protecting group was compatible with with basic and palladium-catalyzed condition, as well as, stable under high acidic medium used for cleaving the peptide from Wang resin. It is worth mentioning that *p*NZ was previously used as the temporary protecting group of the second residue, therefore, washings of the resin should be performed carefully to ensure the avoidance of even traces of the reagents used for its removal. In addition, the neutralization in the following step helped to prevent the undesired

removal of this protecting group. The last amino acid, Boc-Lys(*p*NZ)-OH was introduced with the proper protecting groups due to their availability.
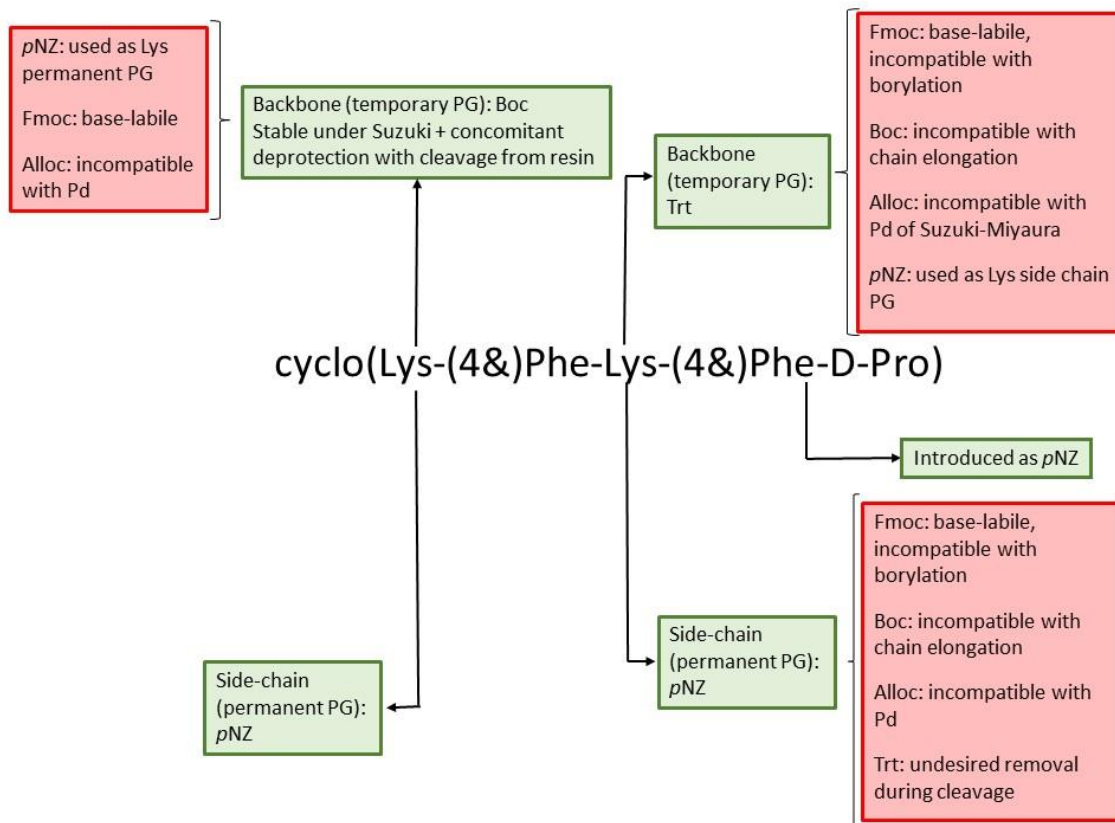
Figure 1.32. Protecting group scheme for the synthesis of cyclo(Lys-(4&)Phe-Lys-(4&)Phe-D-Pro).

Removal of side-chain protecting groups was performed after head-to-tail cyclization to avoid byproducts. *p*NZ removal in solution was studied at two diffent conditions.

The same $SnCl_2$/HCl mixture, which was used to deprotect *p*NZ on solid-phase, was discarded in solution since the reaction did not proceed.

Finally, the strategy to remove *p*NZ in solution was based on reductive conditions with $Na_2S_2O_4$. This reaction was especially difficult and required long reaction times to achieve full deprotection.

After having synthesized the biaryl bicyclic peptide containing two lysines, we envisaged the potential exploration of what we called the bridge effect. We questioned ourselves whether the presence of the biaryl staple could have some

beneficial or detrimental effects into these new synthesized peptides. As it will be discussed in Chapter 2, the properties that we decided to study were the permeability by passive diffusion, one of the existing mechanisms to cross the blood-brain barrier, the protease resistance and their cytotoxicity.

In general, stapled peptides are considered to be privileged structures with enhanced permeability and biostability, for this reason it was interesting to test whether the biaryl motif also follows this tendency. Furthermore, bicyclic peptides could have an increase in these properties due to the head-to-tail cyclization. Therefore, we decided to rule out that possibility by studying separately the effect of the biaryl bridge and the head-to-tail cyclization.

A set of three control peptides was prepared to achieve this goal (Figure 1.33). A linear peptide H-Lys-Phe-Lys-Phe-D-Pro-OH, a linear stapled H-Lys-(4&)Phe-Lys-(4&)Phe-D-Pro-OH and a head-to-tail cyclic cyclo(-Lys-Phe-Lys-Phe-DPro-). It should be taken into account that the synthesis of each peptide followed a different scheme owing to the significant differences with the parent bicyclic peptide.
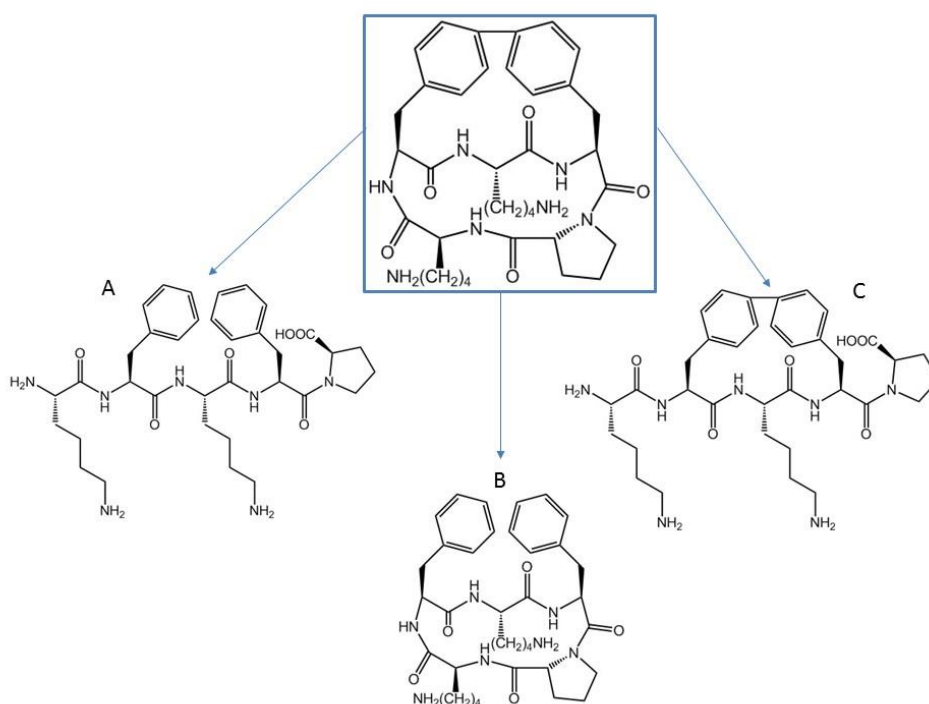
Figure 1.33. Lysine family: parent bicyclic peptide remarked in the box and the set of three control peptides being (A) linear H-Lys-Phe-Lys-Phe-D-Pro-OH, (B) head-to-tail cyclic cyclo(Lys-Phe-Lys-Phe-D-Pro) and (C) linear stapled H-Lys-(4&)Phe-Lys-(4&)Phe-D-Pro-OH.

The linear pentapeptide was synthesized using standard Fmoc/*t*Bu SPPS with 2-chlorotrityl resin and concomitant cleavage and deprotection of Boc side-chain protecting groups. The head-to-tail cyclic peptide was prepared with a similar protocol by using mild cleavage conditions (2% TFA/ 98% DCM) to maintain lysine side-chains protected until cyclization in solution was finished, once cyclic peptide was formed, Boc removal in solution was carried out. The linear stapled peptide was prepared with the same protocol of the bicyclic but using Boc as lysine protecting group which was removed during the cleavage from the resin.
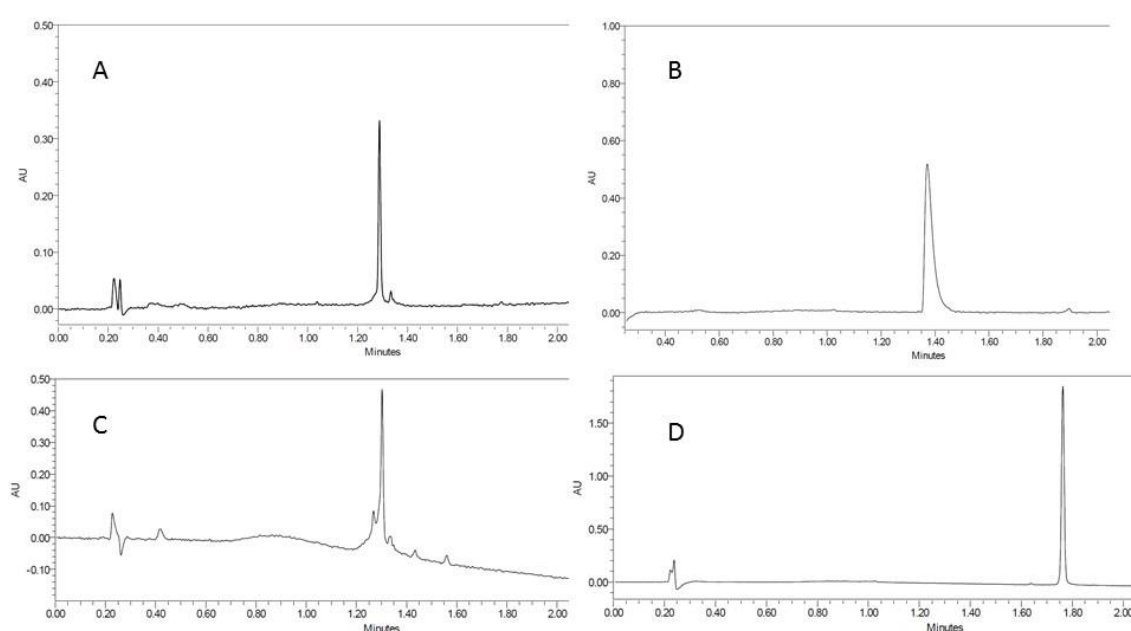
Figure 1.34. UPLC chromatogram of the pure peptides in a gradient 0-100% MeCN in 2 min. Column BEH C$_{18}$, 3.5 μm, 2.1x50mm. A) linear, H-Lys-Phe-Lys-Phe-D-Pro-OH, t$_R$= 1.27min B) head-to-tail cyclic, cyclo(-ys-Phe-Lys-Phe-D-Pro), t$_R$= 1.40min C) linear stapled, H-Lys-(4&)Phe-Lys-(4&)Phe-D-Pro-OH, t$_R$= 1.28min D) bicyclic, cyclo(Lys-(4&)Phe-Lys-(4&)Phe-D-Pro), t$_R$= 1.76min.

1.4.2 Arginine family

Introduction of other positively charged residues was also considered. Arginine was selected due to the presence of guanidinium functional groups in the side-chain.

Previous studies in the group unveil the relevance of this functional group in protein surface recognition[187,188]. Dr. M. Martinell's thesis proved that linear peptides displaying different guanidinium groups were able to target p53 tetramerization domain surface, due to the presence of negative charges in the α-helices of this protein.

Moreover, Dr. S. Gordo thesis studied the use of calixarenes displaying four guanidinium groups to recover the self-assembly of mutated p53TD proteins, involved in adrenocortical carcinoma common in south of Brazil[156].

Synthesis of the biaryl bicyclic pentapeptide displaying two arginine residues at the variable positions of the scaffold did not introduce much complexity to the general strategy. Pbf protecting group, was selected due to its stability towards basic and palladium-catalyzed conditions. Furthermore, owing to the compatibility of the guanidinium groups with the head-to-tail cyclization conditions, it was not necessary to maintain the side-chain protecting groups during the cyclization, being concomitantly removed during cleavage from the resin at high acidic conditions.
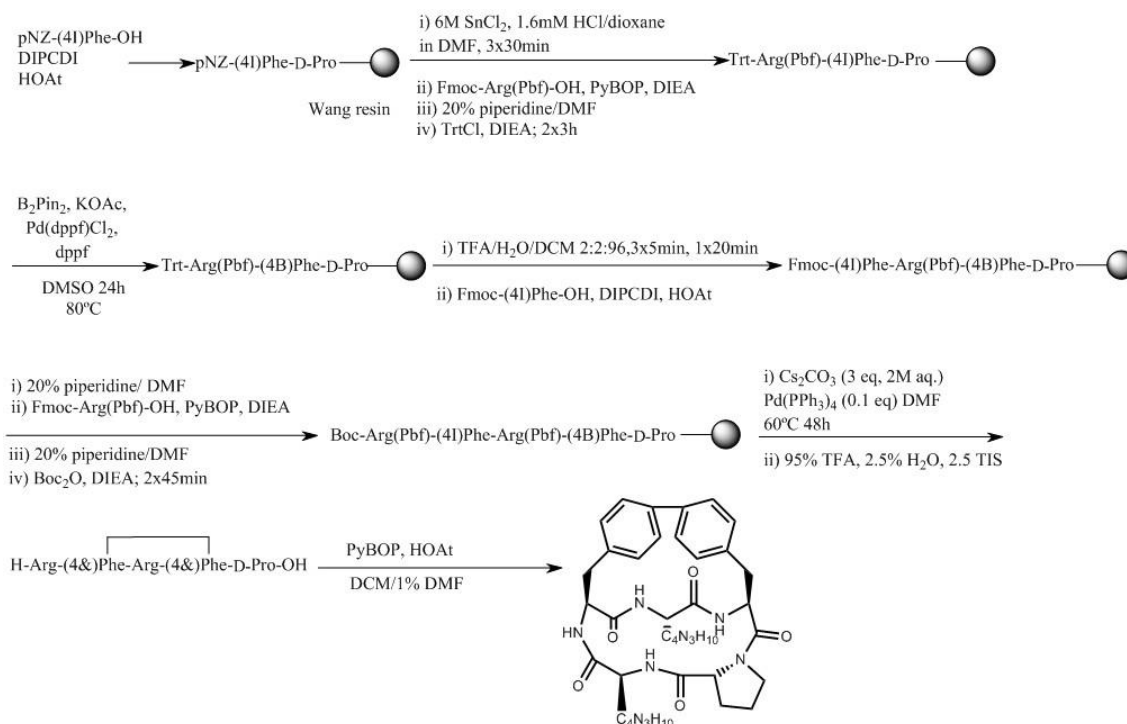
Figure 1.35. SPPS strategy of cyclo(Arg-(4&)Phe-Arg-(4&)Phe-D-Pro).

As for the lysine family, three control peptides (linear, linear stapled and head-to-tail cyclic) were prepared to evaluate the bridge effect in the case of the arginine family. The linear pentapeptide used standard Fmoc/*t*Bu SPPS with 2-chlorotrityl resin and cleavage from the resin at high acidic conditions with concomitant deprotection of arginine side-chains. The head-to-tail cyclic peptide was prepared under the same protocol but including the last step of head-to-tail cyclization in solution. The linear stapled peptide was synthesized using Wang resin with the same protocol of the parent bicyclic peptide finishing once cleavage from the resin was performed.
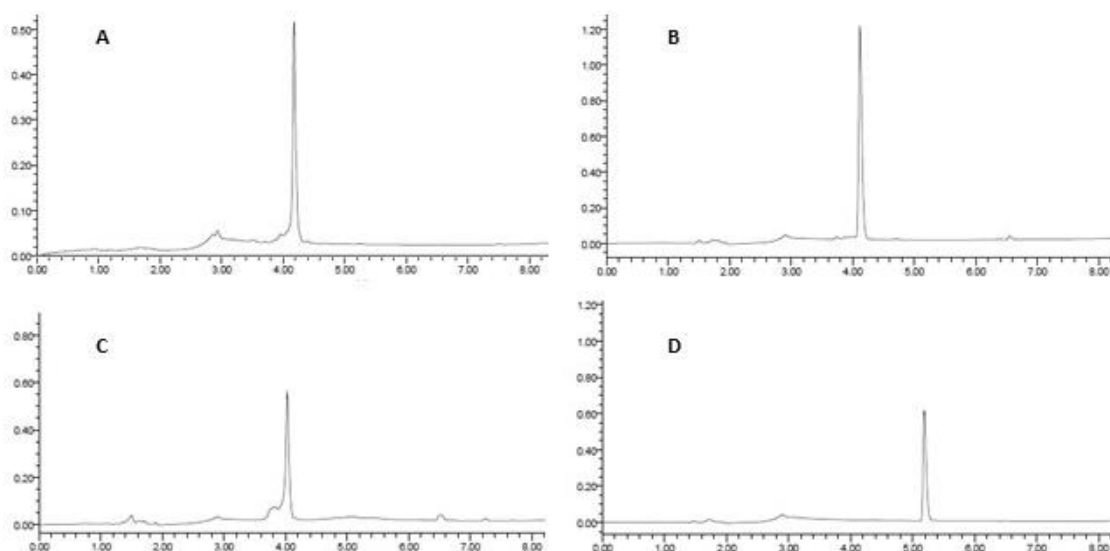
Figure 1.36. UPLC chromatogram of the pure peptides in a gradient 0-100% MeCN in 8 min. Column SunFire C₁₈, 1.7 µm, 4.6x100mm. A) linear, H-Arg-Phe-Arg-Phe-D-Pro-OH, t_R= 4.15min B) head-to-tail cyclic, cyclo(Arg-Phe-Arg-Phe-D-Pro), t_R= 4.07min C) linear stapled, H-Arg-(4&)Phe-Arg-(4&)Phe-D-Pro-OH, t_R= 4.01min D) bicyclic, cyclo(Arg-(4&)Phe-Arg-(4&)Phe-D-Pro), t_R= 5.20min

1.4.3 Serine family

In addition to the incorporation of positively charged amino acids, we aimed to prove the versatility of the synthetic strategy to incorporate residues with other kind of functional groups. In this context, serine amino acid was selected.

Serine was commercially available with benzyl protecting group in the side-chain. This protecting group was orthogonal with the choosen methodology, which means that no extra steps were required to be incorporated during the synthesis.

In fact, primary alcohol present in serine side-chain was also reactive under Miyaura borylation and Suzuki cross-coupling reaction conditions which required its suitable protection. Benzyl protecting group demonstrated to be stable under these conditions. Moreover, concomitant cleavage from the resin and deprotection were performed under 95% TFA avoiding additional steps in solution due to the lack of possible side reactions during head-to-tail cyclization. The synthesis of the serine biaryl bicyclic peptide is shown in Figure 1.37.
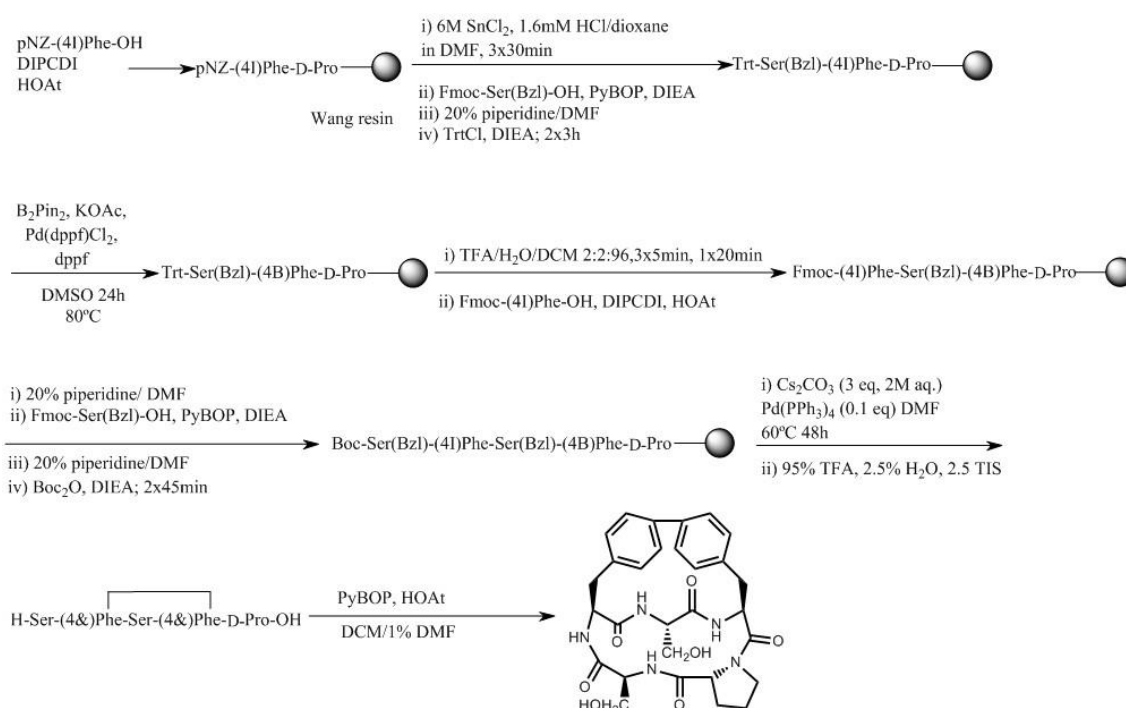
Figure 1.37. SPPS strategy of cyclo(Ser-(4&)Phe-Ser-(4&)Phe-D-Pro).

Due to the interest of studying the effect of the biaryl bridge in this hydrophilic peptide, three controls peptides were prepared. The linear version was synthesized using standard Fmoc/*t*Bu strategy in 2-chlorotrytil resin and using high acidic cleavage conditions to obtain the unprotected peptide. Head-to-tail cyclic peptide was prepared

under similar conditions but with a final cyclization in solution step. Finally, linear stapled peptide was synthesized as the biaryl bicyclic until cleavage from the resin was performed, then Porapak™ column and HPLC-semipreparative purification of the crude rendered the desired bicyclic peptide.
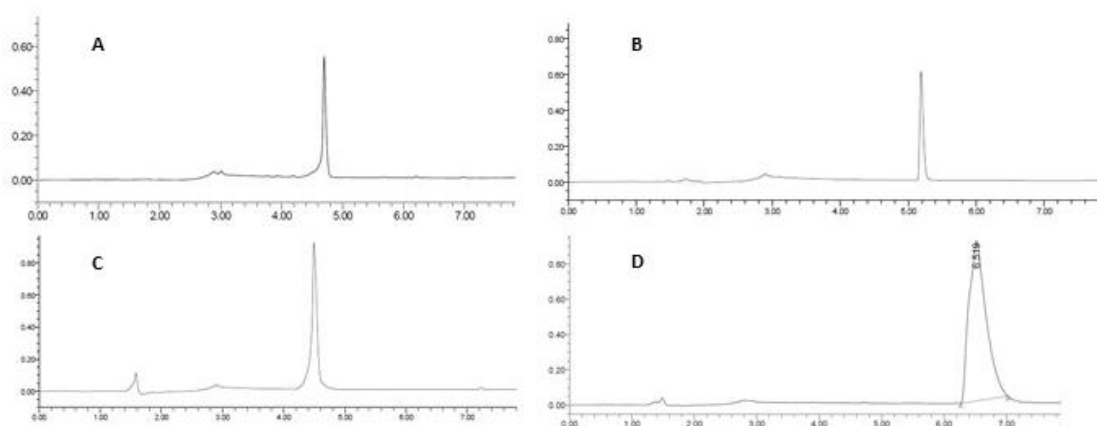
Figure 1.38. UPLC chromatogram of the pure peptides in a gradient 0-100% MeCN in 2 min. Column BEH C$_{18}$, 1.7 µm, 2.1x50mm. A) linear, H-Ser-Phe-Ser-Phe-D-Pro-OH, t$_R$= 4.64min B) head-to-tail cyclic, cyclo(Ser-Phe-Ser-Phe-D-Pro), t$_R$= 5.18min C) linear stapled, H-Ser-(4&)Phe-Ser-(4&)Phe-D-Pro-OH, t$_R$= 4.43min D) bicyclic, cyclo(Ser-(4&)Phe-Ser-(4&)Phe-D-Pro), t$_R$= 6.54min

1.4.4 Expanding the ring size of the cyclodimers and introducing γ-branched amino acids

Another type of peptide which was attempted to be synthesized was the ones with the following sequence cyclo(Ala-(4&$_1$)Phe-Leu-Leu-(4&$_1$)Phe-D-Pro-Ala-(4&$_2$)Phe-Leu-Leu-(4&$_2$)Phe-D-Pro). The sequence of this peptide was based on the first model of the cyclodimers but the chain was extended to twelve amino acids. This peptide included the two new residues between the aromatic amino acids, and the last residue was alanine. The stapling between phenyalanines was established between the *para* positions of the aromatic rings to be able to compare this dodecapeptide with the previously synthesized cyclodimers. The selected aliphatic residues were two L-leucines.

Following the same strategy described for the cyclodimers of the model peptide, the novel cyclodimer with 12 residues was synthesized. Specifically, the aim was not only to expand the size of the cyclodimers but also to study the effect of the introduction of two γ-branched amino acids (leucine) in their structure. It is worth to be mentioned that γ-branched amino acids, such as leucine, have a high helix-forming tendency (Figure 1.40).

Not only had we hypothesized that this fact could affect the overall conformation of the cyclodimers but also the introduction of these amino acids may have an impact on the Suzuki and/or the head-to-tail cyclization reactions. So, depending on the side-chain of the residues and the presence of one or two, the Suzuki and cyclization reactions may be favoured or hindered.
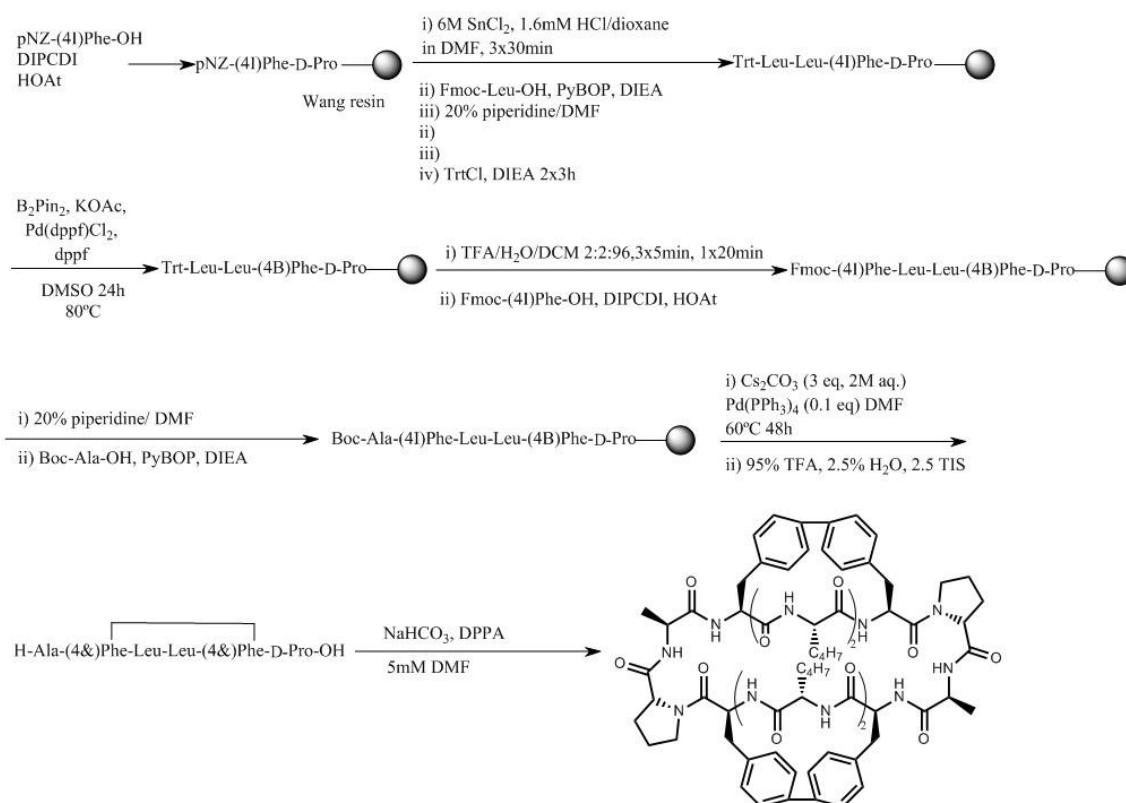
Figure 1.39. SPPS strategy of cyclo(Ala-(4&₁)Phe-Leu-Leu-(4&₁)Phe-D-Pro-Ala-(4&₂)Phe-Leu-Leu-(4&₂)Phe-D-Pro).

After performing the synthesis of the peptide, no remarkable differences during the borylation, Suzuki or cyclization reactions were observed. So it seems that the incorporation of an extra amino acid between the stapled phenylalanine and the fact that these amino acids are γ-branched were not able to favour or hinder these reactions in a relevant manner, at least for this specific peptide sequence. Nevertheless, in order to confirm this hypothesis a representative study including more cyclodimer peptide sequences would be required.
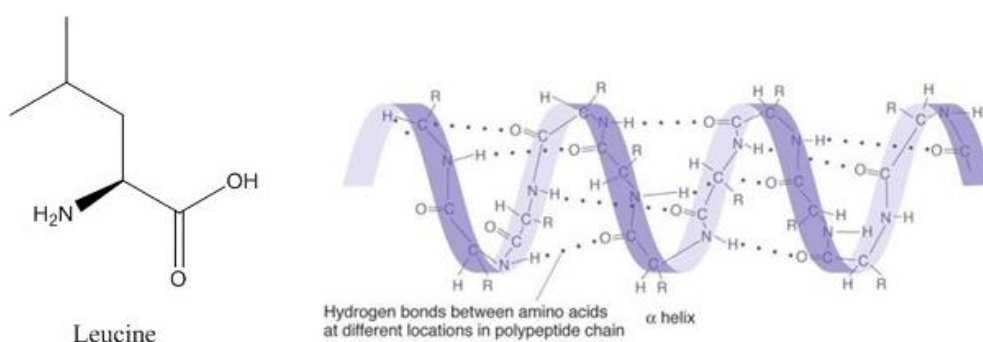
Figure 1.40. α-helix and β-sheet tendency of leucine amino acids.
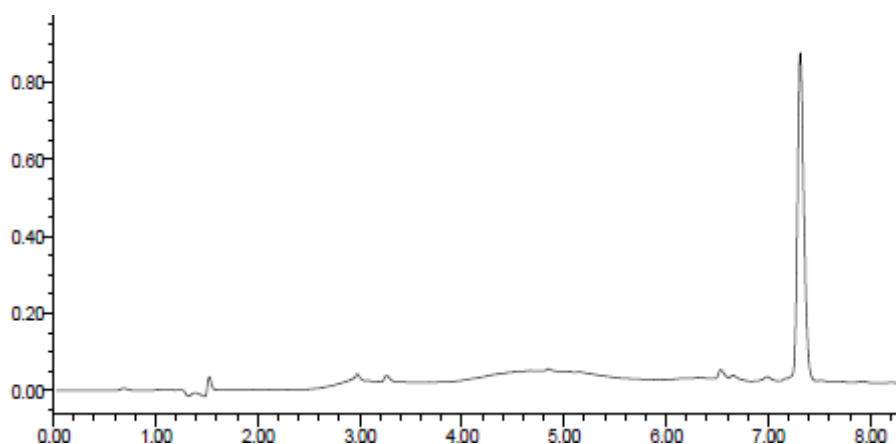
Figure 1.41. HPLC chromatogram of pure peptide cyclo(Ala-(4&1)Phe-Leu-Leu-(4&1)Phe-D-Pro-Ala-(4&2)Phe-Leu-Leu-(4&2)Phe-D-Pro) in a 0-100% MeCN in 8min gradient. Column SunFire C_{18} 3.5μm, 4.6x100mm, t_R=7.34min.

This new cyclodimer was studied by circular dichroism. Samples were dissolved in the same buffer to compare the results with the previous studied cyclodimers.
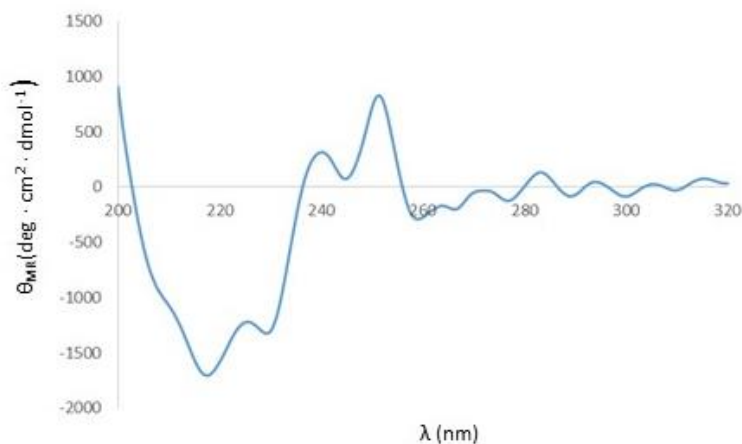
Figure 1.42. CD spectrum of cyclo(Ala-(4&)Phe-Leu-Leu-(4&)Phe-D-Pro-Ala-Leu-Leu-(4&)Phe-D-Pro) at 50µM concentration in 10mM ammonium carbonate pH 10 at 25ºC.

As it was observed for the previous *para-para* cyclodimer peptide, there was a negative band at 227nm while in this case there were two others at 218nm and 208nm, similar to the CD spectra of α-helix conformation. Nevertheless, it was not possible to unequivocally assign the secondary structure of the peptides. The most valuable information that these experiments provide us was the similarity between the peptides with the stapling *para-para* and the clearly different conformation observed with the one in *meta-meta.*

In summary

Biaryl bicyclic peptides were obtained using a solid-phase peptide synthesis approach based on the on-resin Miyaura borylation and Suzuki cross-coupling reactions. The last step of head-to-tail cyclization in solution was extensively studied. Furthermore, monomeric peptides as well as cyclodimers can be obtained from this last reaction according to the choosen conditions. Specifically, we observed that the effect of the solvent, the base and the coupling reagents have a real influence in the rendered product. Previous methodology was mainly focused on the concentration of the head-to-tail cyclization in solution. In the light of our latest results, we were able to confirm that concentration is another parameter to be considered. Nevertheless, dilution degree depends also on the different conditions of the set up.

Regarding the cyclodimers of the model peptides, NMR studies together with circular dichroism and computational simulations unveiled the relevance of the stapling positions between the phenyalanine residues. This result was of great interest; although the followed synthetic strategy was the same, the *para-para* and *meta-meta* versions displayed different conformations. In this context, cyclodimer ring was also expanded by the introduction of two amino acids between the stapling. This new construct, stapled in *para-para,* displayed a similar conformation as the *para-para* model scaffold, once again demonstrating the effect of the bridged positions in the conformation of the product.

Regarding the involved positions of the biaryl, monomeric peptides also showed significant differences in the run molecular dynamic simulations. Rigidity of the *para-para* peptide was higher than for the *meta-meta* version.

Although non trivial and despite the low final yields, the challenging synthesis of these complex bicyclic peptides have been successfully achieved and expanded to other functionalities.This straightforward design allowed the synthesis of different kind of

bicyclic peptides modifying the character of the introduced amino acids. Using an appropriate protecting group scheme, different families of peptides were prepared for further characterization assays. Therefore, this strategy paves the way to gaining access to mono or bicyclic peptides introducing a biaryl motif in their structures and allowing the incorporation of different functional groups; this being of great relevance for the possible application of these compounds in protein surface recognition.

Bibliography

[182] J. Klose, A. Ehrlich, M. Bienert, Influence of proline and β-turn mimetics on the cyclization of penta- and hexapeptides, *Letters in Peptide Science* **1998**, *5*, 129-131.

[183] J. Spengler, J.C. Jiménez, K. Burger, E. Giralt, F. Albericio, Abbreviated nomenclature for cyclic and branched homo- and hetero-detic peptides, *J. Peptide Res.* **2005**, *65*, 550.

[184] H. G. Kuivila, J. F. Reuwer, Jr., J. A. Mangravite, Electrophilic displacement reactions: XV. Kinetics and mechanism of the base-catalyzed protodeboronation of areneboronic acids, Can. *J. Chem* **1963**, *41*, 3081-3090.

[185] A. J. J. Lennox, G. Lloyd-Jones, Selection of boron reagents for Suzuki-Miyaura coupling, *Chem. Soc. Rev.* **2014**, *43*, 412-443.

[186] C. Adamo, C. Amatore, I. Ciofini, A. Jutand, H. Lakmini, Mechanism of the palladium-catalyzed homocoupling of arylboronic acids: key involvement of a palladium peroxo complex, *J. Am. Chem Soc.* **2006**, *128*, 6829-6836.

[187] X. Salvatella, M. Martinell, M. Gairi, M. G. Mateau, M. Feliz, A. D. Hamilton, J. de Mendoza, E. Giralt, A tetraguanidinium ligand binds to the surface of the tetramerization domain of protein p53, *Angewandte Chemie* **2004**, *43*, 196-198.

[188] M. Martinell, X. Salvatella, J. Fernández-Carneado, S. Gordo, M. Feliz, M. Menéndez, E. Giralt, Synthetic ligands able to interact with the p53 tetramerization domain. Towards understanding a protein surface recognition event, *ChemBioChem.* **2006**, *7*, 1105-1113.

CHAPTER 2

UNDERSTANDING THE EFFECT OF THE BRIDGE

The introduction of the biaryl staple motif in the scaffold on these peptides was inspired by natural products that also contain this feature such as vancomycin or aciculitins. To fully expand their potential application we need to improve their pharmacological and pharmacokinetic properties. Stapling has recently emerged as a powerful tool in peptide field demonstrating that the incorporation of hydrophobic motifis may result in better pharmacological and pharmacokinetic properties.

Evaluation of lead candidate pharmacological and pharmacokinetic properties is usually carried out during the final stages of drug discovery and development. This can also be a problem when the candidate does not show good properties leading to the failure of the potential drug. Therefore, incorporation in the early stages of pharmacological tests is an interesting strategy that is being considered.

In this context and after having synthesized biaryl bicyclic peptides, we focused on evaluating the properties that the staple can induce in these compounds[189]. From the chemical point of view, the molecule should be stable and the synthesis scalable without further inconveniences. Regarding the pharmacological properties, the aim is to have a compound with high affinity for the binding site of the target protein but being also selectively enough as it should be safe and nontoxic. Pharmacokinetics studies should demonstrate that the molecule is bioavailable (capable of reaching the target) and biostable with an adequate half-life time and biodistribution.

In this chapter, we decided to evaluate some of these relevant properties in the case of the biaryl bicyclic stapled peptides by taking advantage of some gold-standard *in vitro* techniques established in our laboratory.

As it was mentioned before, thanks to the presence of the head-to-tail cyclization some of these pharmacological and/or pharmacokinetic properties are also commonly improved. Therefore, to study what we call the bridge effect some control peptides were also synthesized. Peptides studied were composed of the bicyclic, the head-to-tail cyclic, the linear stapled and the linear peptides. Taking into account the structure of each one, the linear stapled peptide only contains the biaryl motif, which allowed us to study the effect of its introduction without considering extra cyclization. The

comparison of this peptide with the bicyclic provided information whether it is better or not to have the head-to-tail cycclizations regarding the studied properties. Moreover, the bicyclic peptide was also compared with the head-to-tail cyclic displaying again information of the biaryl motif as an extra constraint. Finally, the linear peptide was the control used to demonstrate that, as for some years has been claimed, pharmacological properties of peptidomimetics including rigidification motifs are improved.

2.1   Permeability through biological barriers

As it was previously mentioned, bioavailability and biodistribution of drug candidates should be carefully evaluated to ensure that molecules are able to reach their target. Peptides are being increasingly used as therapeutics to treat or cure different diseases. Talking about peptides as potential drug candidates, the evaluation of their accessibility to the target should also be confirmed by permeability studies.

These studies are important as many peptides are designed to target intracellularly. Therefore, the balance between hydrophilicity and hydrophobicity is of great importance when designing drugs to achieve good cell membrane penetration. This preliminary evaluation should avoid the potential failure of promising leads during drug development.

We aimed to study whether the presence of the biaryl hydrophobic motif increased or the potential permeability of stapled peptides.

As permeability study, we decided to use an *in vitro* model of the passive diffusion transport existing at the blood-brain barrier (BBB). From all the different cell barriers, the BBB is especially difficult to cross due to the presence of tight junctions between brain capillary endothelial cells, limiting paracellular diffusion. Furthermore, over the years drug delivery to the brain has gained many relevance, mainly due to the important number of CNS diseases that are still an unmet medical need.

Parallel artificial membrane permeability assay (PAMPA) is the gold-standard of *in vitro* assays to evaluate permeability across biological membranes by passive diffusion. However, it is worth mentioning that this technique focuses only in the study of permeability by means of passive diffusion. Considering the small size of the presented peptides, it was important to study this transport mechanism.

2.1.1 Lysine family

The four members of the family were studied under the same conditions by PAMPA. To mimic the BBB, an extract of lipids from porcine brain origin was used in the PAMPA set-up.

PAMPA evaluation of these peptides provided the required information about the importance of introducing this biaryl staple. In Table 2.1, the obtained results are shown in terms of effective permeability and percentage of transport. Standard deviation was calculated considering triplicates of the compounds. Propranolol was used as a positive control. This compound is a β-adrenergic antagonist which has the ability to cross the BBB by passive diffusion (Figure 2.1)
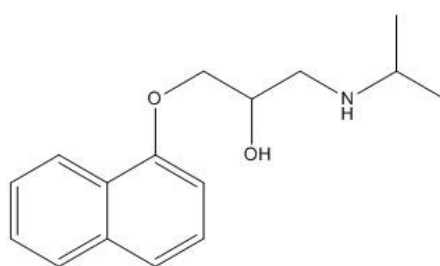
Figure 2.1. Structure of propranolol.

Table 2.1. Percentage of transport (%T), effective permeability (P$_e$) in the PAMPA after 4h.

Compound	P$_e$(x10^6) cm/s	T(%) (4h)
Bicyclic: cyclo(Lys-(4&)Phe-Lys-(4&)Phe-D-Pro)	14.3± 3.3	22.6± 0.6
Linear Stapled: H-Lys-(4&)Phe-Lys-(4&)Phe-D-Pro-OH	9.2 ± 1.8	16 ± 2.6
Head-to-tail Cyclic: cyclo(Lys-Phe-Lys-Phe-D-Pro)	1.4 ± 0.1	2.9 ± 0.2
Linear: H-Lys-Phe-Lys-Phe-D-Pro-OH	1.5 ± 0.1	3.1 ± 0.3
Propranolol	5.8 ± 0.5	18.2 ± 0.8

The different analogues were able to cross the BBB-PAMPA assay with high permeability values, since all of them had an effective permeability higher than $1\cdot10^{-6}$ cm/s which correlates with a good transport prediction *in vivo*[190]. Nonetheless, it is worth noting that the obtained values of the peptides displaying the biaryl motif (linear stapled and bicyclic versions) were higher than the others in one order of magnitude (Figure 2.2), which means that this structural feature favoured transport across the BBB by passive diffusion. Values obtained for the head-to-tail cyclic version were similar to the displayed by the linear peptide. These results unveiled the fact that head-to-tail cyclization did not enhance BBB permeability by passive diffusion even if the lack of *N* and *C*-terminus charges could seem to imply this. Finally, the difference obtained between the bicyclic and the linear stapled candidate was less than one order of magnitude while the complexity related to its synthesis was higher. Therefore, one can wonder whether it was worth or not to include in addition of the biaryl motif a head-to-tail cyclization to have more permeable compounds.

In summary, the obtained results proved that introduction of the staple was a tool for increasing the permeability of linear and the cyclic peptides while cyclization itself was not as powerful as a tool in terms of increasing the transport across membranes.
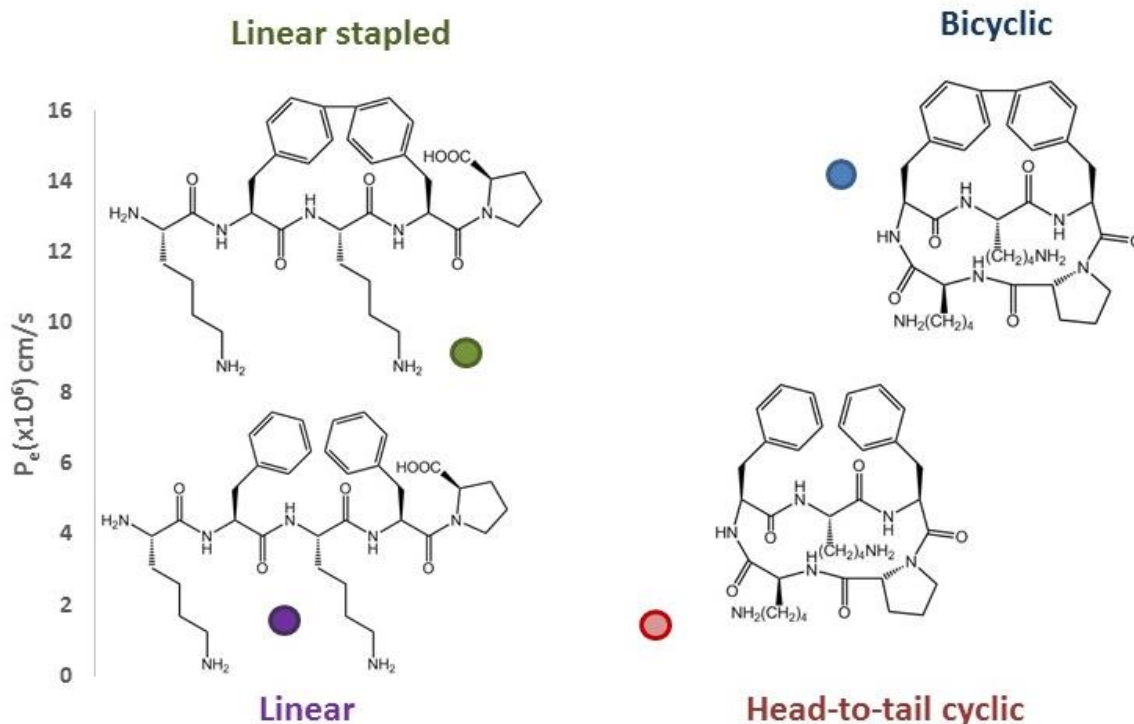
Figure 2.2. Effective permeability in the PAMPA after 4h for lysine derivatives.

Low unwanted retention in the membrane was observed by calculating the mass balance for these peptides after the PAMPA assay. It is worth noting that high membrane retention was not always an indication of better transport as it could be an indication that the compound will get stack in the membrane but not reaching the brain side of the barrier. Standard deviation of the means demonstrate the robustness of PAMPA assay.

2.1.2 Arginine family

After having obtained such positive results for the introduction of the biaryl staple in the lysine derivatives, we decided to prove whether this motif was beneficious for only some kind of peptides or whether it could be used in a wider range of compounds.

Arginine family was also studied by PAMPA assay to evaluate passive diffusion permeability across the BBB (Figure 2.3).
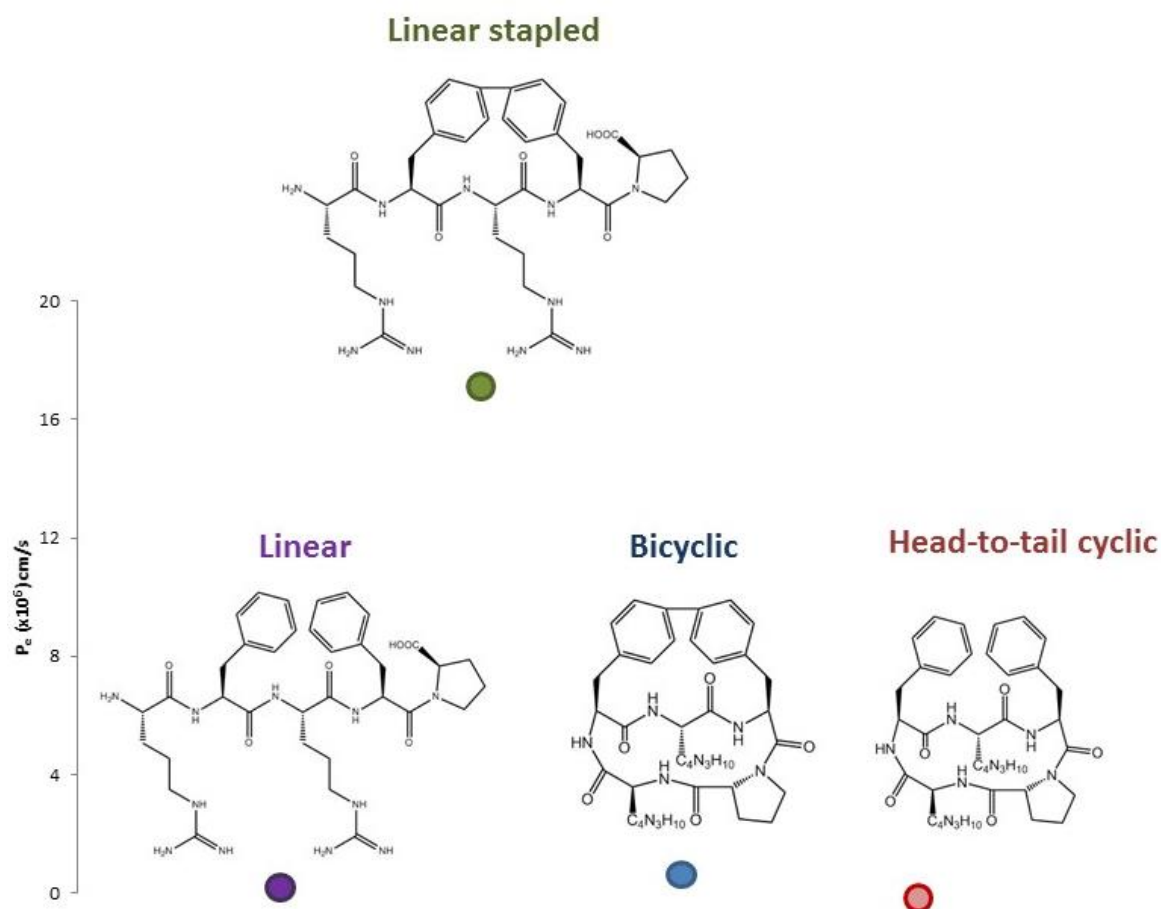
Figure 2.3. Effective permeability in the PAMPA after 4h for arginine derivatives.

The results obtained for the arginine containing peptides were peculiar, as well as, unexpected. On the contrary to what was observed for the lysine family, most compounds did not display good transport prediction *in vivo* based on the P_e values found in the PAMPA assay *in vitro*. Sourprisingly, the most permeable was the linear stapled. This result could mean that the biaryl bridge enhanced permeability. Nevertheless, the permeability of the bicyclic peptide was low, as well as the displayed for the linear and the head-to-tail versions. When analysing in depth the acceptor compartments of the arginine bicyclic peptide, the appearance of a new peak was detected. This new peak did not correspond to degradation of the sequence and the obtained mass values could not be assigned to any possible peptidic side reaction or

degradation. It is worth mentioning that this new peak had greater permeability than the bicyclic peptide itself. We hypothesized that this new product corresponded to the interaction of the peptide with membrane lipids. It has been reported that arginine can interact with membrane lipids[191]. Low unwanted retention in the membrane was observed for the linear and the linear stapled analogues by calculating the mass balance of these peptides after the PAMPA assay.

High membrane retention was also observed for the head-to-tail peptide and the bicyclic one. Even if the four members of the family contained two arginine residues, it was possible to observe a different behaviour due to completely different three-dimensional structure. Head-to-tail cyclization seems to affect the conformation in a manner that is more prone to interact and be retained by membrane lipids.

Table 2.2. Percentage of transport, effective permeability (P_e) in the PAMPA after 4h for arginine derivatives. Standard deviation of the means demonstrated again the robustness of the method.

Compound	P_e(x10^6) cm/s	T(%) (4h)
Bicyclic: cyclo(Arg-(4&)Phe-Arg-(4&)Phe-D-Pro)	0.7 ± 0.1	1.4 ± 0.2
Linear Stapled: H-Arg-(4&)Phe-Arg-(4&)Phe-D-Pro-OH	16.9 ± 1.8	25.5 ± 1.9
Head-to-tail Cyclic: cyclo(Arg-Phe-Arg-Phe-D-Pro)	$0.02 \pm 3.5 \cdot 10^{-3}$	$0.03 \pm 7.5 \cdot 10^{-3}$
Linear: H-Arg-Phe-Arg-Phe-D-Pro-OH	0.1 ± 0.1	0.2 ± 0.1
Propranolol	6.2 ± 0.1	10.8 ± 0.3

2.1.3 Serine family

We decided to analyze the effect of the biaryl bridge in hydrophilic but not charged peptides. Therefore, serine family was also studied by PAMPA (Figure 2.4).
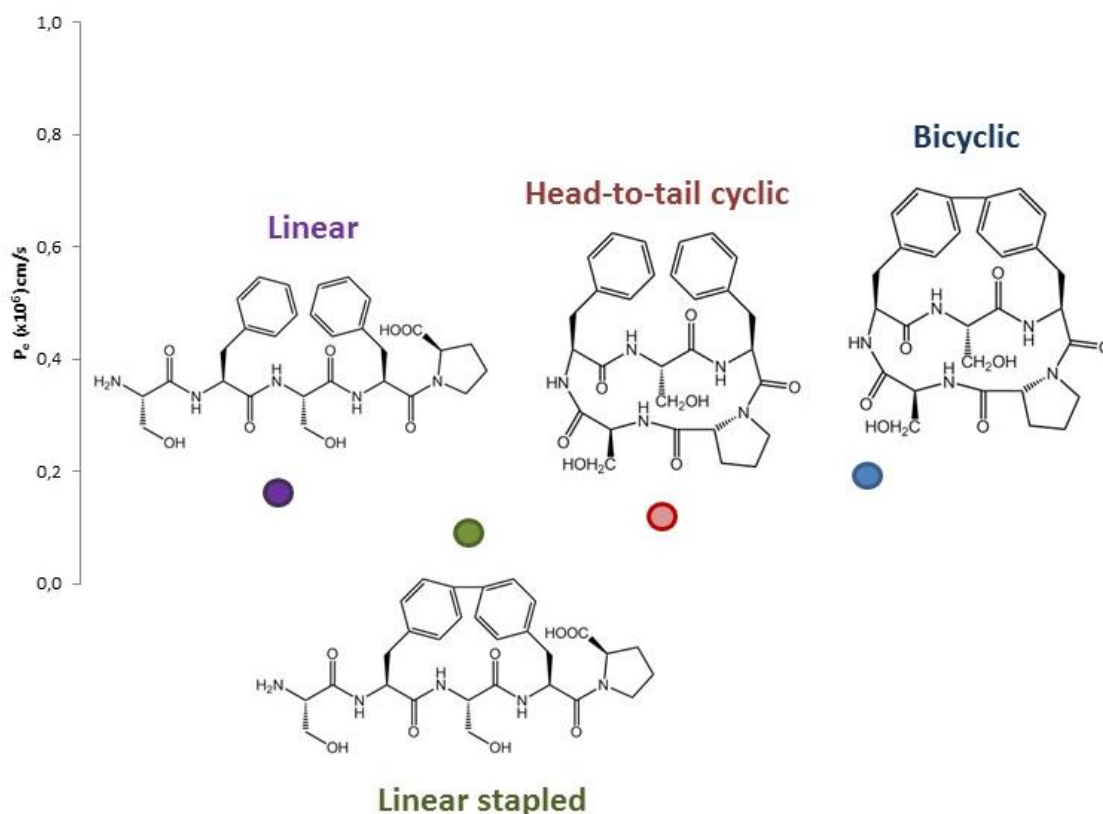
Figure 2.4. Effective permeability in the PAMPA after 4h for serine derivatives.

The values obtained for all the compounds of this family were in the range of low permeability $<1 \cdot 10^{-6}$ cm/s. Similar results were obtained for the linear, linear stapled and head-to-tail cyclic versions while a really slight increasement of transport was detected for the bicyclic peptide analogue.

Comparing these results with the previously obtained for the other peptides tested by PAMPA, low permeability was attributed to the presence of the two serine amino acids. The theory that equilibrium between hydrophobicity and hydrophilicity of the peptides is required to achieve good membrane permeability was reinforced. These peptides contain two serines which display the hydroxyls groups in their side-chains and do not include a long hydrophobic carbon chain (like lysine) that could balance the polarity of the alcohols.

In this case, neither the stapling nor the head-to-tail cyclization, were enough to detect a positive effect. The combination of both strategies was required to cause a slight increase in transport values.

Table 2.3. Percentage of transport, effective permeability (P_e) in the PAMPA after 4h for serine derivatives.

Compound	P_e(x10^6) cm/s	T(%) (4h)
Bicyclic: cyclo(Ser-(4&)Phe-Ser-(4&)Phe-D-Pro)	$0.2 \pm 5 \cdot 10^{-2}$	$0.4 \pm 9 \cdot 10^{-2}$
Linear Stapled: H- Ser-(4&)Phe-Ser-(4&)Phe-D-Pro-OH	$0.1 \pm 3 \cdot 10^{-3}$	$0.2 \pm 6 \cdot 10^{-3}$
Head-to-tail Cyclic: cyclo(Ser-Phe-Ser-Phe-D-Pro)	$0.1 \pm 4 \cdot 10^{-3}$	0.3 ± 10^{-2}
Linear: H-Ser-Phe-Ser-Phe-D-Pro-OH	$0.1 \pm 5 \cdot 10^{-2}$	0.3 ± 0.1
Propranolol	6.2 ± 0.2	10.8 ± 0.3

These experiments allowed us to affirm that the biaryl staple by itself increased passive diffusion permeability for compounds that in their linear version had also good permeability while for those which were not permeable, as the serine containing linear peptide, the introduction of the staple was not enough.

As it was described for the lysine and arginine families, low unwanted retention in the membrane was observed for the linear, head-to-tail cyclic and bicyclic peptides by calculating their mass balance after the PAMPA assay. It is worth mentioning that, the linear stapled version of the serine family had a non neglictible retention of 40%. Standard deviation of the means proved one more time the robustness of this technique.

2.1.4 Effect of the amino acids in the variable position of the bicyclic scaffold

If we compared the three biaryl bicyclic peptides from the lysine, arginine and serine families, in addition to unveil the effect of the head-to-tail cyclization, as well as, the biaryl stapling, it allowed us to understand the effect of the two amino acids in the variable positions (Figure 2.5).
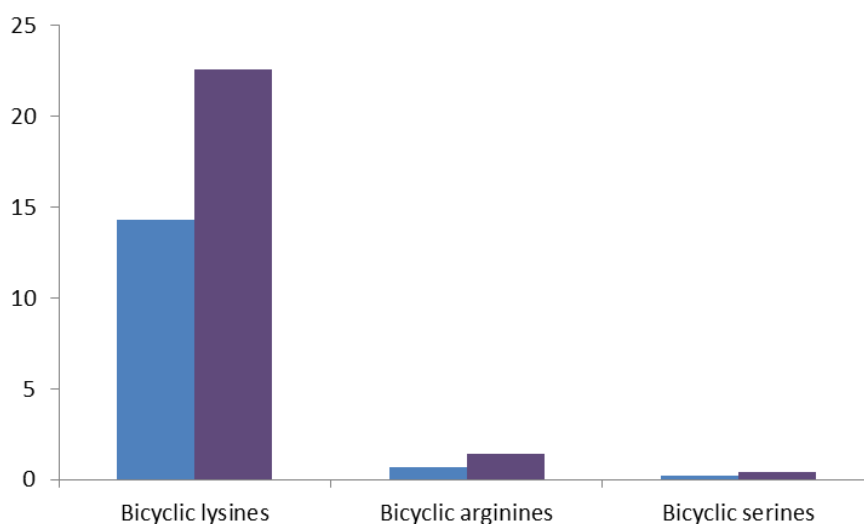
Figure 2.5. Comparison of the effective permeability (P_e (x10^6) cm/s) in blue and the percentage of transport after 4h (T(%)) in purple for the bicyclic peptides of the three studied families.

Lysine and arginine residues represented positively charged amino acids, although amino and guanidinium groups are quite different and behave different in terms of permeability. On the other side, serine represented uncharged polar amino acids.

High retention membrane for the arginine bicyclic peptide avoids passive diffusion permeation of this compound. Nevertheless, the other two bicyclic peptides displaying serines and lysines did not show significant retention in the membrane, which means that this effect was not directly correlated with the presence of the biaryl hydrophobic staple. This result was important, since the attachment to the membrane was a

negative effect when aiming to have peptides with the ability to cross a particular biological membrane by passive diffusion, withouth getting stack

Regarding the values of permeability and transport for the other two analogues, the lysine bicyclic peptides proved to be more permeable by passive diffusion than the serine bicyclic peptide.

In addition to the different permeability observed for lysine and serine bicyclic peptides, it should also be noticed than the physicochemical properties are very different, due to the different balance of hydrophobicity and hydrophilicity. For instance, solubility of the serine bicyclic peptide proved to be better than for the lysine bicyclic peptide. On the other hand, for surface recognition purposes, the presence of the amino group at the end of the side-chain of lysine is more promising than the alcohol present in the side-chain of serine.

2.2   Biostability in human serum

During the development of the biaryl bicyclic peptides, we hypothesized that the introduction of the head-to-tail cyclization together with the biaryl bridge should provide a significant increase in half-life of the peptides. Therefore, for the lysine, arginine and serine families, we evaluated the different four members to be able to compare half-lives and understand the effect of these two motifs regarding biostability in human serum.

Therefore, the peptides were incubated with 90% human serum at 37°C for 24h and aliquots were taken at different time-points. Immediate precipitation of serum proteins was assessed by adding methanol, in which the peptides were fully soluble. After subsequent centrifugation, the supernatant was analysed by HPLC-UV at 220 nm and MALDI-TOF MS to confirm integrity or degradation.

2.2.1 Lysine family

The linear peptide was rapidly degradated in less than 30 min, which was the first time-point, demonstrating the low biostability that linear peptides commonly display. Enhanced stability was observed for cyclic peptides (linear stapled and head-to-tail cyclic). Remarkably, the bicyclic analogue was mostly no degradated after more than 24h (Figure 2.6).
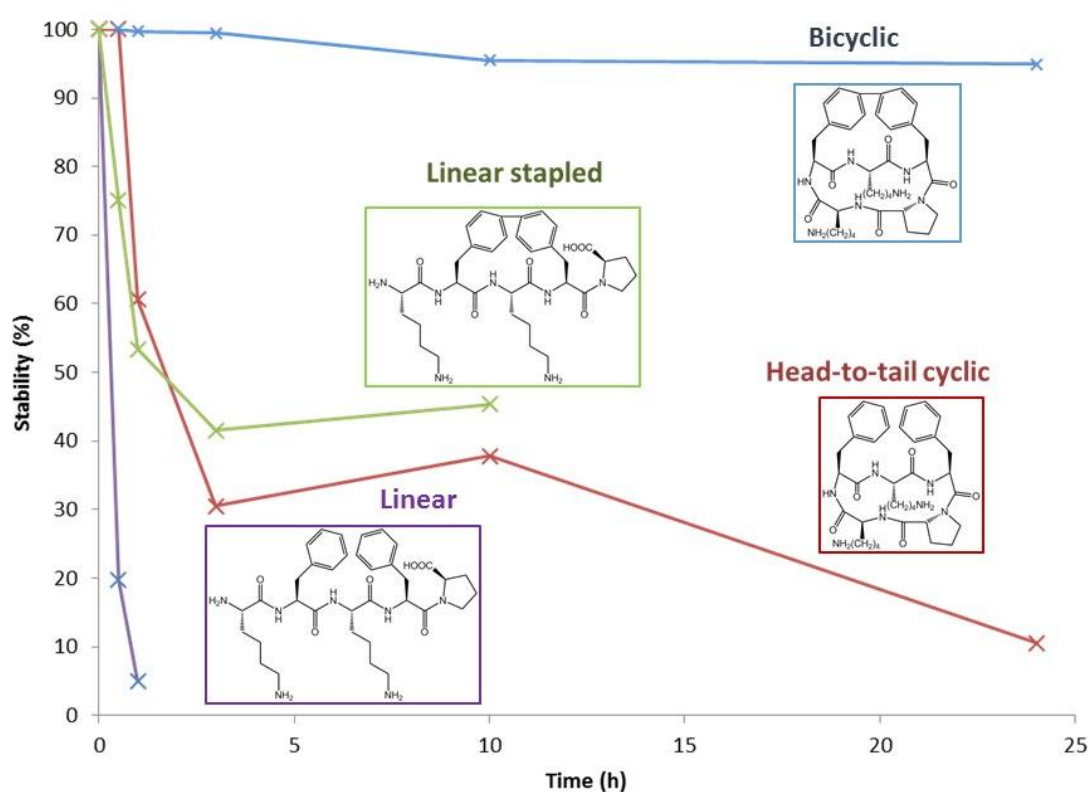
Figure 2.6. Biostability of the lysine derivatives expressed as the percentage of remaining product at different incubation times.

For the linear control peptide, HPLC-MS analysis determined multiple fragmentations within the peptide making difficult to understand the fast pattern of degradation but confirming its high lability. Linear stapled was present at all the time-points but the concentration decreased and new peaks of shorter retention time appeared as degradation fragments. The biaryl staple motif seemed to be one of the difficult

moieties to be degraded in peptide sequences. Head-to-tail cyclic corresponding HPLC peak continously decreased and new peaks at similar retention time appeared probably the open versions. Finally, the bicyclic peptide was found out in all the time-points and no significant changes were observed in the HPLC spectra even after 24h.

2.2.2 Arginine family

Similar results were obtained for this family. Fast degradation of the linear version was observed. In this experiment, the head-to-tail cyclic peptide despite having improved the half-life time was degrataded after 3h. The linear stapled and the bicyclic peptides proved to be stable after more than 24h (Figure 2.7).
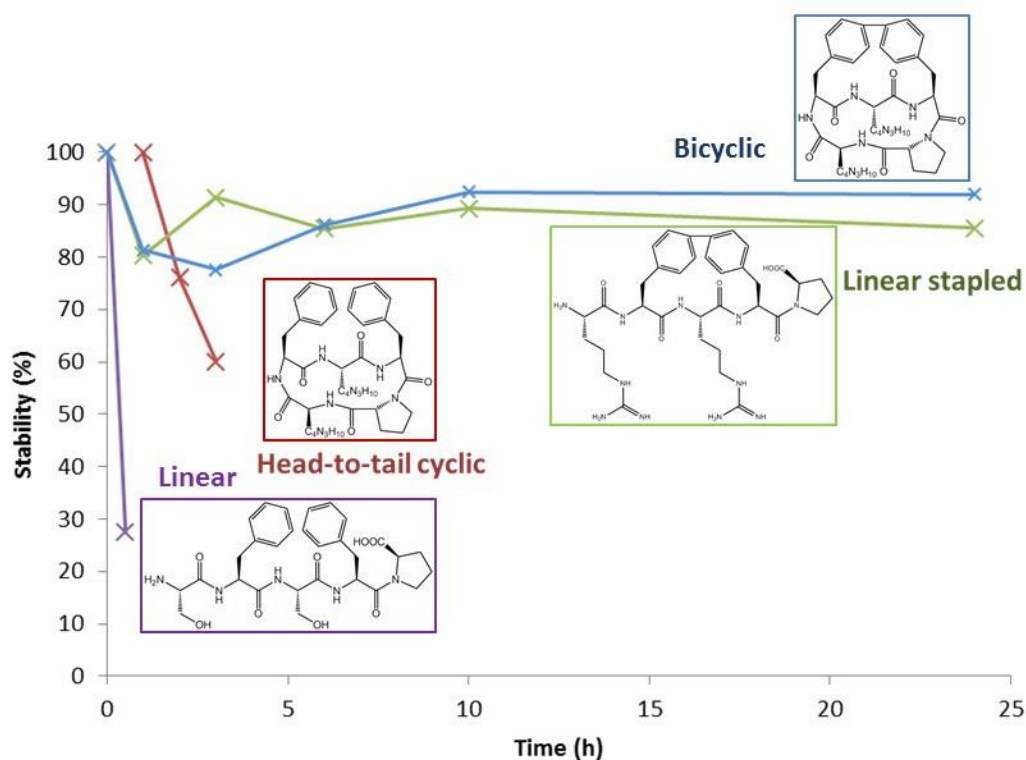
Figure 2.7. Biostability of the arginine derivatives expressed as the percentage of remaining product at different incubation times.

2.2.3 Serine family

In this third family, all the peptides were finally degraded. As in the previous cases, linear version of the peptide was degradated in less than 30min (Figure 2.8).
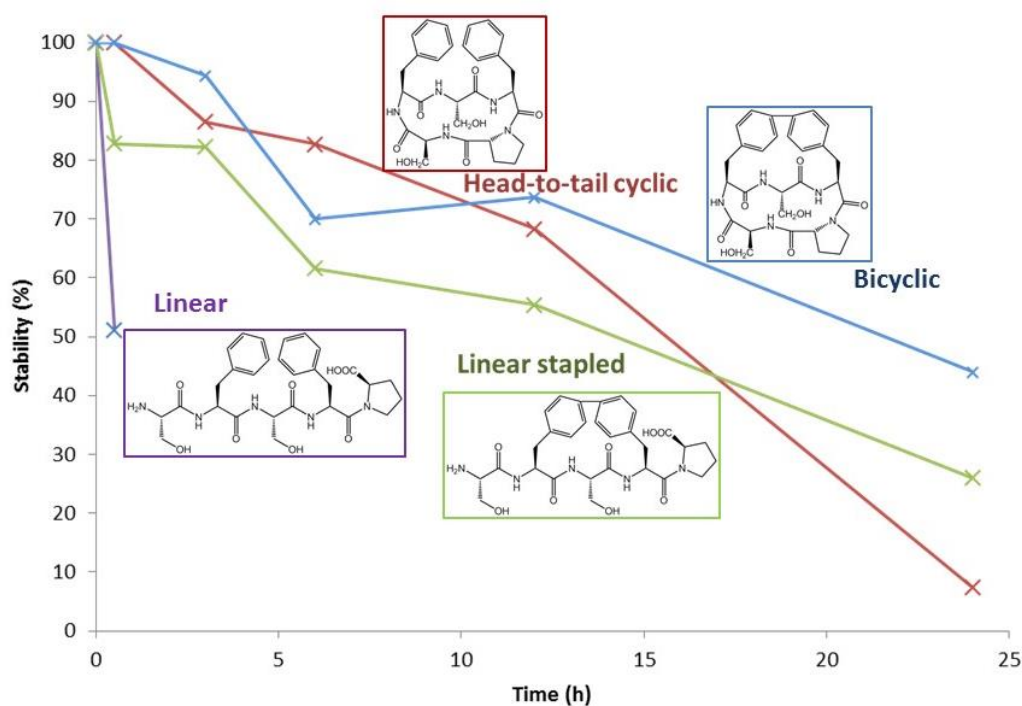
Figure 2.8. Biostability of the serine derivatives expressed as the percentage of remaining product at different incubation times.

Half-life for head-to-tail cyclic, linear stapled and bicyclic analogues proved to be increased to more than 12h. At that time-point, 80 and 75% of the bicyclic and head-to-tail cyclic, respectively, were still present.

In the light of these results, we could confirm that, as expected, head-to-tail cyclization, as well as, biaryl stapling were very powerful tools to remarkably enhance

protease resistance of linear peptides. Combination of both strategies gave access to privileged bicyclic constructs that proved to be highly resistant compounds

2.3 Cell viability assay for the lysine peptide family

The human serum stability results together with the passive diffusion permeability studies pointed out the relevance of the bicyclic lysine peptide being one of the most stable in human serum and the most permeable across the blood-brain barrier by passive diffusion. For this reason, we decided to further study this compound testing some other relevant properties such as the cytotoxicity and the risk of immunogenicity, which can be a concern in medium size peptides.

Therefore, the cytotoxicity of the four members of the lysine family was studied by MTT assay. In this context, we also aimed to guarantee that the incorporation of the biaryl staple did not produce cell death.

MTT assay relies on the conversion of tetrazolium, a yellow water-soluble salt, into insoluble blue formazan crystals by the reductive reaction shown in Figure 2.9. This reaction takes place mainly in the cytoplasm although also occurs in mitochondria and cell membrane.
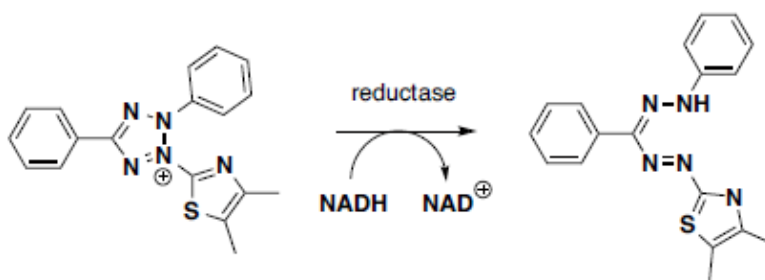
Figure 2.9. Reduction of the tetrazolium salt to formazan. Detection of formazan crystals formed by fluorescence allow performance of the cell viability MTT assay.

Cell viability was tested in HeLa cells at two different concentrations, 200µM and 500µM. As shown in Table 2.4 compounds did not display significant cytotoxicity values at these slightly high concentrations.

At this point, it worth mentioning that for future biological applications of the described peptides in this thesis, related to the recovery of the self-assembly of mutated p53 tetramerization domain proteins, maximum amount considered to be used in the circular dichroism experiments was approximately 300µM. Therefore, appropriate cell viability achieved at 500µM could enable the use of these compounds as possible protein-protein interaction enhancers withouth security concerns.

Table 2.4. Cytotoxicity values for lysine derivatives at 200 and 500 µM concentrations expressed as percentage of cell survival.

	Linear	Linear stapled	Head-to-tail cyclic	Bicyclic
200 µM	75	>99	84	80
500 µM	69	58	71	58

However, at 500 µM the linear stapled and the bicyclic analogues proved to be more cytotoxic than the linear and head-to-tail cyclic versions. This fact could be explained due to the higher protease resistance that these analogues possessed. The degradation of the linear and head-to-tail cyclic peptides could prevent from higher cell death by shortening compound exposure. Nonetheless, the obtained values for all them were reasonable for the potential use of these biaryl containing peptides.

2.4 Immunogenicity of the bicyclic lysine analogue

In addition, immunogenicity is another highly relevant property for novel molecule with new moieties. Peptides fall halfway between small molecules and biologics, thus allowing them to trigger an immunogenic response in the human body. We therefore explored the potential immunogenic risk of the bicyclic peptide.

Bicyclic peptide, without conjugation to any other protein such as KLH or BSA, was inoculated into four mice. A nonapeptide peptide, MiniAp-3[192,] was incorporated as a positive control in this study. Each animal was treated with 10 doses of 50 µg of peptide each, the first dose with Freund's complete adjuvant and the remaining ones with Freund's incomplete adjuvant. After performing the inoculations, we bled the mice and then measured by ELISA the antibodies specifically generated against the peptides. The comparison of the serum before (black dots) and after (white dots) the inoculations proved that the bicyclic peptide was not rising an immunogenic response (Figure 2.10).
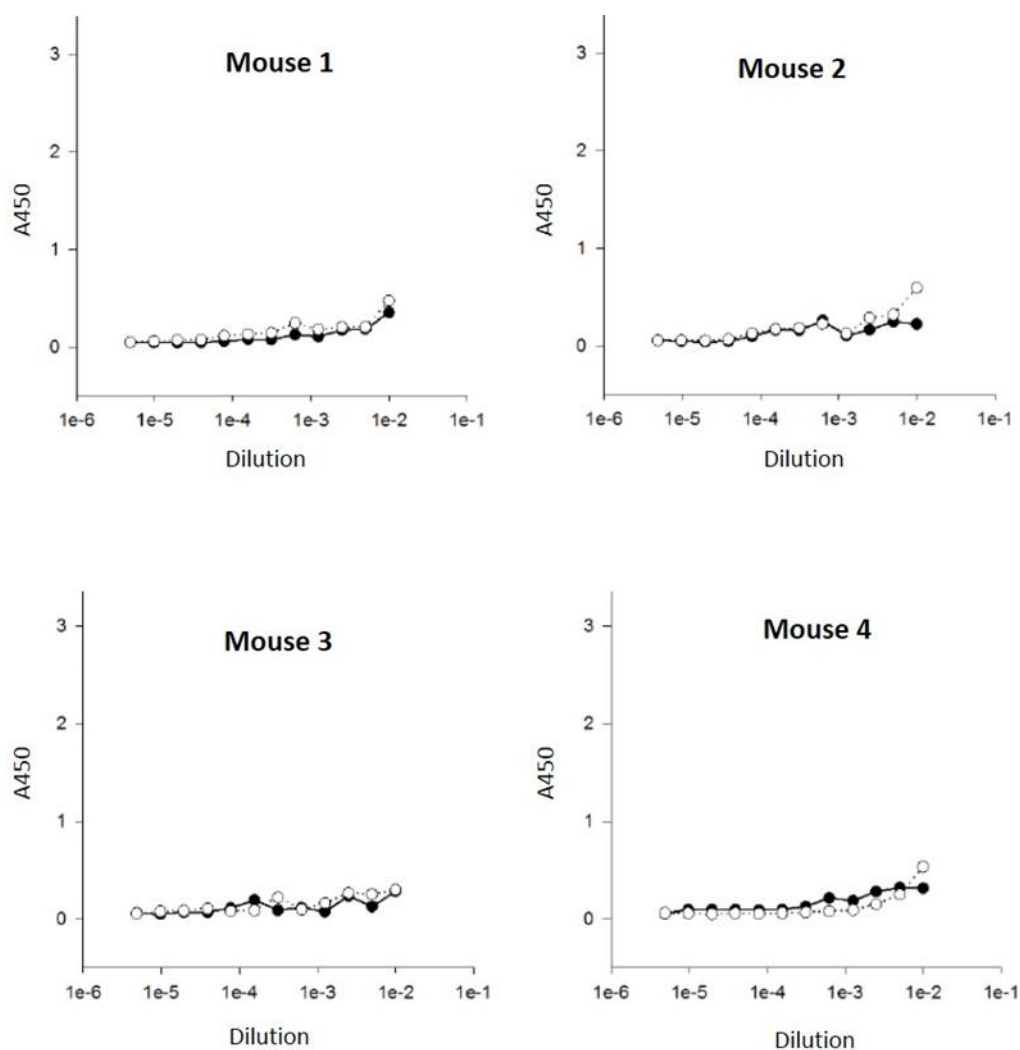
Figure 2.10. Immunogenicity response of the bicyclic peptide, in black bleeding after 7 innoculations and in white bleeding after 10 innoculations, observing no significant response.

Results of the control peptide, which was known to raise immunogenic response, are shown in Figure 2.11.
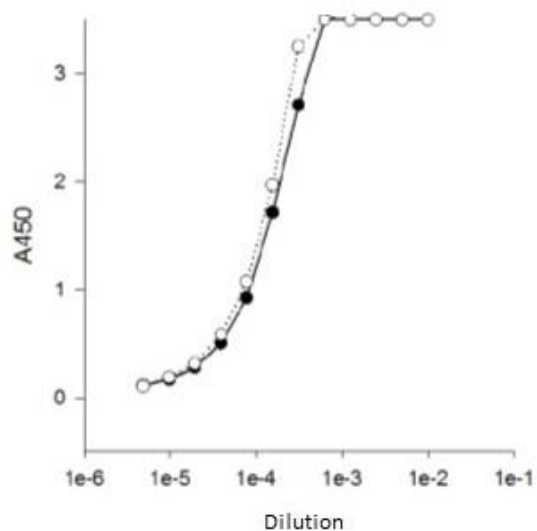
Figure 2.11. Immunogenicity of the control peptide, in black bleeding after 7 innoculations and in white bleeding after 10 doses, immunogenic response was observed.

Comparing the profile of the bicyclic peptide with the control it is possible to consider that the risk of immunogenic response for this bicyclic peptide is low.

In summary

The different synthesized families of compounds were studied in order to unveil the effect of the biaryl bridge incorporation.

Passive diffusion permeability across the blood-brain barrier and assessed by PAMPA pointed out the importance of the introduction of this hydrophobic staple. Nonetheless, the relevance of this motif is also dependent on the sequence of amino acids. Lysine family had good passive diffusion permeability, probably due to the hydrophobic-hydrophilic balance that lysine amino acid present at the variable positions of the general scaffold. In this case, both linear stapled and bicyclic peptides displayed similar transport values. On the contrary, serine amino acid difficulted the permeability by passive diffusion. The bicyclic peptide of this family yielded a slight increase in permeability while the stapling by itself did not show an enhancement. Regarding the arginine family, introduction of the biaryl feature proved a beneficious effect. Although the bicyclic peptide did not show a relevant permeability, high retention to the membrane was accused as the main reason.

We therefore concluded that the bridge introduction enabled passive diffusion permeability by itself or in combination with the head-to-tail cyclization constrain.

In terms of stability, byciclic peptides showed an outstanding increasement in their half-lives in human serum. Non-neglectable protease resistance was also observed for the linear stapled peptides. Specifically, for the arginine family, the linear stapled peptide displayed the same half-lives as the bicyclic one.

Moreover, no cytotoxicity could be attributed to the presence of this stapling after analyzing the MTT assay of the lysine family of compounds. This fact is very relevant for further biological purposes. In this same context, the risk of immunogenic response of the lysine bicyclic peptide was also evaluated. Obtained results were compared with

a control immunogenic peptide (MiniAp-3)[192] to validate the assay. Low or no immunogenic risk can be expected for this compound.

Bibliography

[189] F. Z. Hefti, Requirements for a lead compound to become a clinical candidate, *BMC Neuroscience* **2008**, *9*, 1-7.

[190] L. Di, E. H. Kerns, K. Fan, O. J. McConnell, G. T. Carter, High throughput artificial membrane permeability assay for blood-brain barrier, *Eur. J. Med. Chem.* **2003**, *38*, 223-232.

[191] C. T. Armstrong, P. E. Mason, J. L. Ross Anderson, C. E. Dempsey, Arginine side chain interactions and the role of arginine as a gating charge carrier in voltage sensitive ion channels, Sci. Rep. **2016**, *6*, 21759.

[192] B. Oller-Salvia, M. Sánchez-Navarro, S. Ciudad, M. Guiu, P. Arranz-Gibert, C. Garcia, R. R. Gomis, R. Cecchelli, J. García, E. Giralt, M. Teixidó, MiniAp-4: a venom-inspired peptidomimetic for brain delivery, *Angew. Chem. Int. Ed.* **2016**, *55*, 572-575.

CHAPTER 3

TRP-TRP PEPTIDES: A NEW FAMILY OF BICYCLIC PEPTIDES

After having designed a methodology to carry out the synthesis of biaryl bicyclic pentapeptides, we aimed to demonstrate the versatility of the selected strategy to incorporate other amino acids that we enable new kind of staples.

Owing to the common presence of halotryptophan residue in natural products we envisaged the possibility to include this residue in our synthetic peptides.

The interest of aromatic amino acids for recognition of protein surfaces is well known and widely studied. Tryptophan presence in peptides and proteins is crucial for their biological activity in spite of being low abundant, less than 1% amino acids[193].Therefore, new synthetic methodologies have been applied for the derivatization of the indole group of Trp. One of the most recent is based on direct C-H activation to perform metal-catalyzed C-C coupling[194,195]. This methodology enables the introduction of staples incorporating tryptophan as one of the residues involved.

The indole group of tryptophan can also participate in π–cation interactions[196,197], as happens with phenylalanine amino acids, reinforcing the interest of tryptophan-containing peptides to target protein-protein interactions.

There are several research groups that are working on the derivatization of tryptophan introducing halogens in different position of the indole group[198]. Thanks to a collaboration with Prof. S. Ballet from the Vrije Universiteit Brussel, we could explore new staple entities by using halotryptophan analogues developed in his group.

3.1   En route to the synthesis of Trp-Trp stapled peptides

Taking advantage of the methodology established to perform C-C bond formation on resin by using Miyaura-Suzuki cross-coupling reactions, bicyclic pentapeptides with Trp-Trp stapling were obtained.

Starting materials provided by our collaborator Prof. S. Ballet were (5Br)Trp, (6Br)Trp, (7Br)Trp, Fmoc-(5Br)Trp, Fmoc-(6Br)Trp and Fmoc-(7Br)Trp. All the amino acids sent as Fmoc derivatives were directly introduced in the synthesis while the unprotected halotryptophans were converted into the corresponding *p*nz-derivatives. The derivatization of these residues, as in the general methodology for the synthesis of the biaryl bicyclic peptides described in Chapter 1, was performed in order to avoid diketopiperazine formation when deprotecting the halotryptophans that were placed as second amino acid.

We envisaged performing the synthesis of these Trp-Trp peptides using the same methodology as for the phenylalanine-based bicyclic pentapeptides although low reaction rates were expected due to the fact that the amino acids to be cross-linked are bromine instead of iodine derivatives.

Suzuki reaction can be performed with different halides or also pseudohalides, such as triflates (OTf). Nevertheless, the reactivity of the compounds is highly dependent on the selected halide as it follows[199]: R-I > R-OTf > R-Br >> R-Cl

Several examples based on the use of bromine derivative instead of iodide have been reported but with slighty lower yields[200] also very dependent on the final molecule. Therefore, we maintained the same conditions (solvent, temperature, base and catalyst) but reaction time was increased.

According to the positive results obtained for the lysine bicyclic pentapeptide described in Chapter 2, we decided to mimic this sequence and change the stapling, which also would provide us some relevant information about the effect of the bridge in the same sequence (understood as the same three remaining amino acids).

It is worth noting that not only the stapling is different but also the amino acids that are cross-linked. Therefore, the sequence is not exactly the same (Lys-Phe-Lys-Phe-D-Pro described in Chapter 2 and Lys-Trp-Lys-Trp-D-Pro for the new stapled peptides to be analyzed in the present Chapter).

The strategy followed to perform the synthesis of the Trp-Trp peptides is shown in Figure 3.1.
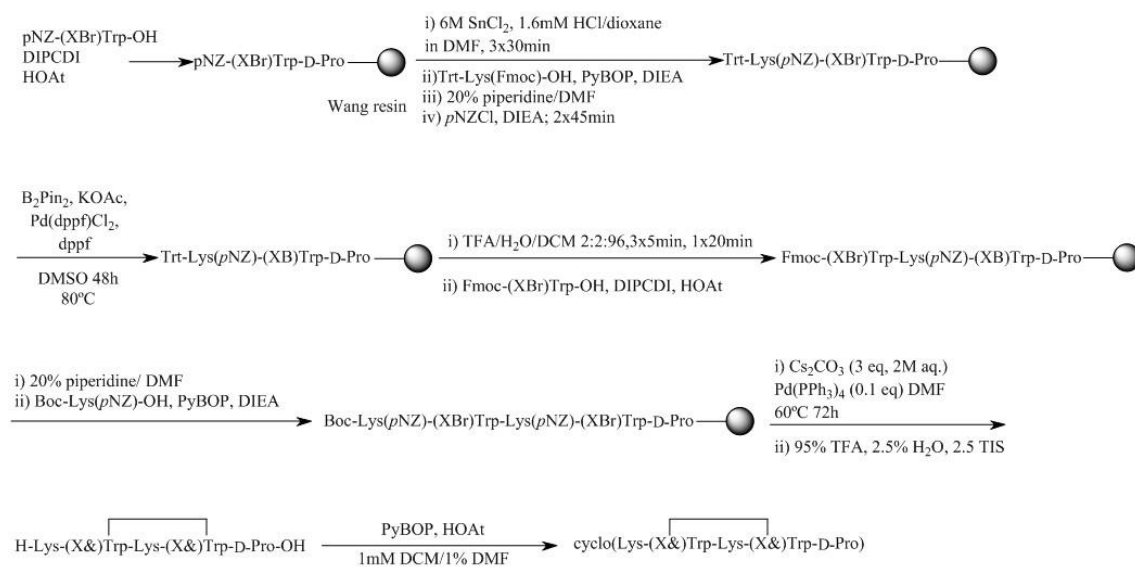
Figure 3.1. General methodology to synthesize Trp-Trp stapled peptide based on the general methodology presented in Chapter 1. X=5,6,7 denotes the position of Br in the indole of Trp.

From all the different possible combinations, the selected peptides to be synthesized were the ones displaying the same substitution in both tryptophans introduced in the sequence, namely (5&)Trp-(5&)Trp, (6&)Trp-(6&)Trp and (7&)Trp-(7&)Trp. We did not observe significant changes in reactivity depending on halogen position of the indole ring.

The three different Trp-stapled bicyclic peptides were obtained and characterized (Figures 3.2, 3.3, 3.4 and 3.5)
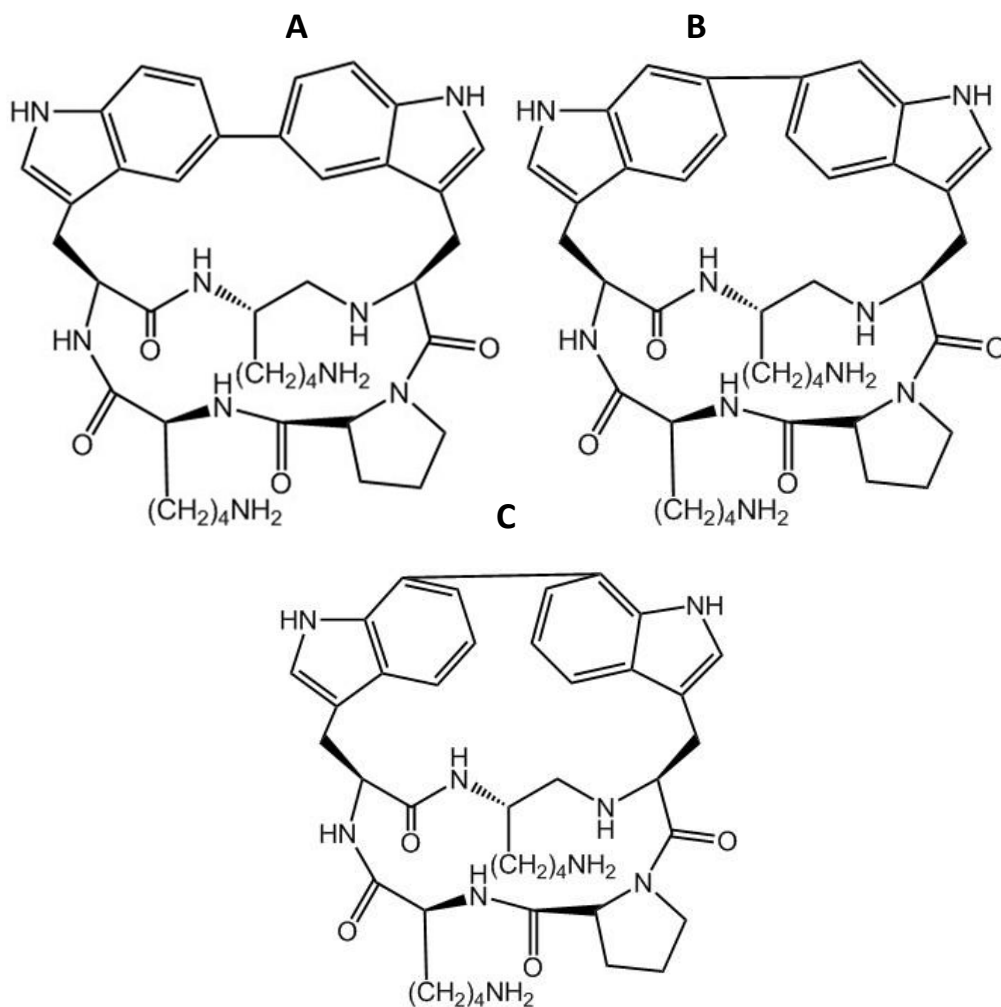
Figure 3.2. Structures of the Trp-Trp bicyclic stapled peptides. A) (5&)Trp-(5&)Trp, B) (6&)Trp-(6&)Trp and C) (7&)Trp-(7&)Trp.
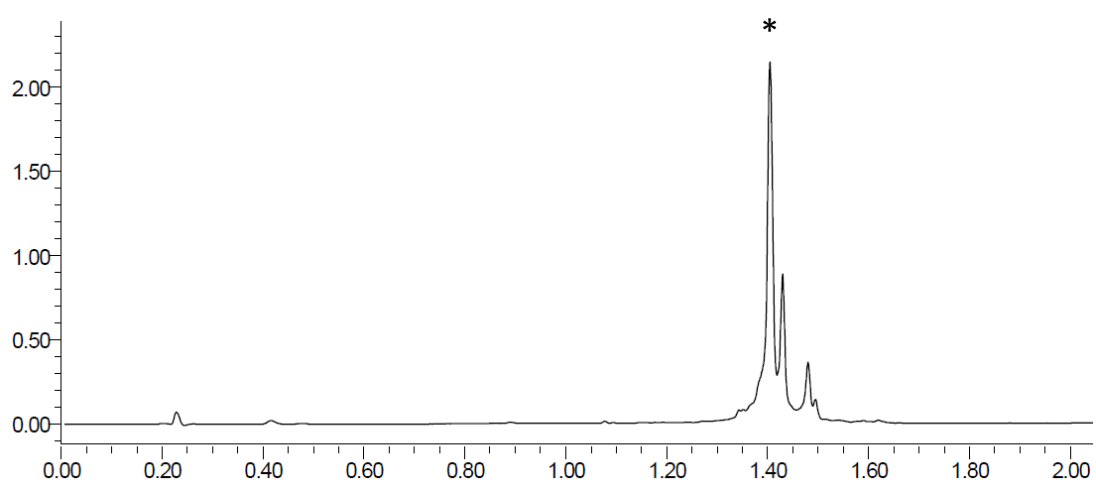
Figure 3.3. UPLC chromatogram of the crude peptide cyclo(Lys-(5&)Trp-Lys-(5&)Lys-D-Pro) in a 0-100% MeCN in 2 min gradient. Column BEH C$_{18}$, 1.7 μm, 2.1x50mm, t$_R$=1.45min. * denotes the desired product
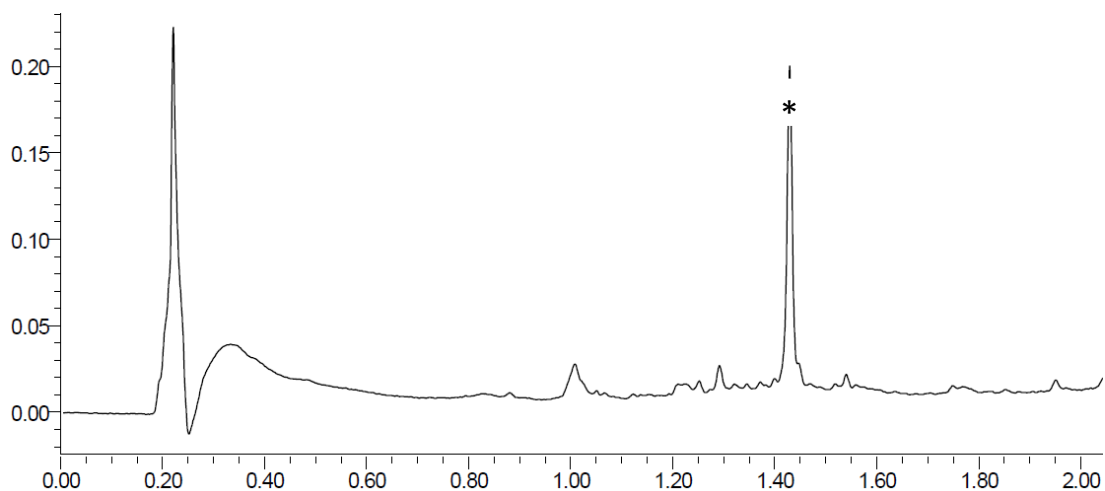
Figure 3.4. UPLC chromatogram of the crude peptide cyclo(Lys-(6&)Trp-Lys-(6&)Trp-D-Pro) in a 0-100% MeCN in 2 min gradient. Column BEH C$_{18}$, 1.7 μm, 2.1x50mm, t$_R$=1.44min. * denotes the desired product
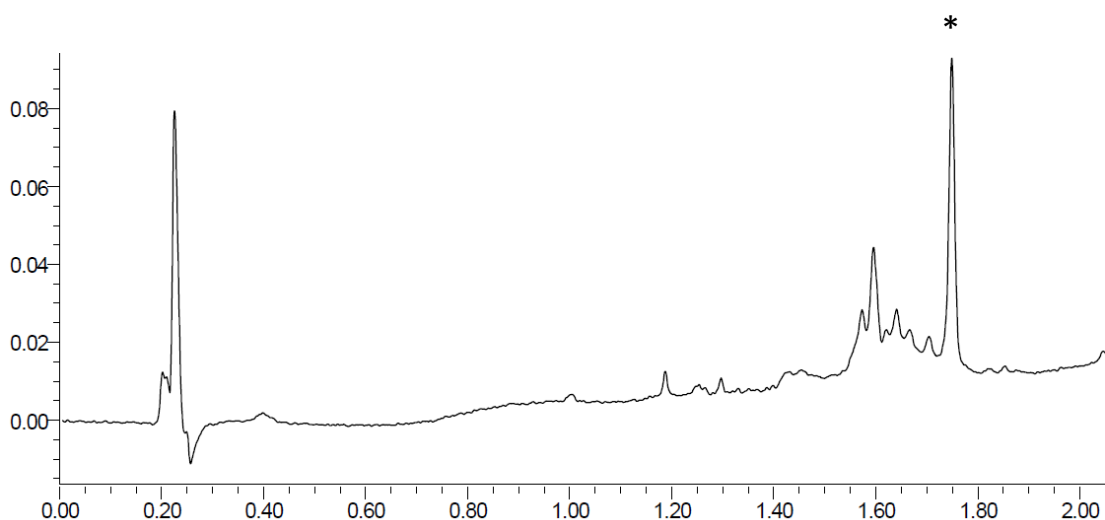
Figure 3.5. UPLC chromatogram of the crude peptide cyclo(Lys-(7&)Trp-Lys-(7&)Trp-D-Pro) in a 0-100% MeCN in 2 min gradient. Column BEH C$_{18}$, 1.7 μm, 2.1x50mm, t$_R$=1.75min. * denotes the desired product

3.2 Bromine containing peptides

Having performed the synthesis of the bicyclic peptides, we envisaged the possibility to prepare head-to-tail cyclic peptides with the same sequence and displaying bromines

at different positions of the aromatic indole ring. To be able to compare them with the bicyclic versions, the substitution of the tryptophans was the same for the two residues introduced in each sequence.

The synthesis of these compounds was performed using standard Fmoc/*t*Bu chemistry in 2-chlorotrytil resin, since bromine is compatible with this methodology. Head-to-tail cyclization was carried out in solution followed by the removal of the remaining protecting groups. The chromatograms of the compounds are shown in Figure 3.6, 3.7 and 3.8.
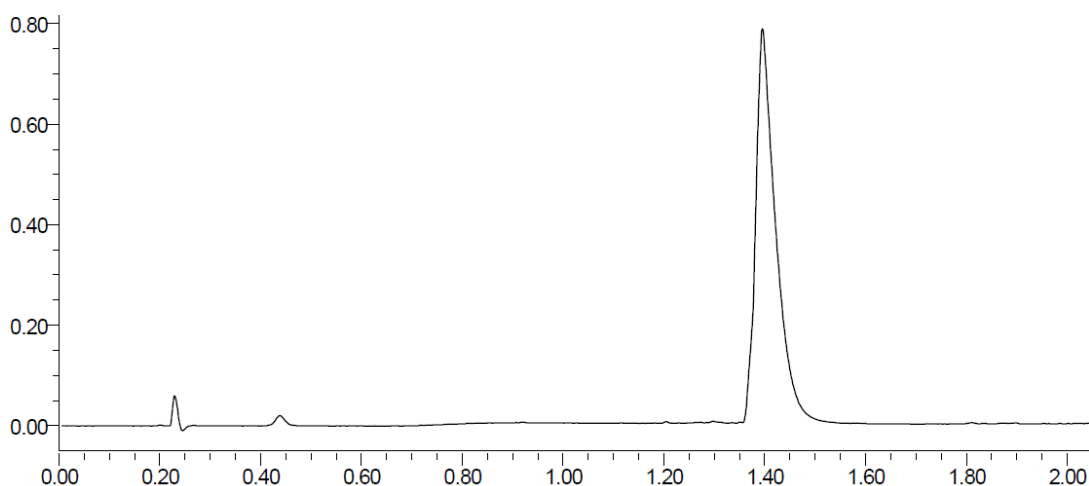
Figure 3.6. UPLC chromatogram of the crude peptide cyclo(Lys-(5Br)Trp-Lys-(5Br)Lys-D-Pro) in a 0-100% MeCN in 2 min greadient. Column BEH C$_{18}$, 1.7 µm, 2.1x50mm, t$_R$=1.35min. .
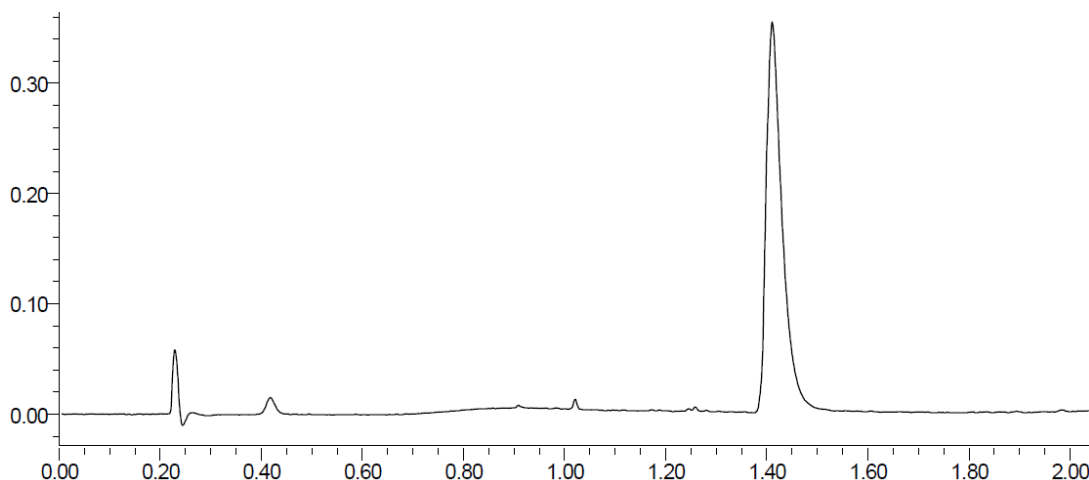
Figure 3.7. UPLC chromatogram of the crude peptide cyclo(Lys-(6Br)Trp-Lys-(6Br)Lys-D-Pro) in a 0-100% MeCN in 2 min gradient. Column BEH C$_{18}$, 1.7 µm, 2.1x50mm, t$_R$=1.35min. .
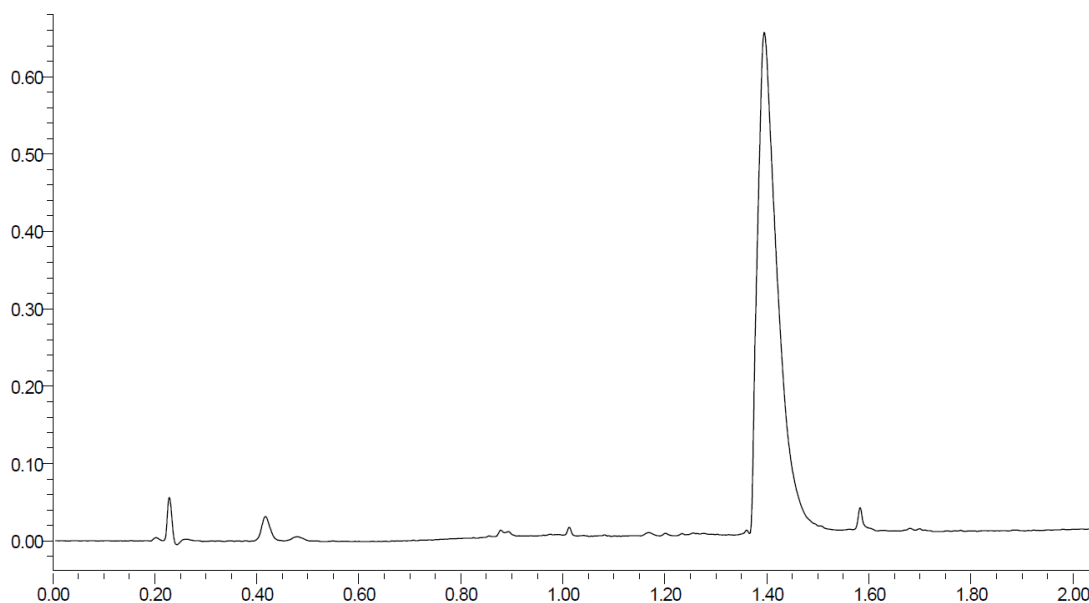
Figure 3.8. UPLC chromatogram of the crude peptide cyclo(Lys-(7Br)Trp-Lys-(7Br)Lys-D-Pro) in a 0-100% MeCN in 2 min gradient. Column BEH C$_{18}$, 1.7 μm, 2.1x50mm, t$_R$=1.35min. .

3.3 PAMPA assay: Parallel Artificial Membrane Permeability Assay

Considering the interest of unveiling the effect of the tryptophan stapling for improving pharmacological properties of peptides, we decided to evaluate the potential permeability of the different stapled peptides by passive diffusion using the PAMPA *in vitro* model. Head-to-tail monocyclic bromine-containing peptides were also studied in the assay.

Furthermore, we aimed to have some control peptides to be able to conclude whether the incorporation of the Trp-Trp staple and/or the presence of bromine can have an impact in passive diffusion permeability.

Therefore, two control peptides were prepared both with the two non-halogenated tryptophans. The first control was the linear version of this peptide (H-Lys-Trp-Lys-Trp-DPro-OH), expected to be non-permeable while the second control was the head-to-tail cyclic version. The chromatograms of the corresponding products are shown in Figures 3.9 and 3.10.
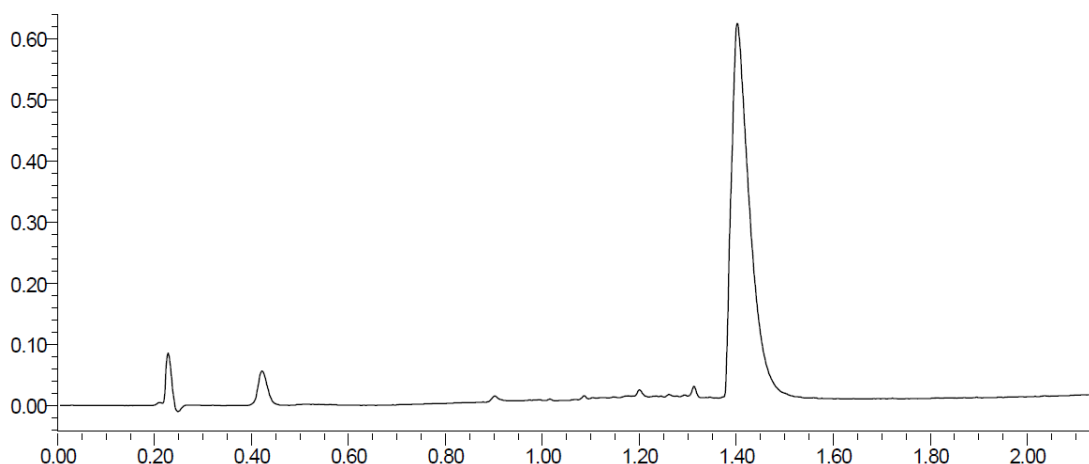
Figure 3.9. UPLC chromatogram of the crude peptide cyclo(Lys-Trp-Lys-Trp-D-Pro) in a 0-100% MeCN in 2 min gradient. Column BEH C$_{18}$, 1.7 μm, 2.1x50mm, t$_R$=1.43min.
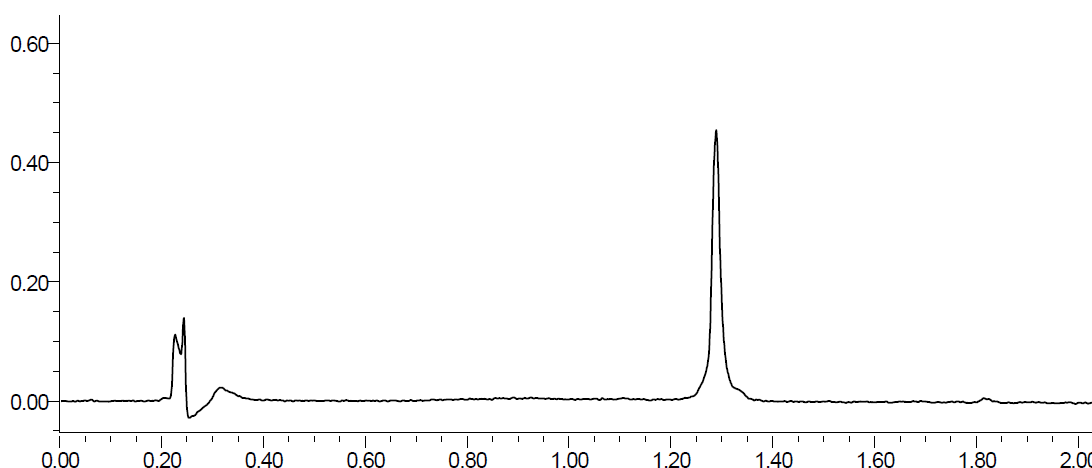
Figure 3.10. UPLC chromatogram of the crude peptide H-Lys-Trp-Lys-Trp-D-Pro-OH in a 0-100% MeCN in 2 min gradient. Column BEH C$_{18}$, 1.7 μm, 2.1x50mm, t$_R$=1.27min.

Both controls were prepared using standard solid-phase Fmoc/*t*Bu strategy in 2-chlorotrytil resin. Cleavage for the obtention of the linear peptide (H-Lys-Trp-Lys-Trp-D-Pro-OH) was performed using 95% TFA, 2.5% TIS, 2.5% H$_2$O to also remove the Boc protecting groups used in both lysine and tryptophan side-chains. Cleavage of the peptide to be cyclized in solution was carried out at 2% TFA, 98% DCM to maintain lysine side-chain protecting group and avoid side reactions during the last step of head-to-tail cyclization in solution. After macrocyclization, a solution of 50% TFA in DCM was used to remove Boc protecting groups in solution and rendered the final cyclic product,cyclo(Lys-Trp-Lys-Trp-D-Pro).

The obtained results for PAMPA are summarized in Tables 3.1 and 3.2.

Table 3.1. Effective permeability and transport after 4h assayed by PAMPA comparing the different Trp-Trp stapled peptides with cyclo(Lys-Trp-Lys-Trp-D-Pro).

Compound	P_e(x10^6) cm/s	T(%) (4h)
Bicyclic 5,5: cyclo(Lys-(5&)Trp-Lys-(5&)-Trp-D-Pro-)	3.8 ± 1.9	7.4 ± 2.4
Bicyclic 6,6: cyclo(Lys-(6&)Trp-Lys-(6&)-Trp-D-Pro-)	3.7 ± 0.6	7.2 ± 1.0
Bicyclic 7,7: cyclo(Lys-(7&)Trp-Lys-(7&)-Trp-D-Pro-)	7.6 ± 1.0	13.7 ± 1.5
Head-to-tail cyclic: cyclo(-KWKWp-)	2.7 ± 0.2	5.3 ± 0.3

Table 3.2. Effective permeability and transport after 4h assayed by PAMPA comparing the different bromine-containing peptides with cyclo(Lys-Trp-Lys-Trp-D-Pro) and linear H-Lys-Trp-Lys-Trp-D-Pro-OH.

Compound	P_e(x10^6) cm/s	T(%) (4h)
Cyclic 5Br: cyclo(Lys-(5Br)Trp-Lys-(5Br)-Trp-D-Pro-)	4.7 ± 0.4	8.9 ± 0.7
Cyclic 6Br: cyclo(Lys-(6Br)Trp-Lys-(6Br)-Trp-D-Pro-)	4.6 ± 0.1	8.9 ± 0.2
Cyclic 7Br: cyclo(Lys-(7Br)Trp-Lys-(7Br)-Trp-D-Pro-)	1.3 ± 0.6	2.6 ± 1.1
Head-to-tail cyclic: cyclo(Lys-Trp-Lys--Trp-D-Pro-)	2.7 ± 0.2	5.3 ± 0.2
Linear: H-Lys-Trp-Lys-Trp-D-Pro-OH	$0.1 \pm 3 \cdot 10^{-3}$	0.2 ± 10^{-2}
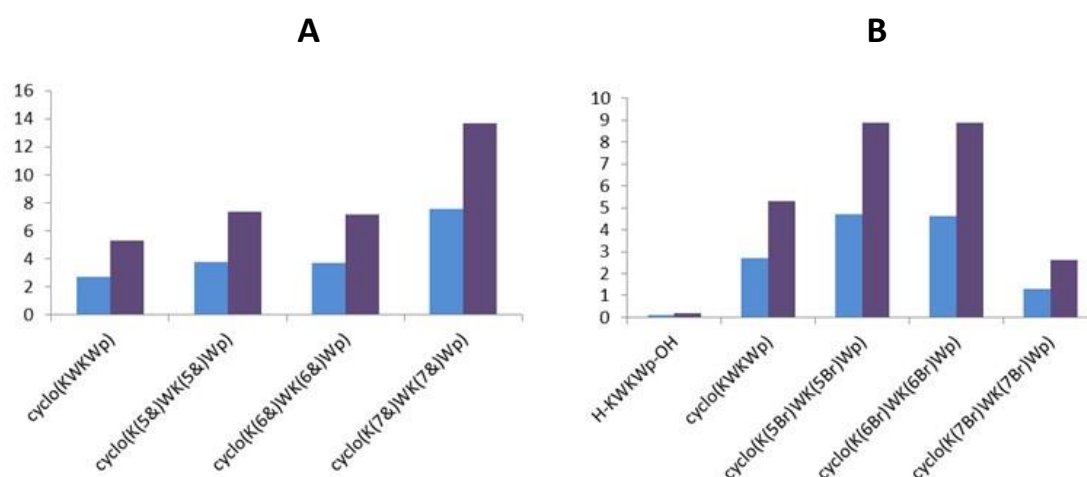
Figure 3.11. Effective permeability and transport after 4h in PAMPA assay. A) Comparison of cyclo(Lys-Trp-Lys-Trp-D-Pro) with Trp-Trp stapled peptides and B) Comparison of cyclo(Lys-Trp-Lys-Trp-D-Pro) and linear H-Lys-Trp-Lys-Trp-D-Pro-OH with the bromine-containing peptides. In blue P_e(x10^6) cm/s and in purple T(%) (4h).

As it can be seen in Figure 3.11.A, the introduction of the staple represented an increase of permeability although it depends on the cross-linked positions. Moreover, as displayed in Figure 3.11.B, having bromine in the sequence also appeared to translate into higher permeability also depending on the position of the bromine in the indole ring[201].

By introducing a staple, permeability values for the head-to-tail cyclic and the linear peptides can be increased. It is known[201] that having an halogen in phenylalanine ring increases the transport. This effect is also displayed when bromine atoms were present in the indole group of tryptophans. In our case, linear control peptide was not permeable, which means that cyclization, as well as, avoidance of the *N*- and *C*- termini charges in this kind of molecules are key factors for the transport. The effect of macrocyclization was also pointed out in the different families studied in Chapter 2 of the present thesis.

Studying in detail the different brominated cyclic peptides, regarding the effect of the position of bromine, values of permeability for the substitution in position 5 and 6 were practically the same while a decrease was observed in the substitution at position 7. This effect could not be explained due to the charge density of this position, since 5, 6 and 7 positions of the indole group are all electrophiles.

In the case of the bicyclic stapled peptides, stapling between 5-5 and 6-6 positions rendered similar results while stapling between positions 7 showed an interesting increase in permeability, being this compound the most permeable one.

In fact, the results were curious since while substitution at position 7 for bromine proved to give the less permeable head-to-tail cyclic peptide, when stapling tryptophans between the same 7 positions, the resulting bicyclic peptide was the most permeable. We hypothesize that the different results in Trp-Trp stapled peptides come from the different structures adopted from the molecules. As explained in Chapter 1 for crosslinking of phenylalanines between positions 4 and positions 3, significant differences can arise from the constraint of the structures and the length of the bonds between the aromatic residues involved in the stapling. Molecular modelling could be an interesting prove to validate the hypothesis.

3.4   Effect of stapling: Trp-Trp vs Phe-Phe

On the other hand, after having prepared these new stapled compounds it became interesting to compare their permeability values obtained by PAMPA with the ones corresponding to the analogues stapled between two phenylalanines (Figure 3.12).
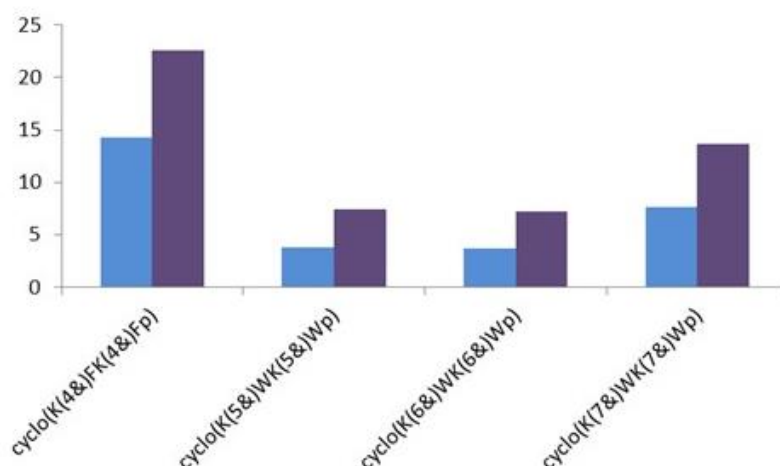
Figure 3.12. Effective permeability and transport after 4h in PAMPA assay. Comparison of the Trp-Trp stapled peptides with cyclo(-K(4&)F(4&)Fp-), fully explained in Chapter 2. In blue P_e(x10^6) cm/s and in purple T(%) (4h).

The bicyclic peptide with the stapling between the two phenylalanines was more permeable than the one displaying Trp-Trp stapling. Nonetheless, the difference was significantly smaller than when the Phe-Phe stapled peptide was compared with the other three control peptides (linear stapled, head-to-tail cyclic and linear).

This result demonstrated the relevance of introducing a second cycle through the biaryl staple in order to increase passive diffusion permeability independently of the particular stapling. Therefore, we can conclude that the stapling provides higher permeability although the nature of this stapling, meaning the amino acids involved as well as the positions cross-linked, can slightly modify the increase of the transport.

Having compared the different bicyclic peptides it became interesting to see the real impact that stapling induced in the different previous sequences in front of the linear and cyclic versions (Figure 3.13)
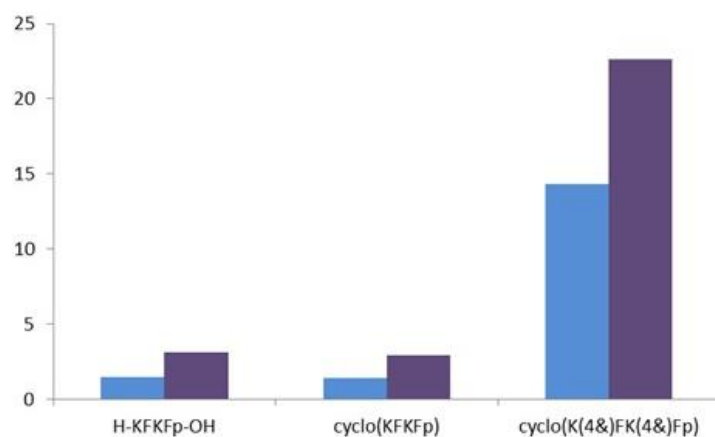
Figure 3.13: Effective permeability and transport after 4h in PAMPA assay. Comparison of the linear, head-to-tail cyclic and biaryl bicyclic peptides with phenyalanines analyzed in Chapter 2. In blue P_e(x10^6) cm/s and in purple T(%) (4h).

In both cases, Phe-Phe and Trp-Trp, the staple introduces an increase in permeability, which is higher in the case of Phe-Phe.

Finally, the comparison between all the different head-to-tail cyclic peptides synthesized during the thesis was also carried out.
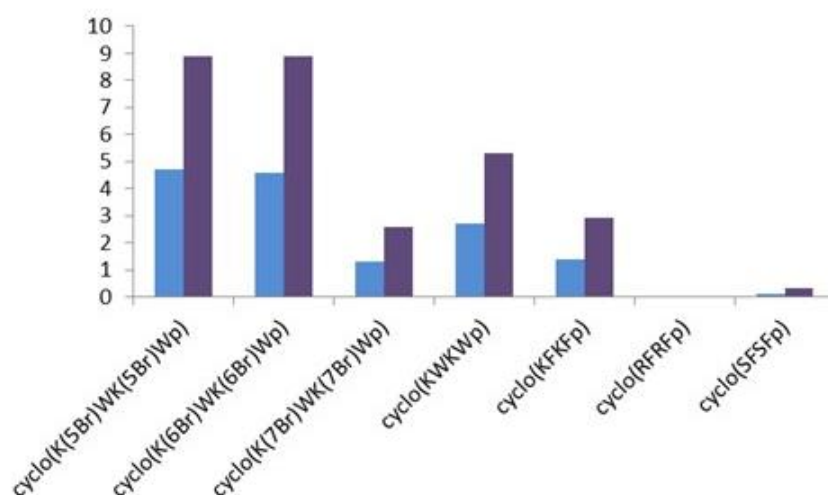
Figure 3.14. Effective permeability and transport after 4h in PAMPA assay. Comparison of the head-to-tail cyclic Trp-bromine containing peptides with the head-to-tail cyclic Phe versions described in Chapter 2. In blue P_e(x10^6) cm/s and in purple T(%) (4h).

Permeability values of the Trp-bromine containing peptides were higher than for the head-to-tail cyclic peptide with phenylalanines.

3.5 Cell viability assay

Encouraged by the good passive diffusion permeability values obtained for the bromine-containing peptides, we decided to evaluate the effect of this halogen in terms of cytotoxicity.

Linear and cyclic versions, H-Lys-Trp-Lys-Trp-D-Pro-OH and cyclo(Lys-Trp-Lys-Trp-D-Pro), were also tested as controls.

Cell viability assay was performed at two different concentrations, 200μM and 500μM, in HeLa cells. XTT cell proliferation assay was carried out. This is an effective method to measure cell growth and cytotoxicity. XTT reagent is a colourless product that becomes orange upon reduction (Figure 3.15). The XTT formazan product is soluble and can be used in real-time assays. Measurements of the plaque can be done until reaching optimal absorbance at 475nm to achieve better quantification. Obtained cell viability values are shown in Table 3.3.

XTT tetrazolium

XTT formazan

Figure 3.15. Reduction of XTT tetrazolium to form the colored formazan derivative.
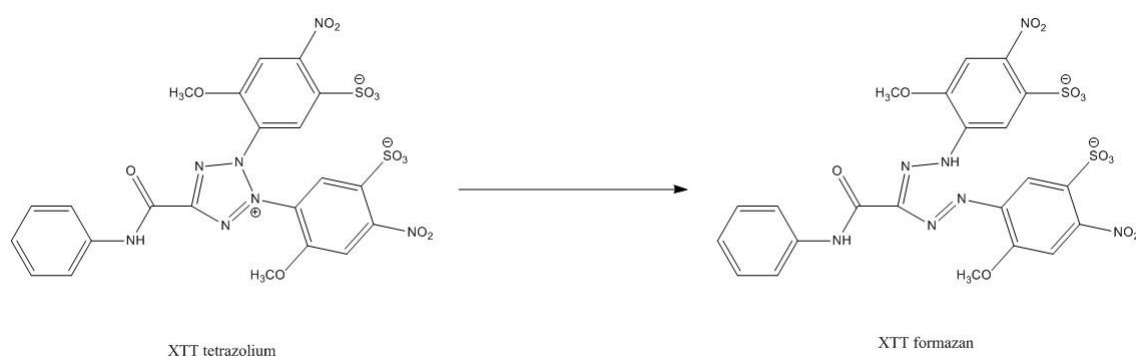
At 200 µM concentration, no cell death was detected for any of the tested peptides. When increasing concentration, while the linear and head-to-tail cyclic peptides showed some cytotoxicity, bromine-containing peptides remained the same. The only exception was observed for compound with bromine at position 5, showing only 11% of cell survival. This could point out towards the importance of the halogen substitution at the tryptophan aromatic ring.

Table 3.3. Cytotoxicity values for linear, head-to-tail cyclic and bromine-containing peptides at 200 and 500 µM concentrations expressed as percentage of cell survival.

	200µM	500µM
Linear: H-Lys-Trp-Lys-Trp-D-Pro-OH	94	79
Head-to-tail cyclic: cyclo(Lys-Trp-Lys-Trp-D-Pro)	100	68
Cyclic 5Br: cyclo(Lys-(5Br)Trp-Lys-(5Br)Trp-D-Pro)	98	11
Cyclic 6Br: cyclo(Lys-(6Br)Trp-Lys-(6Br)Trp-D-Pro)	100	100
Cyclic 7Br: cyclo(Lys-(7Br)Trp-Lys-(7Br)Trp-D-Pro)	100	100
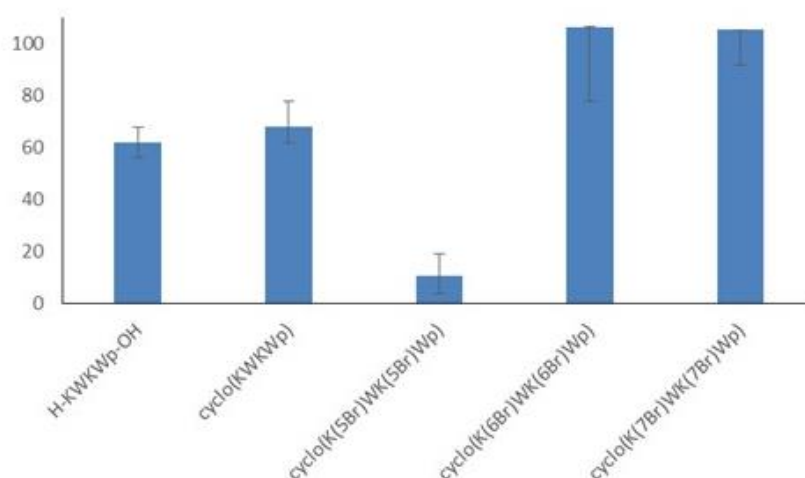
Figure 3.16. Cell viability assay at 500µM concentration of the tested peptides.

In summary

Biaryl bicyclic synthetic methodology was successfully applied to a novel class of stapled peptides, Trp-Trp. Stapling between tryptophan residues at different positions of the indole group were achieved (5&,5&; 6&,6&; 7&,7&). Although longer reaction times for Miyaura borylation and Suzuki cross-coupling were required, bromine-containing tryptophans were able to undergo these reactions.

Comparison of the Trp-Trp bicyclic peptides with the Phe-Phe was carried out proving the relevance of the staple nature. In terms of passive diffusion permeability, stapling between phenylalanine residues proved to be more adequate to facilitate the transport.

During the development of this collaboration we realized about the potential of bromine introduction in our scaffold. As previously described in the group, the incorporation of halogens enhanced passive transport. Moreover, halogen substituted positions in the indole group were also relevant for permeability, since different results were obtained for the synthesized compounds. The reduced synthetic complexicity of the cyclic Trp-bromine containing peptides in front of the bicyclic compounds and the great similarity in passive transport, draw our interest in them.

XTT assay proved that bromine halogen was not cytotoxic when incorporated into these peptides at low concentration, 200μM. Increasing the tested concentration up to 500 μM, cell death was only critical for the compound cyclic 5Br. This unexpected result was again a proof of the relevance of bromine substitution position in the indole group. Noteworthly, at the highest tested concentration, cyclic 6Br and cyclic 7Br were significantly less cytotoxic than the linear and cyclic control versions.

In addition, halotryptophan amino acids can be a great importance due to their potential applications. On one side, the exploration of our methodology demonstrated

that they can participate as reagents to render more complex peptides. On the other side, more interesting properties can be derived from these residues, such as antimicrobial activity has been described for Bittner *et al.*[202]

Bibliography

[193] E. M. Sletten, C. R. Bertozzi, Bioorthogonal chemistry: fishing for selectivity in a sea of functionality, *Angewandte Chemie* **2009**, *48*, 6974-6998.

[194] L. Ackermann, Carboxylate-assisted transition-metal-catalyzed C-H bond functionalizations: mechanism and scope, *Chem. Rev.* ***2011,*** *111*, 1315–1345.

[195] J. Wencel-Delord, T. Dröge, F. Liu, F. Glorius, Towards mild metal-catalyzed C-H bond activation, *Chem. Soc. Rev.* **2011**, *40*, 4740–4761.

[196] W. E. C. Harries, s. Khademi, R. M. Stroud, The role of tryptophan cation-pi interactions on ammonia transport through the AmtB ammonia channel, *International Congress Series* **2007**, *1304*, 15-21.

[197] G. W. Gokel, Indole, the aromatic element of tryptophan, as a pi-donor and amphiphilic headgroup, *International Congress Series* **2007**, *1304*, 1-14.

[198] T. Willemse, K. Van Imp, R. J. M. Goss, H. W. T. Van Vlijmen, W. Schepens, B. U. W. Maes, S. Ballet, Suzuki-Miyaura diversification of amino acids and dipeptides in aqueous media, *ChemCatChem.* **2015**, *7*, 2055-2070.

[199] R. Rossi, F. Bellina, M. Lessi, Selective palladium-catalyzed Suzuki-Miyaura reactions of ployhalogenated heteroarenes, *Advanced synthesis&catalysis* **2012**, *354*, 1181-1255.

[200] L. Shen, S. Huang, Y. Nie, F. Lei, An efficient microwave-assisted Suzuki reaction using a new pyridine-pyrazole/Pd(II) species as catalyst in aqueous media, *Molecules* **2013**, *18*, 1602-1612.

[201] M. Malakoutikah, B. Guixer, P. Arranz-Gibert, M. Teixido, E. Giralt, "À la carte" peptide shuttles: tools to increase their passage across the blood-brain barrier, *ChemMedChem* **2014**, *9*, 1594-1601.

[202] S. Bittner, R. Scherzer, E. Harlev, The five bromotryptophans, *Amino Acids* **2007**, *33*, 19-42.

CHAPTER 4

TARGETING THE TETRAMERIZATION DOMAIN OF MUTATED P53 PROTEIN

One of the main potential applications of peptides as therapeutic agents is to target protein-protein interactions (PPIs).

Despite of the current interest in this topic, targeting PPIs is not as trial and easy as it could be imagined. The designed compounds must selectively recognise the protein surface, whose conformational flexibility in the unbounded state and post-translational modifications may introduce extra complexity.

Most of the existing peptides targeting PPIs are used as inhibitors of this interaction, as it was previously explained. Nevertheless, enhancement or restoration of the stability and/or activity of the system can be more interesting but complicated. While inhibition can be achieved by preventing the binding of the protein partners, restoring the stability or activity should also mimic the interaction which is responsible for the response. Few examples of stabilization of protein complexes can be found in literature[155,203,204].

Moreover, biophysical studies are often performed in artificial environments that scarcely represent physiological conditions. Nonetheless, such techniques, like circular dichroism (CD), are able to provide information regarding protein-protein and protein-ligand interactions using minimal amount of the always valuable target protein, as well as, the selected ligands. In addition, thermodynamic and kinetic information can also be obtained by further analysis.

Following the previous studies developed in our group by Dr. S. Gordo, we now studied the interaction of the arginine bicyclic peptide with p53 tetramerization domain to recover the self-assembly of R337H p53 tetramerization domain mutant.

4.1   The protein targets

4.1.1 p53TD: wild-type protein

Major attention in p53 protein has been focused in the DNA binding domain while previous work in the laboratory initiates the efforts to study the tetramerization domain.

The highly p53TD symmetric tetramer, better defined as a dimer of dimers, is a short domain of 32 residues. Although it could be described as a peptide due to its reduced size, is frequently referred to as a protein.

The structure of this tetramerization domain was solved both by NMR spectroscopy[205] and X-ray crystallography[206] (Figure 4.1)

A   **B**
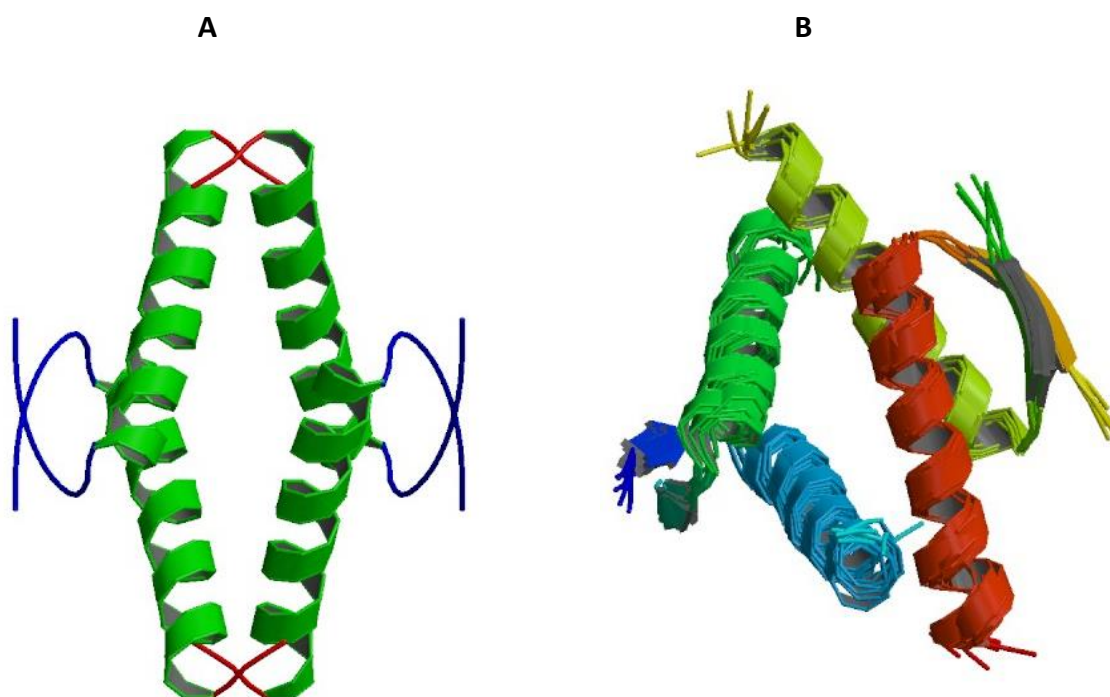
Figure 4.1. A) Crystal structure of p53TD, PDB source 1AIE entry B) NMR solved structure of p53TD, PDB source 2J0Z entry.

Between residues E326 and R333 a β-strand is present, while residues comprised between R335 and A355 or K357 (different residues according to the source of information) are structured as an α-helix, both secondary structures linked by a sharp turn at G334. The arrangement of the dimers buries a hydrophobic core constituted by the four α-helical bundles with two β-sheets at opposite faces exposed to the surface.

High folding tendency of the protein without requiring the use of folding agents and just influenced by the working concentration was connected with a strong driving force, the hydrophobic effect. Side-chains of residues I334, G334, F338 and F341 form a small hydrophobic pocket that cause the V-sharp adopted by monomers in the structure. Folding of the protein is believed to take place through dimerization of monomers and then, dimerization of two dimers. Initially, two monomers interact by hydrogen bonding in the antiparallel β-sheet formed, as well as, a relevant salt bridge between R337 and D352 side-chains is established. A hydrophobic interface comprising F328, L330, I332, F338, F341 and N345 residues resulted from the primary dimer formation. The interaction between two primary dimers takes place between the α-helices burying side-chains of residues M340, L344, A347, L348 and L350 from the solvent. The generated hydrophobic core helps to overcome the entropic cost of the folding and result in a highly stable tetrameric structure. In fact, it is worth mentioning that monomers and dimers are not thermodynamically stable in the case of the wild-type protein.

The role of different amino acids in p53 protein is well known due to the high number of studies developed[147,207]. The hydrophobic core has been conserved throughout evolution[208] since these residues are crucial for tetramer formation[147] domain.

4.1.2 R337H: protein mutant

Previous research developed in our group focused on the studies of three different mutants of the p53 tetramerization domain: R337H, G334V and L344P. Due to its high biological relevance, we selected R337H mutant in this thesis.

Mutation of arginine 337 to histidine (R337H) is the most important mutation in this domain. Nonetheless, neither crystal nor NMR solves structure is accessible at the PDB.

The 0.3% of the general population in southern Brazil presented this mutation, which is not only associated with pediatric adrenocarcinoma but also common in Brazilian Li-Fraumeni (LF) and Li-Fraumeni-like (LFL) families. Recent studies suggested that the inheritance of this point mutation may significantly contribute to breast cancer in Brazil population[209].

Mutant R337H can fold into a tetrameric structure but it presents lesser stability than the wild-type p53TD. We pointed out the relevance of a salt bridge between R337 and D352 to stabilize the primary dimer. The point mutation does not only involve a different side-chain but, specifically, a group with a lower pK_a. If H337 is protonated, pH≤pK_a=6.5, the tetramer can be formed in a stable way like the wild-type p53TD. However, at higher pH the histidine is not protonated causing the neutralization of the salt bridge and leading to an unstable tetramerized domain.

These results also concordats with the tissue specificity observed in adrenocortical carcinoma, in which adrenal cells may present pH~7.9 under certain situations[210].
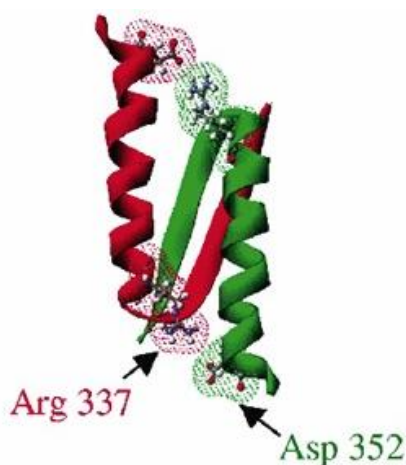
Figure 4.2. Residues involved in the salt bridge. R337 is lacking in the mutant.

4.2   Gaining access to the target proteins: p53TD and R337H

4.2.1 Recombinant p53TD wild-type

Previous work in our group established an initial protocol in order to obtain wild-type p53TD. The method is based on the overexpression in *Escherichia coli* cultures and it finally yields milligrams of the pure desired protein. Following this protocol, the expression was repeated to gain access to the ^{15}N-labelled proteins with the initial purpose of NMR experiments. Expression in bacteria is the general preferred method to obtain labelled proteins in suitable amounts.

The clone used for the expression of the wild-type p53TD was a kind gift from Dr. M. G. Mateu from Cambridge University. This DNA sequence encodes the protein fragment between residues 311-367 (named as p53_tetS), which is nearly twice longer than the structured tetramerization domain, p53TD. The two flanking tails proved to yield better expression levels and despite the fact that they are randomly coiled they do not affect the structure. Minimal media was used to perform ^{15}N-labelled protein production. The obtained protein was highly soluble and well-folded without requiring the use of folding agents.

Figure 4.3. p53_tetS encoded amino acid sequence (311-367).

Purification was performed using a FPLC apparatus. The first stage of purification was a cation-exchange chromatography (CATEX), that could be performed owing to the high isolectric point of p53_tetS, which is around 8.3. Extracted from the soluble fraction of cell lysates, the protein got attached to the cation-exchange column and then eluted in a sodium chloride gradient. Afterwards, size-exclusion chromatography (SEC) was

carried out separating the remaining proteins according to their size. Finally, buffer exchange was performed and the protein was lyophilized being resistant to this process and properly folded when redissolved again.

It is worth mentioning that in the previous work (S. Gordo, Ph.D thesis, 2008), the established protocol of purification by FPLC was carried out at room temperature without facing degradation problems of the protein throughout the purification process. Nevertheless, when purifying at room temperature, our protein was not detected by gel electrophoresis after size-exclusion chromatography.
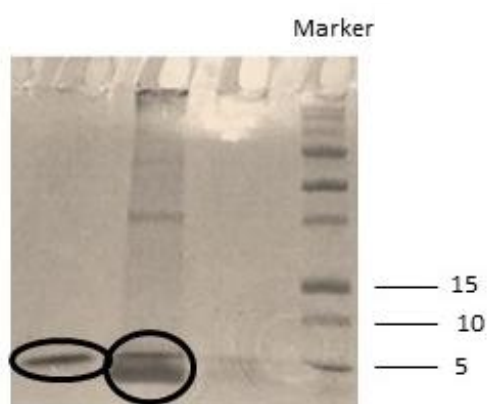
Figure 4.4. SDS-PAGE of cation exchange FPLC purified p53-tetS of the diferent samples.

4.2.2 Recombinant R337H mutant

Clone of the mutant R337H with the flanking tails was obtained by site-directed mutagenesis of the p53_tetS, this clone was prepared by Dr. Susana Gordo in our group.

Using this clone, it was successfully expressed and purified R337H mutant with the flanking tails following the same protocol established for the wild-type protein and performing the FPLC purification at 4°C in this case (Figure 4.5).
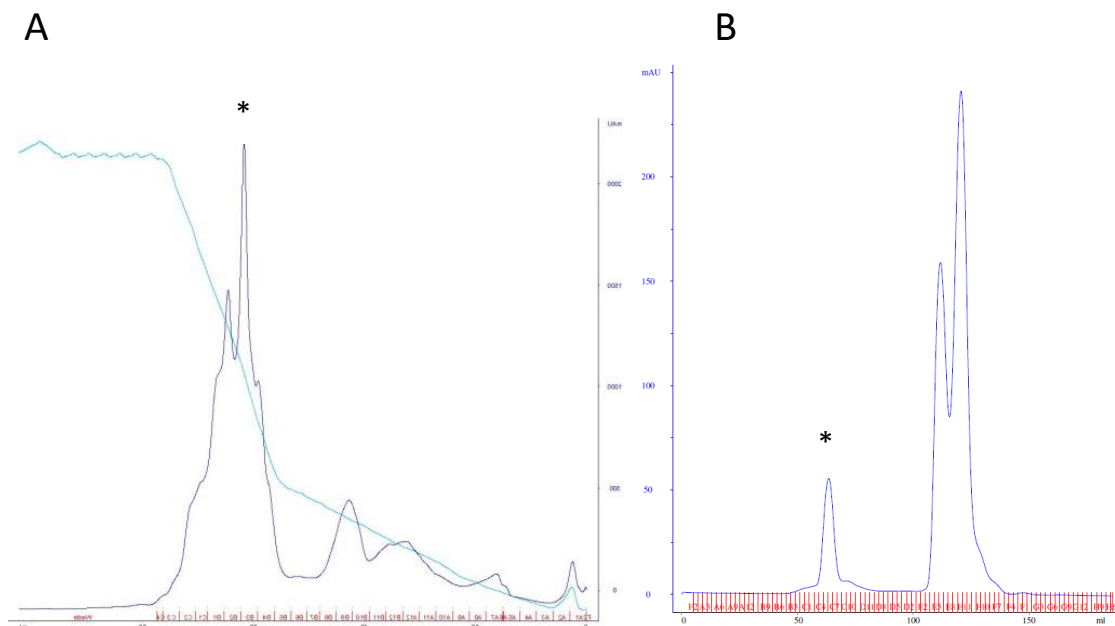
Figure 4.5. A) Cation exchange purification of the mutant R337H with the flanking tails B) Size exclusion purification of the mutant R337H with the flanking tails. *denotes the desired protein

Characterization of the obtained mutant protein was also performed by gel electrophoresis. First, calibration of the size-exclusion column was carried out. Some proteins of known molecular weight were injected into the size-exclusion column to determine their elution volume (V_e). The partition coefficient, K_{av}, was calculated for the different proteins and represented according to their molecular weight to obtain a calibration curve (equation of K_{av} is shown in Figure 4.6).

$$K_{av} = \frac{V_e - V_o}{V_c - V_o}$$

Figure 4.6. Equation to calculate the partition coefficient, K_{av}. V_e corresponds to the elution volume measured from the chromatogram and related to the molecular size of the molecule. V_o corresponds to the void volume, the elution volume of molecules that are excluded from the gel filtration medium because they are larger than the largest pore in the matrix and pass straight through the packed bed. V_c is the column volume.

Table 4.1. Elution volume obtained in SEC and calculated partition coefficient for three control proteins. V_c was 120 mL while V_o was the elution volume of Blue Dextran 2000, V_o=45.45 mL.

	Molecular weight (MW)	Elution volume (V_e)	K_{av}
Ribonuclease A	13,7	80,5	0,47
Chymotrypsinogen	25	74,1	0,38
Ovalbumin	43	61,4	0,21
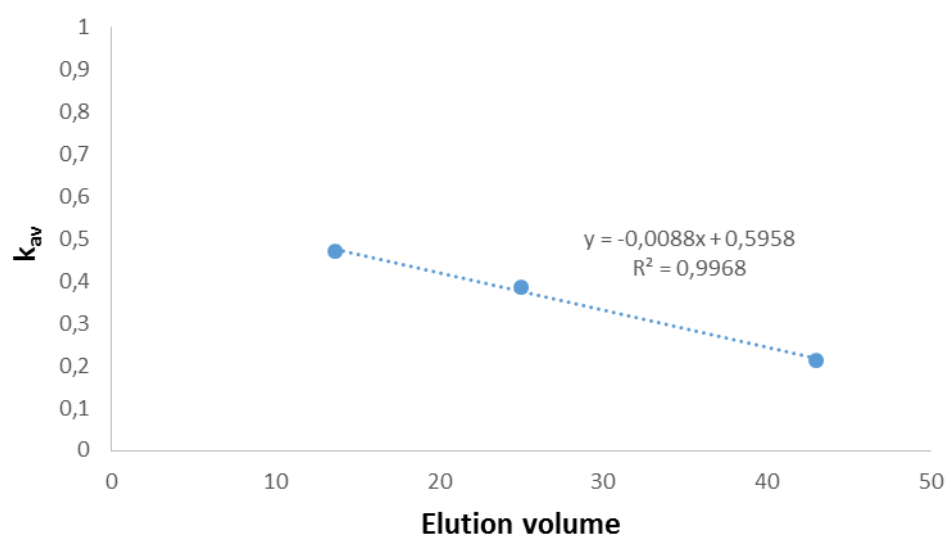
Figure 4.7. Calibration of the used SEC column with three control proteins and estimation of the molecular weight corresponding to the purified mutant R337H.
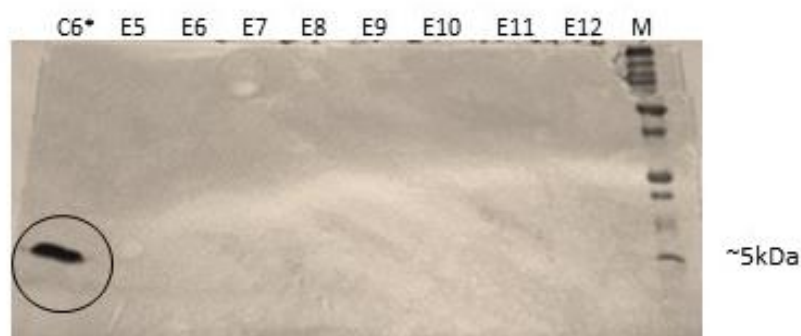
Figure 4.8. SDS-PAGE of the mutant R337H after size exclusion chromatography purification. C6 corresponds to the fraction labelled with * in Figure 4.5.B.

SDS-PAGE confirmed the presence of the mutant R337H with the flanking tails in fraction C6 of SEC (Figure 4.8 B). This result was surprising for us as we expected that small size proteins elute at higher volumes.

At the elution volume of the R337H mutant protein, V_e=63.5mL, the obtained molecular weight corresponded to a specie of 48kDa. This value was higher than the expected (25kDa). Nonetheless, this effect was previously described in the literature[207] and could be explained by the non espherical shape of the protein.

4.2.3 Chemical synthesis of the target proteins: p53TD and R337H mutant

The proteins without labelling were chemically synthesized using the Liberty Blue microwave assisted automatic peptide synthesizer. In this case, we decided to synthesize the sequence that constituted the tetramerization domain without the flanking regions. Therefore, the synthesized sequences were significantly smaller, from 57 to 37 amino acids. Two different synthetic protocols were used to attempt the synthesis of these proteins (Table 4.2).

Ac-KKPLDGEYFTLQIRGRE**R**FEMFRELNEALELKDAQAG-NH$_2$

Figure 4.9. Sequences of p53TD and R337H mutant without the flanking tails.

Table 4.2. Comparison of the two synthetic protocols used in the Liberty Blue automatic microwave assisted peptide synthesizer to carry out the chemical synthesis of the proteins p53TD and mutant R337H. The main differences in both protocols were found in the used coupling reagents and the cleavage conditions.

	Protocol 1	**Protocol 2**
Scale	0.1mmol	0.1mmol
Chemistry	Fmoc/*t*Bu	Fmoc/*t*Bu
Resin	Chem Matrix Rink Amide	Chem Matrix Rink Amide
Loading	0.45mmol/g	0.47mmol/g
Activator/Base	HBTU/DIEA	DIC and Oxyma
Cleavage conditions	85% TFA, 5% H_2O, 5% Anisole, 2.5% EDT 2.5% Thiophenol 2.5h	1st step: 82.5% TFA, 5% H_2O, 5% TIS, 5% Phenol, 2.5% EDT 3h 2nd step: 95% TFA, 2.5% H_2O, 2.5% TIS 1.5h

During the first attempt using protocol 1, p53TD wild-type and mutant R337H were synthesized but very few amounts were obtained after cleavage from the resin, implying a non-efficient synthetic procedure. The obtained proteins were characterized using a RP-C$_4$ column obtaining better resolution (Figure 4.10). Exact mass determination confirmed the successful synthesis of both proteins.

B
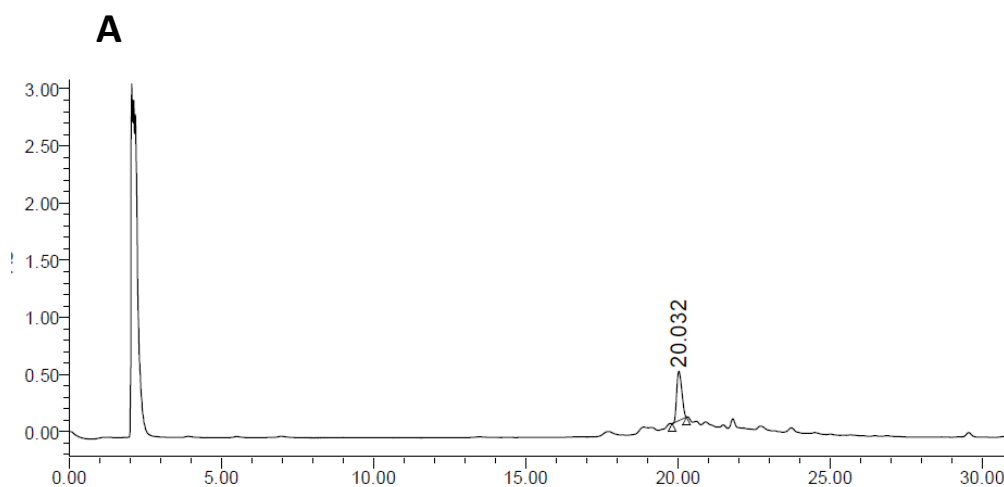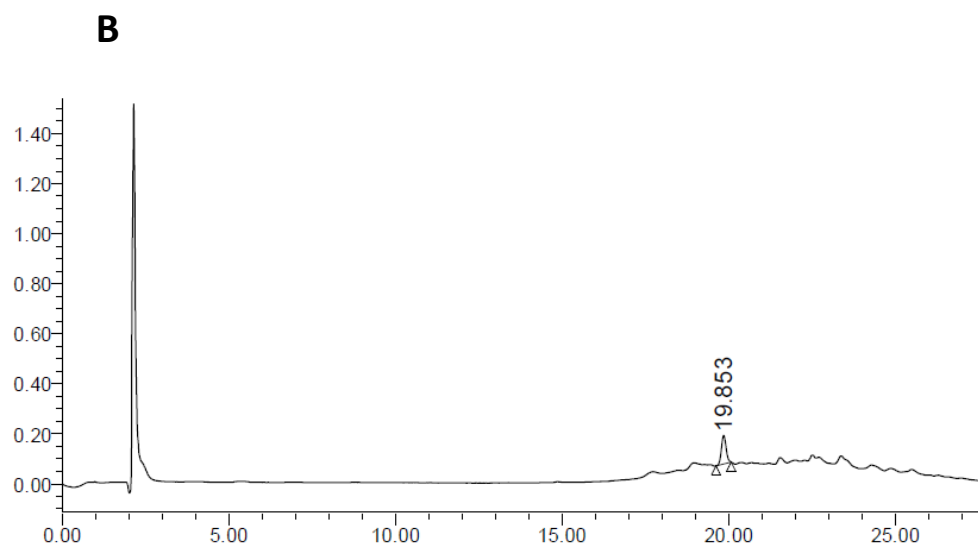
Figure 4.10. A) HPLC chromatogram of the pure protein p53TD in a gradient 50-100% MeCN in 30 min. Column C₄ (ref), t_R=20.03 min B) HPLC chromatogram of the pure protein R337H in a gradient 50-100% MeCN in 30 min. Column C₄ (ref), t_R=19.85min.

On the other hand, the synthetic protocol 2 provided higher amounts of the desired proteins.

Purification was done by HPLC-semipreparative using a RP-C_{18} column. The UPLC chromatogram of the corresponding pure proteins p53TD and R337H are shown in Figure 4.11 and 4.12.

A
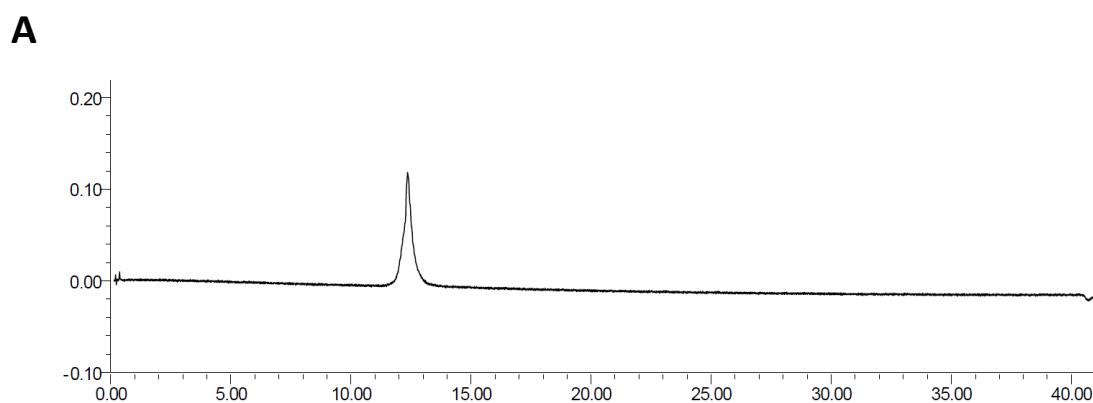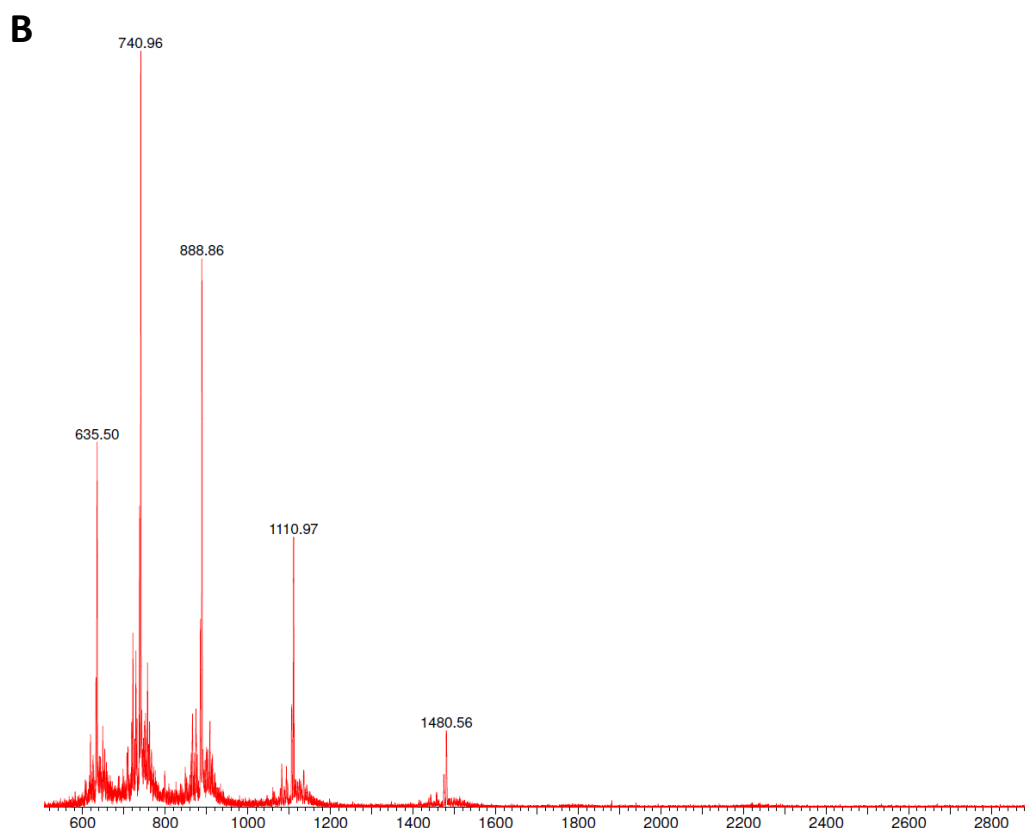
Figure 4.11. A) UPLC chromatogram of pure protein p53TD in a 10-70% MeCN gradient in 40min, column BEH C$_{18}$ 1.7μm, 2.1x50mm, t$_R$= 12.36min. B) Mass spectrum of pure protein p53TD in a 0-100% MeCN gradient in 2min, column BEH C$_{18}$ 1.7μm, 2.1x50mm, t$_R$= 1.37min. [M+3H$^+$]/3 expected= 1481.00, [M+3H$^+$]/3 found= 1480.56; [M+4H$^+$]/4 expected= 1111.00, [M+4H$^+$]/4 found= 1110.97; [M+5H$^+$]/5 expected= 889.00, [M+5H$^+$]/5 found=888.86.
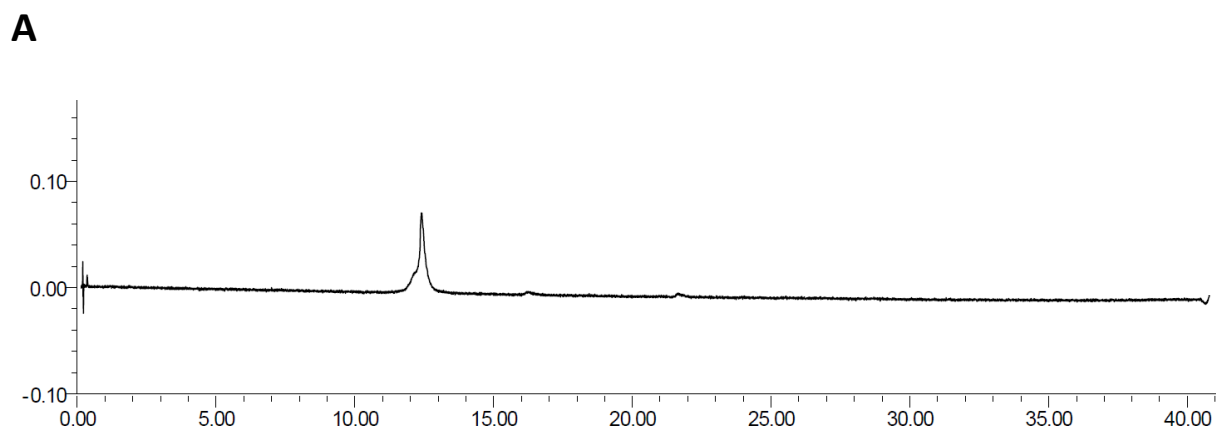
B
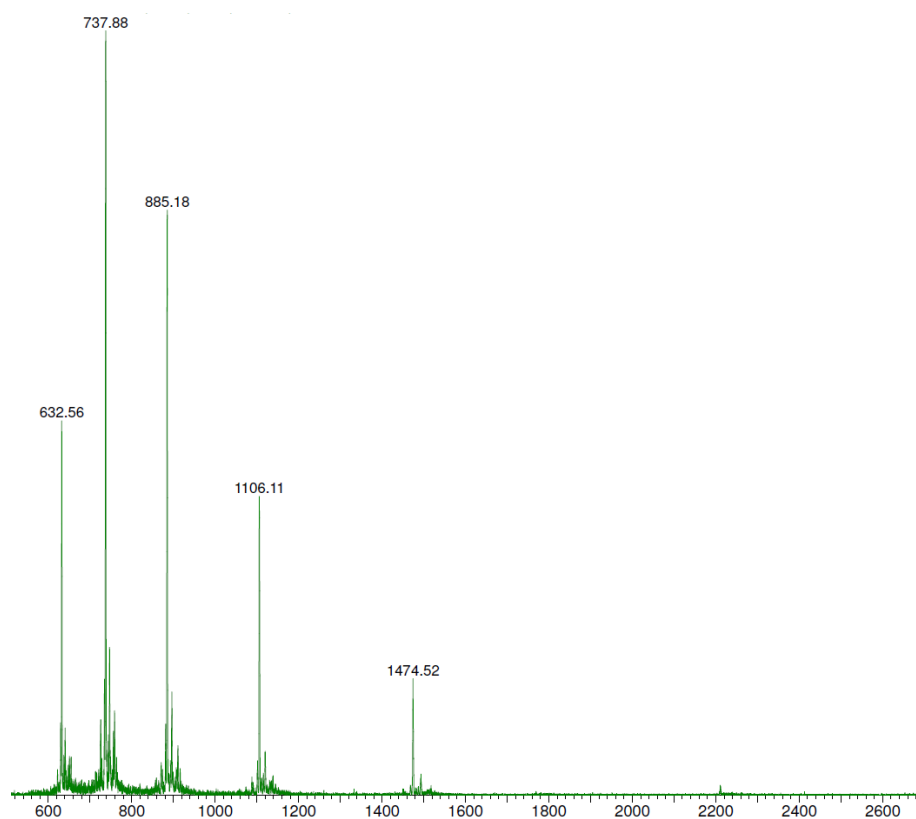
Figure 4.12. A) UPLC chromatogram of pure protein R337H in a 10-70% MeCN gradient in 40min, column BEH C$_{18}$ 1.7µm, 2.1x50mm, t$_R$= 12.41min. B) Mass spectrum of pure protein p53TD in a 0-100% MeCN gradient in 2min, column BEH C$_{18}$ 1.7µm, 2.1x50mm, t$_R$= 1.38min. [M+3H$^+$]/3 expected=1474.65, [M+3H$^+$]/3 found=1474.52; [M+4H$^+$]/4 expected= 1106.24, [M+4H$^+$]/4=1106.11; [M+5H$^+$]/5 expected= 885.19, [M+5H$^+$]/5=885.18.

Proteins were quantified by UV-Vis absorbance at 280 nm taking advantage of the presence of one tryptophan in their sequences (ε_{280}= 1280M^{-1}cm^{-1})[211]. 2.77mg of p53TD and 6.18mg of R337H were obtained after purification of part of the crude. Proteins were lyophilized in aliquots of 1400µM to be stored at -20ºC for further studies.

4.3 Biophysical characterization of the target proteins

4.3.1 NMR characterization of the target proteins

^{1}H-NMR and ^{15}N-HSQC were recorded for the ^{15}N-R337H protein. The signals were aconfirmed using the previous assignment described in the literature[187]. At the lower part of the spectra (Figure 4.12, δ_H ~8ppm and δ_C ~128ppm) some degradation signals were observed, indicating the importance of carefully preserving the protein sample.
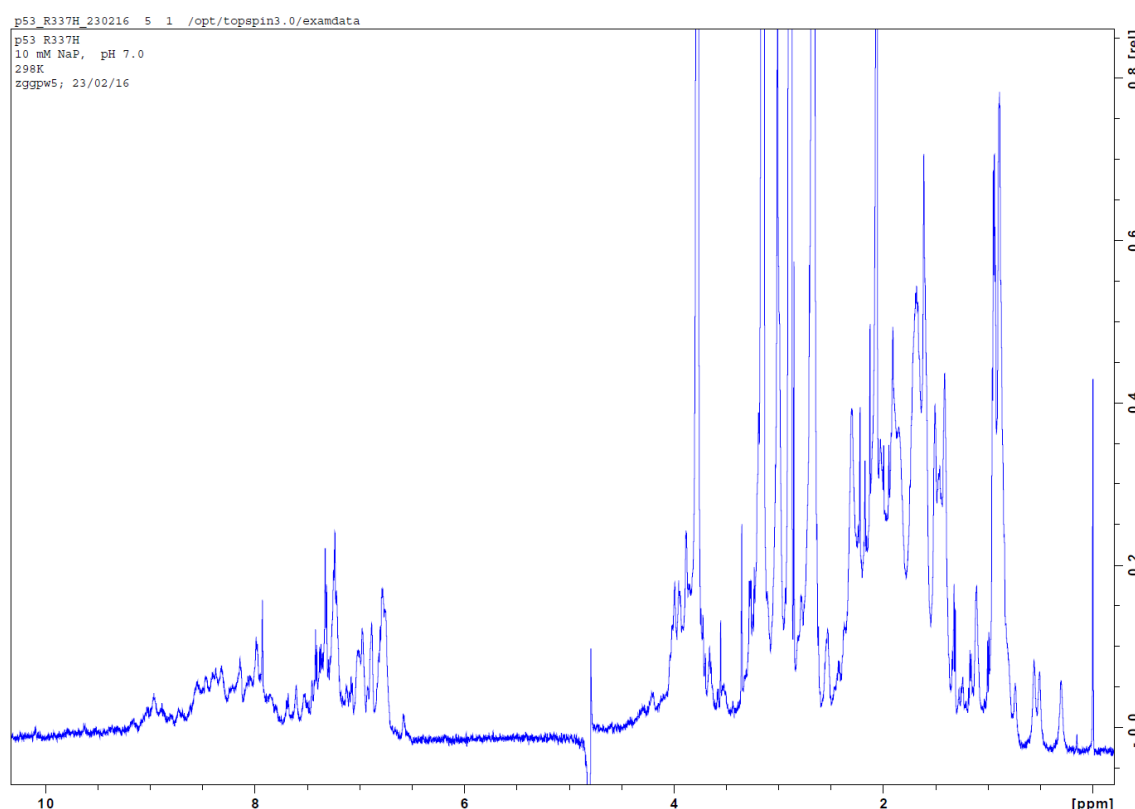
Figure 4.13. [1]H-MNR spectrum of the mutant protein ^{15}N-R337H in 20mM sodium phosphate at pH 7.0, 298K, 100μM monomer, 600MHz.

Up-field ^{1}H resonances in the range between 0.4ppm and -1.0ppm were used as a probe for the structural assessment[212,213,214]. As described in the literature[215] mutant R337H displayed up-field protons due to the rearrangements promoted by this point mutation (Figure 4.11, 0.2ppm (s), 0.45ppm (d)).
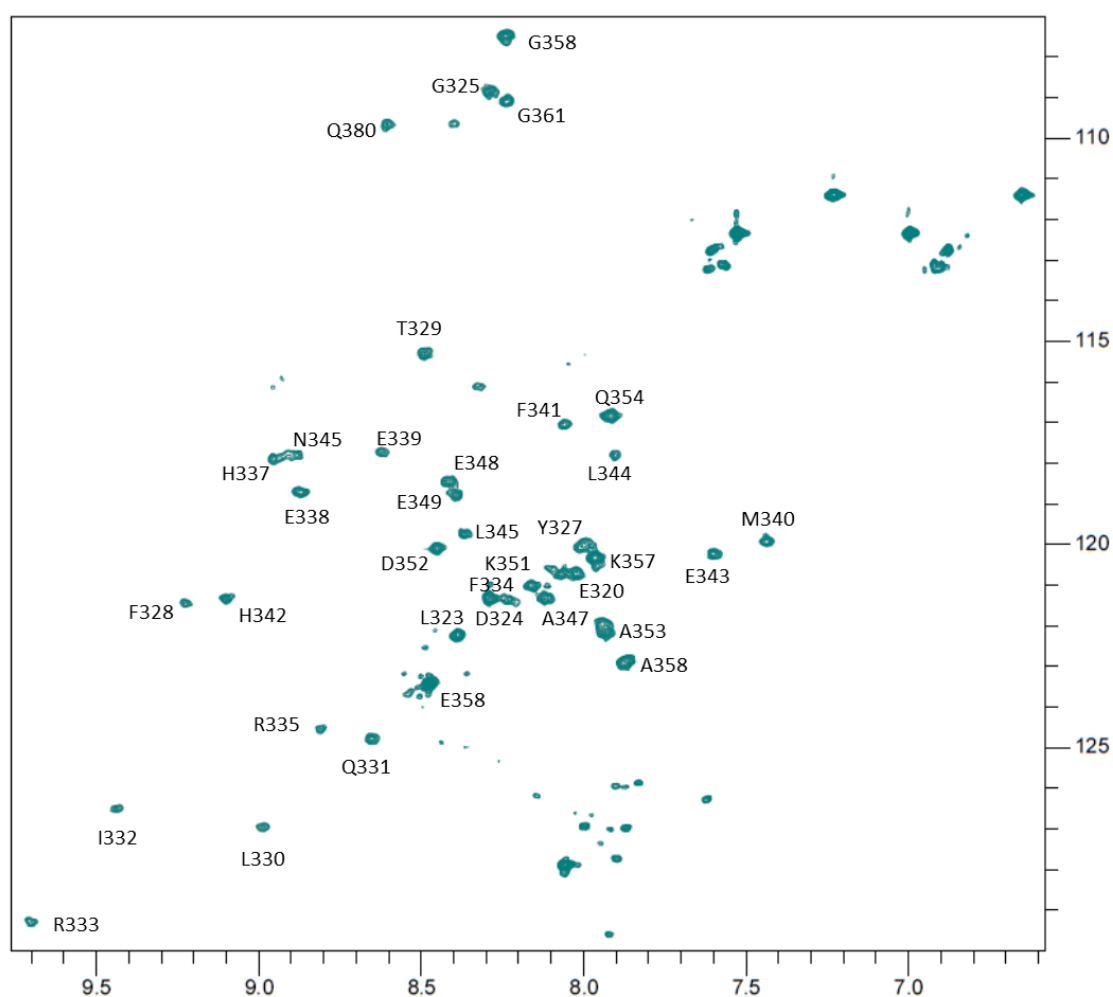
Figure 4.14. Assigned ^{15}N-^{1}H-HSQC spectrum of the mutant protein ^{15}N-R337H in 20mM NaPi at pH 7.0, 298K, 100µM monomer, 600MHz.

Although not ^{15}N-labelled, chemically synthesized p53TD and mutant R337H were also studied by NMR. Monodimensonal ^{1}H-NMR spectra were perfomed paying special attention to the up-field since, as it was previously mentioned; this region is a useful and sensitive probe for structural assessment[212,213,214]. In the spectra region between 0.4 ppm and -1.0 ppm, signals from protons, frequently from methyl groups, that are close in the space to aromatic groups, were observed.

At the NMR concentration, 100μM, mutant R337H presented a ^{1}H-NMR spectrum similar to the one corresponding to the p53TD wild-type. Marked signals in Figure 4.15 confirming the folding as a tetramer of both proteins. Although equilibrium with a certain amount of monomeric form could no be excluded by these NMR experiments.

Resonances in the up-field regions were not assigned due to the proximity to an aromatic ring. A closer look to the three-dimensional structure of the protein allowed understanding the obtained NMR results. Wild-type, p53TD, possess four aromatic amino acids whose position relies on the V-shape adopted by the monomer and the primary dimer formed during the folding process. Residue F338 is particularly sensitive to mutation R337H due to their proximity, explaining the up-field protons corresponding to this amino acid in the spectrum. It is also worth noting that this mutation introduces a fifth aromatic residue, histidine at position 337.

δH (ppm)
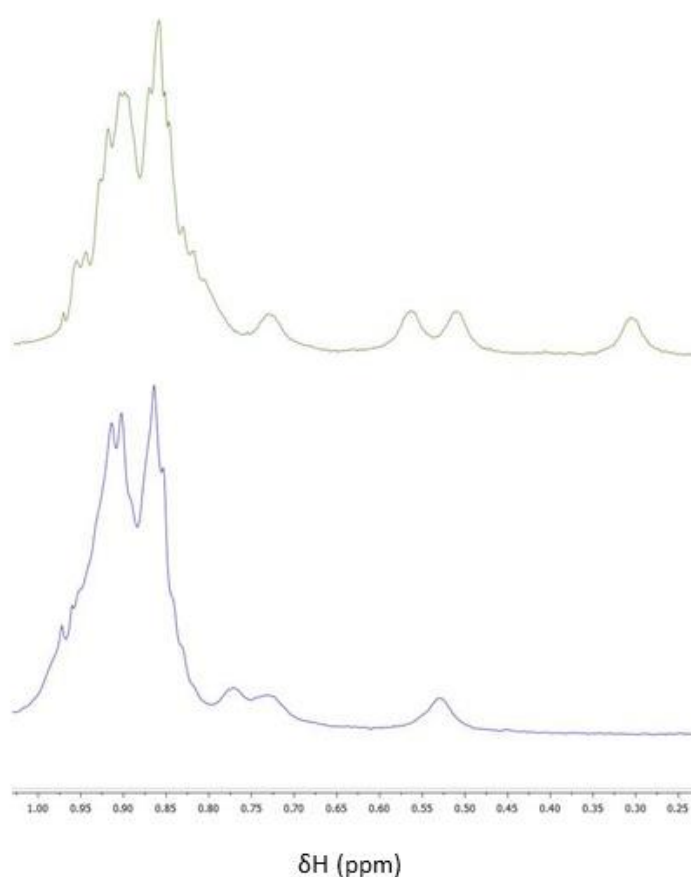
Figure 4.15. Comparison of the up-field ^{1}H-NMR spectra of proteins p53TD and mutant R337H in 20mM sodium phosphate at pH7.0, 298K, 100μM monomer concentration, 600MHz.

4.3.2 Circular dichroism

4.3.2.1 Comparison between p53TD and R337H: CD spectra and unfolding experiments

Circular dichroism (CD) enabled rapid characterization of the global structure of proteins. The CD spectra of the wild-type p53TD and the mutant R337H, both obtained from the chemical synthesis, under the same conditions are shown in Figure 4.16.
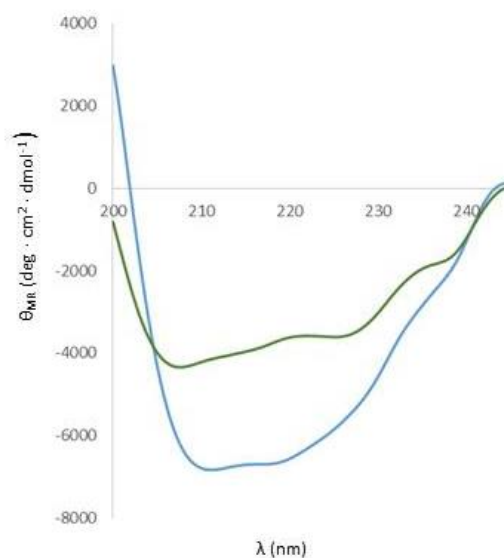
Figure 4.16. CD spectra of the p53TD wild-type (in blue) and the mutant R337H (in green) at 20µM in 25mM sodium phosphate buffer pH7, 100mM NaCl, 25ºC. Ellipticity was normalized to the mean residue concentration, θ$_{MR}$.

The spectrum of the wild-type p53TD displayed the characteristic features of a protein containing α-helices, with two negative bands at 222nm and 208nm. Parameter q (θ$_{220}$/ θ$_{208}$) was 1.0, which corresponds to the existence of interacting helices (q ≥1). This result confirmed the tetramerization of the wild-type protein spontaneously at this buffer conditions and concentration[216].

Mutant R337H presented similar levels of secondary structure than the wild-type protein[148] , with a well-defined α-helix conformation. Nonetheless, less ellipticity was observed and a more flat spectra was recorded close to 222nm negative band. Parameter q was 0.84, also close to 1 but smaller than the obtained for the wild-type p53TD protein.

Thermal stability of the proteins was also assessed by circular dichroism, tracking the changes in the ellipticity at 220nm when increasing the temperature of the samples from 15ºC to 95ºC at a heating rate of 1.5ºC/min. At this wavelength, the results would provide information about the loss of secondary structure of the proteins upon heating. This experiment enables to understand the difference in stability that the mutant R337H presents in front of the wild-type p53TD. The unfolding curves for both proteins are shown in Figure 4.15.
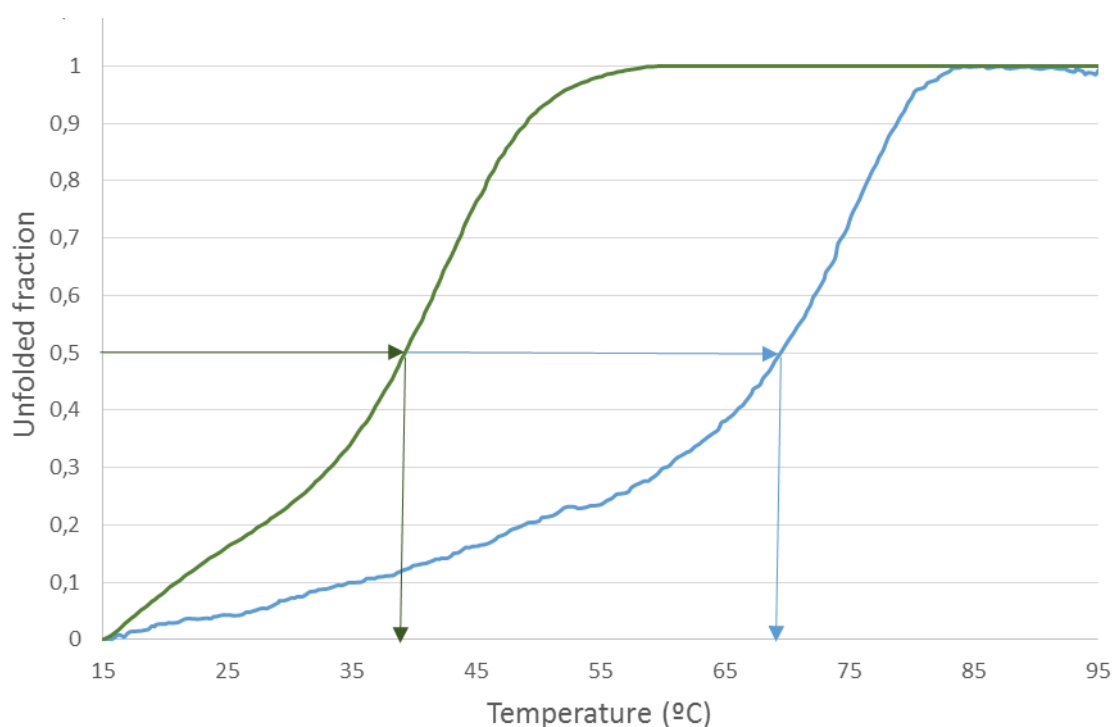
Figure 4.17. CD melting curves of p53TD wild-type (in blue) and mutant R337H (in green) at 20µM protein monomer concentrations in 25mM sodium phosphate buffer pH7, 100mM NaCl.

The unfolding mechanism for p53TD wild-type was described as a two-state process in which the folded tetramer is directly converted into the unfolded monomer[211]. As it is shown in Figure 4.17, the range of transition temperatures was narrow for p53TD,

implying a highly cooperative unfolding process. Owing to the fact that the tetramer dissociation is coupled to the unfolding process, the melting profile of the wild-type is not perfectly symmetric, having a longer plateau in the low-temperature part of the graphic.

Regarding to the mutant R337H, the melting curve was more symmetrical than the obtained for the wild-type. These results suggested that the unfolding process which takes place is not completely coupled with the dissociation process of the tetramer.

In Figure 4.18 we exemplified the possible reversible mechanism than can also involve an insoluble monomer state.
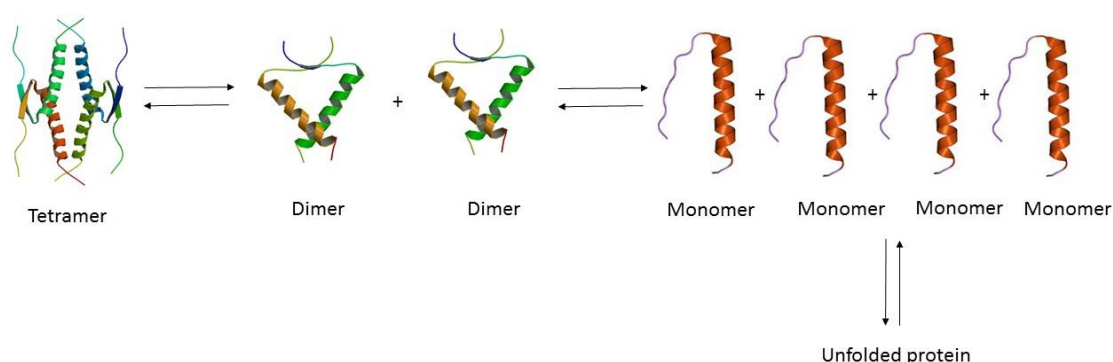
Figure 4.18. Proposed folding mechanism for p53TD.

The reversibility of the process was validated by comparison of the CD spectra at 15°C (the initial temperature of the unfolding experiment) before and after running the melting assay. The good overlapping of both spectra validated the denaturalization process withouth degradation, due to the reversibility observed.

Although no degradation of the proteins during the experiment was expected, being able to ensure this hypothesis was important. Furthermore, the recovery of the initial ellipticity at 15°C and the lack of precipitate traces in the quartz cells allowed us to discard possible precipitation of insoluble proteins, which was something we

considered when observing the unfolding curve of the mutant R337H at a different rate of heating (Figure 4.19).

The unfolding experiment for the mutant R337H protein was recorded at two different rates, 1.5ºC/min and 2ºC/min, both being slow for allowing achieving the equilibrium at every step of the process.
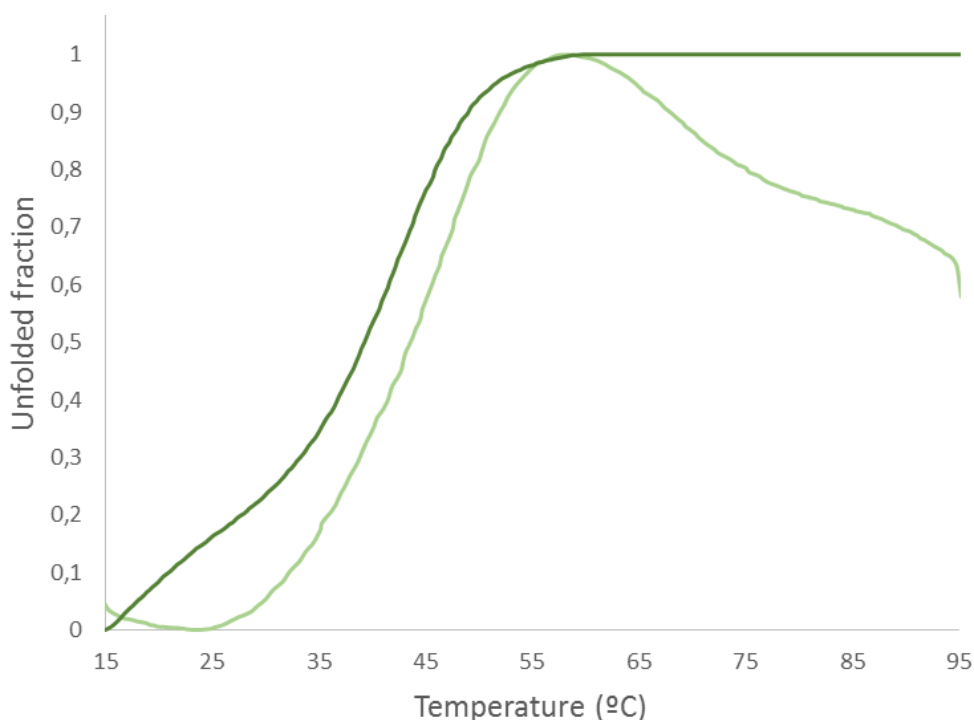
Figure 4.19. CD melting curves of the mutant R337H at a heating rate of 1.5ºC/min (in dark green) and at a heating rate of 2ºC/min (in light green) at 20 µM monomer concentrations in 25mM sodium phosphate buffer pH7, 100mM NaCl.

These results of the comparison in Figure 4.19, together with the presence of the maximum before reaching the final plateau in the curve at a 2ºC/min heating rate, reinforced our hypothesis that for mutant R337H, the unfolding process is not completely coupled to the dissociation of the tetramer.

It is possible that 2ºC/h was a heating rate not slow enough to allow the protein to reach the equilibrium at every step of the unfolding process.

It became interesting for us to know the CD spectra of the proteins during the unfolding experiment. Therefore, we recorded CD spectra of the proteins wild-type and R337H mutant at different temperatures (from 15℃ to 95℃) with the aim of comparing the obtained spectra (Figure 4.20).
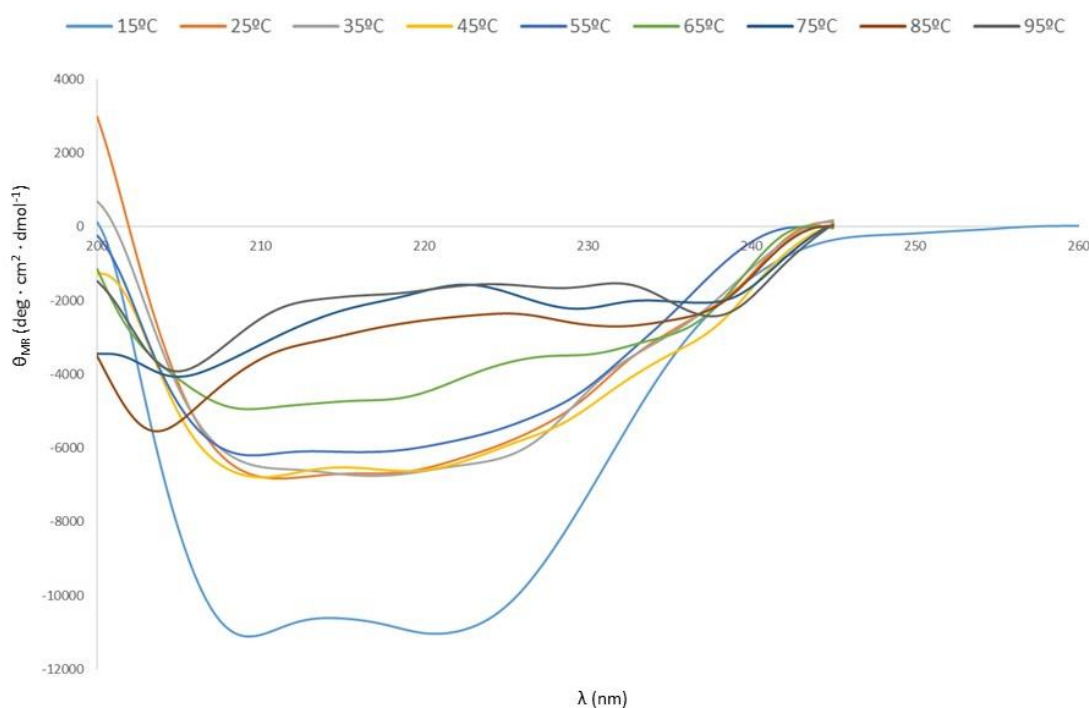
Figure 4.20. CD spectra of the p53TD wild-type at different temperatures (from 15ºC to 95ºC) and at 20 ¡µM concentration of the monomer in 25mM sodium phosphate buffer pH7, 100mM NaCl. Ellipticity was normalized to the mean residue concentration, θ_{MR}.

Analyzing the obtained spectra from 15℃ to 95℃, it was possible to observe significant changes in the ellipticity of the wild-type protein. Until 55℃, the protein displayed two minima at 222 and 208nm, evidencing the presence of an α-helix secondary structure. The most different spectra was the one recorded at 65℃, the closest one at the half unfolding transition temperature (T_{05}). In this spectrum there was a considerable lose of the ellipticity at the α-helix minima, which denoted the loss of the secondary structure, although no signs of random coil was still detected. At 85℃ and 95℃, the obtained spectra unveiled the lack of structure of the protein by the negative band around 200nm characteristic of a random coil structure.

The study of the same sample at different temperatures confirmed the results obtained in the unfolding assay. As expected, helicity was being lost while increasing the temperature with an abrupte change when reaching the thermal stability temperature due to the high cooperativity of the process. Higher temperature values provided a CD spectra characteristic of a random coil. The same CD spectra comparison at different temperatures (from 15ºC to 95ºC) was also carried out for the mutant R337H.
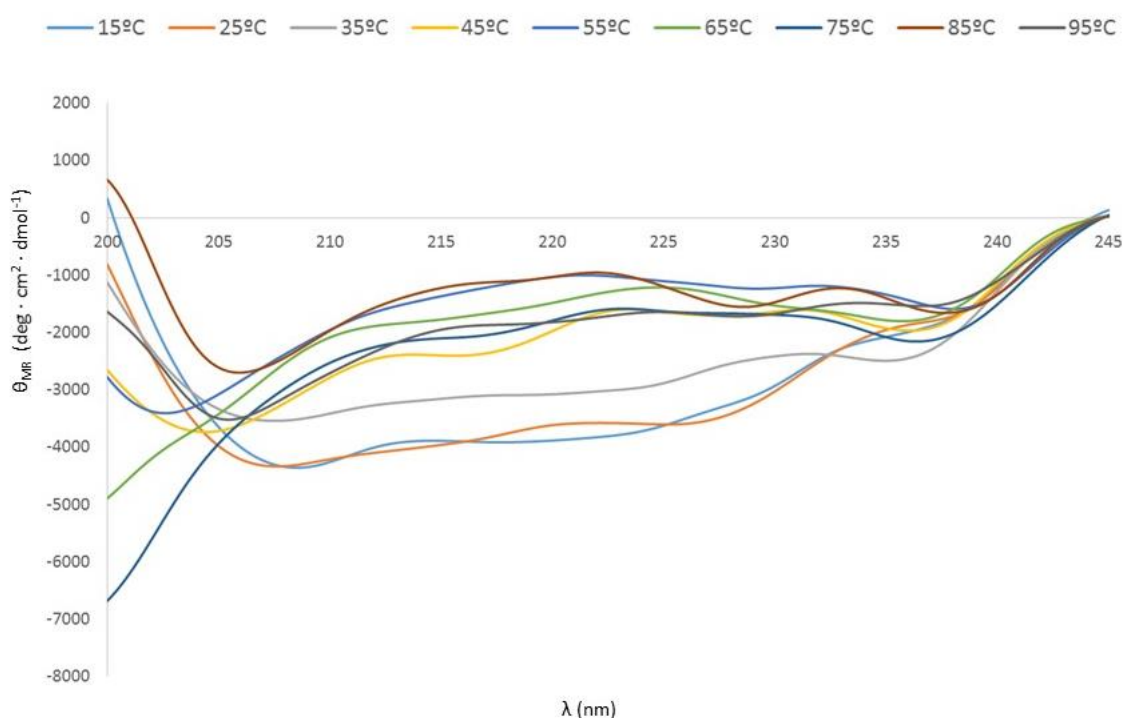
Figure 4.21. CD spectra of the mutant R337H at different temperatures (from 15ºC to 95ºC) and at 20μM concentration of the monomer in 25mM sodium phosphate buffer pH7, 100mM NaCl. Ellipticity was normalized to the mean residue concentration, θ_{MR}.

As it was observed for the wild-type p53TD, the overlapping of spectra at different temperatures provided information regarding the loss of secondary structure. From 15ºC until 35ºC spectra, α-helical conformation was observed with the characteristic negative bands at 222 and 208nm. At 45ºC, the spectrum did not display those bands and a new band around 200nm appeared, corresponding to the random coil structure. This band was more clearly observed when increasing temperature.

These results were similar to the obtained for the wild-type p53TD, although the loss of secondary structure was produced at lower temperature, as it was expected. Again, his analysis was in concordance with the unfolding assay for the mutant R337H mutant protein, whose T_{05} was shifted at lower temperatures in comparison with the wild-type of p53TD.

The obtained results were compared with p53TD wild-type and mutant R337H obtained by expression with the flanking tails by Dr. S. Gordo in the lab. It should be taken into account that the length of the proteins are differents (Table 4.2).

Table 4.2. Comparison of the sequences of p53TD wild-type and mutant R337H obtained by Dr. S. Gordo by recombinant expression in *E. coli* and the synthesized proteins in the present thesis.

	Source	AA*
p53TD from expression	Expression	
NTSSSPQPKKKPLDGEYFTLQIRGRERFEMFRELNEALELKDAQAGKEPGGSRAHSS	in *E. coli*	57
p53TD		
KKPLDGEYFTLQIRGRERFEMFRELNEALELKDAQAG	Synthesis	37
R337H from expression	Expression	
NTSSSPQPKKKPLDGEYFTLQIRGREHFEMFRELNEALELKDAQAGKEPGGSRAHSS	in *E. coli*	57
R337H		
KKPLDGEYFTLQIRGREHFEMFRELNEALELKDAQAG	Synthesis	37

Lower thermal stability values were observed for both p53TD and R337H proteins in their short versions, in addition to a larger difference between their melting temperatures.

Less stability was expected during these unfolding experiments since the synthetic proteins did not contain the flanking tails that could help in stabilizing the folded tetrameric proteins, especially in the case of the mutant R337H, whose stability is critical.

Therefore, the novel constructs proved to be appropriate for the stability studies and were promising in order to have a shorter sequence that can also mimic the full length protein without requiring its whole synthesis or expression.

4.3.2.2   Effect of the pH in the mutant R337H

The stability of mutant R337H has been described to be sensitive to the pH in the physiological range[148.] This effect was expected due to the different pK_a of the mutated residue, histidine and the possible protonation of its side-chain. At acidic pH (lower than pK_a =7.7), imidazole ring present in the side-chain of histidine H337 is protonated, which enables the formation of the native salt bridge with D352 (which in the wild-type p53TD is formed with R337). Unfolding experiments for the mutant R337H were performed at different pH to study this pH-sensitivity effect (Figure 4.22).

Acid pH unfolding curves presented T_{05} of 46°C, which are above the value estimated in the unfolding curve at pH7. Thermal stability of the mutant R337H can be highly increased with slight modification of the buffer conditions. At basic medium, when the salt bridge can be formed, higher values of T_{05} were obtained.
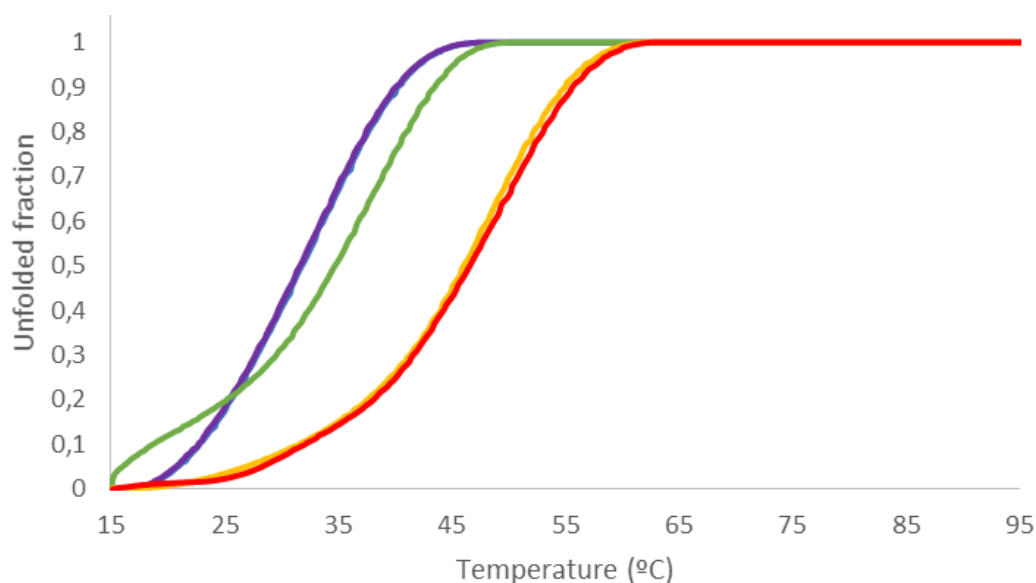
Figure 4.22. CD melting curves of the mutant R337H at a heating rate of 1.5ºC/min in a variable scale of pH from 5 to 9 at 20µM monomer concentrations in 25mM sodium phosphate buffer pH7, 100mM NaCl.

We did not only observe a shift of the unfolding curve, but also a change in the shape of this curve. The symmetry of the melting curve was different depending on the pH conditions of the buffer, implying that the interactions established are relevant for the formation of the folded state. In the narrow range of pH 6-8 important changes can be detected, which strongly suggested that protonation of H337 side-chain was the responsible of the different unfolding curves by modifying the equilibrium of the tetramerization. It is also important for the reproducibility of the assay to notice that at pH 5 and 6 and pH 8 and 9, the unfolding curves perfectly overlap (Figure 4.22). The T_{05} value obtained at different pH are represented in Figure 4.23.
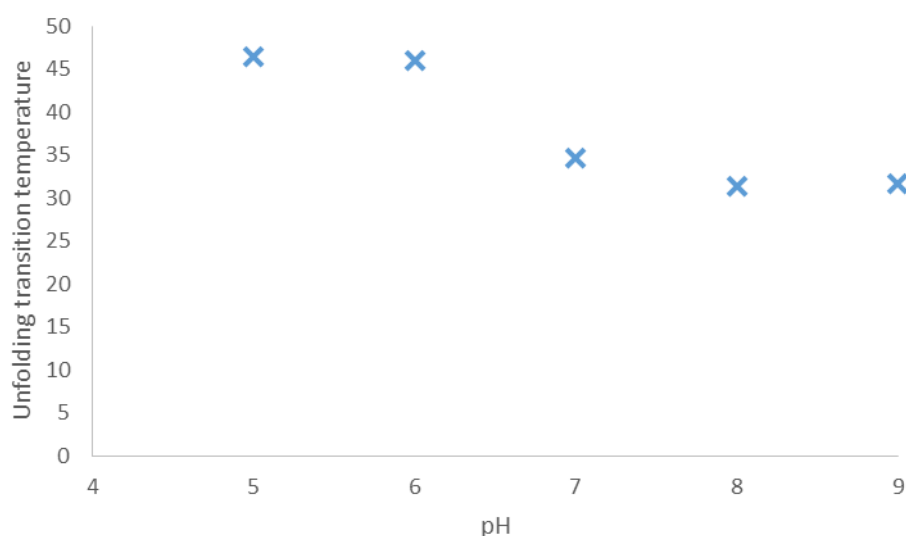
Figure 4.23. Half unfolding transition temperature (T$_{05}$) values of mutant R337H in buffer 25mM NaPi, 250mM NaCl and at different pH.

Important changes at the thermal stability were observed between pH 6 and 8. At acidic conditions the T$_{05}$ was around 46°C while in basic media was 31°C. The significant change pointed out the sensitivity of the mutant, mainly due to histidine H337 presence.

Furthermore, in order to study and compare the stability of the mutant in front of the wild-type it was clear that the pH of work should be neutral or acid. Since the experiments done at closer physiological conditions were more interesting to extract conclusions resembling the *in vivo* situation, we decided to evaluate the following unfolding experiments at pH 7. CD spectra of the mutant at different pH conditions were also recorded, Figure 4.24.
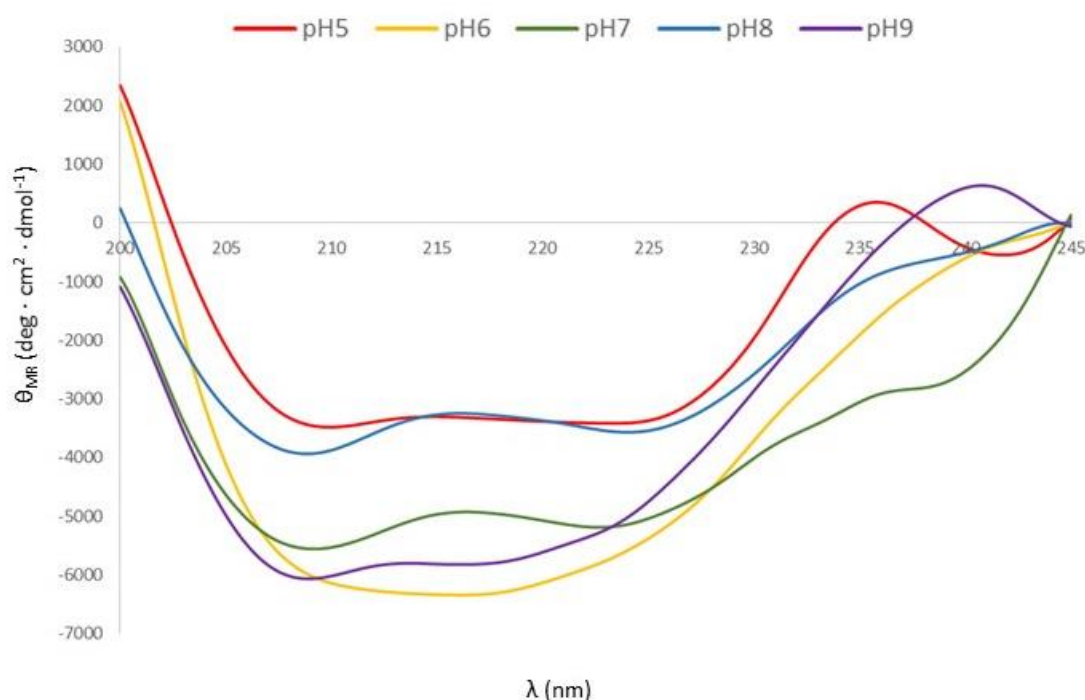
Figure 4.24. CD spectra of mutant R337H in buffer 25mM sodium phosphate, 250mM NaCl, at pH5 (in red), pH6 (in yellow), pH7 (in green), pH8 (in blue) and pH9 (in purple).

Despite of the clear tendency observed by increasing the pH, CD spectra of the mutant R337H at different pH could not be correlated directly with the previous unfolding experiment. CD spectrum at pH 5 showed a more flat negative band while CD spectrum at pH 9 displayed more clear negative bands that the one at pH 5 and at pH 7. Nonetheless, the tendency was not follow by experiments at pH 6 and 8. The amount of tetramer and monomer at the beginning of the experiment could have an impact in the obtained results.

Regarding the shape of the curves, CD spectra at acidic pH displayed a flat minimum having a number of interaction helices q=1. On the other hand, CD spectra at basic pH displayed two clear minima at 208 and 222nm, whose absolute value was not the same, since $\theta_{220} < \theta_{208}$ the number of interacting helices was q<1.

This results were in agreement with the melting curves analyzed at different pH values. In acidic conditions, the salt bridge can be mimicked and so the unfolding of the mutated protein R337H was shifted at highter temperatures while at basic conditions the tetramer was less stable and the protein was mostly unfolded at the *in vivo* conditons.

4.3.2.3   Ionic strength influence in mutant R337H

The ionic strength of the buffer was another parameter to be explored. As it can be seen in Figure 4.25, unfolding curves of the mutant R337H at pH7 recorded in two different buffers changing only the concentration of NaCl were slightly different.

We observed that the higher the salt concentration, the lower the thermal stability of the R337H mutant protein. While T_{05} was 39ºC with the buffer containing 100mM NaCl, in 250mM NaCl buffer T_{05} was 35ºC. Although this comparison was only done with one single experiment for each salt concentration, similar results were previously described for a similar protein sequence[156].
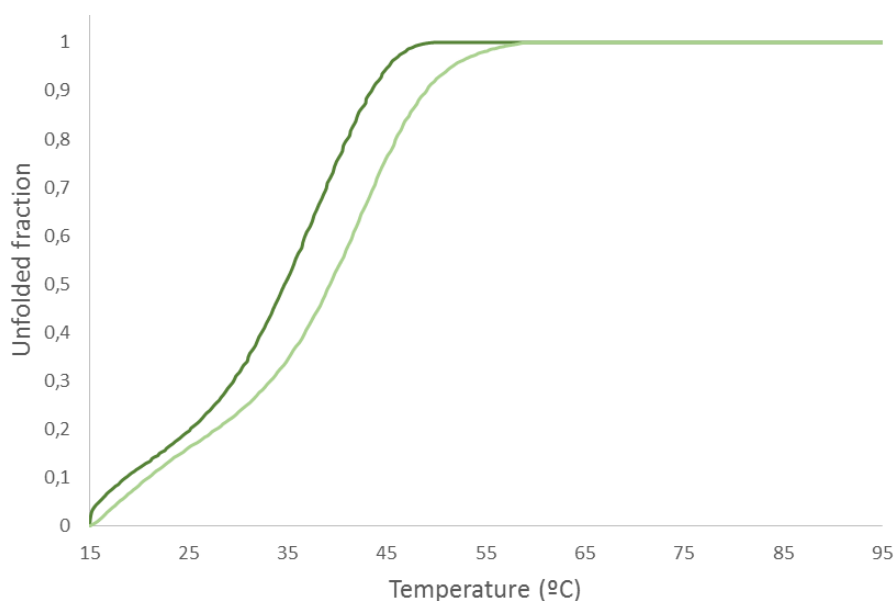
Figure 4.25. Unfolding curves of R337H at 1.5ºC/min in 25mM NaPi buffer with 250mM NaCl at pH7 (in dark green) and with 100mM NaCl at pH 7 (in clear green).

Another interesting fact is that the shape of the melting curves were also slightly different. The unfolding process for the sample with larger salt concentration appeared to be more cooperative than for the sample with less concetration of salts.

We hypothesized that the effect of the ionic strength was related to the ionic interactions that are established between the monomer chains to fold as the native tetramer.

4.4   Towards the stabilization of R337H mutant

In order to determine the stabilization and binding of some of the prepared peptides with the tetrameric state of p53 the most direct way was to measure the effects produced on the thermal stability of the protein.

Two peptides of the arginine family presented in Chapter 1 were evaluated against the established methodology to test the potential recovery of the self-assembly of mutant R337H. Linear stapled (NH$_2$-Arg-(4&)Phe-Arg-(4&)Phe-DPro-COOH) and bicyclic (cyclo(-Arg-(4&)Phe-Arg-(4&)Phe-DPro-) versions were the sequences analyzed. Unfolding curves of the p53TD wild-type and R337H in the presence of different equivalents of the compounds were carried out.

4.4.1 Evaluating arginine bicyclic candidate

Arginine bicyclic peptide was added in 8 or 16 equivalents to a sample containing either p53TD wild-type or R337H mutant in 20µM concentration of the protein monomer. According to the previous results from our group group[156], there are four glutamic residues E336, E339, E343, E346 at each rim of the loops that are expected to interact with the positively charged guanidiniums. For this reason, stoichiometry should be consider as follows; each equivalent of the tetramer displays 8 negative charges, while each equivalent of peptide only contains two positive charges. 1:1 stoichiometry is achieved by adding 4 equivalents of peptide.
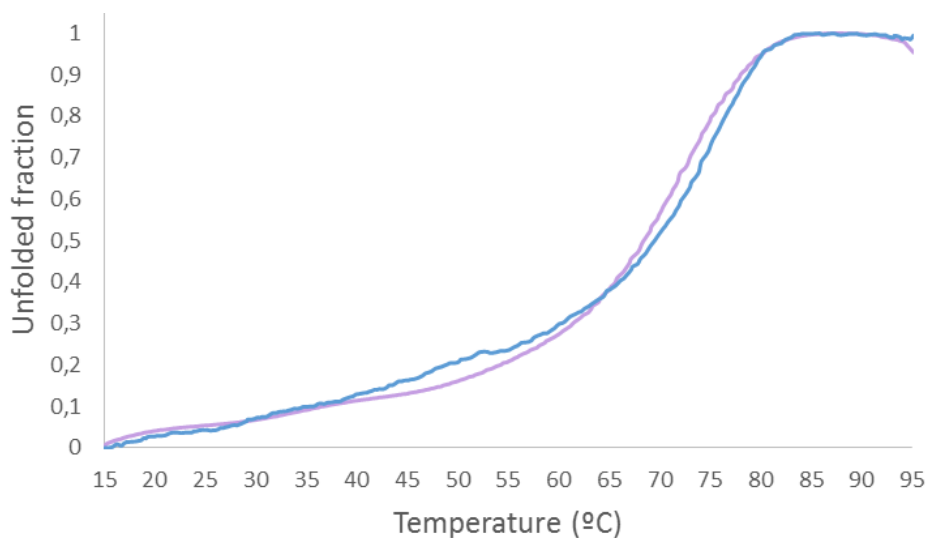
Figure 4.26. Unfolding curves of p53TD at 1.5°C/min in 25mM sodium phosphate buffer with 100mM NaCl at pH7 (in blue), with 8 equivalents of arginine bicyclic peptide (in pale purple).
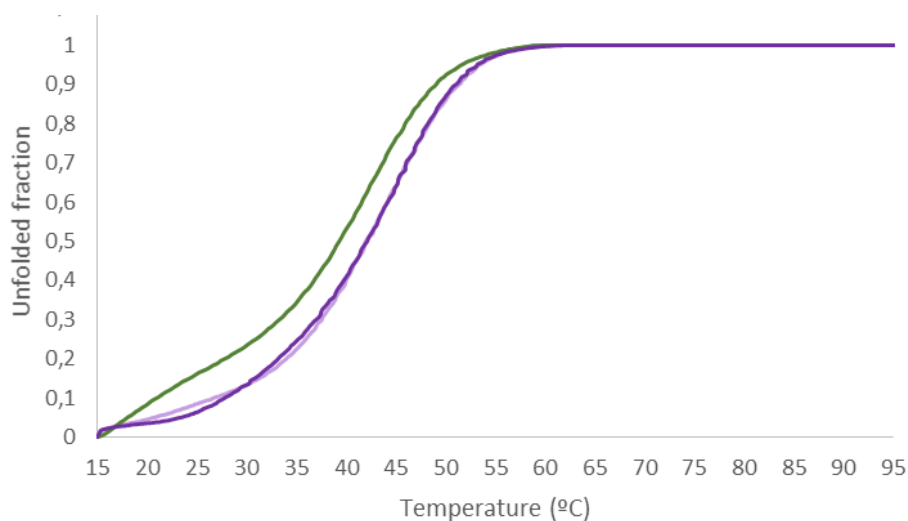
Figure 4.27. Unfolding curves of R337H at 90°C/h in 25mM sodium phosphate buffer with 100mM NaCl at pH 7 (in green), with 8 equivalents of linear stapled arginine bicyclic peptide (in pale purple), with 16 equivalents of arginine bicyclic peptide (in dark purple).

As it is observed in Figure 4.26, introduction of the peptide in the p53TD wild-type protein did not affect the T_{05}. Having proved that no experimental error can be attributed to the incorporation of the ligand, the results of the assay were considered

reliable. An increase of 3°C in the T_{05} was obtained was introducing 8 or 16 equivalents of the arginine bicyclic peptide. No dosis dependence was observed (Figure 4.27).

15°C

25°C

45°C
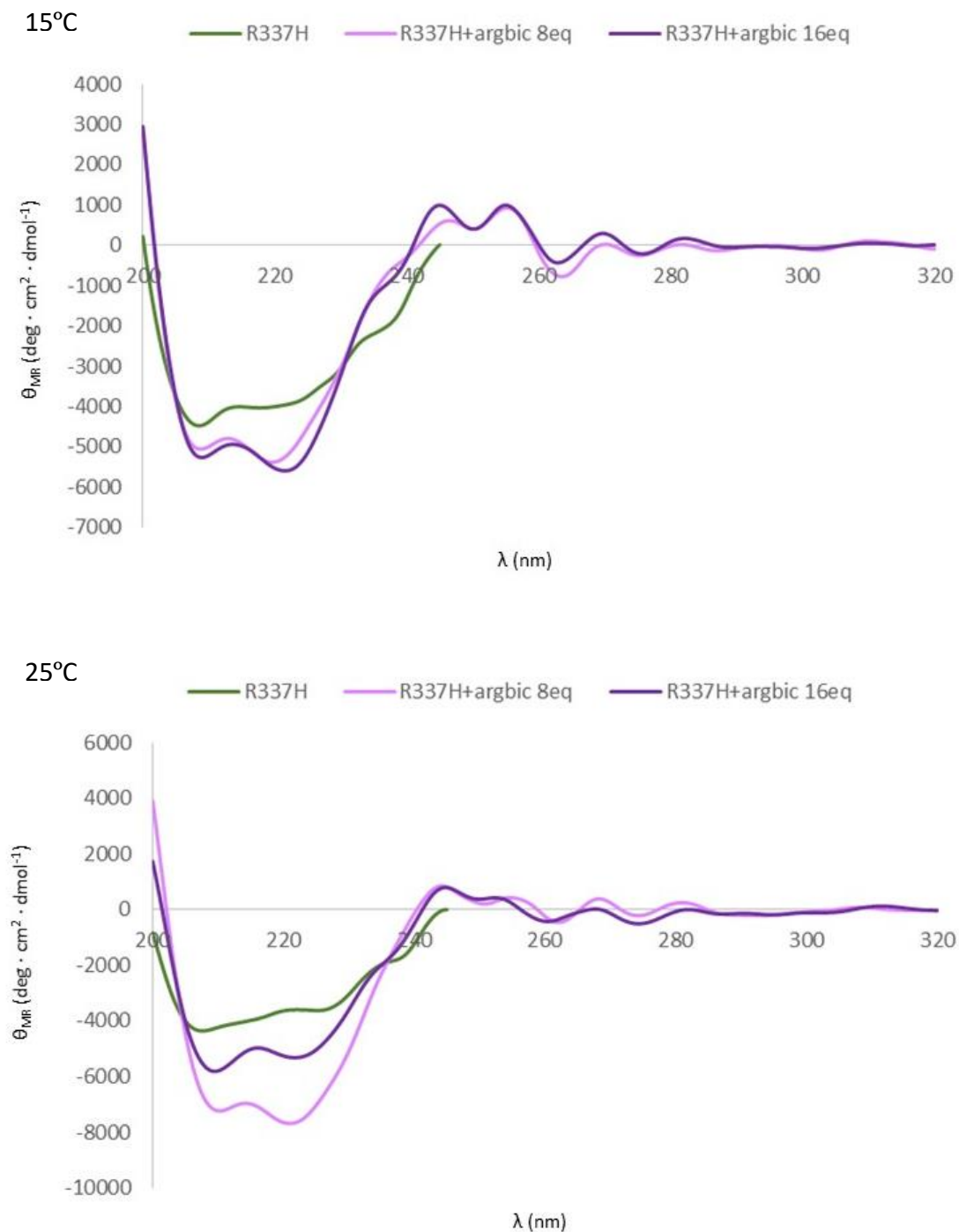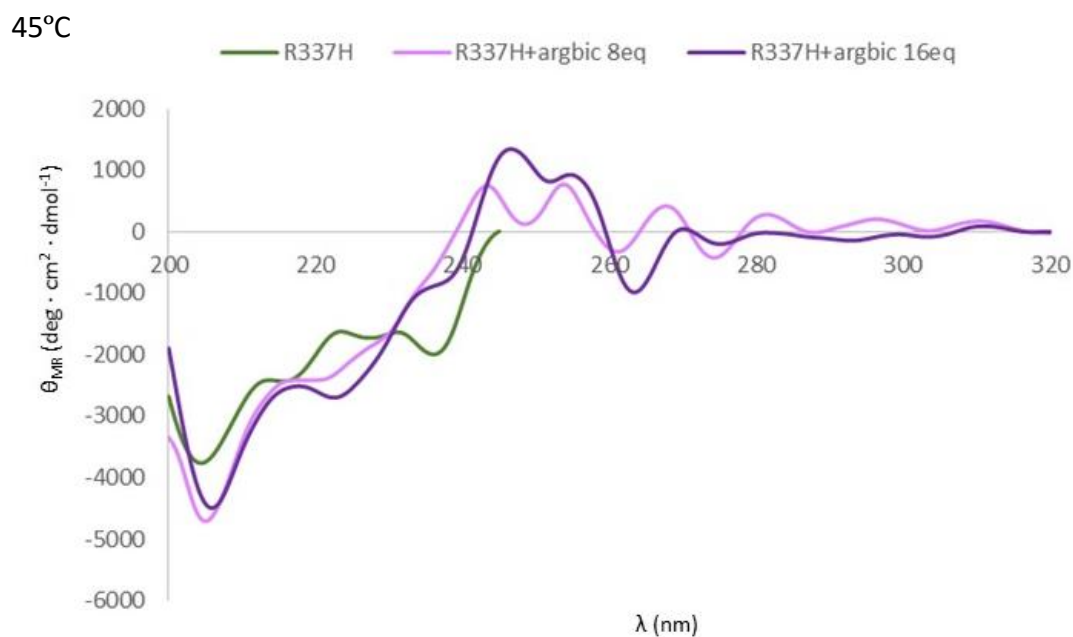
Figure 4.28. CD spectra of R377H mutant at 20µM in 25mM sodium phosphate buffer, 100mM NaCl, pH7, in absence of ligand (in green), 8 equivalent of arginine bicyclic peptide (in light purple), 16 equivalents arginine bicyclic peptide (in purple) at 15°C, 25°C and 45°C.

In Figure 4.28, CD spectra of R337H mutant with arginine bicyclic ligand were represented at different temperatures. The presence of the ligand increased the ellipticity values in all the temperatures analyzed. Noteworthly, α-helical conformation was clearer when introducing the peptide. Furthemore, q value was also increased, confirming the stabilization of the tetramer formed. Nevertheless, when reaching 45°C the random coil structure was observed despite of the introduction of the ligand. This result was expected after reaching only 3°C of stabilization in the previous unfolding curve.

4.4.2 Evaluating arginine linear stapled candidate

Arginine linear stapled was also tested in front of the two proteins. In this case, the ligand exhibited higher flexibility due to the avoidance of the head-to-tail cyclization. Nonetheless, the biaryl bridge acted as a constraint limiting the degrees of freedom.
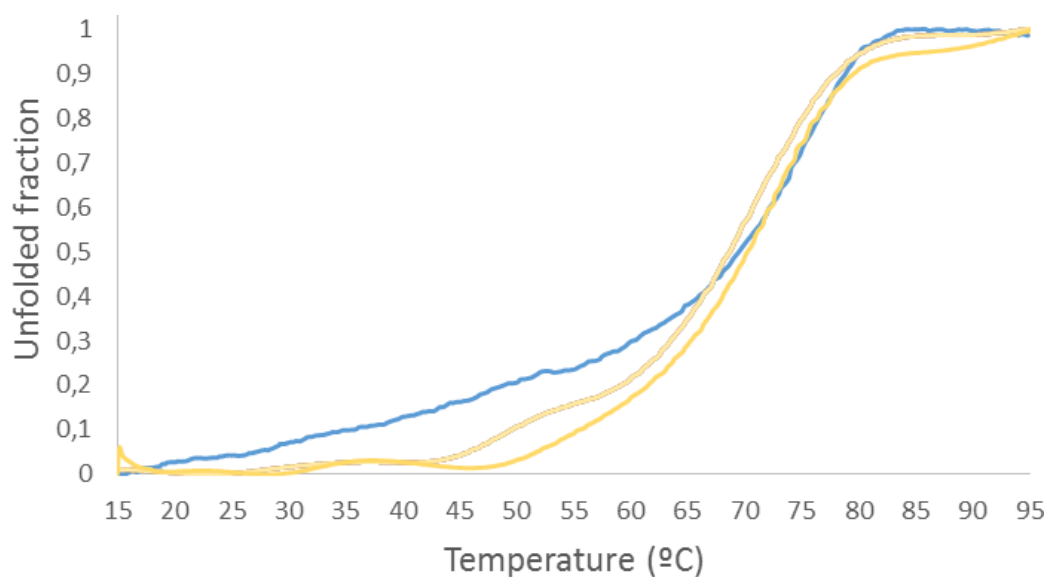
Figure 4.29. Unfolding curves of p53TD at 1.5ºC/min in 25mM sodium phosphate buffer with 100mM NaCl at pH7 (in blue), with 8 equivalents of arginine linear stapled peptide (in pale yellow), and with 16 equivalents of arginine linear stapled peptide (in yellow).
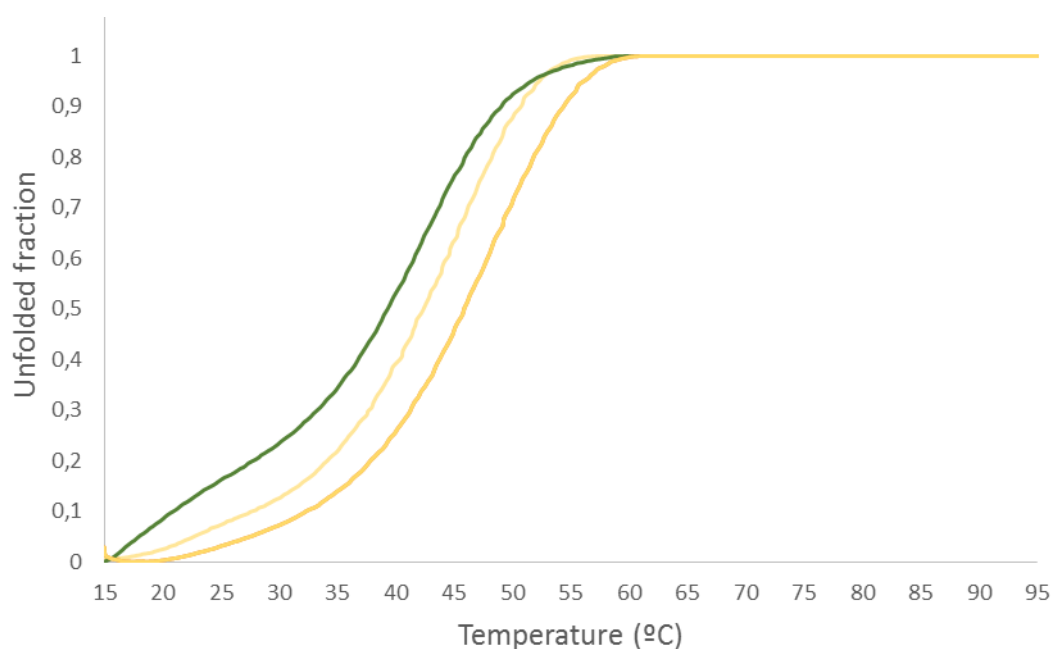
Figure 4.30. Unfolding curves of R337H at 1.5ºC/min in 25mM sodium phosphate buffer with 100mM NaCl at pH7 (in green), with 8 equivalents of arginine linear stapled peptide (in pale yellow), and with 16 equivalents of arginine linear stapled peptide (in yellow).

No significant differences were observed when adding the arginine linear stapled peptide to p53TD wild-type (Figure 4.29). On the other hand, the peptide caused a

relevant enhancement of the thermal stability of the R337H mutant. 8 equivalents of the ligand increase 3°C the T_{05}, as displayed for the arginine bicyclic peptide, while 16 equivalents increase it in 7°C. In this case, there was a dose dependent effect only for the unfolding of the R337H mutant (Figure 4.30).

CD spectra at different temperatures in presence of this ligand were also recorded (Figure 4.31). In this case, the profile of the CD spectra changed when incorporating the arginine linear stapled peptide. In addition of increasing the ellipticity, the two minimals characteristical of α-helical conformation that R337H mutant presented, were changed towards only one negative band at the same region, which could correlate to a q=1, implying tetramer stabilization. At 45°C the band of random coil was much less intense than the one corresponding to the α-helix, being in agreement with the unfolding experiment, specially with 16 equivalents.
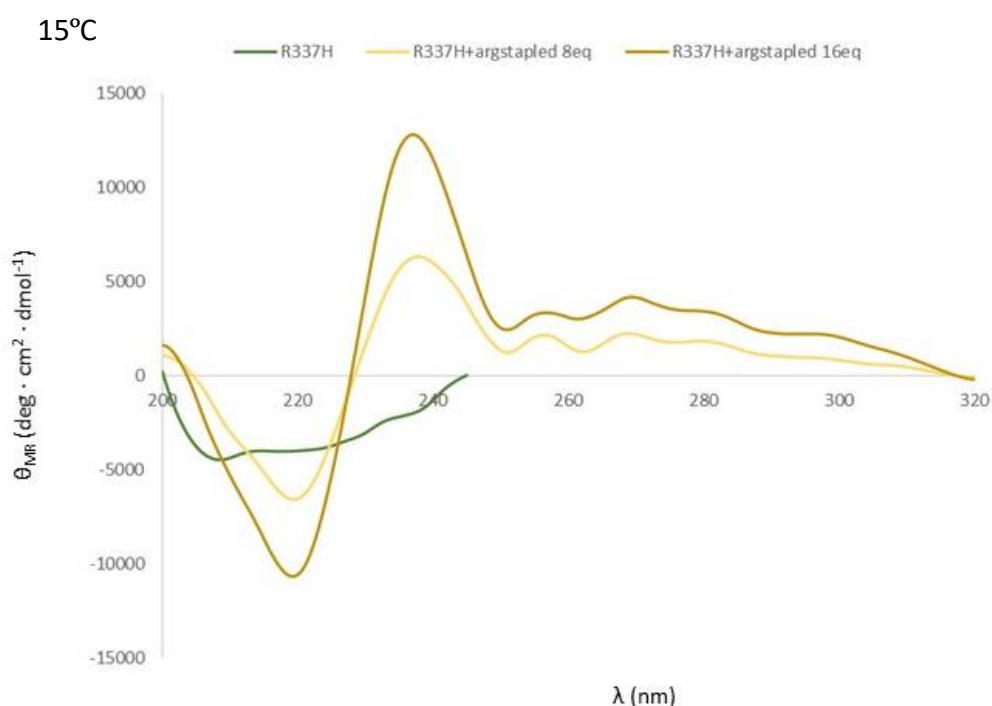
25°C
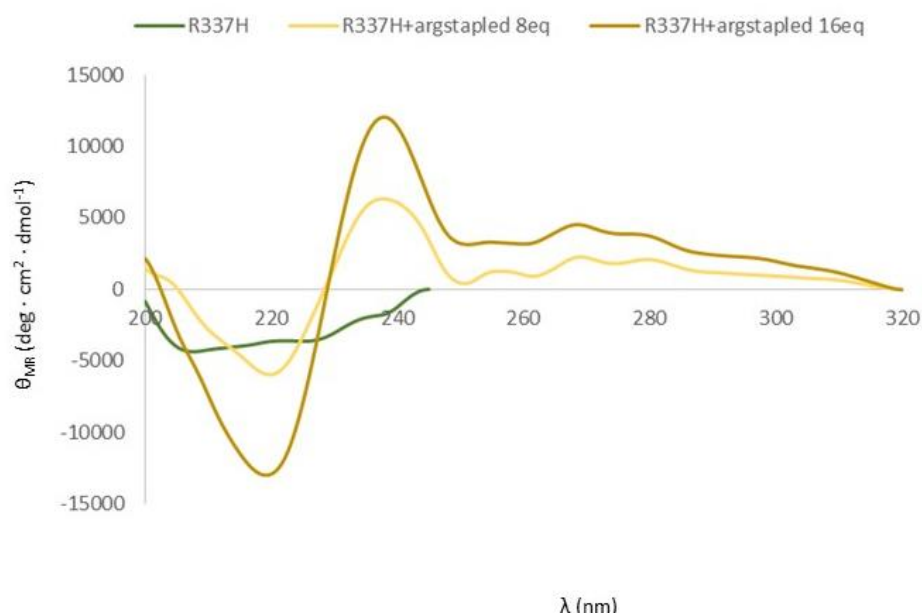
45°C
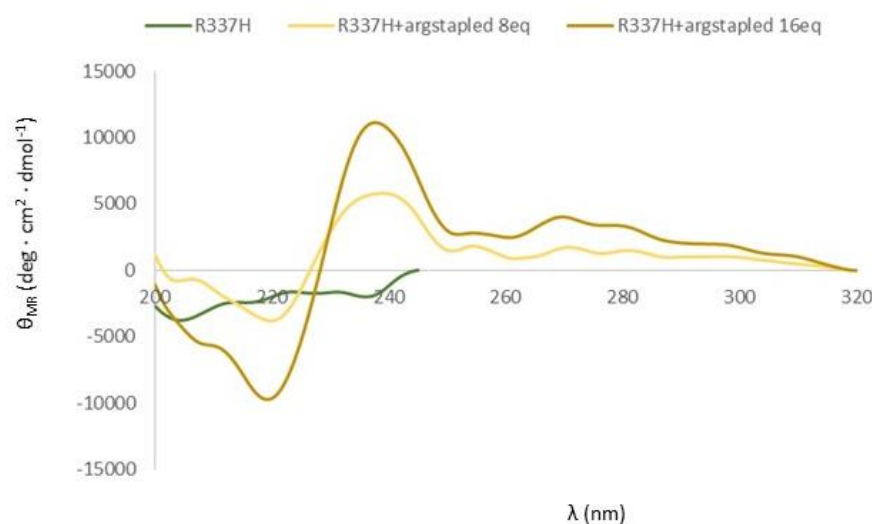
Figure 4.31. CD spectra of R377H mutant at 20µM in 25mM sodium phosphate buffer, 100mM NaCl, pH7, in absence of ligand (in green), 8 equivalent of arginine linear stapled peptide (in light yellow), 16 equivalents arginine linear stapled peptide (in yellow) at 15°C, 25°C and 45°C.

Promising results for the arginine linear stapled peptide encouraged us to further study this peptide. As previously mentioned, a good peptide candidate, in addition of interacting with the protein target should not be toxic. Therefore, cytotoxicity was evaluated using XTT assay at two different concentrations, 200µM and 500µM, higher than the ones used in the CD unfolding experiments. 100% of cell survival was estimating after 24h incubation of the arginine linear stapled peptide with HeLa cells.

As demonstrated in Chapter 2, the introduction of the biaryl staple did not introduce cytotoxicity.

4.5   Computational studies

4.5.1 Docking studies

To determine the binding mode of different synthesized peptides, as well as the theoretical binding energy, a coupled protocol between docking and molecular dynamics simulations was conducted. The p53TD structure was retrieved from Protein Data Bank (PDB: 1OLG) and used as template. The binding site was defined to encompass the different amino acids reported in the literature to be involved in binding and protein recognition. The docking was computed for the p53TD wild-type structure as well as the R337H mutant. In both cases, the binding site was the same, as depicted in figure 4.32.

In table 4.3, the scores obtained in each docking simulation sceneario are presented. It is worth highlighting how the linear version exhibited a better score in the R377H, while in the remaining cases, the docking scores were profiled at similar levels. These results were in excellent agreement with experimental assays, where lineal staple peptide was able to increase the stability of the folded R377H mutant. However, assuming the inherent scoring errors and docking limitations (i.e, rigid protein, scoring function not suitable for peptides but for small molecule, etc.), 1kcal/mol difference was not large enough to conclusively identify the lineal stapled peptide as the most potent inhibitor.

Table 4.3. Docking scores (expressed in kcal/mol) obtained by MOE using as a template the 1OLG PDB entry. Binding of the linear stapled peptide in the R377H scenario yielded the best score, in agreement with experimental results.

	SCORE (kcal/mol)	
	p53TD wild-type	R337H mutant
Lineal stapled peptide	-7,02	-8,58
Bicyclic peptide	-7,49	-7,39

In table 4.4 a list of representative amino acids that are in contact with the ligand along the top 5 docking predictions of each molecule is shown.

Table 4.4. List of amino acids involved in the interaction of p53TD wild-type (PDB: 1OLG) and peptides arginine bicyclic and arginine linear stapled.

	Arginine bicyclic	Arginine linear stapled
R335	NO	YES
E336	YES	YES
R337	YES	YES
F338	NO	NO
E339	YES	NO
M340	YES	YES
F341	NO	NO
R342	NO	YES
E343	YES	YES
L3444	NO	NO
N345	NO	NO
E346	NO	YES
A347	NO	NO
L348	YES	NO
E349	NO	NO
L350	NO	NO
K351	YES	YES

E336, R337, M340, E343 and K351 are the amino acids common in both peptide ligands (Table4.4, labelled in green). It is worth mentioning that in both cases, R337 was one of the few residues involved in the molecular recognition of both peptides, suggesting the impairment a point mutation might induce. The main structural difference when comparing p53TD wild-type and R337H mutant was in the volume ($8Å^3$ higher than in the R337H case) of the binding site.
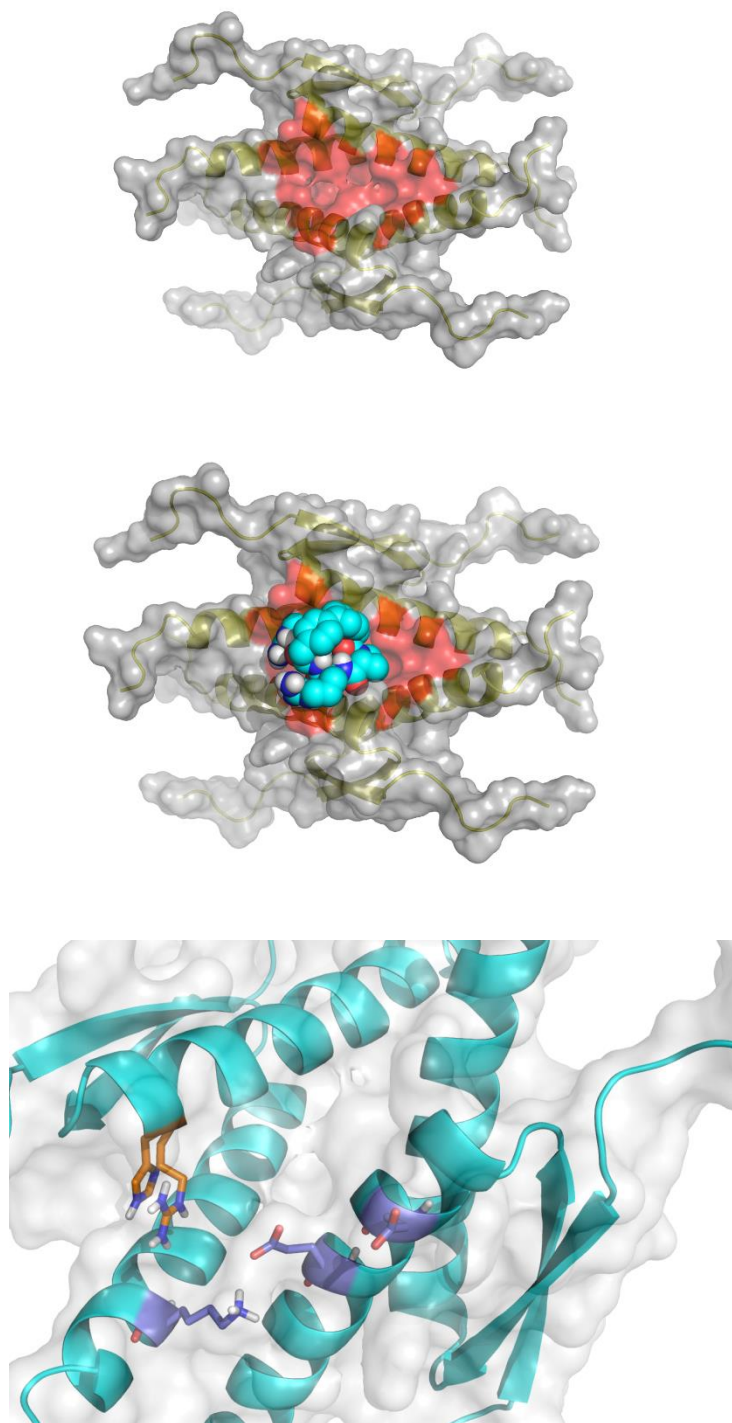
Figure 4.32. Binding site of p53TD (highlited in red surface). For illustrative purpose, the former bicyclic docking prediction is shown to demonstrate the extended protein binding site region covered by the peptide. The structural point mutation R337H is shown in oranged sticks in conjunction with other negatively charged residues lying at the binding site, whose interactions favour the peptide accommodation. As observed, R337H mutation produces a contraction in the binding site that induces the formation of a slightly larger volume.
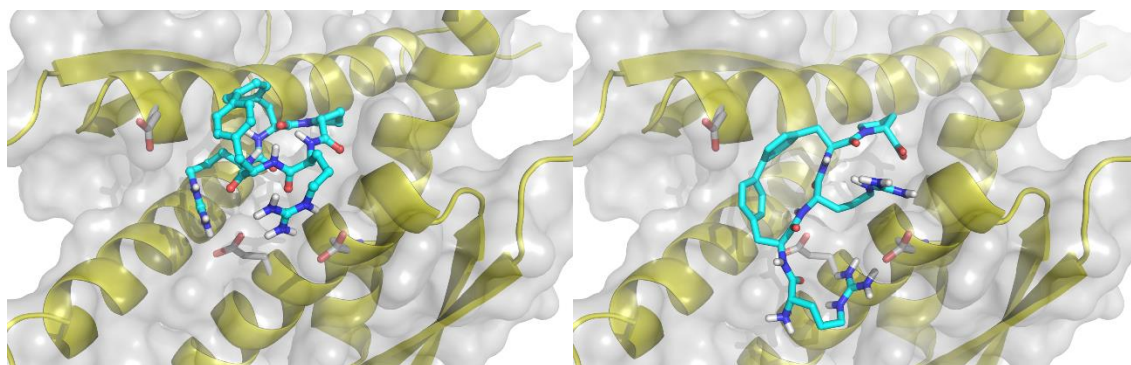
Figure 4.33. Comparison of the established interactions between arginine bicyclic and arginine linear stapled peptides with p53TD.

Nonetheless, some significant differences regarding the established interactions were observed. Relevant residues previously described in the literature[156] to interact with some ligands were E336, E339, E343, E346 and E349.

Arginine bicyclic peptide interacted with three of these contact residues, E336, E339 and E343. Also in the case of arginine linear stapled, three amino acids were common E336, E343 and E346. While the bicyclic version displayed interaction with E339, the linear stapled did it with E346, showing some kind of differences regarding the pose of the peptides in the binding site. This difference could explain the obtained experimental results. Despite of having a very similar binding site, the binding mode of the peptide could be very different. Therefore, molecular dynamic simulations were run to better understand the interaction along the time.

4.5.2 Molecular dynamics

The different predicted bound geometries of linear stapled and bicyclic peptides when partnering with p53TD wild-type and R337H mutant were subjected to short molecular dynamics to determine whether their binding modes were stable along the time. This study was aimed to elucidate if experimental differences could be explained by fundamental peptide stability when bound to p53TD. The lower the stability was, the more reduced the experimental observable.

In both cases, the ligand remained stable and preserved their original bound geometry, although bicyclic version slightly exhibited a more unstable profile. In Fig. 4.34, the root mean square deviation (RMSd) was plotted when comparing each frame simulation with original starting geometry. It is worth highlighting the RMSd achieved a plateau profile in the former 5nanoseconds (5000ps).

Extended MD simulations, in the range of microseconds, would be required to further validate the stability profile as the reduced time was not in the same timescale of the experimental observable (microsend to milliseconds).
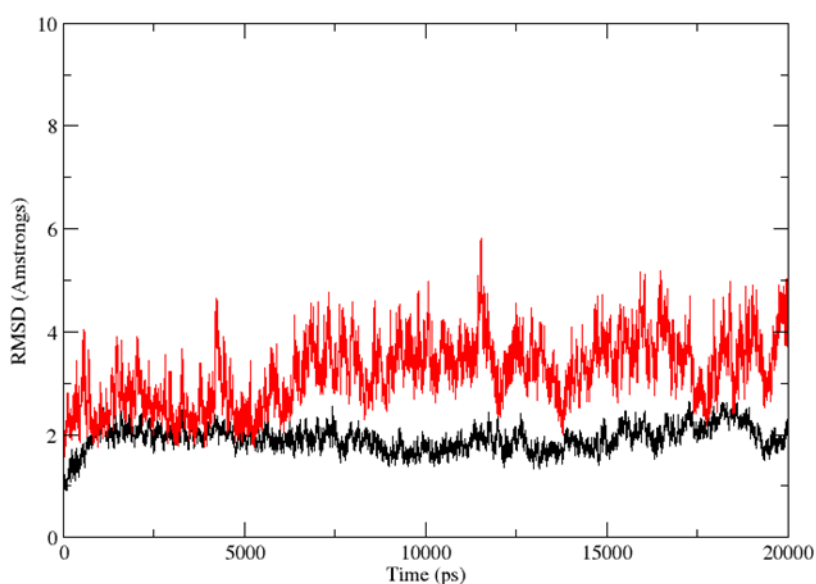
Figure 4.34. RMSd values of linear stapled (in black) and bicyclic (in red) peptides along the simulation time (20nanoseconds). The linear stapled peptide geometry was found to be more stable than the bicyclic peptide analog denoted by its lower RMSd.

In summary

Shorter constructs of p53TD wild-type and R337H mutant were prepared using the automated microwave assited chemical synthesized. After in-detail studies of both proteins, we could confirm that the characterization and study of p53 tetramerization domain and this mutant can be carried out without requiring the full-length proteins or the longer constructs described in the literature[156,217].

Reported circular dichroism experiments have been repeated with the shorter constructs rendering similar results. This fact evidenced that the flanking tails introduced in longer constructs did not affect the folding of the proteins. It is worth mentioning that no folding agents were required despite the reduced size of the proteins.

Difference of tetramer equilibrium between the wild-type and the mutant was of 30ºC. The unfolding curves of the prepared shorter constructs were slightly shifted towards lower temperatures although not in a relevant manner. This observation evidenced the effect of the tails, not incorporated in this case.
Relevance of protonation of the H337 side-chain, as described in the literature, proved to be of great importance. At acid pH, R337H mutant was in the tetrameric state, while basic pH shifted the tetramerization equilibrium at lower temperatures. Moreover, ionic strength of the buffer was another paremeter to be considered. The higher the ionic strength was, the lower the stability of the complex.

Limited self-assembly ability of R337H mutant was targeted with two stapled peptides. The first one, the arginine bicyclic peptide, displayed a slight thermal stabilization which did not increase when using more equivalents. The second compound was the arginine linear stapled version. Increasing the amount of equivalents caused an increased response, pointing towards a dose-dependent ligand. 8 equivalents of the linear stapled peptide caused an increase of 3ºC of the half unfolding transition temperature, as displayed for 8 and 16 equivalents of the arginine bicyclic.

Nonetheless, this increase was of 7ºC when introducing 16 equivalents. This result was very promising for the potential application of the linear stapled compound. In addition of the previously described high passive diffusion permeability P_e of $16.9 \cdot 10^{-6}$ cm/s and outstanding protease resistance in human serum for more than 24h, no cytotoxicity was detected for this compound by XTT assay up to 500µM.

Docking studies illustrated the binding of the compounds to the tetrameric protein establishing contacts with three glutamic acids placed in the surface of the α-helix and just above the hydrophobic pocket located within the strands.
Binding score was the same for the two compounds, -7kcal/mol.

Bibliography

[203] T. J. Vaughan, J. K. Osbourn, P. R. Tempest, Human antibodies by design, *Nat. Biotechnol.* **1998**, *16*, 535-539.

[204] R. P. Junghans, t. A. Waldman, N. F. Landolfi, N. M. Avdalovic, W. P. Schneider, C. Queen, Anti-Tac-H, a humanized antibody to the interleukin 2 receptor with new features for immunotherapy in malignant and immune disorders, *Cancer Res.* **1990**, *50*, 1495-1502.

[205] G. M. Clore, J. Ernst, R. Clubb, J. G. Omichinski, W. M. P. Kennedy, K. Sakaguchi, E. Appella, a. M. Gronenborn, Refined solution structure of the oligomerization domain of tumour suppressor p53. *Nat. Struct. Biol.,* **1995**, *2*, 321-333.

[206] P. D. Jeffrey, S. Gorina, N. P. Pavletich, Crystal structure of the tetramerization domain of the p53 tumor suppressor at 1.7 angstroms, *Science* **1995**, *267*, 1498-1502.

[207] M. McCoy, E. S. Stavridi, j. L. Waterman, A. M. Wieczorek, S. J. Opella, t. D. Halazonetis, Hydrophobic side-chain size is a determinant of the three-dimensional structure of the p53 oligomerization domain, *EMBO J.* **1997**, *16*, 6230-6236.

[208] M. G. Mateau, A. R. Fehrst, Mutually compensatory mutations during evolution of the tetramerization domain of tumor suppressor p53 lead to impaired hetero-oligomerization, *Proc. Natl. Acad. Sci. USA* **1999**, *96*, 3595-3599.

[209] J. Giacomazzi, M. S. Graudenz, C. A. B. T. Osorio, P. Koheler-Santos, E. I. Palmero, M. Zagonel-Oliveira, R. A. D. Michelli, C. S. Neto, G. C. Fernandes, M. I. W. S. Achatz, G. Martel-Planche, F. A. Soares, M. Caleffi, J. R. Goldim, P. Hainaut, S. A. Camey, P. Ashton-Prolla, Prevalence of the TP53 p.R337H mutation in breast cancer patients in Brazil, *PLOS one* **2014**, *9*, e99893.

[210] H. Y. Dai, N. Tsao, W. C. Leung, H. Y. Lei, Increase of the intracellular pH in p53-dependent apoptosis of thymocytes induced by gamma radiation, *Radiat. Res.* **1993**, *90*, 11337-11340.

[211] C. R. Johnson, P. E. Morin, C. H. Arrowsmith, E. Freire, Thermodynamic analysis of the structural stability of the tetrameric oligomerization domain of p53 tumor suppressor, *Biochemistry* **1995**, *34*, 5309-5316.

[212] S. J. Perkins, K. Wuthrich, Conformational transition from trypsinogen to trypsin: 1H nuclear magnetic resonance at 360MHz and ring current calculations, *Journal of Molecular Biology* **1980**, *138*, 43-64.

[213] D. W. Hoyt, R. M. Harkins, M. T. Debanne, M. O'Connor-McCourt, B. D. Sykes, Interaction of transforming growth factor alpha with the epidemial growth factor receptor: binding kinetics and differential mobility within the bound TGF-alpha, *Biochemistry* **1994**, *33*, 15283-15292.

[214] J. Hinshelwood, S. J. Perkins, Conformational changes during the assembly of factor B from its domains by (1)H NMR spectroscopy and molecular modelling: their relevance to the regulation of factor B activity, *J. Mol. Biol.* **2000**, *301*, 1267-1285.

[215] C. Galea, P. Bowman, R. W. Kriwacki, Disruption of an intermonomer salt bridge in the p53 tetramerization domain results in an increased propensity to form amyloid fibrils, *Protein Sci.* **2005**, *14*, 2993-3003.

[216] S. Y. Lau, A. K. Taneja, R. S. Hodges, Synthesis of a model protein of defined secondary and quaternary structure. Effect of chain length on the stabilization and formation of two-stranded alpha-helical coiled-colis, *J. Biol. Chem.* **1984**, *259*, 13253-13261.

[217] R. Kamada, Tetramer stability and functional regulation of tumor suppressor protein p53, Springer theses, **2012**, Japan, Chapter 2.

FUTURE DIRECTIONS

We believed that after the work present in the thesis, there would still be some greatly valuable experiments to be done in order to even improve its quality and future applications.

- ➢ The head-to-tail bromine containing compounds appeared as an interesting opportunity to have antimicrobial peptides. Therefore, we would like to study their potential activity. In this context, protease resistance of these compounds would also be valuable in order to fully assess their pharmacological properties.

- ➢ Further NMR studies of the ^{15}N-labelled p53TD wild-type and R337H mutant with the ligands would allowed better understanding of the interactions occurring.

- ➢ Evaluating other candidates not displaying the guanidinium groups, as well as, the *C*- and *N*-termini against R337H would also enable us to correlate the observed results with the structure of the ligand.

- ➢ In addition, further dynamic simulations would be required to study the binding mode along the time.

CONCLUSIONS

Based on the presented results in the previous chapters and considering the initial objectives of the thesis, the main conclusions that can be drawn are the following:

Objective 1

i. The initial methodology to prepare biaryl bicyclic peptides **has been successfully fulfilled and optimized**. The developed strategy included SPPS, Suzuki-Miyaura cross-coupling reactions on resin and head-to-tail cyclization in solution. Biaryl formation was obtained taking advantage of the previously mentioned coupling reactions (chapter 1, section 2) and was achieved between the ***meta*** or the ***para*** positions of phenylalanines. Proper selection of the compatible and available protecting groups allowed the introduction of different amino acids at the variable positions of the scaffold.

ii. Regarding the last step of head-to-tail cyclization in solution, exhaustive study with the model peptides was carried out to unveil the most appropriate conditions to selectively obtain the **monomeric bicyclic peptides**, as well as, the cyclodimers. **Using PyBOP, HOAt, DIEA, 1mM DCM/1% DMF** the reaction yielded monomeric bicyclic compounds with minimal traces of cyclodimers even working at highly concentrated conditions (100mM of the linear precursor). On the other hand, **cyclodimer synthesis** could not be perfomed in a selective manner using modified head-to-tail cyclization conditions. Their synthesis must be carried out under intial head-to-tail cyclization conditions (**DPPA, NaHCO$_3$, 5mM DMF**) followed by HPLC-semipreparative purification. Furthermore, straightforward SPPS of the cyclodimers was attempted, based on successive Miyaura borylations and Suzuki reactions. Failure of the synthesis was attributed to the remaining palladium coming from the Miyaura and Suzuki reactions, not allowing the evolution of the second borylation reaction.

iii. Conformational studies by molecular dynamic simulations were performed for the bicyclic peptides. The position of the stapling was hypothesized to have a relevant impact in the overall structure. **While the *para-para* showed to be quite rigid** during the simulation times, **the *meta-meta* displayed more flexibility**.

iv. Cyclodimers of the model peptides were also studied. **NMR** characterization and **molecular dynamic simulations** confirmed the existence of **two different conformations**. This result was attributed to the difference in the stapling positions. In addition, circular dichroism spectra revealed existence of secondary structures non random coiled. A similar CD spectrum was obtained for cyclo(-Ala-(4&$_1$)Phe-Ala-(4&$_1$)Phe-D-Pro-Ala-(4&$_2$)Phe-Ala-(4&$_2$)Phe-D-Pro) and cyclo(-Ala-(4&$_1$)Phe-Leu-Leu-(4&$_1$)Phe-D-Pro-Ala-(4&$_2$)Phe-Leu-Leu-(4&$_2$)Phe-D-Pro). Therefore, we concluded that *para-para* stapling induced a similar type of secondary structure.

v. Three different families of peptides (lysine family, arginine family and serine family) were prepared. The verstatily of the synthetic methodology proved to be adequate for the introduction of functional groups. Each family contained not only the bicyclic parent peptides but also a linear, a head-to-tail cyclic and a linear stapled version. SPPS strategy was correspondingly modified in each case in order to obtain the desired products.

Objective 2

i. Passive diffusion permeability for the three families of compounds, mentioned above, was evaluated using BBB-PAMPA. Lysine family showed high permeability due to the hydrophobic-hydrophilic balance that the introduction of these amino acids brought to the sequence. Peptides with the biaryl staple (linear staple version and bicyclic version) displayed higher permeabilitites. Regarding arginine family, the linear stapled peptide displayed highest permeability. In this case, high membrane retention was detected for the head-to-tail cyclic and bicyclic analogs, hypothesizing interaction with the lipids used for mimicking the BBB. Finally, serine family showed poor permeability values, although the bicyclic peptide had a slight improvement. Therefore, the overall conclusion is that **the introduction of the biaryl staple represented an enhancement in passive diffusion permeability across the BBB**.

ii. Protease resistance in human serum displayed similar results for all the families. Linear peptides were degraded during the initial minutes of the assay, while the head-to-tail cyclic and linear stapled versions were more resistant with increased half-lives.

Bicyclic versions were the most stable ones, with very low degradation even after 24-48h of incubation. It is worth mentioning that the arginine linear stapled peptide displayed a half-life similar to the arginine bicyclic peptide.

iii. MTT assay in HeLa cells proved that the introduction of **the biaryl staple did not introduce cytotoxicity to the scaffold at 200µM and 500µM concentrations**. Moreover, risk of immunogenicity for lysine bicyclic peptide assayed in mice, was very low.

Objective 3

i. Introduction of **Trp-Trp staple was successfully achieved**. The synthesis of these peptides was carried out following the previously described methodolody, based on SPPS, Suzuki-Miyaura on resin and head-to-tail cyclization in solution. In this case, stapling was performed from halotryptophan provided by Prof. S. Ballet group. Stapling was performed on positions 5-5, 6-6 or 7-7 of the indole group of tryptophan. **Head-to-tail bromine containing peptides** were also synthesized to study the effect of the halogen in the indole group of tryptophan and at the different positions.

ii. BBB-PAMPA showed the enhanced permeability of both Trp-Trp peptides and head-to-tail bromine containing peptides. When compared with the Phe-Phe peptides we observed that **the nature of the stapling was crucial.** Better results were obtained for the peptides stapled between phenylalanines (described in chapter 2). Head-to-tail cyclic peptides prepared during the thesis were also compared, displaying **higher values the ones with bromine** at the different positions of the indole. Moreover, slight differences were also observed according to the bromine position in the indole.

iii. XTT assay in HeLa cells demonstrated that the head-to-tail bromine containing peptides **were not cytotoxic except for the one with bromine at position 5 at the indole group and at concentrations of 500µM**.

Objective 4

i. ^{15}N-labelled R337H mutant with the flanking tails was succesfully expressed in *E. coli* and purified by cation exchange and size exclusion chromatrography by FPLC. ^{1}H-^{15}N-HSQC-NMR was obtained and properly assigned. On the other hand, **chemical synthesis of p53TD wild-type and R337H mutant without the flanking tails was achieved** using Liberty Blue automatic microwave assisted peptide synthesizer.

ii. Circular dichroism displayed the characteristic **α-helical profile**. Unfolding curves demonstrated the lesser stability of the R337H mutant with a significant difference of **30ºC** in front of the wid-type, regarding the transition temperature. Futhermore, as described in the literature, we observed that R337H mutant was less stable when the buffer had more ionic strength, as well as, in basic media. Noteworthly, the heating rate to perform the unfolding experiments was very relevant to achieve the equilibrium between the folded and unfolded fractions at every step. Reversibility of the process was assessed after evaluating the initial temperature before and after carrying out the unfolding experiments.

iii. The capacity to recover the self-assembly of R337H for the arginine bicyclic peptide was evaluated. A slight increase of 3ºC in the transition temperature (T_{05}) was observed with 8 or 16 equivalents of the peptide. On the other hand, a more promising result was obtained for the **arginine linear staple peptide.** A significant difference of **7ºC** was observed when introducing 16 equivalents of the peptide. The same experiments were perfomed with p53TD wild-type. In this case, unfolding curves in the absence or presence of the ligands were the same. Moreover, the arginine linear stpaled peptide was **non-cytotoxic in HeLa cells at concentration of 500μM**.

iv. Docking studies demonstrated that the **guanidinium groups of the arginine peptides interacted with the glutamic acids E336, E339, E343 and E346 of the protein p53.** A slightly better docking score was obtained for the arginine linear stapled peptide.

MATERIAL AND METHODS

PEPTIDE SYNTHESIS

Protected amino acids were supplied by Iris Biotech (Marktredwitz, Germany). Wang® resin was obtained from PCAS BioMatrix Inc. (Quebec, Canada). DIEA, DIPCDI and ninhydrin were purchased from Fluka Chemika (Buchs, Switzerland), and HOAt from GL Biochem Shangai Ltd. (Shangai, China). Solvents for SPPS, such as DMF and DCM, were purchased from SDS (Barcelona, Spain) and trifluoroacetic acid (TFA) from Scharlau (Barcelona, Spain). Other chemical reagents were acquired from Aldrich (Milwaukee, WI) with the highest purity commercially available. Syringes for SPPS and Eppendorf tubes were provided by Scharlau and Falcon tubes by Deltalab. PAMPA plates and system solution were supplied by pION (Woburn, MA USA), and porcine polar brain lipid extract (PBLEP) by Avantis Polar Lipids (Alabaster, AL). The basic instruments used were a lyophilizer (Virtis, Frezzmobile 25 EL), oven (Selecta, Digitronic), vortex (Merck Eurolab, MELB1719 (EU)), magnetic stirrer (IKA, RCT basic), centrifuge (Eppendorf, 5415R), GUT-BOX™ (pION Aqueous Boundary Layer Thickness @ Double-Sink™), pipettes (Gilson, Pipetman P2, P20, P200, P1000), and Shimadzu UV-2501 PC UV-VIS spectrophotometer.

Characterization of the peptides and purity assessment

HPLC-analytical scale

HPLC analyses were performed on a Waters Alliance 2695 with an automated injector and a photodiode array detector 2998 Waters (Waters, Milford, MA) using a SunFire™ C_{18} column, 3.5μm, 4.6x100mm. EmpowerPro 2 software was used to process the data. Detection was performed at 220nm. The analyses were carried out with a linear gradients of CH_3CN (0.036% TFA) in H_2O (0.045% TFA) over 8 min at a flow rate of 1 mL/min. Different gradients were explored to assess separation of the peak corresponding to the product from the impurities and enable HPLC-semipreparative purification.

UPLC

UPLC analyses were performed on a Waters Acquity with an automated injector and a photodiode array detector Waters (Waters, Milford, MA) using a BEH C_{18} column, 1.7μm, 2.1x50mm. Data was processed with an EmpowerPro 3 software. Detection was performed at 220 nm. The analyses were carried out with linear gradients CH_3CN,

UPLC grade, (0.036% TFA) in H$_2$O (0.045% TFA) over 2min at a flow rate of 0.61 mL/min.

UPLC-ESI-MS

UPLC-MS analyses were performed on a Waters Acquity with an automated injector and a photodiode array detector Waters (Waters, Milford, MA) coupled to an electrospray ion source ESI-MS Micromass ZQ. A BEH C$_{18}$ column, 1.7µm, 2.1x50mm was used. Data was processed with Masslynx 4.1 software. The instrument was operated in the positive ESI (+) ion mode. Detection was performed at 220 nm and the analyses were carried out with linear gradients CH$_3$CN, UPLC grade, (0.07% formic acid) in H$_2$O (0.1% formic acid) over 2min at a flow rate of 0.61mL/min. Samples were introduced, in a volume (1-100µL) whose absorbance was between 0.2-0.4, into the mass spectrometer ion source directly through an UPLC autosampler.

MALDI-TOF MS

Mass spectrometry characterization of some peptides was carried out using a MALDI-TOF Applied Biosystem 4700. 1µL of the peptide in a solution with a concentration around 1 mg/mL was mixed with 1µL of α-cyano-4-hydroxycinnamic acid (ACH) matrix, and then seeded on the MALDI plate and air-dried. For the matrix, 10mg/mL solution of ACH was prepared in CH$_3$CN/H$_2$O 1:1 (v/v) with 0.1% TFA.

LTQ-FT MS

Some of the peptides were analyzed using a high resolution mass spectrometer to obtain their exact mass. Samples were dissolved in 200µL of H$_2$O:MeCN and diluted in H$_2$O:MeCN 1% formic acid for MS analysis. The analysis was performed in a LTQ-FT Ultra (Thermo Scientific) and the samples were introduced by automated nanoelectrospray. A NanoMate (Advion BioScience, Ithaca, NY, USA) infused the samples through the ESI Chip, which consists of 400 nozzles in a 20x20 array. Spray voltage was 1.7kV and delivery pressure was 0.3psi. MS conditions were: NanoESI, positive ionization, capillary temperature 200ºC, tube lens 119V, ion spray voltage 2kV and m/z 100-2000amu.

General method for solid-phase peptide synthesis

SPPS were performed at different scales between 100-1000μmols. L-amino acids were used except for D-proline. Peptide elongations were carried out in 20-mL or 60-mL polypropylene syringes, each fitted with a polypropylene porous disk. Solvents and soluble reagents were removed by filtration. Washings between steps were done with DMF (3x30s), MeOH (3x30s) and DCM (3x30s) using 10mL of solvent/g resin each time. During couplings the resin was stirred using an orbital shaker.

Solid-phase Miyaura borylation[53]

The resin was transferred to a glass vial and treated with bis(pinacolato)diboron (B_2Pin_2) (4 equiv.), $PdCl_2(dppf)$ (0.18 equiv.), 1,1'-bis(diphenylphosphanyl)ferrocene (dppf) (0.09 equiv.) and KOAc (6 equiv.) in DMSO. The mixture was then heated at 85°C for between 24h and 36h.

The resin was then filtered and washed with DMF, DMF/H_2O, MeOH and DCM. An aliquot of the resulting borono resin was cleaved with 95% TFA/ 2.5% H_2O/ 2.5% TIS for 1 h. Following TFA evaporation, the crude peptide was dissolved in H_2O:CH_3CN 1:1, and then analyzed by HPLC and characterized by MS.

Solid-phase Suzuki reaction[53]

The resin was transferred to a glass vial and treated with Cs_2CO_3 (3 equiv.) and $Pd(PPh_3)_4$ (0.1 equiv.) in DMF. The mixture was stirred and heated at 65°C for 48 h. The resin was then filtered and washed with DMF, MeOH and DCM. After the Suzuki reaction, the peptides were cleaved from the resin.

Purification of the crude peptides

In order to remove remains of palladium (from the Suzuki-Miyaura and borylation reactions), a Porapak™ RP cartridge was required as an intermediate purification step prior to the head-to-tail cyclization of the compounds already bearing the biaryl bridge.

First, the column was washed with MeOH (2 volumes) and equilibrated with H_2O (1 volume). After the column had dried, the sample was charged in less than 1.5 mL methanol or CH_3CN/H_2O 1:1. The gradient started with 100% H_2O, followed by a step

by step increasing of 5%. Manual pressure was applied to achieve a constant flux and facilitate elution.

Samples of the fractions were injected in the HPLC and HPLC-MS apparatuses in order to detect the product. Those fractions containing the peptide were collected and lyophilized. The flow rate and the size of the Porapak column were selected taking into account the amount of crude peptide to be purified.

Final HPLC-semipreparative purification was carried out.

HPLC purification performed in a Waters system with 2545 binary gradient module, a 2767 manager collector, and a 2998 photodiode array detector with MassLynx 4.1 software. To different columns were used according to the amount of crude peptide to be purified. In higher scales XBridge C_{18} 5μm, 19x150mm column was used while in purification of lower scales or worse separation of the crudes Vydac column C_{18} 5μm, 250x10mm.

The solvents were prepared as CH_3CN (0.1% TFA) and H_2O (0.1% TFA). The flow rate was 20 mL/min for XBridge column and 5 mL/min for Vydac column. HPLC and/or UPLC analyses were performed to validate the correct purification of the peptides. Purity and identity was assessed by analytical UPLC-MS.

Head-to-tail cyclization in solution

- **Initial cyclization conditions**

After cleavage from the resin and Porapak^{TM} purification the linear precursor peptide was dissolved in DMF at a final concentration of 5mM. DPPA (2 equiv.) and $NaHCO_3$ (8 equiv.) were used. The pH was measured, adjusted if necessary at 8-9 with more $NaHCO_3$.

The reaction was stirred at room temperature for 24-48h.

- **Optimization cyclization experiments**

In experiments 1, 2 and 5 the linear precursors were dissolved in DMF at 5, 50 and 100mM concentration. DPPA (2 equiv.) and NaHCO$_3$ (8 equiv.) were used and the pH adjusted at 8-9 with NaHCO$_3$. The reactions were stirred at room temperature for 48h. In experiments 3, 4, 6, 7, 8 and 9 the linear precursors were dissolved in DCM with 1% of DMF at 1, 0.5, 5, 10, 50 and 100mM concentrations. PyBOP (2 equiv.), HOAt (1 equiv.) and DIEA (6 equiv.) were used. pH was adjusted at 8-9 with DIEA. The reactions were stirred at room temperature for 48h.

- **Optimized cyclization conditions**

After cleavage from the resin and Porapak^{TM} purification, linear precursor was treated with PyBOP (2 equiv.), HOAt (1 equiv.), DIEA (6 equiv.) in DCM/ 1% DMF at a final concentration 1mM. The reaction was stirred at room temperature for 24 h-48 h.

A final purification step by RP-HPLC on a C$_{18}$ column was required to obtain the pure cyclic peptides.

Amino acid derivatization *p*NZ-(4I)Phe-OH and *p*NZ-(3I)Phe-OH

The amino acid was prepared from 2g (6.88mmol) of H-(4I)Phe-OH. *p*-nitrobenzyl chloroformate (1 equiv.) was dissolved in dioxane (3mL). Sodium azide (1.2 equiv.), previously dissolved in water (2mL), was added to this solution. This mixture was vigorously stirred at room temperature for 3h. The amino acid dissolved in dioxane (16mL) and 2% aq. NaHCO$_3$ (16mL) was then introduced dropwise. The mixture was allowed to react for 24h at room temperature. The pH was kept at 9-10 and readjusted when needed. Completion of the reaction was monitored by thin layer chromatography (TLC).

The crude product was separated in 50% H$_2$O/ 50% MTBE (100 mL), and the aqueous phase was extracted with MTBE (2x50 mL). The pH was adjusted to 4 with aqueous HCl 12N. The product precipitated as a white solid. Finally, it was filtered, washed, resuspended in water, and lyophilized.

Amino acid derivatization *H*-(XBr)Trp-OH x=5,6 or 7 by Tom Willemse, from Prof. S. Ballet laboratory

Were prepared by Tom Willemse according to:

D. R. M. Smith, T. Willemse, D. S. Gkotsi, W. Schepens, B. U. W. Maes, S. Ballet , R. J. M. Goss, *Org. Lett.* **2014**, *16*, 2622-2625

- **5-Bromotryptophan**

Formula: $C_{11}H_{11}BrN_2O_2$; **HPLC:** t_R = 10.7 min; **MS (ESI$^+$):** 283 [M+H, ^{79}Br]$^+$, 285 [M+H, ^{81}Br]$^+$; **^{1}H NMR (300 MHz, D$_2$O):** ∂ 7.67 (1H, d, *J* = 1.8), 7.30 (1H, d, *J* = 8.7), 7.25 - 7.19 (2H, m), 4.23 (1H, dd, *J* = 7.1, 5.5), 3.32 (1H, dd, *J* = 15.4, 5.4), 3.24 (1H, dd, 15.4, 7.2); **^{13}C NMR (75 MHz, D$_2$O):** 172.3, 135.2, 128.5, 126.8, 124.9, 120.8, 113.8, 112.3, 106.3, 55.6, 26.0.

- **6-Bromotryptophan**

Formula: $C_{11}H_{11}BrN_2O_2$; **HPLC:** t_R = 10.8 min; **MS (ESI$^+$):** 283 [M+H, ^{79}Br]$^+$, 285 [M+H, ^{81}Br]$^+$; **^{1}H NMR (300 MHz, D$_2$O):** ∂ 7.55 (1H, d, *J* = 1.7), 7.39 (1H, d, *J* = 8.5), 7.18 (1H, s), 7.15 (1H, dd, *J* = 8.5, 1.7), 4.24 (1H, dd, *J* = 7.0, 5.5), 3.35 (1H, dd, *J* = 15.4, 5.5), 3.27 (1H, dd, *J* = 15.4, 7.1); **^{13}C NMR (75 MHz, D$_2$O):** ∂ 172.3, 137.3, 126.2, 125.8, 122.6, 119.8, 115.2, 114.8, 106.9, 53.6, 26.0.

- **7-Bromotryptophan**

Formula: $C_{11}H_{11}BrN_2O_2$; **HPLC:** t_R = 10.7 min; **HRMS (ESI$^+$)**; found 283.0057 [M+H, ^{79}Br]$^+$, expected 283.0077; found 285.0045 [M+H, ^{81}Br]$^+$, expected 285.0057; **^{1}H NMR (300 MHz, D$_2$O):** ∂ 7.54 (1H, dd, *J* = 8.0, 0.8), 7.36 (1H, dd, *J* = 7.6, 0.6), 7.26 (1H, s), 6.99 (1H, t, *J* = 7.8), 4.25 (1H, dd, *J* = 5.5, 7.1), 3.38 (1H, dd, *J* = 5.3, 15.7), 3.29 (1H, dd, *J* = 7.0, 15.5); **^{13}C NMR (75 MHz, D$_2$O):** ∂ 172.4, 135.1, 128.2, 126.2, 124.8, 121.0, 117.9, 108.1, 104.8, 53.7, 26.2.

Amino acid derivatization Fmoc-(XBr)Trp-OH x=5,6 or 7, provided by Tom Willemse form Prof. S. Ballet laboratory

The Fmoc-protected building blocks were synthesized according to the following procedure:

The corresponding bromotryptophan hydrochloric acid salt (500 mg, 1.57 mmol) was dissolved with Na_2CO_3 (1.2 eq, 1.89 mmol) in 10mL H_2O. To this was added a solution of Fmoc-OSu (1.1 eq, 1.72mmol) in 10mL dioxane. The reaction mixture was stirred overnight at room temperature. Reaction completion was checked by HPLC and the mixture was concentrated. The resulting aqueous phase was acidified with 1N HCl (pH = 1) and extracted with CH_2Cl_2 (4x 30 mL). The combined organic phase was washed with 1N HCl, dried over $MgSO_4$ and concentrated by rotary evaporation. The resultant crude was triturated with a mixture of CH_2Cl_2/hexane and filtered over a glass frit. The obtained pink solid was further purified with flash column chromatography (CH_2Cl_2/MeOH/AcOH 97:2:1, for r_{ref} see individual compound) and concentrated to obtain as a white solids.

- **Fmoc-5-Bromotryptophan**

Yield: 561 mg (71%); HPLC: t_{ret}= 18.9 min; TLC: r_{ref}= 0.19 (CH_2Cl_2/MeOH/AcOH 97:2:1); MW ($C_{26}H_{21}BrN_2O_4$): 505.3680 g/mol; LC/MS: (ESI+) [M+Na$^+$, ^{81}Br]: 527, [M+Na$^+$, ^{79}Br]: 525; [M+H$^+$, ^{81}Br]: 507, [M+H$^+$, ^{79}Br]: 505; HRMS (ESI+): Calculated for: $C_{26}H_{20}{}^{81}BrN_2O_4NaH_p{}^+$: 529.0556, found: 529.0552 ;^{1}H-NMR (500 MHz, DMSO-d$_6$): 1H-NMR (500 MHz, DMSO-d6): δH 12.65 (1H, br s), 11.06 (1H, s), 7.87 (2H, d, J= 7.7 Hz), 7.75 (1H, d, J= 1.3 Hz), 7.70 (1H, d, J= 8.1 Hz), 7.63 (2H, dd, J= 15.6 Hz, 7.5 Hz), 7.39 (2H, q, J= 7.1 Hz), 7.22-7.32 (4H, M), 7.17 (1H, dd, J= 8.5 Hz, 1.7 Hz), 4.14-4.22 (4H, M), 3.15 (2H, dd, J= 14.5 Hz, 4.6 Hz), 2.99 (2H, dd, J= 14.5 Hz, 9.8 Hz)

Consistent with literature data: Chen C. H. et al., *Org. Biomol. Chem.*, **2014**, 12, 9764

- **Fmoc-6-Bromotryptophan**

Yield: 589 mg (75%); HPLC: t_{ret}= 18.9 min; TLC: r_{ref}= 0.16 (CH_2Cl_2/MeOH/AcOH 97:2:1); MW ($C_{26}H_{21}BrN_2O_4$): 505.3680 g/mol; LC/MS: (ESI+) [M+Na$^+$, ^{81}Br]: 527, [M+Na$^+$, ^{79}Br]: 525; [M+H$^+$, ^{81}Br]: 507, [M+H$^+$, ^{79}Br]: 505 HRMS (ESI+): Calculated for: $C_{26}H_{20}{}^{81}BrN_2O_4NaH_p{}^+$: 529.0556, found: 529.0579; ^{1}H-NMR (500 MHz, DMSO-d$_6$): δH 12.66 (1H, br s), 10.98 (1H, s), 7.87 (2H, d, J= 7.5 Hz), 7.62-66 (3H, M), 7.51 (2H, M), 7.37-41 (2H, M), 7.27 (2H, M), 7.19 (1H, d, J= 2.3 Hz),7.09 (1H, dd, J= 8.3 Hz, 1.4 Hz), 4.15-4.22 (4H, M), 3.16 (1H, dd, J= 14.5 Hz, 4.5 Hz), 2.99 (1H, dd, J= 14.5 Hz, 9.8 Hz)

-Fmoc-7-Bromotryptophan

<u>Yield:</u> 592 mg (75%); <u>HPLC:</u> t_{ret}= 19.3 min; <u>TLC:</u> r_{ref}= 0.22 (CH$_2$Cl$_2$/MeOH/AcOH 97:2:1); <u>MW</u> (C$_{26}$H$_{21}$BrN$_2$O$_4$): 505.3680 g/mol; <u>LC/MS:</u> (ESI+) [M+Na$^+$, ^{81}Br]: 527, [M+Na$^+$, ^{79}Br]: 525; [M+H$^+$, ^{81}Br]: 507, [M+H$^+$, ^{79}Br]: 505; <u>HRMS (ESI+):</u> Calculated for: C$_{26}$H$_{20}$^{81}BrN$_2$O$_4$NaH$_p$$^+$: 529.0556, found: 529.0511; ^{1}H-NMR (500 MHz, DMSO-d$_6$): δH 12.71 (1H, br s), 11.09 (1H, s), 7.86 (2H, d, J= 7.5 Hz), 7.70 (1H, d, J= 8.1 Hz), 7.64 (1H, d, J= 7.5 Hz), 7.61 (1H, d, J= 7.5 Hz), 7.58 (1H, d, J= 7.9 Hz), 7.39 (2H, m),7.24-7.31 (4H, M), 6.93 (1H, t, J= 7.7 Hz), 4.19-4.24 (2H, M), 4.17 (2H, m), 3.19 (1H, dd, J= 14.5 Hz, 4.3 Hz), 3.19 (1H, dd, J= 14.5 Hz, 10.4 Hz)

Amino acid derivatization *p*NZ-(XBr)Trp-OH x=5,6 or 7

The amino acid was prepared from the received amount of H-(XBr)Trp-OH. The same derivatization procedure for *p*NZ-(4I)Phe-OH was used.

The products precipitated as yellow pale solids which finally were filtered, washed, resuspended in water and lyophilized.

Loading of the first amino acid onto Wang resin

The peptides were synthesized manually on solid-phase using standard Fmoc/*t*Bu chemistry. Wang resin (1.42 mmol/g) was used as support. Coupling of the first amino acid Fmoc-DPro-OH (8 equiv.) was performed using DIPCDI (4 equiv.) in 90% DCM / 10% DMF and DMAP (0.8 equiv.) at room temperature overnight. The solution was filtered, and the resin was washed with DMF, DCM and MeOH several times. The Fmoc group was removed by treatment with 20% piperidine solution in DMF (1x5 min, 1x10 min, 1x15 min), and the loading of the resin was quantified by measuring the absorbance of the filtrate at 290 nm (ε=5900). The capping of the remaining reactive positions of the resin was carried out with acetic anhydride (20 equiv.) and DIEA (20 equiv.) in DMF at room temperature for 30 min. The resin was washed again with DMF, DCM and MeOH.

Loading of the first amino acid onto Chlorotrityl resin

The peptides were synthesized manually on solid-phase using Fmoc standard chemistry. 2-CTC resin was used as support (1.57 mmol/g), and the coupling of the first

amino acid Fmoc-DPro-OH (1 equiv.) was performed with DIEA (3 equiv.) in 15% DMF and 85% DCM at room temperature for 20min. An extra excess of DIEA (3 equiv.) was then added, and the mixture was stirred and allowed to react for 90min. At this point, 0.8 mL/g resin MeOH was added, and the reaction was maintained for another 15min. When the time was over, the solution was filtered, and the resin was washed with DMF and DCM several times. Loading was determined as for the Wang resin.

Identification tests

Colorimetric tests were used throughout SPPS. These tools enable to monitor coupling and deprotection steps of a particular residue in the sequence in an easily and quickly qualitative manner.

- **Kaiser test or ninhydrin test**[218]

Ninhidrin or Kaiser test was used so as to monitor each coupling or deprotection step by detecting the presence of primary amines attached to the resin. This test is based in the formation of the ninhidrin chromophore by condensation of the amine with a molecule of ninhydrin to yield a Schiff base. This reaction can only be performed when ammonia or primary amines are present due to the requirement of an alpha proton for the Schiff base transfer.

For this reason, this test was used to check whether the coupling or the deprotection reactions are finished. In order to carry out this assay, some beads of the previously washed resin (with DCM) are transferred into a glass tube. Then, six drops of the reagent solution A and two drops of the reagent solution B are added into the tube, which is heated up to 110ºC for 3min. A yellow or orange solution with naturally coloured beads indicated a negative result, which means the absence of primary amines, while a dark blue or purple solution and beads communicate a positive test with primary amines attached to the resin.

Reagent solution A was obtained according to the following protocol. 40g of phenol were added to 10mL of ethanol. The mixture was heated until total solution of the solid was obtained. At the same time, a solution of 65mg of KCN in 100mL of water was added to pyridine, freshly distilled over 100mL of ninhydrin. Both solutions were stirred for 45min with 4g of Amberlite MB-3 resin, filtered and mixed.

Reagent solution B was a solution of 205mg of ninhydrin in 50mL of absolute ethanol. This reagent should be maintained in high-proof container to be protected from light.

- **Chloranil test[219]**

The chloranil test was used for detection of primary and secondary amines in coupling and deprotection steps. In SPPS, this test was used in order to monitor accomplishment of amino acid coupling onto secondary amines such as prolines.

Resin beads were transferres into a glass tube after being washed with methanol. 200 μL of acetaldehyde was added for both primary and secondary amines test or acetone for secondary amines test, followed by 50μL chloranil solution (750mg of 2,3,5,6-tetrachloro-1,4-benzoquinone in 25mL of toluene). The solution was stirred at room temperature for 5min. The presence of free amineswais detected by a green or blue-coloured solution and beads, while negative test was obtained as yellow, amber or brown solution and beads.

Cleavage conditions

Peptides were cleaved from the Wang resin using a mixture of 95% TFA, 2.5% H_2O and 2.5% TIS. The peptides were stirred for 90 min with the cocktail. The compounds were then filtrated and washed with DCM. After reducing the volume with nitrogen, they were resolved with MeCN:H_2O and lyophilized.

Regarding the sequences prepared with chlorotrityl resin, general cleavage was performed with 50% TFA, 45% DCM and 5% H_2O. When having acid-labile protecting groups in the side-chains, cleavage was carried out at 95% TFA/ 5% DCM to yield the unprotected peptide.

Synthesis and characterization of the peptides

General method to synthesize phe-phe stapled bicyclic pentapeptides

The peptide was prepared starting from Fmoc-DPro-Wang resin. The Fmoc group was removed with 20% piperidine in DMF (1x5 min, 1x15 min). The second amino acid was introduced as pNZ-(4I)Phe-OH or pNZ-(3I)Phe-OH (3 equiv.) and coupled to DIPCDI (3 equiv.) and HOAt (3 equiv.) in DMF at room temperature for 90min. Completion of the

coupling was checked by the chloranil test. *p*NZ was then removed with a solution of 6M SnCl$_2$ and 1.6mM HCl/dioxane (3x30min). The resin was washed with DMF, DMF/H$_2$O, H$_2$O/THF, THF, MeOH and DCM (3x each). The third amino acid, coupled with PyBOP (3 equiv.) and DIEA (6 equiv.) in DMF at room temperature for 1h, depends on the sequence requiring a different protecting group scheme. At tripeptide level, Miyaura borylation was performed following the general method for this reaction on resin. The Trt temporary protecting group was then removed with 2% TFA/ 2% H$_2$O/ 96% DCM (3x5min, 1x20min). Between the treatments, the resin was washed twice with DCM and, after the last one, also with a solution of 5% DIEA/ 95% DCM. Fmoc-(4I)-Phe-OH or Fmoc-(3I)-Phe-OH (3 equiv.) was introduced with DIPCDI (3 equiv.) and oxyma (3 equiv.) in DCM/DMF. Again, deprotection of the Fmoc group preceded the coupling of the last amino acid (3 equiv.), different for each sequence, which was activated with TBTU (3 equiv.) and DIEA (6 equiv.). The Suzuki reaction was performed following the general method. Cleavage from the resin was then carried out with a mixture of 95% TFA/ 2.5% DCM/ 2.5% H$_2$O under stirring for 1h at room temperature. After TFA evaporation, the crude product was dissolved in 50% H$_2$O/ 50% MeCN and lyophilized. Palladium was then removed by elution through a Porapak^{TM} RP cartridge with increasing amounts of MeCN in H$_2$O. The fractions containing the product, even when not completely pure, were pooled and lyophilized. To finish the synthesis, the peptide was cyclized using the general method. Remaining protecting groups in some sequences are deprotected under required conditions in solution.

The crudes were purified by HPLC-semipreparative using C$_{18}$ column. Fractions containing the peptides were lyophilized. The pure peptides were analysed by HPLC, UPLC and characterized by UPLC-MS and exact mass determination.

General method to synthesize trp-trp stapled bicyclic pentapeptides

The peptide was prepared starting from Fmoc-DPro-Wang resin. The Fmoc group was removed with 20% piperidine in DMF (1x5min, 1x15min). The second amino acid was introduced as *p*NZ-(XBr)Trp-OH (x=5,6 or 7) (2 equiv.) and coupled to DIPCDI (2 equiv.) and HOAt (2 equiv.) in DMF at room temperature for 90 min. Completion of the coupling was checked by the chloranil test. *p*NZ was then removed with a solution of 6M SnCl$_2$ and 1.6 mM HCl/dioxane (3x30min). The resin was washed with DMF,

DMF/H$_2$O, H$_2$O/THF, THF, MeOH and DCM (3x each). Trt-Lys(Fmoc) was coupled with PyBOP (3 equiv.) and DIEA (6 equiv.) in DMF at room temperature for 1 h. Fmoc protecting group was removed (1x1min, 1x3min, 1x5min). *p*NZ was introduced using *p*NZCl (3 equiv.) and DIEA (30 equiv.) in DMF at room temperature (2x45min). At tripeptide level, Miyaura borylation was performed following the general method for this reaction on resin for 48h. The Trt temporary protecting group was then removed with 2% TFA/ 2% H$_2$O/ 96% DCM (3x5min, 1x20min). Between the treatments, the resin was washed twice with DCM and, after the last one, also with a solution of 5% DIEA/ 95% DCM. Fmoc-(XBr)-Trp-OH (x=5,6 or 7) (2 equiv.) was introduced with DIPCDI (2 equiv.) and HOAt (2 equiv.) in DCM/DMF. Again, deprotection of the Fmoc group preceded the coupling of the last amino acid, Boc-Lys(*p*NZ)-OH (3 equiv.) which was activated with PyBOP (3 equiv.) and DIEA (6 equiv.). The Suzuki reaction was performed following the general method for 72h. Cleavage from the resin was then carried out with a mixture of 95% TFA/ 2.5% DCM/ 2.5% H$_2$O under stirring for 1h at room temperature. After TFA evaporation, the crude product was dissolved in 50% H$_2$O/ 50% MeCN and lyophilized. Palladium was then removed by elution through a Porapak^{TM} RP cartridge with increasing amounts of MeCN in H$_2$O. The fractions containing the product, even when not completely pure, were pooled and lyophilized. To finish the synthesis, the peptide was cyclized using the general method, and next *p*NZ in lysines side-chains were removed by means of Na$_2$S$_2$O$_4$ (8 equiv.) and a mixture of equal parts of H$_2$O, MeCN and EtOH. After 24 h, the reagents were added again, and at 48 h the reaction was completed. The solvent was then evaporated and the crude was dissolved in 50% H$_2$O/ 50% MeCN and lyophilized.

The crudes were purified by HPLC-semipreparative using C$_{18}$ column. Fractions containing the peptides were lyophilized. The pure peptides were analysed by HPLC, UPLC and characterized by UPLC-MS and exact mass determination.

cyclo(Ala-(4&)Phe-Ala-(4&)Phe-D-Pro)

The peptide was prepared using the standard methodology for phe-phe stapled peptides.

The third introduced amino acid was Fmoc-Ala-OH, followed by Fmoc deprotection, trytil protecting group was incorporated in the main chain using TrtCl (10 equiv.) and DIEA (30 equiv, 2x3h) . Ninhydrin test was used to ensure full protection.

The last amino acid was Boc-Ala-OH, which contains the required protecting group for concomitant Suzuki reaction.

HPLC t_R (G 0-100% CH_3CN/H_2O in 8min): 5.04min; UPLC-MS t_R (G 0-100% CH_3CN/H_2O in 2min): 1.54min, $[M+H^+]_{expected}$=532.25, $[M+H^+]_{found}$=532.51, HRMS (ESI): 532.2554 calcd. for $C_{29}H_{34}N_5O_5$; $[M+H^+]_{found}$=532.2535; yield not quantified, synthesized in small trials for obtimization of the head-to-tail cyclization protocol

cyclo(Ala-(3&)Phe-Ala-(3&)Phe-D-Pro)

The peptide was prepared using the standard methodology for phe-phe stapled peptides.

As described for the analogue with 4&, Fmoc-Ala-OH and Boc-Ala-OH were used as the third and fifth amino acids, respectively.

In this peptide 3-iodine derivatives were used.

HPLC t_R (G 0-100% CH_3CN/H_2O in 8min): 5.04min; UPLC-MS t_R (G 0-100% CH_3CN/H_2O in 2min): 1.54min, $[M+H^+]_{expected}$=532.25, $[M+H^+]_{found}$=532.51, HRMS (ESI): 532.2554 calcd. for $C_{29}H_{34}N_5O_5$; $[M+H^+]_{found}$=532.2535; yield not quantified, synthesized in small trials for obtimization of the head-to-tail cyclization protocol

cyclo(Ala-(4&₁)Phe-Ala-(4&₁)Phe-D-Pro-Ala-(4&₂)Phe-Ala-(4&₂)Phe-D-Pro)

The peptide was prepared using the standard methodology for phe-phe stapled peptides.

The third introduced amino acid was Fmoc-Ala-OH, followed by Fmoc deprotection, trytil protecting group was incorporated in the main chain using TrtCl (10 equiv.) and DIEA (30 equiv,2x3h) . Ninhydrin test was used to ensure full protection.

The last amino acid was Boc-Ala-OH, which contains the required protecting group for concomitant Suzuki reaction. Head-to-tail cyclization in solution was carried out under the initial conditions, 8eq $NaHCO_3$, 2eq DPPA in 5mM DMF.

HPLC t_R (G 20-100% CH₃CN/H₂O in 8min): 6.18min; UPLC-MS t_R (G 0-100% CH₃CN/H₂O in 2min): 1.58min, [M+H$^+$]$_{expected}$=1063.50, [M+H$^+$]$_{found}$=, HRMS (ESI): 1063.50362 calcd. for $C_{58}H_{67}N_{10}O_{10}$; [M+H$^+$]$_{found}$= 1063.50535; yield (synthesis+purification)=1%

cyclo(Ala-(3&₁)Phe-Ala-(3&₁)Phe-D-Pro-Ala-(3&₂)Phe-Ala-(3&₂)Phe-D-Pro)

The peptide was prepared using the standard methodology for phe-phe stapled peptides.

The third introduced amino acid was Fmoc-Ala-OH, followed by Fmoc deprotection, trytil protecting group was incorporated in the main chain using TrtCl (10 equiv.) and DIEA (30 equiv(2x3h) . Ninhydrin test was used to ensure full protection.

The last amino acid was Boc-Ala-OH, which contains the required protecting group for concomitant Suzuki reaction. Head-to-tail cyclization in solution was carried out under the initial conditions, 8eq NaHCO₃, 2eq DPPA in 5mM DMF.

HPLC t_R (G 20-100% CH₃CN/H₂O in 8min): 6.10min; UPLC-MS t_R (G 0-100% CH₃CN/H₂O in 2min): 1.58min, [M+H$^+$]$_{expected}$=1063.50, [M+H$^+$]$_{found}$=, HRMS (ESI): calcd. for $C_{58}H_{67}N_{10}O_{10}$; [M+H$^+$]$_{found}$=1063.50567; yield (synthesis+purification)=1%

cyclo(Ala-(4&₁)Phe-Leu-Leu-(4&₁)Phe-D-Pro-Ala-(4&₂)Phe-Leu-Leu-(4&₂)Phe-D-Pro)

The peptide was prepared using the standard methodology for phe-phe stapled peptides. In this case, the sequence introduced an extra aminoacid before performing Suzuki reaction. Borylation was also carried out at the tripeptide level. Head-to-tail cyclization in solution was carried out under the initial conditions, 8eq NaHCO₃, 2eq DPPA in 5mM DMF.

HPLC t_R (G 0-100% CH₃CN/H₂O in 8min): 7.34min; UPLC-MS t_R (G 0-100% CH₃CN/H₂O in 2min): 2.0min, [M+H$^+$]$_{expected}$=1373.76, [M+H$^+$]$_{found}$=1373.01, HRMS (ESI): 1373.76564calcd. for $C_{76}H_{101}N_{12}O_{12}$; [M+H$^+$]$_{found}$= 1373.76454; yield could not be estimated due to the purification of an aliquot of the final crude peptide.

cyclo(Lys-(4&)Phe-Lys-(4&)Phe-D-Pro)

The peptide was prepared using the standard methodology for phe-phe stapled peptides.

Trt-Lys(Fmoc)-OH was used as the third amino acid, coupled with PyBOP (3 equiv.) and DIEA (6 equiv.) in DMF at room temperature for 1h. After Fmoc removal, pNZ was introduced using pNZCl (3 equiv.) and DIEA (30 equiv.) in DMF at room temperature (2x45 min). The last amino acid, Boc-Lys(pNZ)-OH (3 equiv.), was activated with TBTU (3 equiv.) and DIEA (6 equiv.). To finish the synthesis, the peptide was cyclized using the general method, and next pNZ in lysines side-chains were removed by means of $Na_2S_2O_4$ (8 equiv.) and a mixture of equal parts of H_2O, MeCN and EtOH. After 24 h, the reagents were added again, and at 48 h the reaction was completed. The solvent was then evaporated and the crude was dissolved in 50% H_2O/ 50% MeCN and lyophilized.

HPLC t_R (G 0-100% CH_3CN/H_2O in 8min): 8.00min; UPLC t_R (G 0-100% CH_3CN/H_2O in 2min): 1.8 min; UPLC-MS t_R (G 0-100% CH_3CN/H_2O in 2min): 1.8 min, $[M+H^+]_{expected}$= 645.36, $[M+H^+]_{found}$= 645.44, HRMS (ESI): calcd. for $C_{35}H_{48}N_7O_5$ 645.3533; $[M+H^+]_{found}$= 645.3536; yield (synthesis+purification): 1%

cyclo(Arg-(4&)Phe-Arg-(4&)Phe-D-Pro)

The peptide was prepared using the standard methodology for phe-phe stapled peptides.

After the introduction of the third amino acid, Fmoc-Arg(Pbf)-OH, Fmoc deprotection was carried out followed by trytil introduction with TrtCl (10 equiv.) and DIEA (30 equiv.) (2x3h). Ninhydrin test was used to ensure full protection.

The last amino acid was Fmoc-Arg(Pbf), which requires Fmoc deprotection and Boc introduction with Boc anhydride (10 equiv.) and DIEA (30 equiv.) (2x45min). Again, ninhydrin test was performed to ensure full protection of the pentapeptide.

Pbf deprotection was performed during the cleavage of the peptide from the resin, avoiding additional reactions in solution. The mixture was evaporated and the crude product was dissolved in 50% H_2O/ 50% MeCN and lyophilized.

HPLC t_R (G 0-100% CH_3CN/H_2O in 8min): 5.20min; UPLC-MS t_R (G 0-100% CH_3CN/H_2O in 2min): 1.45min, $[M+H^+]_{expected}$= 702.83, $[M+H^+]_{found}$= 703.49, HRMS (ESI): 702.38344 calcd. for $C_{35}H_{48}N_5O_{11}$; $[M+H^+]_{found}$= 702.38440; yield (synthesis + purifaction)= 1%

cyclo(Ser-(4&)Phe-Ser-(4&)Phe-D-Pro)

The peptide was synthesized using the standard methodology for phe-phe stapled peptides.

The third amino acid introduced was Fmoc-Ser(Bzl)-OH. Fmoc deprotection was performed followed by trytil protection with TrtCl (10 equiv.) and DIEA (30 equiv.) (2x3h). Ninhydrin test was used to ensure full protection.

The last amino acid was again Fmoc-Ser(Bzl)-OH, requiring Fmoc deprotection and Boc introduction with Boc anhydride (10 equiv.) and DIEA (30 equiv.) (2x45min). Ninhydrin test was also used to ensure full protection of the pentapeptide.

Bzl deprotection was carried out during the cleavage of the peptide from the resin, avoiding additional reaction in solution. The mixture was evaporated and the crude product was dissolved in 50% H_2O/ 50% MeCN and lyophilized.

HPLC t_R (G 0-100% CH_3CN/H_2O in 8min): 6.54min; UPLC-MS t_R (G 0-100% CH_3CN/H_2O in 2min):   1.42min, $[M+H^+]_{expected}$= 564.61, $[M+H^+]_{found}$= 565.32, yield (synthesis + purifaction)= 2%

H-Lys-Phe-Lys-Phe-D-Pro-OH

This peptide was prepared from DPro-CTC (1 equiv.=0.58 mmol). Fmoc-Phe-OH and Fmoc-Lys(Boc)-OH residues (3 equiv.) were attached using DIPCDI (3 equiv.) and HOAt (3 equiv.) as coupling agents. General cleavage procedure of the sequence provided the desired peptide. The mixture was evaporated and the crude product was dissolved in 50% H_2O/ 50% MeCN and lyophilized.

HPLC t_R (G 0-100% CH_3CN/H_2O in 8min): 4.1min; UPLC t_R (G 0-100% CH_3CN/H_2O in 2min): 1.3 min; UPLC-MS t_R (G 0-100% CH_3CN/H_2O in 2min): 1.3 min, $[M+H^+]_{expected}$= 666.39, $[M+H^+]_{found}$= 666.29, HRMS (ESI): calcd. for $C_{35}H_{52}N_7O_6$ 666.3974; $[M+H^+]_{found}$= 666.3970; yield (synthesis+purification): 44%

H-Arg-Phe-Arg-Phe-D-Pro-OH

This peptide was prepared from DPro-CTC (1 equiv.=mmol). Fmoc-Phe-OH and Fmoc-Arg(Pbf)-OH residues (3 equiv.) were attached using DIPCDI (3 equiv.) and HOAt (3 equiv.) as coupling agents. Cleavage of the sequence with 95% TFA/ 5% DCM provided the desired peptide. The mixture was evaporated and the crude product was dissolved in 50% H_2O/ 50% MeCN and lyophilized.

HPLC t_R (G 0-100% CH_3CN/H_2O in 8min): 4.15min; UPLC-MS t_R (G 0-100% CH_3CN/H_2O in 2min): 1.21min, $[M+H^+]_{expected}$= 721.86, $[M+H^+]_{found}$= 721.36, HRMS (ESI): 721.40238 calcd. for $C_{35}H_{51}N_{11}O_6$; $[M+H^+]_{found}$= 721.40385; yield (synthesis+purification): 40%

H-Ser-Phe-Ser-Phe-D-Pro-OH

This peptide was prepared from DPro-CTC (1 equiv.=mmol). Fmoc-Phe-OH and Fmoc-Ser(Bzl)-OH residues (3 equiv.) were attached using DIPCDI (3 equiv.) and HOAt (3 equiv.) as coupling agents. Cleavage of the sequence with 95% TFA/ 5% DCM provided the desired peptide. The mixture was evaporated and the crude product was dissolved in 50% H_2O/ 50% MeCN and lyophilized.

HPLC t_R (G 0-100% CH_3CN/H_2O in 8min): 4.64min; UPLC-MS t_R (G 0-100% CH_3CN/H_2O in 2min): 1.39min, $[M+H^+]_{expected}$= 585.64, $[M+H^+]_{found}$= 584.24, HRMS (ESI): 584.27149 calcd. for $C_{29}H_{38}N_5O_8$; $[M+H^+]_{found}$= 584.27122 ; yield (synthesis+purification): 30%

cyclo(Lys-Phe-Lys-Phe-D-Pro)

This peptide was prepared by cyclization of previously synthesized linear peptide following the general cyclization method. Cleavage conditions in this synthesis involved 2% TFA/ 98% DCM to maintain Boc protecting groups in lysine side-chains. Boc removal was achieved by adding a 75% TFA/ 25% DCM solution to the peptide. The mixture was stirred at room temperature for 4 h. The reaction was monitored by TLC (50% AcOEt/ 50% DCM) using the ninhydrin staining solution. The solvent was evaporated and the crude product was dissolved in 50% H_2O/ 50% MeCN and lyophilized.

HPLC t_R (G 0-100% CH$_3$CN/H$_2$O in 8min): 6.0 min; UPLC t_R (G 0-100% CH$_3$CN/H$_2$O in 2min): 1.4 min; UPLC-MS t_R (G 0-100% CH$_3$CN/H$_2$O in 2min): 1.4 min, [M+H$^+$]$_{expected}$= 648.38, [M+H$^+$]$_{found}$= 649.23, HRMS (ESI): calcd. for C$_{35}$H$_{50}$N$_7$O$_5$ 648.3868; [M+H$^+$]$_{found}$= 648.3878; yield (synthesis+purification): 15%

cyclo(Arg-Phe-Arg-Phe-D-Pro)

This peptide was prepared by cyclization of previously synthesized linear peptide following the general cyclization method. Cleavage was performed with 95% TFA/ 5% DCM to remove Pbf protecting groups in arginine side-chains. The mixture was evaporated, and the crude product was dissolved in 50% H$_2$O/ 50% MeCN and lyophilized.

HPLC t_R (G 0-100% CH$_3$CN/H$_2$O in 8min): 4.07min; UPLC-MS t_R (G 0-100% CH$_3$CN/H$_2$O in 2min): 1.23min, [M+H$^+$]$_{expected}$= 704.84, [M+H$^+$]$_{found}$= 704.54, HRMS (ESI): 704.39909 calcd. for C$_{35}$H$_{50}$N$_{11}$O$_5$; [M+H$^+$]$_{found}$= 704.39812; yield (synthesis+purification): 29%

cyclo(Ser-Phe-Ser-Phe-D-Pro)

This peptide was prepared by cyclization of previously synthesized linear peptide following the general cyclization method. Cleavage was performed with 95% TFA/ 5% DCM to remove Bzl protecting groups in serine side-chains. The mixture was evaporated, and the crude product was dissolved in 50% H$_2$O/ 50% MeCN and lyophilized.

HPLC t_R (G 0-100% CH$_3$CN/H$_2$O in 8min): 5.18min; UPLC-MS t_R (G 0-100% CH$_3$CN/H$_2$O in 2min): 1.49min, [M+H$^+$]$_{expected}$= 566.63, [M+H$^+$]$_{found}$= 566.18, HRMS (ESI): 566.26092 calcd. for C$_{29}$H$_{36}$N$_5$O$_7$; [M+H$^+$]$_{found}$= 566.26057; yield (synthesis+purification): 35%

H-Lys-(4&)Phe-Lys-(4&)Lys-D-Pro-OH

The peptide was synthesized from D-Pro-CTC (1 eq=0.53 mmol). The general procedure was used to prepare this sequence. The Trt-Lys(Fmoc)-OH residue was required as in the bicyclic peptide synthesis. In this particular sequence, Fmoc was exchanged for Boc to facilitate removal of these protecting groups. Cleavage of the sequence provided

the desired unprotected peptide. The mixture was evaporated and the crude product was dissolved in 50% H_2O/ 50% MeCN and lyophilized.

HPLC t_R (G 0-100% CH_3CN/H_2O in 8min): 5.3min; UPLC t_R (G 0-100% CH_3CN/H_2O in 2min): 1.3 min; UPLC-MS t_R (G 0-100% CH_3CN/H_2O in 2 min): 1.3 min, $[M+H^+]_{expected}$= 664.37, $[M+H^+]_{found}$= 664.49, HRMS (ESI): calcd. for $C_{35}H_{50}N_7O_6$ 664.3817; $[M+H^+]_{found}$= 664.3818; yield (synthesis+purification): 3 %

H-Arg-(4&)Phe-Arg-(4&)Phe-DPro-OH

The peptide was synthesized from DPro-CTC (1 eq=mmol). The general procedure was used to prepare this sequence. The Fmoc-Arg(Pbf)-OH residue was required as in the bicyclic peptide synthesis, exchanging Fmoc protecting group for Trt before performing Miyaura borylation and for Boc before carrying out Suzuki cross-coupling. Cleavage of the sequence with 95% TFA/ 5% DCM provided the desired unprotected peptide. The mixture was evaporated and the crude product was dissolved in 50% H_2O/ 50% MeCN and lyophilized.

HPLC t_R (G 0-100% CH_3CN/H_2O in 8min): 4.01min; UPLC-MS t_R (G 0-100% CH_3CN/H_2O in 2min): 1.18min, $[M+H^+]_{expected}$= 720.85, $[M+H^+]_{found}$= 720.36, HRMS (ESI): 719.38673 calcd. for $C_{35}H_{49}N_{11}O_6$; $[M+H^+]_{found}$=719.38097; yield (synthesis+purification): 2.5%

H-Ser-(4&)Phe-Ser-(4&)Phe-D-Pro-OH

The peptide was synthesized from D-Pro-CTC (1 eq=mmol). The general procedure was used to prepare this sequence. The Fmoc-Ser(Bzl)-OH residue was required as in the bicyclic peptide synthesis, exchanging Fmoc protecting group for Trt before performing Miyaura borylation and for Boc before carrying out Suzuki cross-coupling. Cleavage of the sequence with 95% TFA/ 5% DCM provided the desired unprotected peptide. The mixture was evaporated and the crude product was dissolved in 50% H_2O/ 50% MeCN and lyophilized.

HPLC t_R (G 0-100% CH_3CN/H_2O in 8min): 4.43min; UPLC-MS t_R (G 0-100% CH_3CN/H_2O in 2min): 1.37min, $[M+H^+]_{expected}$= 582.63, $[M+H^+]_{found}$=582.21, HRMS (ESI): 582.24857 calcd. for $C_{29}H_{35}N_5O_8$; $[M+H^+]_{found}$=582.24837; yield (synthesis+purification): 20%

cyclo(Lys-(5&)Trp-Lys-(5&)Trp-D-Pro)

The peptide was prepared using the standard methodology for trp-trp stapled peptides.

pNZ-(5Br)Trp-OH and Fmoc-(5Br)Trp-OH were used as the second and fourth amino acids, respectively.

UPLC t_R (G 0-100% CH_3CN/H_2O in 2 min): 1.45min; UPLC-MS t_R (G 0-100% CH_3CN/H_2O in 2min): 1.68min, $[M+H^+]_{expected}$= 710.90, $[M+H^+]_{found}$= 709.30, yield (synthesis+purification): 2%

cyclo(Lys-(6&)Trp-Lys-(6&)Trp-D-Pro)

The peptide was prepared using the standard methodology for trp-trp stapled peptides.

pNZ-(6Br)Trp-OH and Fmoc-(6Br)Trp-OH were used as the second and fourth amino acids, respectively.

UPLC t_R (G 0-100% CH_3CN/H_2O in 2min): 1.44min; UPLC-MS t_R (G 0-100% CH_3CN/H_2O in 2min): 1.69min, $[M+H^+]_{expected}$= 710.90, $[M+H^+]_{found}$= 709.80, (synthesis+purification): 5%

cyclo(Lys-(7&)Trp-Lys-(7&)Trp-D-Pro)

The peptide was prepared using the standard methodology for trp-trp stapled peptides.

pNZ-(7Br)Trp-OH and Fmoc-(7Br)Trp-OH were used as the second and fourth amino acids, respectively.

UPLC t_R (G 0-100% CH₃CN/H₂O in 2min): 1.75min; UPLC-MS t_R (G 0-100% CH₃CN/H₂O in 2min): 1.75min, [M+H⁺]$_{expected}$= 710.90, [M+H⁺]$_{found}$=709.70, yield (synthesis+purification): 3%

cyclo(Lys-(5Br)Trp-Lys-(5Br)Trp-D-Pro)

This peptide was prepared from DPro-CTC (1 equiv.=mmol). Fmoc-(5Br)Trp-OH and Fmoc-Lys(Boc)-OH residues (3 equiv.) were attached using DIPCDI (2 equiv. for Trp and 3 equiv. for Lys) and HOAt (2 equiv. for Trp and 3 equiv. for Lys) as coupling agents. Cleavage of the sequence with 2% TFA/ 98% DCM provided the desired peptide. General cyclization method was used. Boc removal was performed with 50% TFA/ 50% DCM solution. The mixture was stirred at room temperature for 2 h. The reaction was monitored by TLC (50% AcOEt/ 50% DCM) using the ninhydrin staining solution. The solvent was evaporated and the crude product was dissolved in 50% H₂O/ 50% MeCN and lyophilized.

UPLC t_R (G 0-100% CH₃CN/H₂O in 2min): 1.35min; UPLC-MS t_R (G 0-100% CH₃CN/H₂O in 2min): 1.42min, [M+H⁺]$_{expected}$= 884.69, [M+H⁺]$_{found}$= 883.93, HRMS (ESI): 882.22962 calcd. for $C_{39}H_{50}N_9O_5Br_2$; [M+H⁺]$_{found}$= 882.22829; yield (synthesis+purification): 15%

cyclo(Lys-(6Br)Trp-Lys-(6Br)Trp-D-Pro)

This peptide was prepared from DPro-CTC (1 equiv.=mmol). Fmoc-(6Br)Trp-OH and Fmoc-Lys(Boc)-OH residues (3 equiv.) were attached using DIPCDI (2 equiv. for Trp and 3 equiv. for Lys) and HOAt (2 equiv. for Trp and 3 equiv. for Lys) as coupling agents. Cleavage of the sequence with 2% TFA/ 98% DCM provided the desired peptide. General cyclization method was used. Boc removal was performed with 50% TFA/ 50% DCM solution. The mixture was stirred at room temperature for 2 h. The reaction was monitored by TLC (50% AcOEt/ 50% DCM) using the ninhydrin staining solution. The solvent was evaporated and the crude product was dissolved in 50% H₂O/ 50% MeCN and lyophilized.

UPLC t_R (G 0-100% CH$_3$CN/H$_2$O in 2min): 1.35min; UPLC-MS t_R (G 0-100% CH$_3$CN/H$_2$O in 2min): 1.42min, [M+H$^+$]$_{expected}$= 884.69, [M+H$^+$]$_{found}$= 883.99, HRMS (ESI): 882.22962 calcd. for C$_{39}$H$_{50}$N$_9$O$_5$Br$_2$; [M+H$^+$]$_{found}$= 882.22969; yield (synthesis+purification): 15%

cyclo(Lys-(7Br)Trp-Lys-(7Br)Trp-D-Pro)

This peptide was prepared from DPro-CTC (1 equiv.=mmol). Fmoc-(7Br)Trp-OH and Fmoc-Lys(Boc)-OH residues (3 equiv.) were attached using DIPCDI (2 equiv. for Trp and 3 equiv. for Lys) and HOAt (2 equiv. for Trp and 3 equiv. for Lys) as coupling agents. Cleavage of the sequence with 2% TFA/ 98% DCM provided the desired peptide. General cyclization method was used. Boc removal was performed with 50% TFA/ 50% DCM solution. The mixture was stirred at room temperature for 2 h. The reaction was monitored by TLC (50% AcOEt/ 50% DCM) using the ninhydrin staining solution. The solvent was evaporated and the crude product was dissolved in 50% H$_2$O/ 50% MeCN and lyophilized.

UPLC t_R (G 0-100% CH$_3$CN/H$_2$O in 2min): 1.35min; UPLC-MS t_R (G 0-100% CH$_3$CN/H$_2$O in 2min): 1.42min, [M+H$^+$]$_{expected}$= 884.69, [M+H$^+$]$_{found}$= 883.99 , HRMS (ESI): 882.22962 calcd. for C$_{39}$H$_{50}$N$_9$O$_5$Br$_2$; [M+H$^+$]$_{found}$= 882.22973; yield (synthesis+purification): 10%

H-Lys-Trp-Lys-Trp-D-Pro-OH

This peptide was prepared from DPro-CTC (1 equiv.=mmol). Fmoc-Trp(Boc)-OH and Fmoc-Lys(Boc)-OH residues (3 equiv.) were attached using DIPCDI (3 equiv.) and HOAt (3 equiv.) as coupling agents. Cleavage of the sequence with 95% TFA/ 5% DCM provided the desired peptide. The mixture was evaporated and the crude product was dissolved in 50% H$_2$O/ 50% MeCN and lyophilized.

UPLC t_R (G 0-100% CH$_3$CN/H$_2$O in 2min): 1.26min; UPLC-MS t_R (G 0-100% CH$_3$CN/H$_2$O in 2min): 1.18min, [M+H$^+$]$_{expected}$= 744.90, [M+H$^+$]$_{found}$=744.10, HRMS (ESI): 744.41916 calcd. for C$_{39}$H$_{54}$N$_9$O$_6$; [M+H$^+$]$_{found}$=744.41898; yield (synthesis+purification): 60%

cyclo(-Lys-Trp-Lys-Trp-D-Pro)

This peptide was prepared from DPro-CTC (1 equiv.=mmol). Fmoc-Trp(Boc)-OH and Fmoc-Lys(Boc)-OH residues (3 equiv.) were attached using DIPCDI (3 equiv.) and HOAt (3 equiv.) as coupling agents. Cleavage of the sequence with 2% TFA/ 98% DCM provided the desired peptide. Cyclization was performed with the general method followed by Boc removal with 50% TFA/ 50% DCM solution. The mixture was stirred at room temperature for 2 h. The reaction was monitored by TLC (50% AcOEt/ 50% DCM) using the ninhydrin staining solution. The solvent was evaporated and the crude product was dissolved in 50% H_2O/ 50% MeCN and lyophilized.

UPLC t_R (G 0-100% CH_3CN/H_2O in 2min): 1.40min; UPLC-MS t_R (G 0-100% CH_3CN/H_2O in 2min): 1.25min, $[M+H^+]_{expected}$= 726.90, $[M+H^+]_{found}$=726.70, HRMS (ESI): 726.40859 calcd. for $C_{39}H_{52}N_9O_5$; $[M+H^+]_{found}$=726.40721; yield (synthesis+purification): 50%

MOLECULAR BIOLOGY: PROTEIN EXPRESSION AND PURIFICATION

Protein expression

The clone for the recombinant production of the wild-type tetramerization domain of p53 (residued 311-367 inserted into the expression vector pET23b+) was a kind gift from Dr. M.G.Mateu.

The plasmid of the mutant R337H was obtained by Dr. S. Gordo using Site-Directed Mutagenesis.

- **General procedure for large scale protein expression**

1ng of plasmid was transformed into 100μL of competent cells BL21(DE3), plated in LB-agar with antibiotics and incubated O/N at 37°C. A single colony was inoculated into 50mL of sterile LB medium, containing the antibiotics and the culture was growth O/N at 37°C with vigorous shaking. The large scale culture was set up by inoculating the O/N growth culture (1/1000 dilution) in 3L-flask (1L), previously centrifuged and redissolved with the sterile M9 minimal medium with antibiotics, and it was then incubated with vigorous shaking at 37°C until OD_{600} reached ~ 0.9[a]. Then, protein expression was induced by addition of solid IPTG to 500μM and the cultures were further incubated at 25°C shaking O/N. Cells were harvested by centrifugation in 1L-hermetic bottles at 3,500xg for 15min at 4°C and the cell pellets were resuspended with 40mM MES pH6 with protease inhibitors, 40-50mL buffer per litre of culture. The mixtures were flash-frozen in liquid nitrogen and stored at -80°C.

- **Media composition and stock solutions**

M9 minimal medium

For 1L culture: 6.8 g Na_2HPO_4, 3g KH_2PO_4, 0.5g NaCl, 780mL miliQ H_2O heat-sterilized. Then, 2mL $MgSO_4$ 1M, 2mL solution Q, 10mL vitamins mix*, 20mL D-glucose 0.2g/mL*, 5mL $^{15}NH_4Cl$ 0.2g/mL*

[a]OD_{600}: optical density at 600nm (determined by UV)

- Sterilized by filtering through a 0.2μm membrane

Vitamins mix
For 100ml:
50mg thiamine hydrochloride
10mg D-biotin
sterilized through filtration at 0.2μm and stored at -20°C.

LB-agar plates
1L LB medium
15g agar
heat-sterilized
Antibiotics were added when the solution was not hot. 20mL were plated per dish and stored at 4°C.

Antibiotics

p53TD and R337H plasmids had resistance to ampicillin antibiotic. Nonetheless, instead of ampicillin, carbenicillin was recommended due to its less sensitivity to the drop in pH of the groth medium that is common in bacterial growth.

Sodim carbenicillin was sterilized by filtration through 0.2μm membrane and stocked at a concentration 100mg/mL in water at -20°C. An aliquot was used containing 100μg/mL.

Protein purification

The purification procedure was described by Mateu et al(ref1 susana). Some appropriate modifications were carried out.

Cells were defrozen and lysed by tip-sonication (0.7 power) in an ice-bath (10 cycles of 10s-sonication with 10s-pause). Cell debris were pelleted by centrifugation at 35,000xg for 40min at 4ªC and the clarified supernatant was immediately filtered through a 0.2μm membrane. The metholodogy proposed to flash-frozen in liquid nitrogen and store at -20ªC. However, in all the cases proteins were immediately purified without further

Cation exchange purification by FPLC

50-75ml of cell extracts were loaded into a 5mL HiTrap SP-Sepharose at 2ml/min and extensively washed with 40mM MES ph 6 until A_{280} <0.1AU. Proteins were eluted with 0-0.7M NaCl gradient (0-70% of 40mM MES pH 6, 1M NaCl) in 20cv at 2ml/min, collecting 3mL fractions. Proteins eluted at ~200mM NaCl.

Size exclusion by FPLC

Fractions of 3-5mL were injected into a Superdex 75 preparative grade 16x60 column at 1ml/min 40mM MES pH 6, 200mM NaCl, collecting 3mL fractions. Proteins eluted at ~100mL.

Exchanging the buffer

3.5kDa cut-off Amicon centricons were used to ultracentrifugated the proteins fractions (previously the membrane was rinsed to remove the glycerol).
Several dilutions were done with the buffer of interest to ensure complete remove of purification buffer.

Protein fraction were unified and lyophilized.

Monomeric protein concentration was determined by UV spectrometry in water (ε_{280nm}= 1280$M^{-1}cm^{-1}$). Molecular weight was determined by MALDI-MS using freshly prepared ACH matrix (10mg/mL, H_2O:MeCN, 1:1, 1%TFA).
Sample was stored after lyophilisation at -20°C.

General protocols for molecular biology

Plasmid transformation into competent cells

Competent cells BL21(DE3), frozen at -80°C, were thawed on ice and gently mixed by finger-flicking. 10μL of cells were transferred into a pre-chilled sterile 1.5mL tube and ~1ng of plasmid was added and mixed gently by finger-flicking. Mixture was incubated on ice for 30min, pulse heated for 30-45s in a 42°C water bath (without shaking) and cooled on ice for 2min. 500μL of fresh LB medium (better pre-heated at 37°C) were added and cells were incubated at 37°C for approximately 1h shaking vigorously. The

sample was plated into LB-agar plates (pre-heated at 37ºC) containing cabenicillin antibiotic and evenly spread with a sterile spreader until complete absorption.

Plates were incubated upside-down at 37ºC O/N. Plates with grown colonies were sealed with parafilm and stored upside-down at 4ºC being used in less than one month of storage to avoid possible contamination.

SDS-PAGE (Sodium dodecyl sulfate-PolyAcrylamide Gel Electrophoresis)

For analysing p53TD and mutant R337H by SDS-PAGE, 15% poly-acrylamide gels with 10% glycerol were used, since this type of gel allow better detection and resolution of low molecular weight species. The results were compared with standar 15% poly-acrylamide gels without observing significant difference. Actual improvement was detected when gels were run 2/3 of the total length, facilitating detection of the lower bands of both samples and the marker.

Gel composition (for 4 gels of 0.75mm thickness):

Glicerol containing gels

	resolving	stacker
Acryl:bisacrylamide (37:5:1)	8mL	2mL
Tris-HCl 3M pH 8.5	6.7mL	2.1mL
miliQ water	2.6mL	4mL
SDS 20%	100µL	32µL
Glycerol 87%	2.4mL	-
APS 15% (w/v)	200µL	80µL
TEMED	8µL	8µL

Standard 15% PA gels

	resolving	stacker
Acryl:bisacrylamide (37:5:1)	8mL	2mL
Tris-HCl 3M pH 8.5	6.7mL	2.1mL
miliQ water	2.6mL	4mL
SDS 20%	100µL	32µL
Glycerol 87%	2.4mL	-
APS 15% (w/v)	200µL	80µL
TEMED	8µL	8µL

Protein samples were mixed 1:1 with loading buffer 2x and denatured by heating 5min at 95°C. The samples were loaded into the wells together with the marker (nom), used for detection of low molecular weight species. The gel was run at 150V for 1h or until the bands reached 2/3 of the total length.

Coomassie blue stainer was used due to the brightness and clearness of the protein bands. Staining was accelerated by heating in the microwave for 30s. Then, the gel was kept into the hot Coomassie solution for 30min-1h. Distaining was performed with an initial water wash and then for 15-30min in water.

LOADING BUFFER 2X:

250 µL Tris-HCl 0.5M pH 6.8

2mL glycerol 87%

250µL miliQ water

4mL SDS 20%

1mL bromophenol blue 0.4% (w/v)

RUNNING BUFFER:

For 1L (pH 8.3-8.8)

15.14g TRIZMA® base

72.07g glycine

5g SDS

DYING

For 1L

0.25g Coomassie® blue G250

100mL AcOH

MATERIALS AND REAGENTS

CHEMICALS

Salts and reagents (molecular biology grade)	Sigma-Aldrich
Acryl-bisacrylamide (37:5:1)	Amresco
Agar	Conda Laboratories
Antibiotics	Duchefa
APS (electrophoresis grade)	Sigma
Coomassie	BioRad
Glycerol 87%	Merck
Isotope labeled reagents	Cambridge Isotope Laboratories
LB	Conda Laboratories
Protease inhibitors cocktail (without EDTA)	Roche
SDS-PAGE molecular weight ladders	BioRad
TEMED (electrophoresis grade)	Sigma

SOLVENTS

AcOH	SDS
EtOH	Panreac
HCl	Scharlau
milliQ water (resistivity >18M$\Omega \cdot$cm^{-1}	MilliQ Plus filtration system (Millipore)

MATERIALS

Amicon centricones 3.5kDa	Millipore
Centrifuge polypropylene hermetic tubes	Beckman Coulter

HiTrap SP-Sepharose column	GE Healthcare
Quartz cells	Hellman
Superdex 75 preparative grade	GE Healthcare

INSTRUMENTATION

Electrophoresis cells	Mini-protean® BioRad (SDS-PAGE)
Centrifuges	Beckman Coulter, rotor (J25-50)
	Eppendorf 5415R, benchtop centrifuge
Sonicator	IKASONIC U200-S, IKA Labortechnik
FPLC	ÄKTA Explorer, Amersham Bioscience ®
pH meter	Crison GLP21
UV-Vis spectrometer	Eppendorf UV Biophotometer

PROTEIN CHEMICAL SYNTHESIS

Solid Phase Peptide Synthesis of the proteins

The synthesis of the p53 tetramerization domain (residues 320-356) and the mutant R337H were carried out automatically under the following conditions.

1st protocol

Sequence p53TD	Ac-KKPLDGEYFTLQIRGRERFEMFRELNEALELKDAQAG-NH$_2$
Chemistry	Fmoc/tBu
Polymeric support	Rinkamide Chem Matrix ®
Functionalization	0.49mmol/g
Scale	0.1mmol
Solvent	DMF
Amino acid excess	0.2M
Coupling reagents	HBTU/DIEA in DMF
Coupling time	120s
Deprotection	Piperidine,DIEA in DMF
Double coupling	2K, 11L, 12Q, 13I, 14R, 16Q, 17E, 18R, 22F, 23R, 28A, 30E, 35Q

Sequence R337H	Ac-KKPLDGEYFTLQIRGREHFEMFRELNEALELKDAQAG-NH$_2$
Chemistry	Fmoc/tBu
Polymeric support	Rinkamide Chem Matrix ®
Functionalization	0.49mmol/g
Scale	0.1mmol
Solvent	DMF
Amino acid excess	0.2M
Coupling reagents	HBTU/DIEA in DMF
Coupling time	120s
Deprotection	Piperidine,DIEA in DMF
Double coupling	2K, 11L, 12Q, 13I, 14R, 16Q, 17E, 18H, 22F, 23R, 28A, 30E, 35Q

2nd protocol

Sequence p53TD	Ac-KKPLDGEYFTLQIRGRERFEMFRELNEALELKDAQAG-NH$_2$
Chemistry	Fmoc/tBu
Polymeric support	Rinkamide-ChemMatrix®
Functionalization	0.47mmol/g
Scale	0.1mmol
Solvent	DMF
Amino acid excess	0.2M
Coupling reagents	DIC/oxyma in DMF
Coupling time	120s
Deprotection	Piperazine,NMP, EtOH, oxyma in DMF
Double coupling	2K,3P,4L,7E,8Y,9F,10T,11L,12Q,13I,14R,16R,18R,19F,22F,23R,24E,25L,28A,29L,30E,31L

Sequence R337H	Ac-KKPLDGEYFTLQIRGREHFEMFRELNEALELKDAQAG-NH$_2$
Chemistry	Fmoc/tBu
Polymeric support	Rinkamide-ChemMatrix®
Functionalization	0.47mmol/g
Scale	0.1mmol
Solvent	DMF
Amino acid excess	0.2M
Coupling reagents	DIC/oxyma in DMF
Coupling time	120s
Deprotection	Piperazine,NMP, EtOH, oxyma in DMF
Double coupling	2K,3P,4L,7E,8Y,9F,10T,11L,12Q,13I,14R,16R,18H(50°C),19F,22F,23R,24E,25L,28A,29L,30E,31L

Synthetic considerations

- ChemMatrix® resin initial conditioning:

  For a proper performance of the resin, it was washed following this procedure:

1.	MeOH	5 x 1min
2.	DMF	5 x 1min
3.	DCM	5 x 1min
4.	DCM + 5% TFA	5 x 1min
5.	DCM + 5% DIEA	5 x 1min
6.	DCM	5 x 1min
7.	DMF	5 x 1min

  Rink-amide linker was present in the commercially available resin.

- Incoporation of the first amino acid onto the resin was performed manually, Fmoc-Gly-OH (3 equiv.), DIPCDI (3 equiv.) and HOAt (3 equiv.) Ninhydrine test was perfomed.

- Synthesizer stock solutions:

  Activators: (1st protocol) HBTU/ DIEA in DMF, (2nd protocol) 0.5M DIC in DMF, 1.0M oxyma in DMF.

  Deprotection: (1st protocol) 20% piperidina, 0.1M HOBt in DMF (2nd protocol) 10% (w/v) piperazine, 90% (v/v) NMP, 10% (v/v) EtOH, 0.1M oxyma in DMF.

- Final Fmoc-deprotection of the peptidyl-resin was performed by hand and the free N-termini were capped with 50eq Ac_2O and 50eq DIEA for 25min. Ninhydrin test was done.

Peptide cleavage and side-chain deprotection

Large scale cleavage was perfomed with:

1st protocol: 85% TFA, 5% H$_2$O, 5% Anisol, 2.5% EDT 2.5% Thiophenol 2.5h

2nd protocol: 1st step: 82.5% TFA, 5% H$_2$O, 5% TIPS, 5% Phenol, 2.5% EDT 3h; 2nd step: 95% TFA, 2.5% H$_2$O, 2.5% TIPS 1.5h

Filtration of the beads to isolated the cleaved products was performed. The solution was evaporated under nitrogen flow and the remaining products were extracted with chilled ether (30mL x 3) and centrifuged at 4,000xg for 10min at 4°C after each extraction. The final peptide pellet was dried under nitrogen and products were solved in H$_2$O:MeCN 50:50.

The crude was analysed by HPLC and the molecular weight was confirmed by UPLC-MS and MALDI-MS.

Peptide purification

The purification was carried out by semi-preparative HPLC, in a reverse C18 column.

Peptide crude was solved into H$_2$O:MeCN (70:30) the day before purying and sonicated for 3h. Solubilty of these peptides was not very good; therefore, the samples were stored at the 2°C O/N. The following day, solutions were clear edand ready to purify. 2mL of the solution were diluted up 9mL with H$_2$O.

8mL fractions were injected in the column containing approximately 25mg of crude. Working at a flow rate of 10mL/min in a 15-50 in 50min gradient.Protein peak appeared at 20min and fractions were collected manually. No better resolution was obtained after attempting several gradients.

The purity of the final crude was determined by analytical RP-HPLC and UPLC-MS, being >98%.

Once lyophilized the peptide was quantified by UV (ε_{280nm}=1280M$^{-1}\Omega^{-1}$ in water). The total yield of the synthesis could not be calculated because not all the crude was purified. Approximately, from Xmg of raw wet crude, 3mg of pure p53TD and 6mg of R337H were obtained.

MATERIALS AND REAGENTS

PEPTIDE SYNTHESIS

Rink-amide ChemMatrix® resin	Matrix Innovation Inc.
Fmoc-amino acids	IRIS Biotech
DIPCDI	Sigma-Aldrich
HOAt	IRIS Biotech
HBTU	IRIS Biotech
Oxyma	IRIS Biotech
Piperazine	Sigma-Aldrich

SOLVENTS AND GENERAL REAGENTS

Ac_2O	Aldrich
ACH	Fluka
MeCN	SDS
AcOH	SDS
DCM	SDS
DIEA	Merk
Et_2O	SDS
DMF	Panreac
EDT	Fluka
HCl	Scharlau
MeOH	SDS
milliQ water ($>18M\Omega \cdot cm^{-1}$)	MilliQ Plus Filtration (MilliPore)
Phenol	Fluka
Piperidine	SDS
TFA (HPLC grade)	Fluorochem
TIS	Fluka

others	Merk, Sigma or Fluka

INSTRUMENTATION

Automatic peptide synthesizer	CEM Liberty Blue microwave assisted automatic peptide synthesizer
Analytic HPLC-PDA	WATERS Alliance 2695
	Photodiode array 2998 UV/Vis detector
	Automatic sampler
	Solvents: H_2O 0.045%, TFA
	MeCN 0.036% TFA
Analytic UPLC-PDA	Waters Acquity
	Photodiode array UV/Vis detector
	Automatic sampler FNT
	Solvents: H_2O 0.045%, TFA
	MeCN (UPLC grade) 0.036% TFA
Analytic UPLC-MS	Waters Acquity
	Photodiode array UV/Vis detector
	Electrospray ion source ESI-MS Micromass ZQ
	Automatic sampler FNT
	Solvents: H_2O 0.1%, FA
	MeCN (UPLC grade) 0.07% FA
Semipreparative HPLC	WATERS Alliance
	Dual 2489 UV/Vis detector
	Automatic sampler 2707
	Quaternary Gradient Module 2545
	Fraction Collector III
	Solvents: H_2O 0.1%, TFA

	MeCN 0.05% TFA
MALDI-TOF	Applied Biosystems 4700, proteomics analyzer
Centrifuges	Beckman Coulter Allegra 21R
	Eppendorf 5415R benchtop centrifuge
Spectrometer	Eppendorf UV Biophotometer

BIOPHYSICS

Parallel artificial membrane permeability assay (PAMPA)

The PAMPA was used to measure the capacity of the peptides to cross the BBB by passive diffusion. The effective permeability (P_e) of the compounds was determined at an initial concentration of 200 μM. The buffer solution was prepared from a commercially concentrated one, supplied by pION. Following the manufacturer's instructions, system solution was adjusted to pH 7.4 using a 0.5 M NaOH solution. The peptides were dissolved in a mixture of buffer solution with 20% of 1-propanol used as cosolvent. The PAMPA sandwich was separated, and the donor well was filled with 195 μL of the compound solution of interest. A magnetic stirrer was placed in each well. The acceptor plate was put into the donor plate, ensuring that the underside of the membrane was in contact with the buffer. Then, 4 μL of a mixture of phospholipids from a porcine polar brain extract (20 mg/mL) in dodecane (composition: 12.6% phosphatidylcholine (PC), 33.1% phosphatidylethanolamine (PE), 18.5% phosphatidylserine (PS), 4.1% phosphatidylinositol (PI), 0.8% phosphatidic acid and 30.9% of other compounds) was added to the filter of each well, followed by 200 μL of buffer solution. The plate was then covered and incubated at room temperature in a saturated humidity atmosphere for 4 h under orbital agitation at 25 μm of unstirred water layer (UWL). After this period, 165 μL/well of the solution from the donor and acceptor plates was transferred to the HPLC vials, except for the bicyclic compound, for which all the fractions were pooled. 100 μL of each linear, stapled and cyclic acceptor samples and 80 μL of the bicyclic acceptor were injected into the HPLC apparatus. Transport was also confirmed by HPLC-MS, which indicated that the integrity of the peptides was preserved. Regarding the donor and initial time samples, the linear compound was injected at 1 μL, the linear stapled peptide at 20 μL, the head-to-tail cyclic peptide at 10 μL, and the bicyclic peptide at 5 μL. The bicyclic acceptor was injected again at 1 and 5 μL owing to the initial large absorbance obtained.

The effective permeability after 4 h was calculated using *equation 1* and the percentage of transport using *equation 2.*

$$T(\%) = \frac{C_A(t)}{C_D(t_0)} \cdot 100 \qquad \textbf{[Equation 1]}$$

$$P_e = \frac{-218.3}{t} \cdot \log\left[1 - \frac{2 \cdot C_A(t)}{C_D(t_0)}\right] \cdot 10^{-6}\, cm/s \qquad \textbf{[Equation 2]}$$

where t is time (h), $C_A(t)$ is the peptide concentration in the acceptor well at time t, and $C_D(t_0)$ is the peptide concentration in the donor well at 0 h. Membrane retention (%R) was calculated from the difference between the total starting amount of peptide and the amount of peptide in the donor and acceptor wells at the end of the assay after 4 h.

Stability in human serum

Peptides at a final concentration of 3 mM were dissolved in HBSS and incubated at 37°C in the presence of 90% human serum for 24 h. At different incubation times (30 min, 1 h, 3 h, 6 h, 10 h, 12 h and 24 h), 50 μL aliquots were treated with 200 μL of methanol to precipitate serum proteins. After 30 min of centrifugation at 4°C, the supernatant was filtered and then analyzed by RP-HPLC to calculate the percentage of intact peptide in the sample.

Cytotoxicity, MTT assay

3500 HeLa cells were seeded in 96-well plates 24 h before starting the assay. After this period, cells with peptides at 200 μM and 500 μM in DMEM (1 mg/mL glucose) supplemented with 10% serum were incubated for 24 h. After 22 h, MTT reagent was added to a final concentration of 0.5 mg/mL. After a 4 h incubation, the medium was discarded and the purple crystals of formazan were dissolved in 200 μL of DMSO. The plate was shaken for 30 min and absorbance was measured at 570 nm. Cell viability was calculated by dividing the absorbance of wells treated with a given peptide by the absorbance of the untreated wells. Measurements were performed in triplicate. As a positive control, cells were incubated with 1% SDS.

Cytotoxicity, XTT assay

5000 HeLa cells were seeded in 96-well plates 24 h before starting the assay. After this period, cells with peptides at 200 µM and 500 µM in DMEM (1 mg/mL glucose) supplemented with 10% serum were incubated for 24 h. Then, medium with peptides was removed and the XTT reagent was added to a final concentration of 0.5 mg/mL. After a 3h incubation, absorbance was measured at 475 nm. The same measure was perfomed after 6h incubation. Cell viability was calculated by dividing the absorbance of wells treated with a given peptide by the absorbance of the untreated wells. 6h incubation values were used for the calculations, since an absorbance higher than 2 is required to ensure achievement of the plateau zone of the fluorescen. Measurements were performed in triplicate. As a negative control, cells were incubated with medium and as positive control 1% of DMSO was introduced.

Nuclear magnetic resonance

NMR experiments were carried out on a Bruker Avance III 600 MHz spectrometer equipped with a TCI cryoprobe. Samples of the cyclodimers were prepared by dissolving the peptides in DMSO. Proteins p53TD wild-type and R337H mutant were dissolved in 25mM NaPi, pH 7 with 10% D_2O at 100µM. Chemical shifts were referenced to internal sodium-3-(trimethylsilyl)propanesulfonate (DSS). Supression of the water signal was achieved by excitation sculpting (368b). Full characterization of the cyclodimers was achieved by doing several experiments not included in the thesis. All experiments for the proteins were perfomed at 298K. Up-field spectra were studied in detail for the proteins as well as the comparison of the ^{1}H-^{15}N-HSQC of the ^{15}N-R337H with the reported.

Circular Dichroism

All circular dichroism experiments were recorded in a Jasco J-810 spectropolarimeter, equipped with a Jasco-CDF-426S Peltier thermostatted cell holder and a Julabo external bath.

CD spectra

Far UV-CD spectra were the average of 3 scans recorded at a scanning rate of 10nm·min^{-1}, with 4s response time, 1nm bandwith and 0.1nm data pitch. Square quartz cells of 1mm (~300µL) path length were used, keeping the HT voltage below 500mV. Blank spectra were also recorded with the phosphate buffer.

The spectra were processed with the software provided by the manufacturer, Spectra Manager. The smoothed blank (with Savitsly-Golay and mean algorithm) was properly substracted to the raw spectrum and CD ellipticity was normalized to the mean residue concentration (formula), θ_{MR}. Spectra were then smoothed using two different algorithms, Savitsly-Golay and mean algorithm both with 25 point window, carefully checking the goodness by comparison with the raw data after each smoothing cycle.

CD unfolding curves

CD unfolding curves were recorded measuring CD ellipticity at 220nm while heating from 15°C to 95°C at 1.5°C min^{-1} with 4s response time, 1nm bandwith and 0.1°C data pitch. Square quartz cells 1mm (~300µL) path length were used, completely filled with the sample.

CD spectra of the initial temperature were also recorded after having performed the full experiment.

Recorded data were processed in Spectra Manager software, normalizing concentration and smoothing by the binomial factor. The initial and final baseline slopes were also corrected by subtraction of a slope straight line. Data were exported to Origin 8.0 software and transformed into the normalized unfolded fraction curve considering a two-state unfolding model.

Comparison of the CD spectra before and after running the unfolding experiment was done in Spectra Manager software.

Samples were recovered after the experiments and stored again at -20°C.

INSTRUMENTATION

NMR

Bruker Avance III 600 MHz

Circular dichroism

Unitat d'Espectroscopia Molecular, Serveis Cientificotècnics de la Universitat de Barcelona

Jasco J-810 spectropolarimeter

Jasco-CDF-426S Peltier thermostatted cell holder

Julabo external bath

COMPUTATIONAL STUDIES

Molecular dynamic simulations of the monomeric bicycles

Structures were created using MOE software. Biphenyl parameters were extracted from gaff forcefield (type cd, head sp^2). The topology file was built from the starting conformation using Parm99 as forcefield. 10ns simulation in Implicit Solvent using Born Solvent Model –BSM- in Amber, setting the internal dielectric constant to 2 and the external to 48 or 8 (DMSO and highly hydrophobic environment, respectively). Temperature was 500K to speed up the system in order to explore conformation far from the initial one, timestep 2fs and 4.000 saved frames. Three systems were simulated: *para-para* in DMSO and in highly hydrophobic environment and *meta-meta* in DMSO.

R conformations for each system were extracted from the clustering trajectory.

System set-up and Hamiltonian Replica Exchange (H-REX) simulations for the cyclodimers

The cyclodimers were built with AmberTools14[220]. The dihedral of the biphenyl bridge was parametrized following the QM-fitting procedures[221]. The peptides were modeled with the Amber99SB-ILDN[222] force field and solvated in a cubic box of DMSO[223]. The LINCS[224] algorithm was used to constrain all bonds, and equations of motion were integrated with a time step of 2 fs. For each replica the system temperature was kept at 300 K by the stochastic velocity rescaling thermostat[225]. For all non-bonded interactions the direct space cutoff was set to 1.0 nm, and the electrostatic long-range interactions were treated using the default particle-mesh Ewald[226] settings. All the simulations were run using GROMACS 4.6.7[227] patched with PLUMED 2.1.3[228] and the H-REX implementation[229].

The H-REX simulations were performed with 16 replicas and with the scaling factor (λ) ranging from 1 to 0.17 following a geometric distribution. Within this framework the acceptance rate was 40-60%. Each peptide was simulated for a cumulative time of 1.92μs. Trajectories were visualized and analyzed with VMD[230].

Docking p53TD with arginine ligands

Protein-ligand docking study was carried out for the whole peptide library using docking module implemented in MOE 2015 (Molecular Operating Environment)[231] The p53 protein conformation was retrieved from Protein Data Bank (PDB id: 1OLG). The preparatory docking steps of the p53TD included addition of missing atoms, removal of duplicated atoms (such in the case of double occupancies), and assignment of the most adequate protonation state of histidine residues at physiological pH (7.4). Crystallographic water molecules closer than 3.5 Å from any protein atom were retained. The p53TD binding site was assigned with SiteFinder module implemented in MOE. In this particular case, the binding site amino acids were identified if their coordinates were at less than 3.5 Amstrongs of p53TD receptor atom. In total, a docking binding site surface larger than 1500 $Å^2$ was generated.

To determine the binding mode of each peptide structure, a docking multilevel strategy, was carried out. Formerly, peptide structures were subjected to conformational analysis using Conformational Search module (MMFF94x force field) in MOE in an energy window of 15 kcal/mol, rendering a total of 1000 conformers. The lowest 100 conformations were placed at any region of the binding site using the Triangle Matcher and scored by London dG methods respectively. The best 15 poses of each compound were further refined using GBVI/WSA dG method consisting in 500 minimization steps to identify potential induced fit effects promoted by the ligand when   bound.   mol.

Molecular dynamics

The simulation began with the complex structure formed by the p53 tetramer structure with the cyclic structure of the peptide built with XLEaP program from the AMBER14 molecular mechanics package. The geometry of the ligand was taken from the first docking predicted binding mode. The Amber ff99SB forcefield was used, together with the reoptimized omega-bond angle parameters[232]. The initial complex structure was first subjected to minimization protocol consisting of

1000 steps of steep decent method followed by 500 steps of conjugate gradient method. The optimized structure was gradually heated to 300 K in 200 ps. Production simulation part was conducted over 50 nanoseconds, using implicit solvent conditions through Generalized Born model formalism[233] with an effective salt concentration of 0.2 M was deployed to mimic the solvation effect. Nonpolar solvation term was approximately represented by surface area term[234]. Integral time step was set to 1 fs. Temperature was regulated using Berendsen thermostat[235] with a coupling time constant of 1 ps. SHAKE algorithm[236] was used to constrain all the covalent bonds involving hydrogen atoms. Snapshots were saved every 2ps. To MD simulation post-analysis included RMSD stability (for both protein and cyclic ligand) and energy interaction profile between the complex through MM/PBSA[237]. This approach estimates the free energy of a system as the sum of molecular mechanics terms as described by the force-field, the solvation free energy using a continuum model and the solute entropy, which can be estimated by quasi harmonic analysis or other means. A total of 500 snapshots equally spaced along the converged part of each simulation were taken for the binding of energy.

Bibliography

[218] A. Madder, N. Farcy, N.G.C. Hoster, H. De Muynck, P. De Clercq, J. Barry, A.P. Davis, A novel sensitive colorimetric assay for visual detection of solid-phase bound amines, *Eur. J.Org. Chem.* **1999**, *11*, 2787-2791.

[219] A. T. Christensen, *Acta. Chem. Scand. Series B.* **1979**, B33, 763.

[220] J. Wang, W. Wang, P. A. Kollman, D. A. Case, Automatic atom type and bond typer perception in molecular mechanical calculations, *J. Molec.Graph. and Modell.* **2006**, *25*, 247260.

[221] I. Ivani, P. D. Dans, A. Noy, A. Pérez, I. Faustino, A. Hospital, J. Walther, P. Andrio, R. Goñi, A. Balaceanu, G. Portella, F. Battistini, J. L. Gelpí, C. González, M. Vendruscolo, C. A. Laughton, S. A. Harris, D. A. Case, M. Orozco, Parmbscl: a refined force field for DNA simulations, *Nat. Methods* **2016**, *13*, 55-8.

[222] V. Hornak, R. Abel, A. Okur, B. Strockbine, A. Roitberg, C. Simmerling, Comparison of multiple Amber force fields and development of improved protein backbone parameters, *Proteins: Struct., Funct, Bionf.* **2006**, *65*, 712-725.

[223] J. Wang, R. M. Wolf, J. W. Caldwell, P. A. Kollman, D. A. Case, Development and testing of a general AMBER force field, *J. Comp. Chem.* **2004**, *25*, 1157-1174.

[224] B. Hess, H. Bekker, H. J. C. Berendsen, J. G. E. M. Fraaije, LINCS: A Linear Constraint Solver for molecular simulations, *J. Comp. Chem.* **1997**, *18*, 1463-1472.

[225] G. Bussi, D. Donadio, M. Parrinello, Canonical sampling through velocity rescaling, *J. Chem. Phys.* **2007**, *126*, 014101.

[226] T. Darden, D. York, L. Pedersen, *J. Chem. Phys.* **1993**, *98*, 10089-10092.

[227] B. Hess, C. Kutzner, D. van der Spoel, E. Lindahl, GROMACS 4: Algorithms for highly efficient, load-balanced, and scalable molecular simulation, *J. Chem. Theory Comput.* **2008**, *4*, 435-447.

[228] G. A. Tribello, M. Bonomi, D. Branduardi, C. Camilloni, G. Bussi, PLUMED 2: new feathers for an old bird, *Comput. Phys. Commun.* **2014**, *185*, 604-613.

[229] G. Bussi, Hamiltonian replica exchange in GROMACS: a flexible implementation, *Mol. Phys.* **2014**, *112*, 379-384.

[230] W. Humphrey, A. Dalke, K. Schulten, VMD- visual molecular dynamics, *J. Molec. Graphics* **1996**, *14*, 33-38.

[231] *Molecular Operating Environment (MOE)*, 2013.08; Chemical Computing Group Inc., 1010 Sherbooke St. West, Suite #910, Montreal, QC, Canada, H3A 2R7, **2016**.

[232] U. Doshi, D. Hamelberg, Reoptimization of the AMBER force field parameters for peptide bond (omega) torsions using accelerated molecular dynamics **2009**, *113*, 16590-16595.

[233] J. Mongan, C. Simmerling, J. A. McCammon, D. A. Case, A. Onufriev, Generalized born model with a simple, robust molecular volume correction, *J. Chem. Theory Comput.* **2006**, *3*, 156-159.

[234] J. Weiser, P. S. Shenkin, W. C. Still, Approximate atomic surfaces from linear combinations of pairwise overlaps (LCPO), *J. Comput. Chem.* **1999**, *20*, 217-230.

[235] H. J. C. Berendsen, J. P. M. Postma, W. F. Gunsteren, A. DiNola, J. R. Haak, Molecular dynamics with coupling to an external bath, *J. Chem. Phys* **1984**, *81*, 3684-3690.

[236] J. P. Ryckaert, G. Ciccotti, H. J. C. Berendsen, Numerical integration of the Cartesian equations of motion of a system with constraints: molecular dynamics of n-alkanes, *J. CompuPhys* **1977**, *23*, 327-341.

[237] P. A. Kollman, I. Massova, C. Reyes, B. Kuhn, S. Huo, L. Chong, M. Lee, T. Lee, Y. Duan, W. Wang, O. Donini, P. Cieplak, J. Srinivasan, D. A. Case, T. E. Cheatham 3rd, Calculating structures and free energies of complex molecules: combining molecular mechanics and continuum models, *Acc. Chem. Res.* **2000**, *33*, 889-897.

RESUMEN EN ESPAÑOL

INTRODUCCIÓN

Desde la primera síntesis llevada a cabo en fase sólida, el uso de los péptidos ha sufrido un importante incremento a lo largo de los años. En la actualidad, más de 500 péptidos se encuentran como posibles fármacos y 60 ya están en el mercado[8].

A lo largo del siglo XX, el desarrollo de fármacos se centró principalmente en el uso de moléculas pequeñas. A finales de siglo, tuvo lugar la aparición de un nuevo tipo de fármacos denominados "biológicos", los cuales están basados en proteínas o ácidos nucleicos. A pesar de que dichos fármacos no se pueden administrar por vía oral, presentan una elevada especificidad, lo que conlleva una reducción de los efectos adversos atribuídos a los fármacos pequeños.

A medio camino entre ambas estrategias se encuentran los péptidos. Dicho tipo de moléculas pretende aprovechar las ventajas de las anteriores y, al mismo tiempo, evitar sus principales inconvenientes (Figura i).
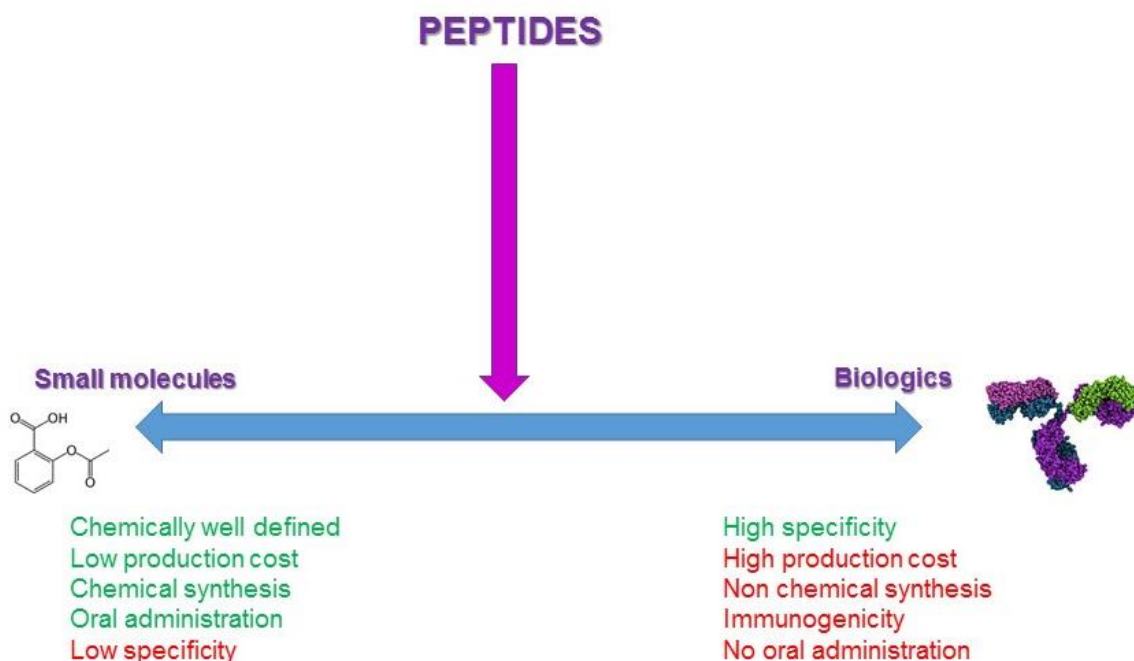

Figura i. Comparación entre moléculas pequeñas, fármacos "biológicos" y péptidos.

Los péptidos son compuestos que suelen presentar una elevada especificidad por su diana terapéutica, dando lugar a una elevada potencia y una reducción de los efectos secundarios. A pesar de ello, es habitual que los fármacos peptídicos muestren baja bioestabilidad, elevada metabolización, carencia de solubilidad y/o permeabilidad a través de membranas biológicas. Todos estos factores dificultan su administración. Actualmente, existen diversas estrategias sintéticas que permiten la adecuada modificación de dichos productos a fin de obtener mejores candidatos a fármacos.

Una de las distintas aplicaciones de los péptidos, ampliamente estudiada en la actualidad, se encuentra en el campo de las interacciones proteína-proteína (IPPs). Las principales ventajas que presentan los péptidos en este campo son las siguientes: i) flexibilidad que permite mejor adaptación a las superficies proteicas, ii) incremento de la selectividad y la potencia mediante su modulación, factor que también comporta una diversidad estructural mayor, iii) tamaño reducido que impide la acumulación de los péptidos en tejidos iv) baja toxicidad en humanos debido a la biocompatibilidad que presentan[18].

Con el objetivo de mejorar las propiedades farmacológicas de los péptidos, tuvo lugar el desarrollo de los peptidomiméticos. Los peptidomiméticos son moléculas que incluyen determinadas modificaciones en los péptidos, preservando su actividad original.

Muchas de las interacciones proteína-proteína son moduladas por péptidos pequeños. Este hecho tiene lugar por la estructura secundaria que los péptidos adoptan. Por ello, existen diversas estrategias que permiten incrementar la tendencia a adquirir dichas conformaciones. Entre ellas, cabe destacar la macrociclación, la *N*-metilación de los aminoácidos incorporados a la secuencia y la introducción de amino ácidos con tendencia a formar giros[19] (Figura ii).

Macrocyclization   *N*-Methylation   Turn inducing amino acids
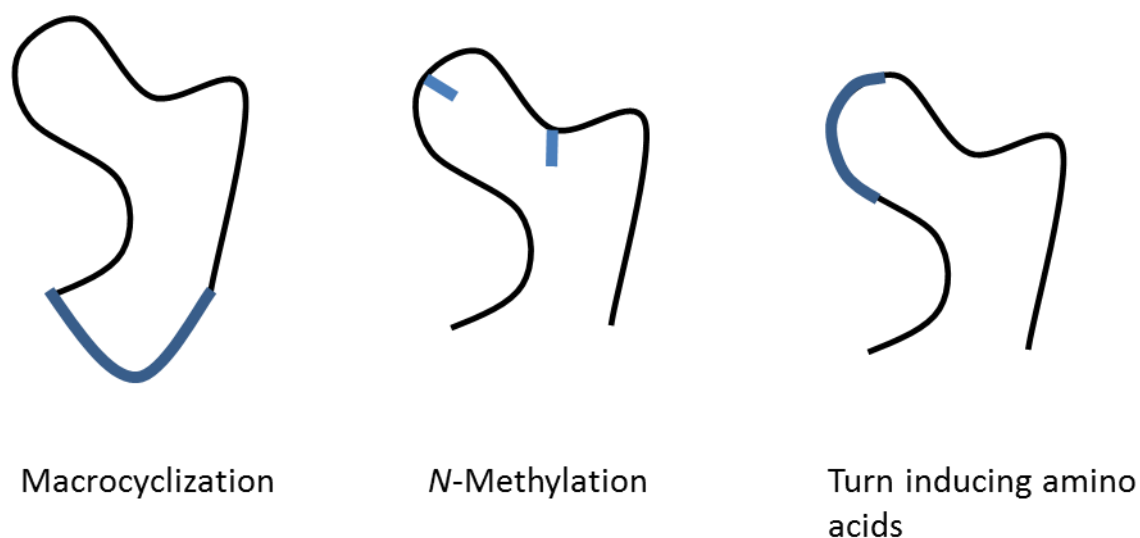
Figura ii. Estrategias generales para favorecer la tendencia de los péptidos a adquirir estructuras secundarias. Adaptado de Pelay *et al.*[19]

De entre las distintas opciones previamente presentadas, las distintas estrategias de macrociclación son de gran importancia[25] (Figura iii).
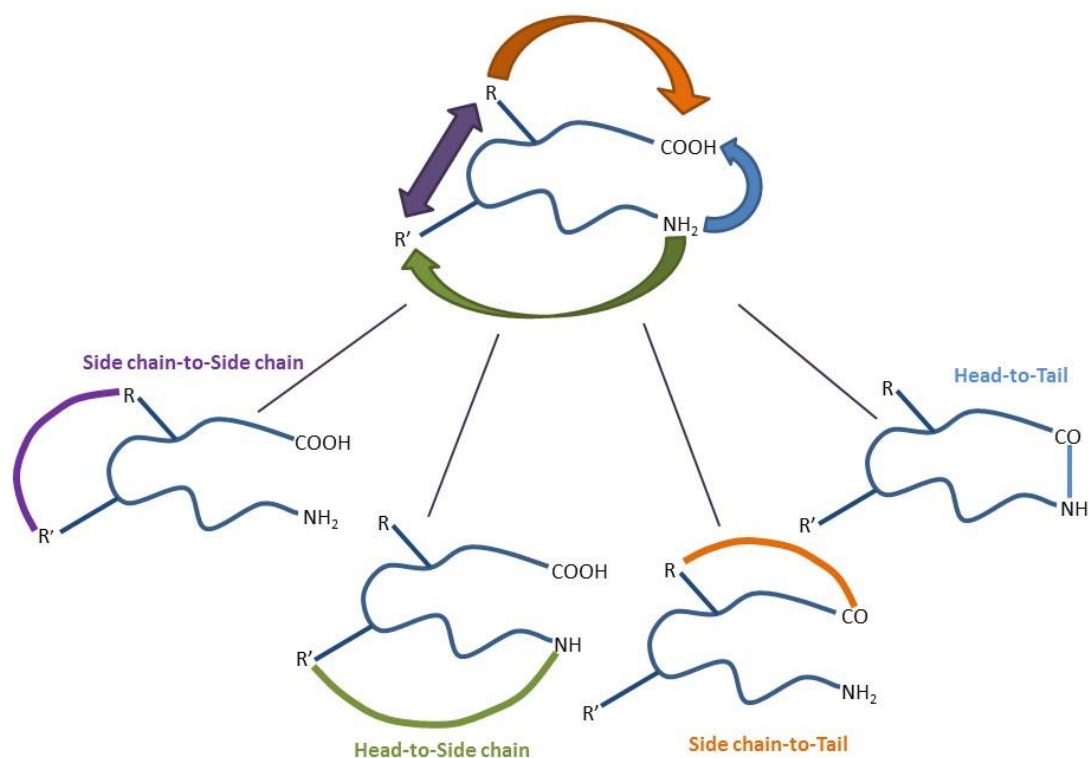

Figura iii. Estrategias de macrociclación. Adaptada de White *et al.*[25]

La ciclación de péptidos tiene lugar entre distintas posiciones de la cadena peptídica. Es posible unir sus extremos, dando lugar a la que se conoce como ciclación cabeza-cola. Por otro lado, se puede unir uno de los extremos con la cadena lateral de algún residuo presente en la secuencia, ciclación cabeza-cadena lateral o cadena lateral-cola. Finalmente, se pueden unir dos cadenas laterales de distintos aminoácidos entre sí, ciclación cadena lateral-cadena lateral.

Además de dichas consideraciones, son también importantes las condiciones en las cuales se realiza la reacción de macrociclación. Se debe tener presente los reactivos así como las condiciones de dilución para evitar la formación de productos secundarios indeseados.

La incorporación de aminácidos que mimeticen determinados giros permite que las macrociclaciones transcurran más fácilmente. Existen distintos tipos de enlaces que se pueden formar en función de los grupos reactivos. Los enlaces pueden ser de tipo amida, lactama, tiol (puente disulfuro) o triazol, entre otros. Las chaperonas o aminoácidos como pseudoprolinas se emplean en síntesis complejas a fin de favorecer la etapa de ciclación.

En este contexto, el uso de péptidos grapa ha sido también ampliamente estudiado. La unión de distintas partes de la secuencia mediante anillos biarilo, azo o C-C ha permitido mejorar las propiedades de los péptidos formados. Además, la incorporación de estos motivos da lugar también a la estabilización de determinadas estructuras, como es el caso de la estructura secundaria de α-hélice[9].

Es importante tener presente que la introducción de determinados motivos da lugar a la rigidificación de su estructura. Estructuras más rígidas se relacionan con un incremento de la especificidad, la afinidad y la estabilidad[34]. No obstante, se debe tener presente que la flexibilidad de las moléculas es importante a fin de permitir la adaptación de los ligandos a sus dianas terapéuticas.

Los anillos biarilo se encuentran presentes en distintas moléculas naturales, como los ejemplos que se muestran a continuación (Figura iv).
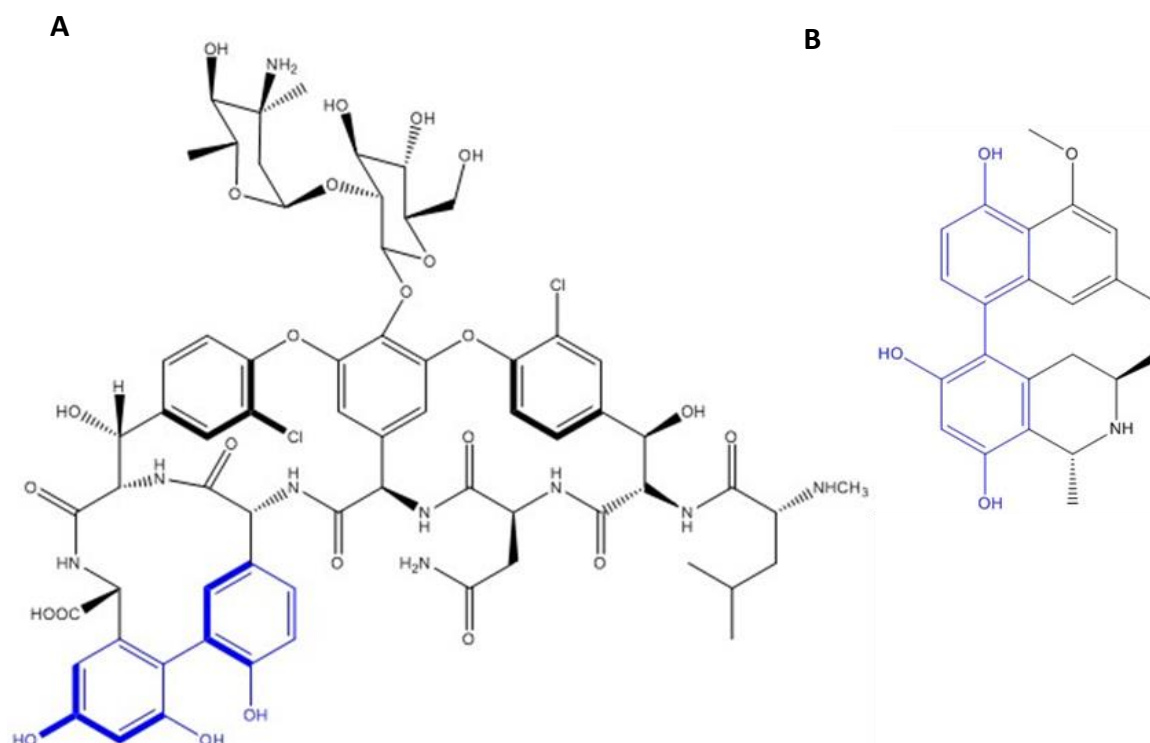
Figura iv. Estructuras de vancomicina (A) y korupensamida A (B).

La formación de este anillo particular puede tener lugar mediante una estrategia de acoplamiento, que permite la formación de un enlace C-C. En este caso, la reacción de Suzuki, compatible con el uso de fase sólida y la presencia de distintos grupos funcionales, es de un gran interés[24,53,58,59,60]. Asimismo, dicha reacción se puede combinar con la reacción de borilación de Miyaura (Figura v).
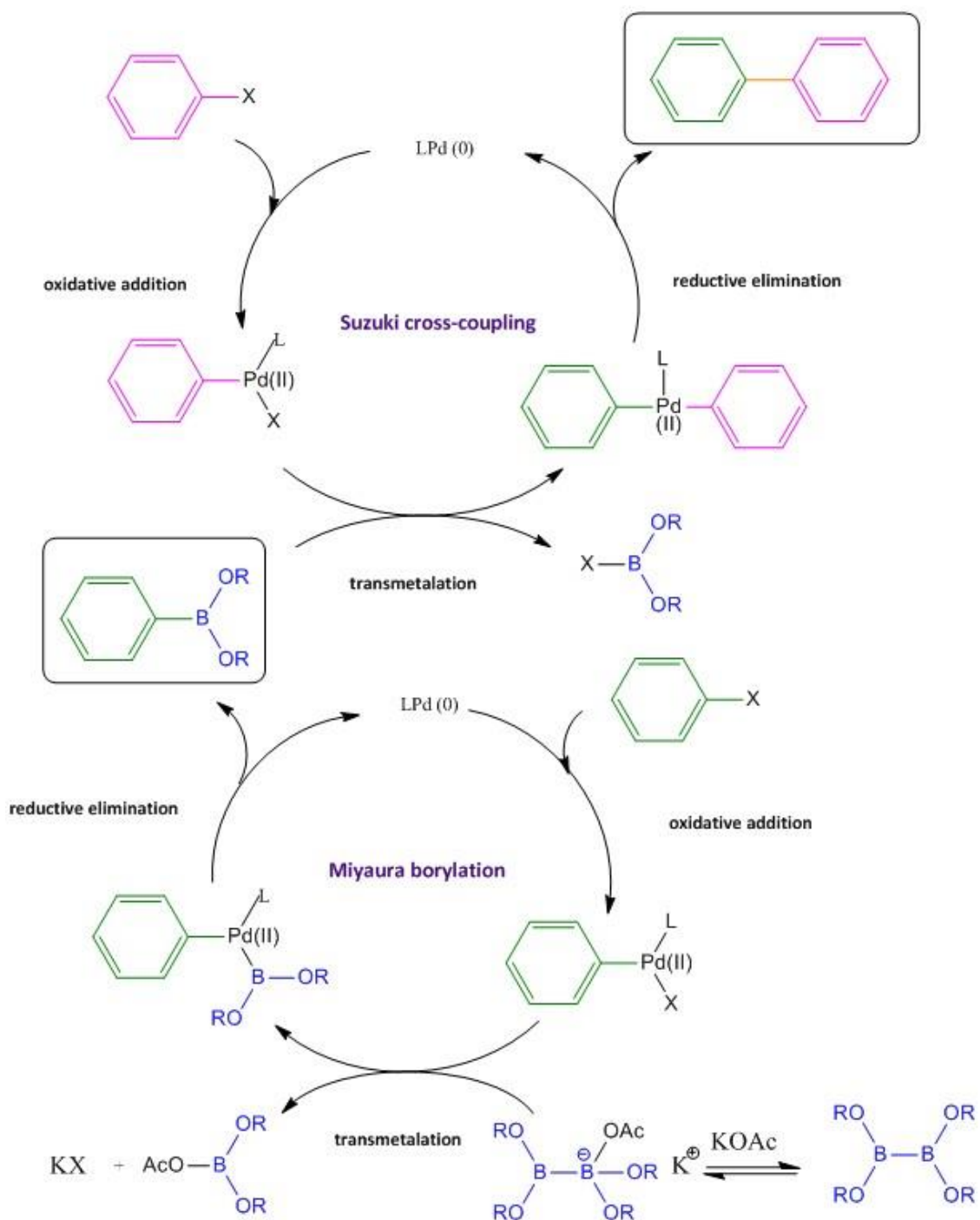
Figura v. Ciclo catalítico de Suzuki-Miyaura. Los productos obtenidos se encuentran en distintos colores, así como el enlace C-C formado (en naranja).

No obstante, cabe destacar que existen otras reacciones catalíticas de formación de enlaces C-C.

La relevancia del aminoácido triptófano es ampliamente conocida en el campo de los productos naturales, siendo éste un importante precursor sintético. Del mismo modo que los anillos biarilo, dicho aminoácido es capaz de participar en interacciones π-catión, las cuales son de elevada importancia en el reconocimiento molecular de superficies proteicas[77].

La proteína p53 es una diana biológica muy importante, debido a su implicación en el control del ciclo celular y la preservación de la integridad genómica en el organismo[123,124]. Principalmente, la proteína p53 se relaciona con el desarrollo de tumores cancerígenos (Figura vi).
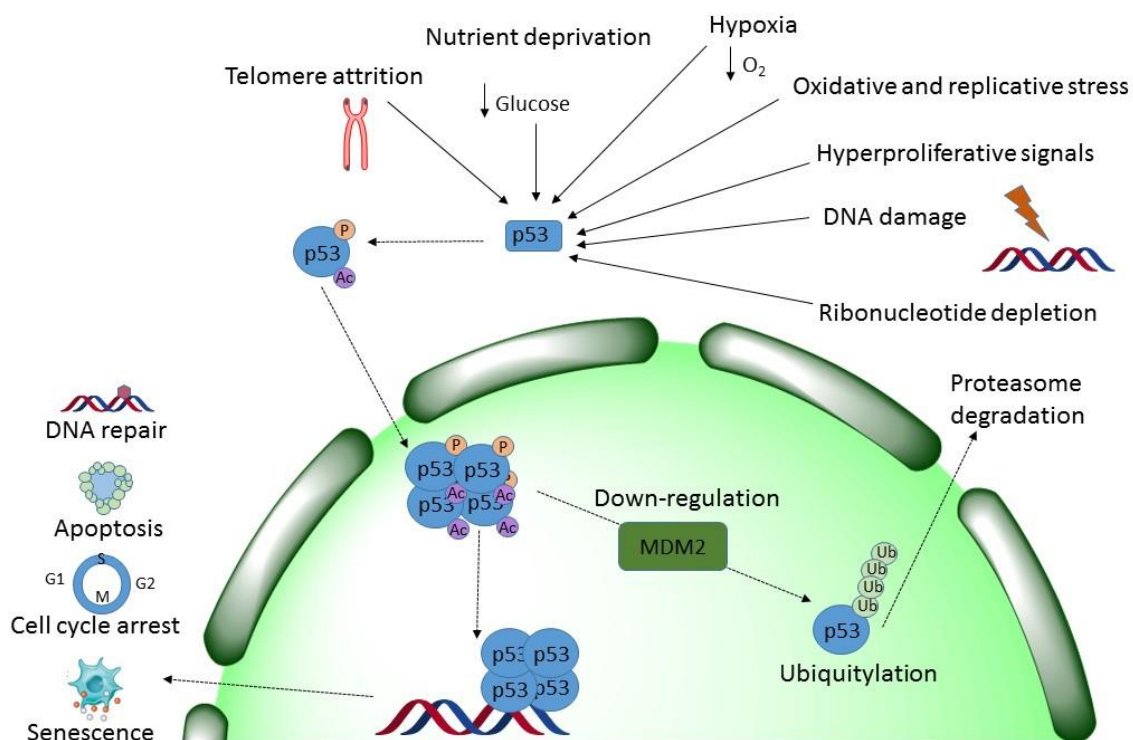
Figura vi. Mecanismos de activación de p53 y sus respuestas celulares.

Desde un punto de vista estructural, la proteína p53 es un dímero de dímeros. La región responsable del plegamiento de la proteína es de un gran interés. Dicha región se conoce como el dominio de tetramerización y está comprendida entre los residuos 326 y 357 de la secuencia peptídica[127].

El mutante R337H de la proteína p53 es el más común asociado al dominio de tetramerización. Dicha mutación está relacionada con el aumento de cáncer en niños (tumor en el córtex adrenal) especialmente en la región sur de Brasil[131]. Asimismo, estudios recientes demuestran una elevada prevalencia de dicha mutación en mujeres con cáncer de mama en la misma región[209].

El mutante R337H es capaz de formar el tetrámero, aunque su estabilidad es baja. Este hecho se ha relacionado principalmente con la participación del residuo R337 en un puente salino con el residuo D352. Esta interacción permite que el tetrámero sea más estable, lo que hace que sea de gran importancia. Por este motivo, el mutante R337H muestra dependencia con el pH. En medios básicos, la cadena lateral del aminoácido mutado histidina no está protonada, lo que da lugar a una desaparición del puente salino.

Basándonos en estudios previos en nuestro grupo (Tesis de Dr. S. Gordo) se empleó la técnica biofísica de dicroísmo circular para estudiar la posible estabilización del tetrámero formado por la proteína R337H en presencia de distintos ligandos.

Debido a la presencia de tumores cerebrales, relacionados con la proteína p53, es muy importante poder acceder al sistema nervioso central (SNC).

La naturaleza altamente protectora de la barrera hematoencefálica (BHE) dificulta en gran medida la penetración de distintas sustancias a través de ella. Esta limitación implica llevar a cabo un estudio exhaustivo de los mecanismos de transporte de sustancias al cerebro. Principalmente, nos dedicamos al estudio del transporte pasivo, que suele tener lugar en moléculas pequeñas. El estudio de la permeabilidad de los distintos péptidos sintetizados a través de la BHE se llevó a cabo mediante el ensayo de "Permeación con Membranas Artificiales en Paralelo", conocido como PAMPA. Para mimetizar la BHE, se empleó una mezcla de un extracto lipídico. Los diferentes productos que se analizaron, se situaron en los compartimentos inferiores del plato de 96 pocillos, mientras que en los superiores se introdujo el disolvente. Después de realizar una incubación de 4h se analizaron ambos compartimentos (Figura vii).
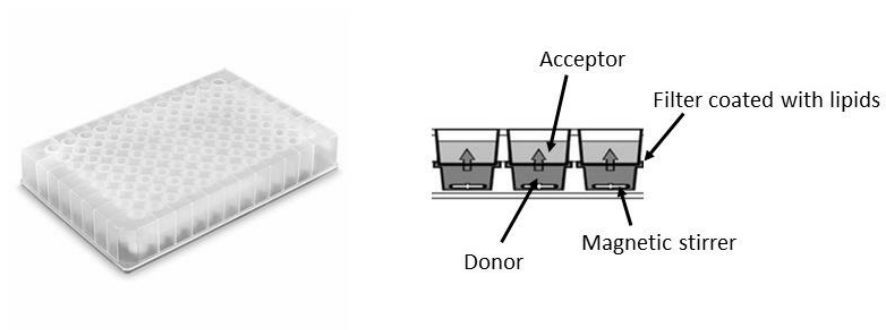
Figura vii. Illustración de la placa usada para el ensayo de PAMPA. Explicacion de los compartimentos que se usaron para realizar el ensayo.

OBJETIVOS

Los objetivos de la presente tesis son los siguientes:

1. Síntesis de péptidos biaril bicíclicos expandiendo la metodología presente en el laboratorio

2. Estudio del efecto de incorporar un anillo biarilo a la estructura de los péptidos, en términos de permeabilidad por transporte pasivo, resistencia a proteasas, viabilidad celular y riesgo de immunogenicidad

3. Preparación de un nuevo tipo de péptidos grapa, Trp-Trp

4. Evaluación de la potencial aplicación de péptidos sintetizados en la tesis para la recuperación del autoensamblaje del mutante R337H del dominio de tetramerización de p53

CAPÍTULO 1. SÍNTESIS DE LOS "PÉPTIDOS BICICLETA"

Los productos naturales son una fuente inexorable de moléculas bioactivas con motivos peculiares presentes en sus estructuras. Entre ellos, existen péptidos macrocíclicos que incluyen motivos biarilo y han demostrado tener actividad biológica relevante[24]. Este tipo de anillos pueden ser sintetizados mediante reacciones de acoplamiento que dan lugar a enlaces C-C, como es el caso de la reacción de Suzuki-Miyaura[55].

De entre las distintas aplicaciones que presentan los péptidos cabe destacar su uso para el reconocimiento molecular de superficies proteicas. Los péptidos lineales son capaces de entrar en determinadas cavidades constituidas en los procesos de interacción entre proteínas. No obstante, dichos compuestos muestran una baja bioestabilidad así como poca permeabilidad a través de membranas celulares. Con el objeto de mejorar dichos inconvenientes, a lo largo de los años, el uso de péptidos modificados ha sufrido un considerable incremento. Los péptidos cíclicos presentan propiedades farmacológicas mejoradas. Dichos péptidos pueden encajarse en la interfase de interacciones proteína-proteína (IPPs) debido a la estructura plana que presentan, permitiendo así la modulación de IPPs. No obstante, existen ciertos casos en los cuales el objetivo es reforzar o estabilizar una interacción proteica en lugar de inhibirla. Se ha descrito que los péptidos de carácter bicíclico, los cuales presentan un volumen tridimensional, son capaces de penetrar en las cavidades constituidas entre proteínas, estabilizando IPPs.

En este primer capítulo, nos centramos en desarrollar una metodología sintética para permitir la obtención de péptidos biaril bicíclicos haciendo uso de fase sólida, reacciones de acoplamiento Suzuki-Miyaura y ciclación cabeza-cola en solución. Este último paso ha sido estudiado en profundidad, dando lugar a la obtención de ciclodímeros. Asimismo, la metodología previamente estudiada en el grupo del Prof. Giralt ha sido expandida a la incorporación de aminoácidos con distintas funcionalizaciones.

El modelo peptídico de los compuestos biaril bicíclicos se basa en una secuencia de cinco aminoácidos; tres de ellos fijos, una D-prolina y dos L-fenilalaninas, mientras que

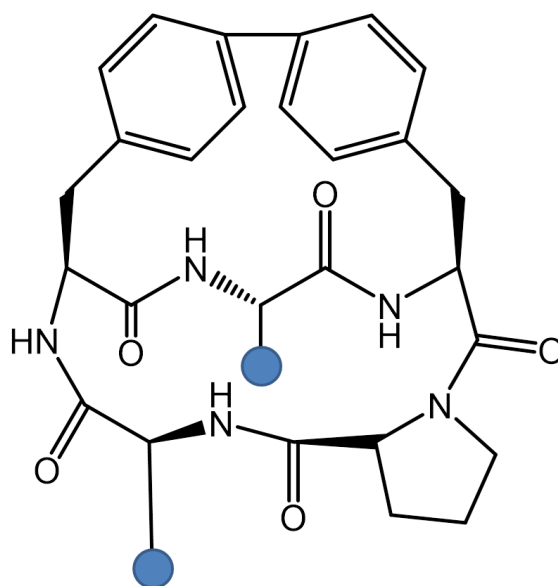los otros dos residuos son variables a fin de introducir cierta versatilidad en la estructura (Figura viii).

Figura viii. Estructura general del péptido modelo.

El tamaño del péptido fue escogido en base a la posibilidad de obtener péptidos cíclicos con rendimientos adecuados y dando lugar a moléculas con una determinada rigidez. El puente C-C permite incrementar la rigidez a la vez que se mejoran las propiedades farmacológicas, por ejemplo, la permeabilidad a través de barreras biológicas[31]. Este mismo motivo da lugar a interacciones π-catión para el reconocimiento molecular de superficies proteicas. Dicho anillo puede constituirse entre las posiciones *meta* o *para* de los anillos aromáticos en las cadenas laterales de fenilalanina.

El aminoácido D-prolina se usa como extremo *C*-terminal en resina, favoreciendo una conformación apta para la ciclación cabeza-cola.

La primera metodología para la obtención de los péptidos modelos se basó en la incorporación de dos alaninas en las posiciones variables. En la Figura ix es posible observar la estrategia sintética usada, en este caso ejemplificada para el péptido con el puente biarilo en las posiciones *para-para.*
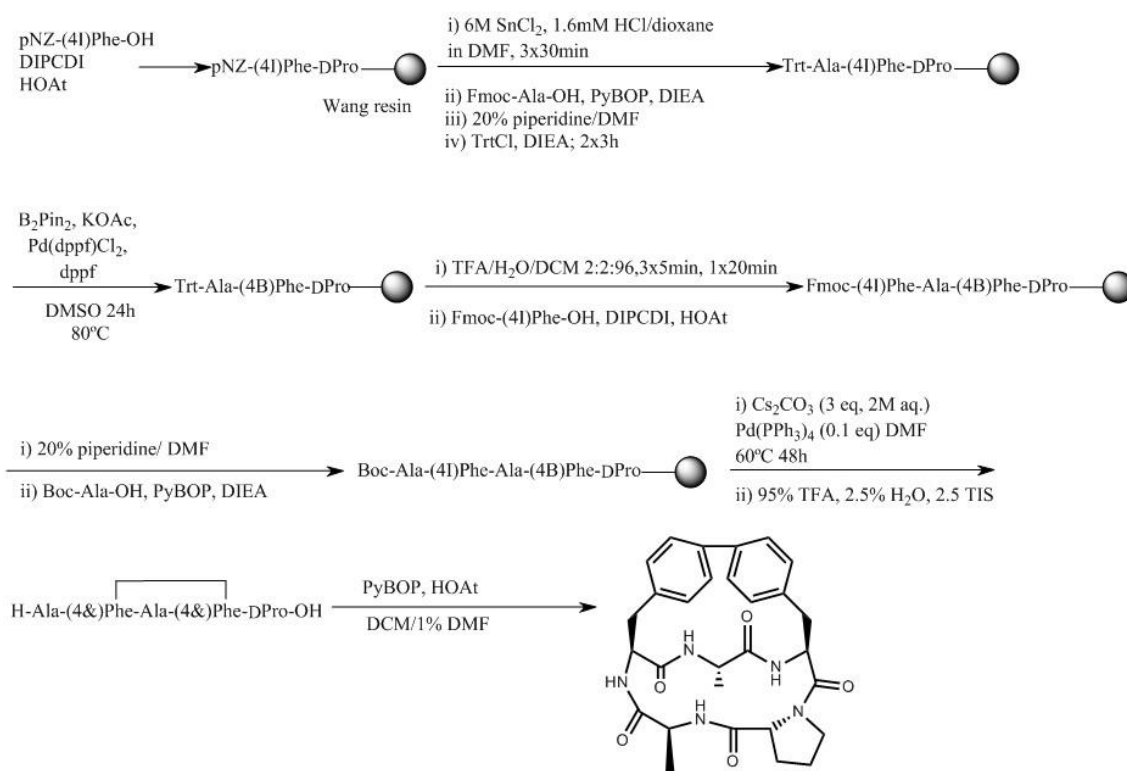
Figura ix. Síntesi en fase sólida de cyloc(Ala-(4&)Phe-Ala(4&)-PheD-Pro) y cyclo(Ala-(3&)Phe-Ala-(3&)Phe-D-Pro).

La metodología se basa en una apropiada modificación de la estrategia Fmoc/*t*Bu. Los grupos protectores fueron cuidadosamente seleccionados a fin de evitar reacciones secundarias indeseadas (*p*NZ en el segundo aminoácido para evitar formación de dicetopiperazinas) o bien debido a su compatibilidad con la borilación de Miyaura o el acoplamiento Suzuki. El biarilo se sintetiza en fase sólida mientras que, posteriormente a la escisión del péptido de la resina, tiene lugar la ciclación cabeza-cola en condiciones de alta dilución. El esquema de grupos protectores se ilustra en la Figura x.
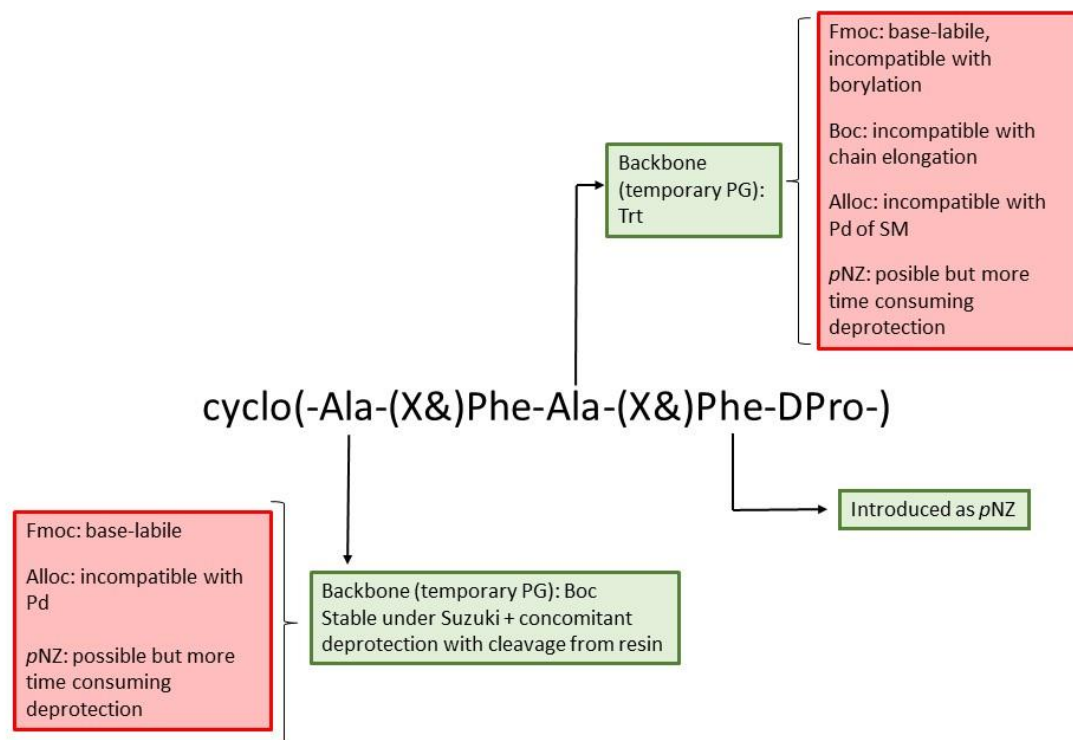
Figura x. Esquema de grupos protectores para el péptido modelo cyclo(-Ala-(X&)Phe-Ala-(X&)Phe-DPro-).

Debido a la complejidad sintética de dichos productos, se llevó a cabo un exhaustivo análisis de los intermedios de reacción. Cabe mencionar que entre los subproductos se encuentran el producto resultante de protodeboronación y el compuesto obtenido tras la incorporación de agua sobre el intermedio sometido a la reacción de Miyaura.

Mediante estudios computacionales fue posible concluir la distinta tensión a la que están sometidas las moléculas según la posición del biarilo. Mientras el biciclo *para-para* mostró una elevada rigidez con una conformación mayoritaria a lo largo de la simulación, el compuesto *meta-meta* presentó una mayor flexibilidad. De modo que, mediante una misma estrategia sintética se obtienen compuestos con distintas conformaciones, lo que en un futuro puede implicar distintos usos.

Durante la preparación de los péptidos modelos se observaron sus correspondientes ciclodímeros (Figura xi). Dichos productos fueron obtenidos durante la última etapa de ciclación cabeza-cola en solución.

La dimerización durante la reacción de Suzuki fue descartada mediante el estudio del producto final de ésta misma.
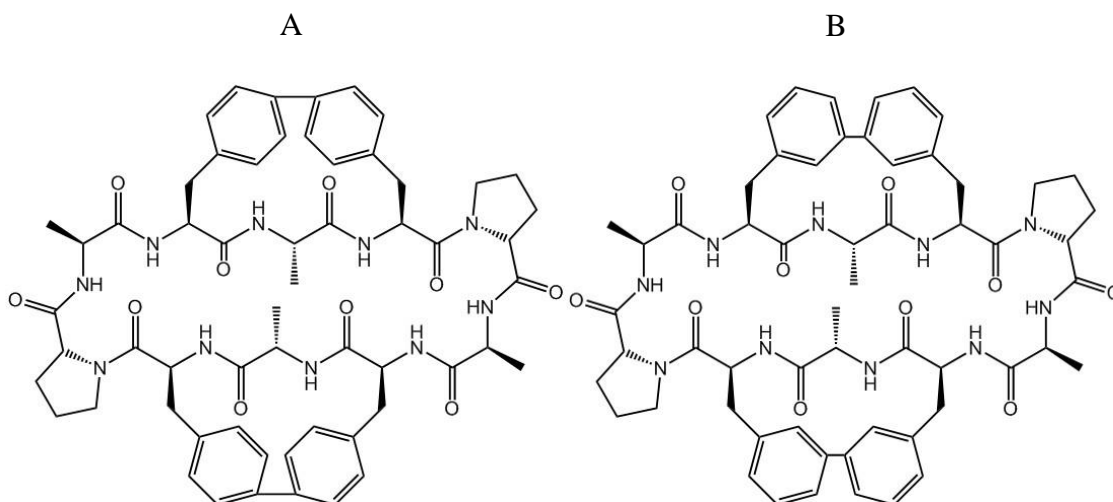
Figura xi. Estructuras correspondientes a los ciclodímeros de los péptidos modelo.

Un extenso estudio sobre las condiciones de ciclación fue llevado a cabo con el objetivo de obtener una metodología que permitiera la obtención de los biciclos monoméricos así como otra para la síntesis de los correspondientes ciclodímeros.

Mediante distintos experimentos fue posible concluir que las condiciones que favorecen la síntesis de los biciclos monoméricos son PyBOP, HOAt, DIEA en DCM/1% DMF. Incluso usando concentraciones más elevadas, los ciclodímeros fueron sólamente hallados en trazas. Sin embargo, el uso de DPPA, NaHCO$_3$ y DMF dan lugar a mezclas de ambos productos. No se obtuvo una metodología exclusiva para la síntesis de los ciclodímeros. Por ello, se intentó llevar a cabo una estrategia de síntesis en fase sólida de dichos productos (Figura xii). No obstante, después de la segunda etapa de borilación no fue posible hallar el producto final ni el material de partida de ésta. Este hecho hizo pensar que existía alguna interferencia con las condiciones de reacción,

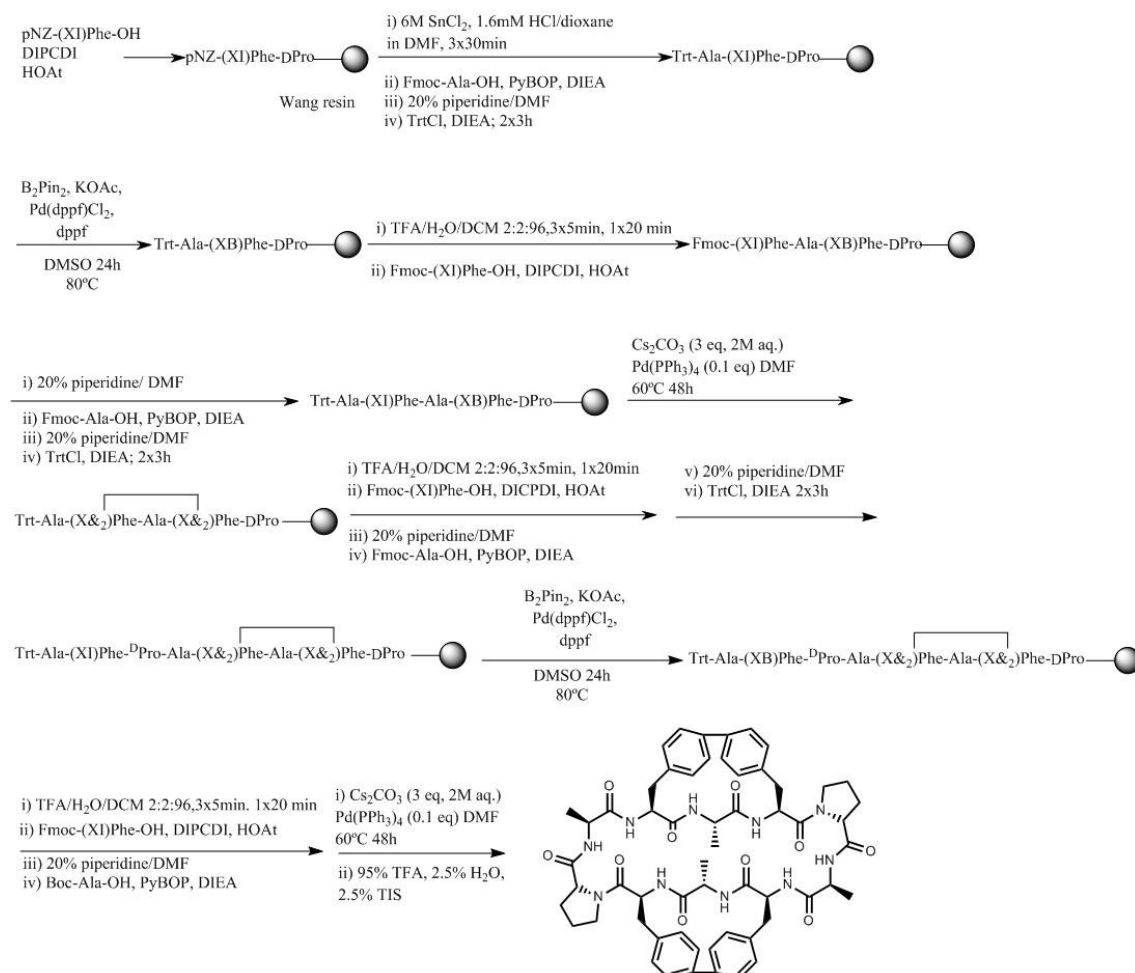como pueda ser la presencia de paladio remanente de las anteriores reacciones de borilación y acoplamiento.

Figura xii. Estrategia de fase sólida propuesta para la obtención de los ciclodímeros.

Los ciclodímeros obtenidos mediante la estrategia original fueron caracterizados por resonancia magnética nuclear (RMN), mostrando conformaciones diferentes según la posición del biarilo. Asimismo, estudios conformacionales *in silico* mostraron diferencias entre dichos compuestos, con una tendencia a plegamiento β.

Con el objeto de confirmar dichos resultados computacionales, se llevó a cabo el estudio por dicroísmo circular. Ambos compuestos mostraron espectros peculiares a la vez que distintos (Figura xiii). Confirmando de este modo las diferentes conformaciones observadas por RMN.
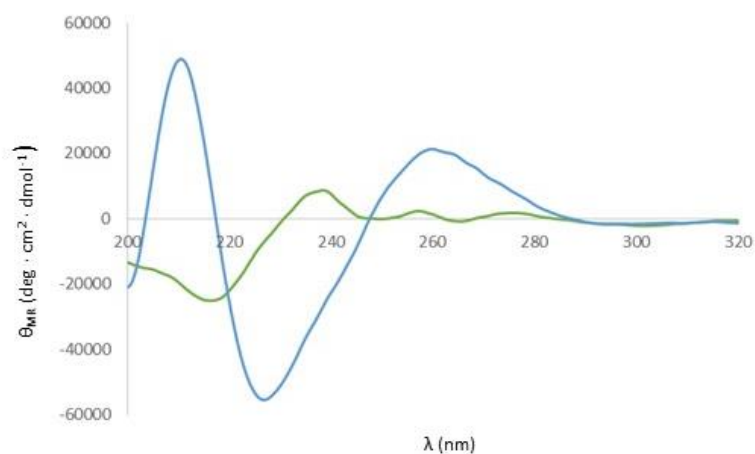
Figura xiii. Espectro de dicroísmo circular de los ciclodímeros *meta-meta* en azul y *para-para* en verde a 25°C en carbonato amónico 10mM pH 10.

La estrategia sintética fue expandida a familias en las que las posiciones variables del pentaciclo fueron modificadas. El enlace *para-para* fue seleccionado, dado la mayor rigidez que presenta. Para ello, la correcta selección de grupos protectores fue un punto clave (Figura xiv).
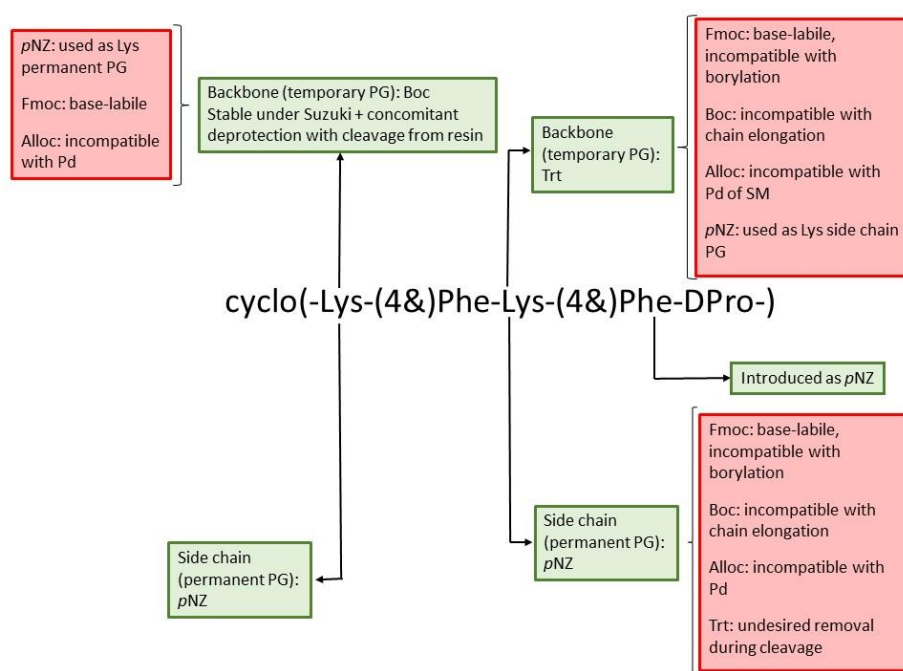

Figura xiv. Esquema de grupos protectores para la síntesi de cyclo(Lys-(4&)Phe-Lys-(4&)Phe-D-Pro).

Esta misma estrategia fue también expandida para la incorporación de arginina o de serina en las posiciones variables del esqueleto peptídico, conteniendo en cada caso en ambas posiciones el mismo aminoácido.

A fin de estudiar el efecto del anillo biarilo en la estructura de los péptidos bicíclicos (capítulo 2), se llevó a cabo la síntesis de familias de compuestos, incluyendo un análogo linear, otro ciclado cabeza-cola y un último linear pero con la introducción del biarilo. En la Figura viii se ejemplifica para la familia de lisina.
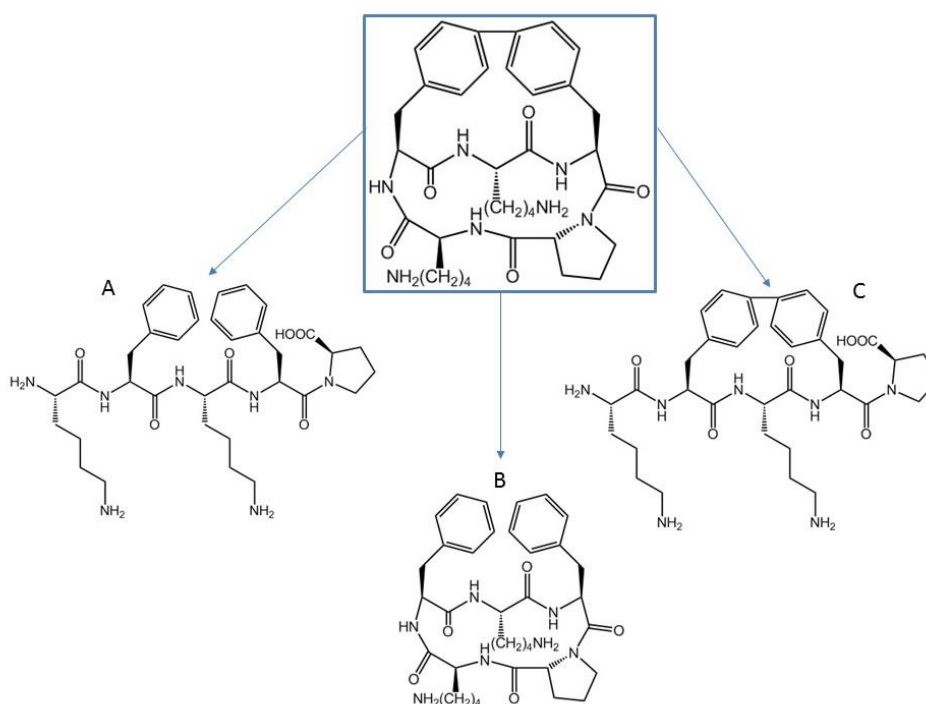
Figura xv. Familia de lisina. Péptido bicíclico destacado en el cuadrado superior. Péptidos control a) lineal H-Lys-Phe-Lys-Phe-D-Pro-OH b) cíclico cabeza-cola cyclo(Lys-Phe-Lys-Phe-D-Pro) y c) lineal grapa/biarilo H-Lys-(4&)Phe-Lys-(4&)Phe-D-Pro-OH.

En cuanto a los ciclodímeros, se realizó la expansión del anillo incorporando dos leucinas entre las fenilalaninas, siendo la secuencia cyclo(Ala-(4&$_1$)Phe-Leu-Leu-(4&$_1$)Phe-D-Pro-Ala-(4&$_2$)Phe-Leu-Leu-(4&$_2$)Phe-D-Pro).

El estudio por dicroísmo circular confirmó la similitud con la versión *para-para* del análogo de alanina. Este hecho refuerza la hipótesis de que la estructura de los péptidos esta mayormente influencia por la tensión infringida por el biarilo.

CAPÍTULO 2: EFFECTO DEL PUENTE BIARILO

Una vez llevada a cabo la síntesis de distintas familias de compuesto biaril bicíclicos, se plantea estudiar la repercusión que tiene la introducción del biarilo. De hecho, en la literatura se describe la mejora de propiedades farmacológicas que presentan los péptidos "grapa"[31]. Por ello, se decidió evaluar la permeabilidad a través de la barrera hematoencefálica, la resistencia a proteasas así como su potencial citotoxicidad.

Para el estudio de permeabilidad a través de la barrera hematoencefálica se usó el ensayo estándar de "Permeación con Membranas Artificiales en Paralelo" (PAMPA)[181]. Se mimetizó la barrera hematoencefálica, testando la potencial permeabilidad por difusión pasiva de las distintas familias de compuestos. Como control positivo, se usó propranolol. En las Figuras xvi-xviii se observa los resultados obtenidos para los distintos compuestos.
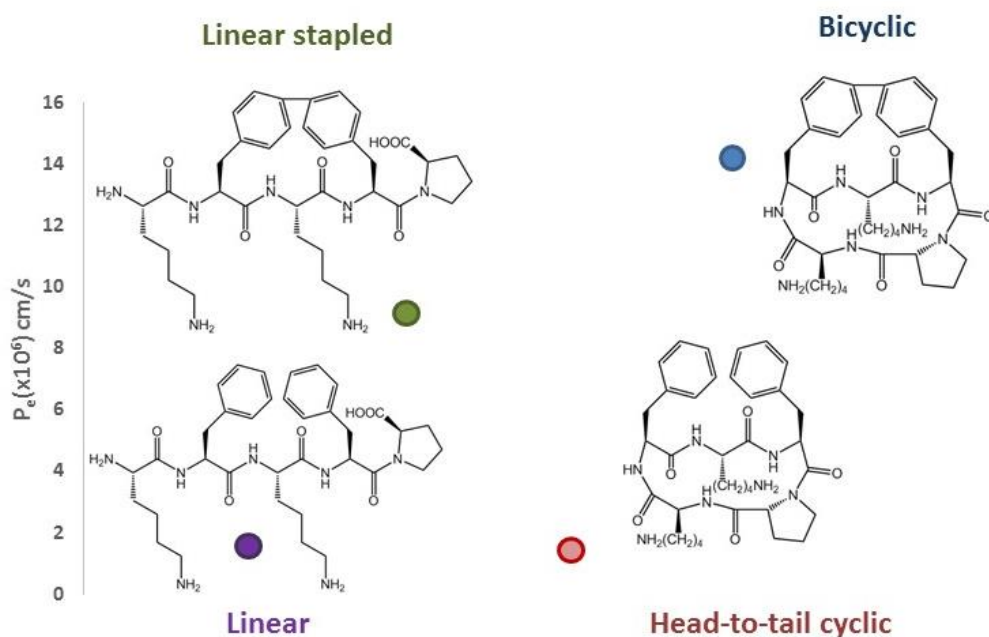

Figura xvi. Permeabilidad efectiva de la familia de lisina en el ensayo PAMPA después de 4h.
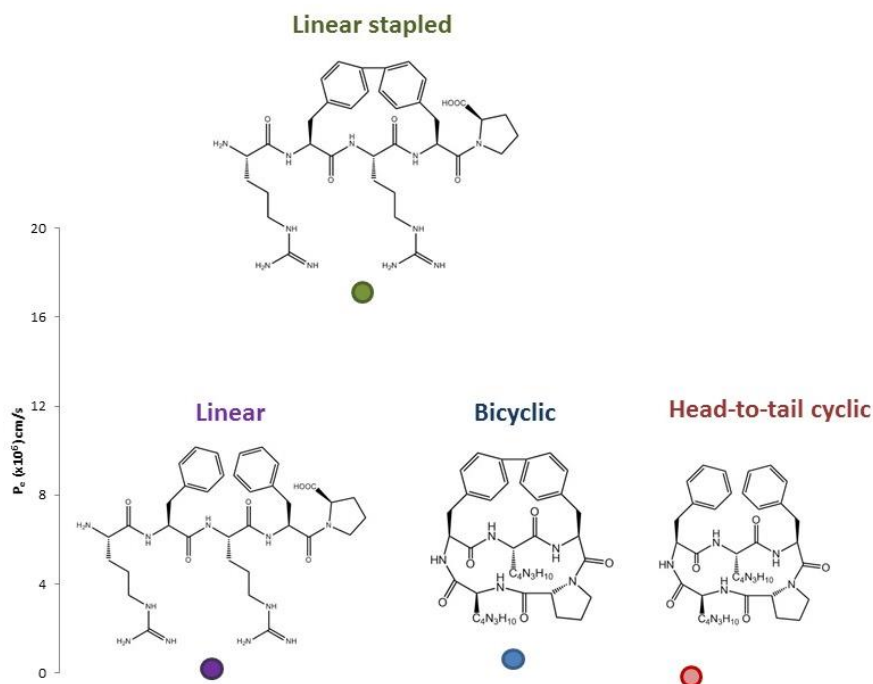
Figura xvi. Permeabilidad efectiva de la familia de arginina en el ensayo PAMPA después de 4h.
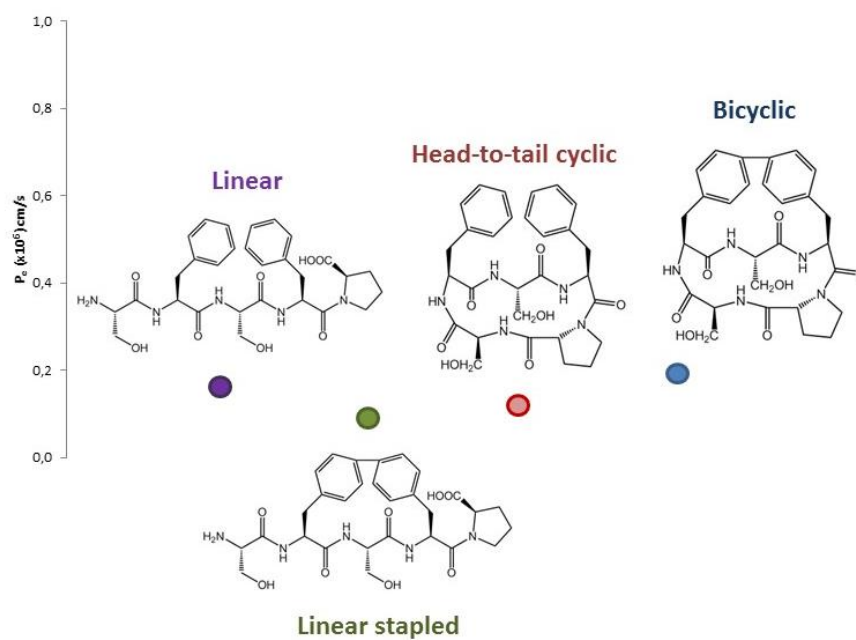

Figura xviii. Permeabilidad efectiva de la familia de serina en el ensayo PAMPA después de 4h.

La familia de lisina mostró una mayor permeabilidad que el resto. Este hecho se atribuye al balance hidrofílico-hidrofóbico que dicho aminoácido incorpora en la secuencia, mejorando de este modo la difusión pasiva y evitando retención en membrana. Significativamente, los dos péptidos que presentan el biarilo fueron los que tuvieron mayor permeabilidad, especialmente el péptido bicíclico. La introducción del biarilo fue también notable en la familia de arginina, aunque cabe mencionar que el péptido bicíclico presentó una elevada retención en membrana que disminuyó su internalización. Finalmente, la presencia de serinas parece disminuir el transporte pasivo, aun así un ligero incremento fue observado en el caso del péptido bicíclico.

En cuanto a la resistencia a proteasas, en este caso los resultados fueron mucho más homogéneos. Los distintos péptidos bicíclicos no mostraron degradación o muy poca (análogo de serina) pasadas 24h. El incremento de estabilidad fue también notable para los compuestos ciclados cabeza-cola así como "grapa". Cabe destacar que el péptido linear biarilo de la familia de arginina mostró una estabilidad similar a la del compuesto bicíclico.

Puesto que los compuestos con futuras aplicaciones médicas deben presentar toxicidades bajas, se decidió llevar a cabo un ensayo de viabilidad celular, MTT en células HeLa, con la familia de lisina. Los resultados mostraron carencia de citotoxicidad para todos los análogos a 200µM. A una concentración superior, 500µM, un ligero incremento de la mortalidad celular fue observado para los compuestos con presencia del biarilo. Este hecho se atribuyó a la mayor estabilidad de estos productos. No obstante, en ningún caso se observaron valores de mortalidad celular a considerar.

Finalmente, el péptido lisina bicíclico fue inyectado en ratones a fin de conocer el potencial riesgo de immunogenicidad. Después de 10 immunizaciones de 50µg cada una, fue posible ver ausencia de respuesta immunogénica. Este hecho concluyó la bondad del diseño, abriendo la puerta a la posibilidad de incorporar estos novedosos compuestos como potenciales ligandos en el reconocimiento de superficies proteicas.

CAPÍTULO 3: PÉPTIDOS TRP-TRP: UNA NUEVA FAMILIA DE PÉPTIDOS BICÍCLICOS

El aminoácido triptófano se encuentra presente en multitud de productos naturales. Uno de los mayores intereses de su incorporación en los péptidos se basa en la propiedad de este aminoácido de participar en interacciones π-catión.

Mediante una colaboración con el Prof. S. Ballet de la Universidad Vrije en Bruselas, se exploraron nuevos péptidos "grapa" a partir de halotriptófanos, desarrollados en dicho grupo.

La obtención de los péptidos bicíclicos fue llevada a cabo mediante la misma estrategia sintética previamente especificada (Figura xix).
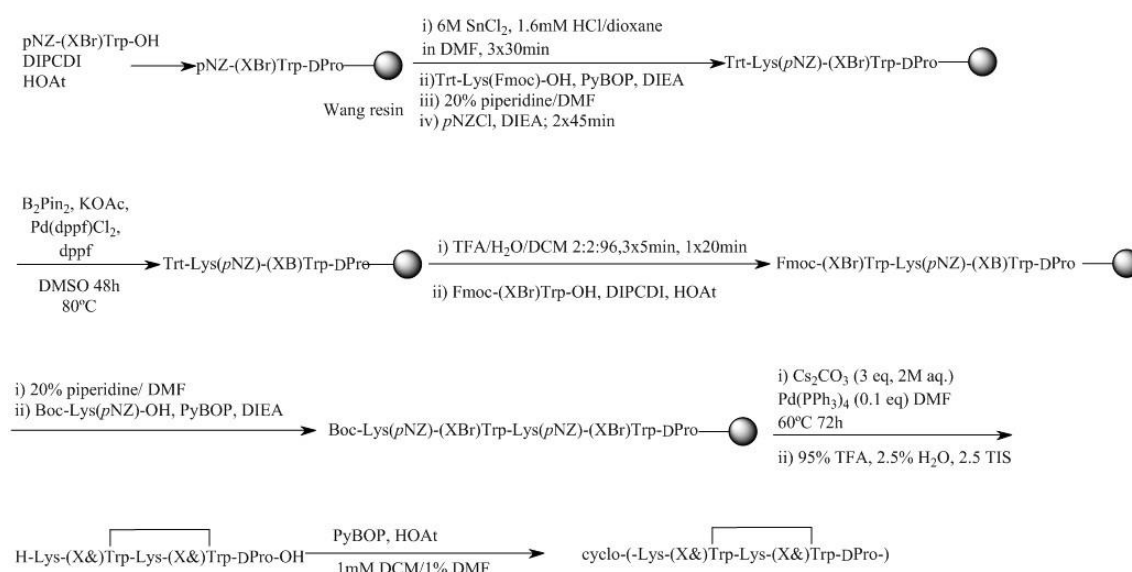

Figura xix. Método general de síntesis de los péptidos Trp-Trp.

En dicho caso, las posiciones 5-5, 6-6 o 7-7 del grupo indol del triptófano fueron unidas mediante enlace C-C (Figura xx).
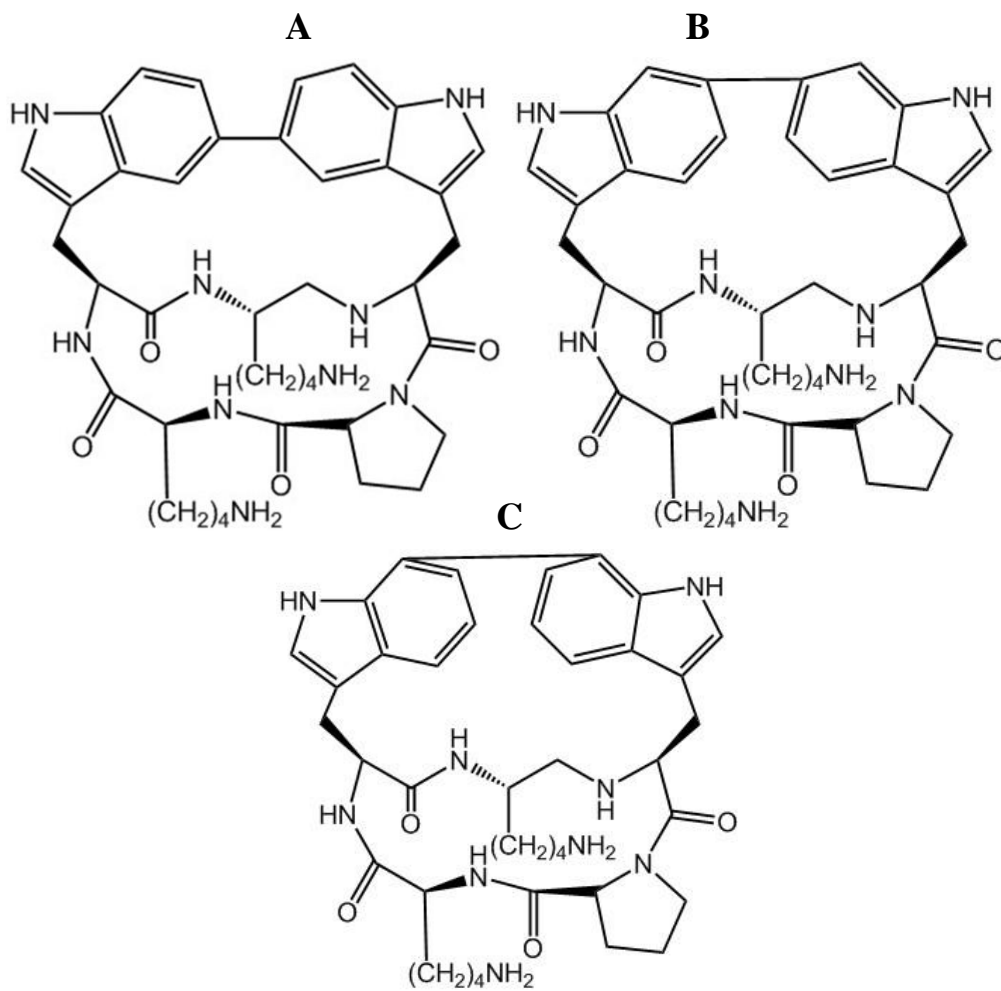
Figura xx. Estructuras de los péptidos Trp-Trp A) 5&Trp-5&Trp, B) 6&Trp-6&Trp and C) 7&Trp-7&Trp.

Los mismos derivados halogenados de triptófano, usados para llevar a cabo la síntesis de los péptidos Trp-Trp, fueron directamente incorporados a la secuencia a fin de preparar péptidos bromados y ciclados cabeza-cola.

Los distintos compuestos, juntamente con los derivados lineal (KWKp) y cíclico cabeza-cola (*cyclo(-KWKWp-)*) fueron sometidos al ensayo PAMPA (Figura xxi).
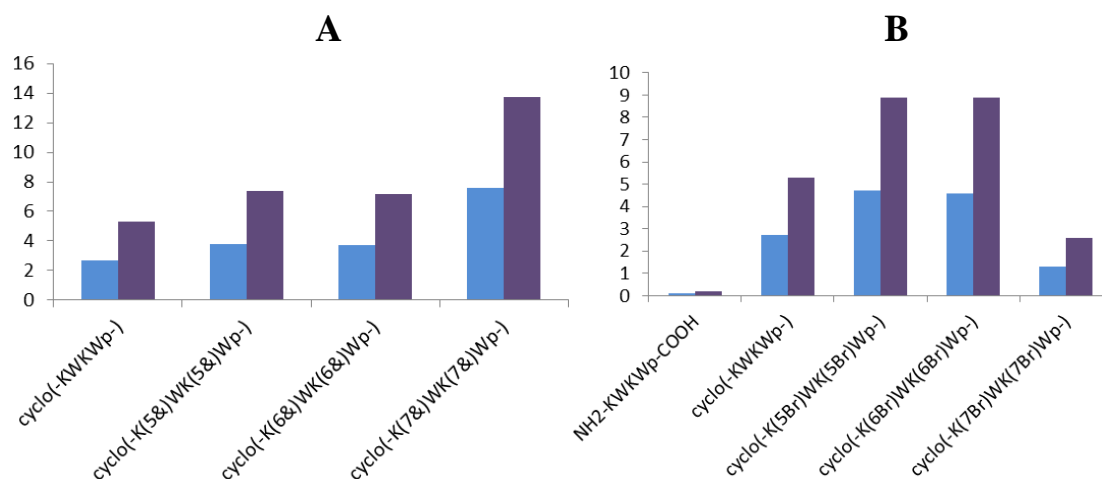
Figura xxi. Permeabilidad efectiva (azul) y transporte (morado) después de 4h en el ensayor PAMPA. A) Comparición de cyclo(-KWKWp-) con los péptidos Trp-Trp B) Comparación de cyclo(-KWKWp-) y NH$_2$-KWKWp-COOH con los péptidos bromados.

Los resultados obtenidos permitieron demostrar que, tanto la incorporación de halógenos en una secuencia cíclica, como la formación de compuestos bicíclicos permiten incrementar el transporte por difusión pasiva.

La comparación con los análogos de biarilo entre fenilalaninas demostró que estos últimos dan lugar a permeabilidades más prometedoras. Este hecho se atribuye a la naturaleza del biarilo.

Puesto que el incremento observado de los péptidos bicíclicos con respecto a los bromados no fue muy significativo se decidió estudiar estos últimos en detalle.

Mediante un ensayo XTT se determinó la viabilidad celular en células HeLA (Figura xxii).
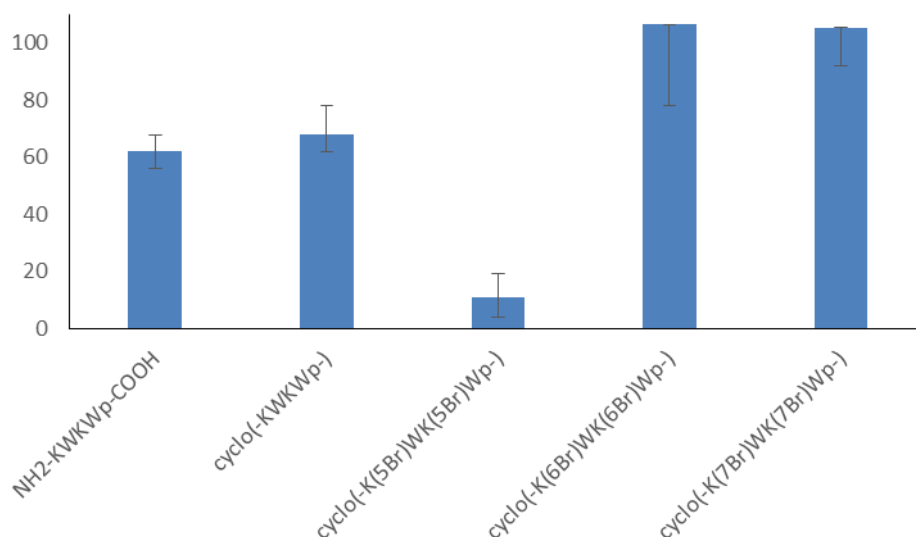
Figura xxii. Ensayo XTT de viabilidad celular a 500µM (células HeLa).

Únicamente el péptido con bromo en las posiciones 5 del grupo indol del triptófano, mostró una elevada mortalidad celular. Este efecto puede ser debido a que al tener un bromo en la posición 5, el péptido cíclico adopte una determinada conformación que resulte ser más tóxica. Asimismo, se observó una mayor viabilidad celular en los casos de los péptidos con bromo en posición 6 y 7 respecto a sus controles cíclico y linear que carecen de dicho halógeno.

Los resultados favorables obtenidos para los compuestos con bromo en 6 y 7, conjuntamente con su menor complejidad sintética respecto a los bicíclicos hacen de ellos péptidos interesantes para estudiar y buscar posibles aplicaciones biológicas.

CAPÍTULO 4: APLICACIÓN DE LOS PÉPTIDOS EN LA RECUPERACIÓN DEL AUTOENSAMBLAJE DE UNA MUTACIÓN DEL DOMINIO DE TETRAMERIZACIÓN DE P53.

La mayoría de los péptidos empleados como moduladores de interacciones proteína-proteína, se basan en la inhibición de éstas. No obstante, la estabilización de dichas interacciones es también una importante diana terapéutica.

Existen diferentes técnicas biofísicas que permiten estudiar interacciones entre las proteínas y sus ligandos empleando mínimas cantidades y permitiendo la obtención de parámetros termodinámicos, como por ejemplo, el dicroísmo circular.

El dominio de tetramerización de p53 (p53TD) es un dímero de dímeros de 32 aminoácidos con una estructura de α-hélice y dos láminas β. El plegamiento de la proteína tiene lugar de forma espontánea en las concentraciones de trabajo, no requiriendo el uso de agentes de plegamiento.

En la presente tesis, nos centramos en el estudio del mutante R337H debido a su relevancia biológica. La mutación de arginina 337 por histidina es la más importante en el dominio de tetramerización. Dicha mutación está relacionada con un carcinoma adrecortical pediátrico, común en el sur de Brasil. Recientes estudios sugieren que la herencia de esta mutación puede contribuir también a cáncer de mama en dicha población.

El mutante R337H puede adquirir el plegamiento funcional a las condiciones de trabajo, del mismo modo que p53TD. Sin embargo, el tetrámero resultante es menos estable y altamente dependiente del pH del medio. Cuando el pH es inferior a 6.5, valor del pk_a de la cadena lateral de histidina, ésta se halla protonada, permitiendo la formación estable del tetrámero. No obstante, a valores de pH superiores a 6.5, la cadena lateral de histidina no está protonada, dando lugar a la desaparición del puente salino y, por consiguiente, la formación de un tetrámero altamente inestable.

El mutante R337H fue obtenido mediante expresión en *E. coli* y purificado usando una etapa de intercambio catiónico y una segunda de exclusión molecular. El espectro de resonancia magnética nuclear bidimensional ^{1}H-^{15}N-HSQC fue asignado empleando la descripción reportada en la literatura[215] (Figura xxii).
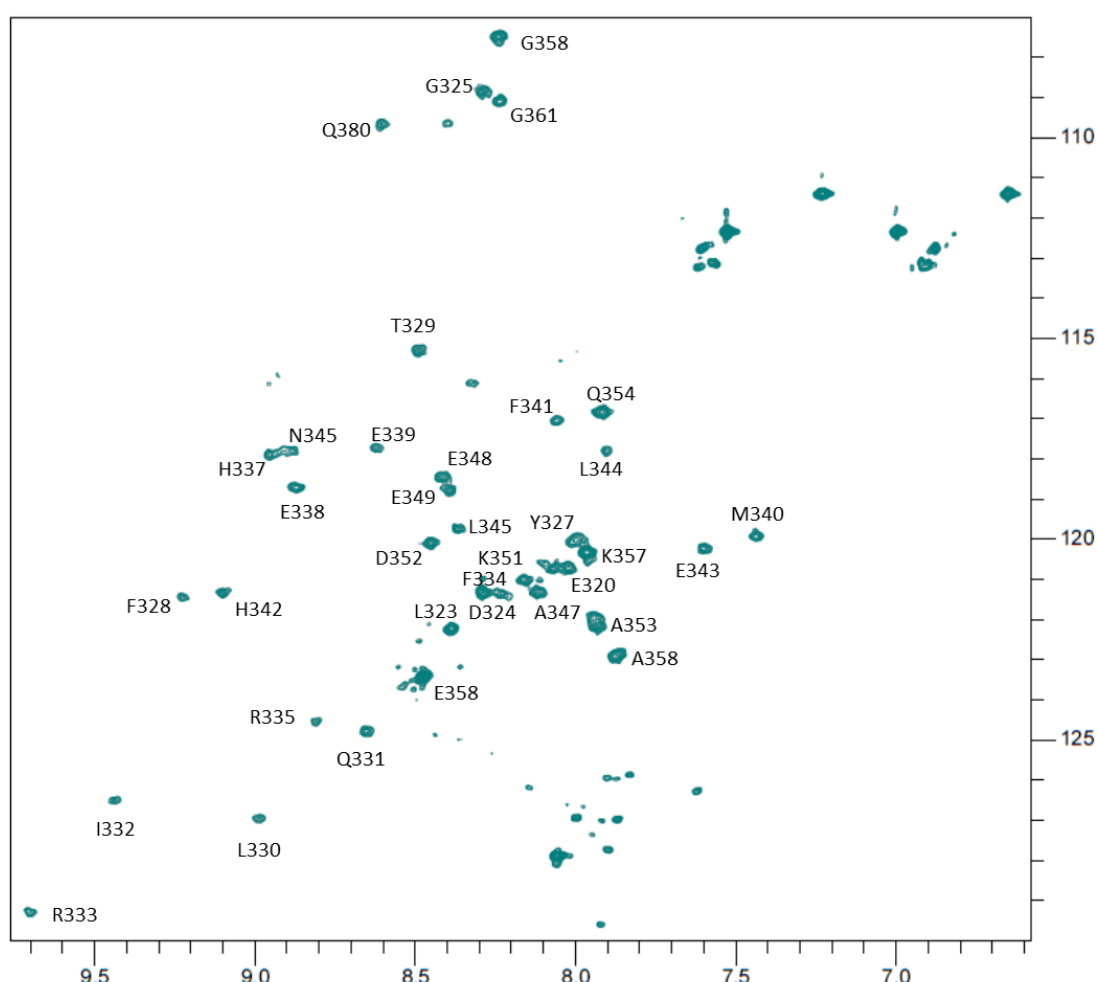

Figura xxii. Espectro de RMN ^{15}N-^{1}H-HSQC de ^{15}N-R337H en 20mM NaPi a pH 7.0, 298K, 100μM monómero, 600MHz.

Ambas proteínas, la nativa y el mutante, fueron también sintetizadas mediante síntesis automática asistida por microondas. La comparación a campo alto del espectro monodimensional de ambas proteínas (nativa y mutante) sin marcaje isotópico, permitió ver diferencias significativas debido a la presencia de H en la posición 337 y la formación del puente salino (Figura xxii).
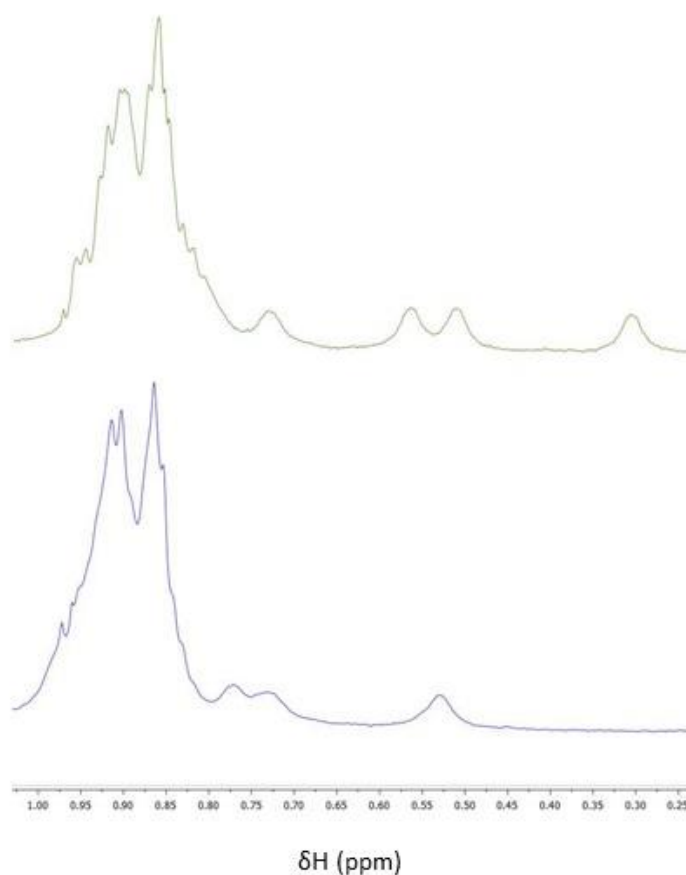
Figura xxiii. Comparación a campo alto del espectro de ^{1}H-RMN de p53TD en azul y el mutante R337H en verde a 20mM NaPi pH 7.0, 298K, 100μM de monómero, 600MHz.

La caracterización de ambas proteínas (nativa y mutante) por dicroísmo circular fue llevada a cabo, observando el mínimo característico de α-hélice. A fin de conocer su estabilidad térmica, se monitorizó la elipticidad a 220nm durante una rampa de temperatura de 15°C a 95°C con una velocidad de 1.5°C/min (Figura xxiv).
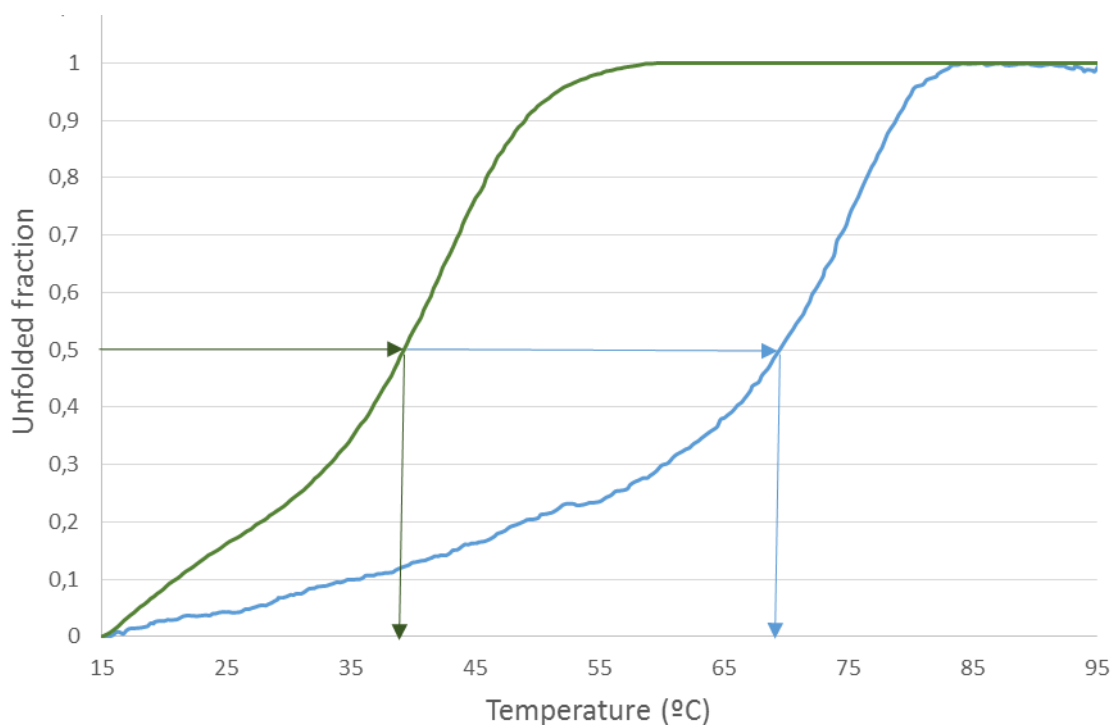
Figura xxiv. Curvas de desplegamiento de p53TD (azul) y R337H (verde) a 20µM monómero en 25mM NaPi pH7, 100mM NaCl.

La mayor estabilidad de la proteína nativa fue reflejada en un incremento de 30°C en la temperatura de transición del deplegamiento respecto al mutante R337H. En ambos casos se observó un proceso altamente cooperativo, dado que se adquirió el 100% de desplegamiento en un rango estrecho de temperaturas. La evolución del dicroísmo circular de las proteínas a lo largo del ensayo se presenta en las Figuras xxv y xvi.
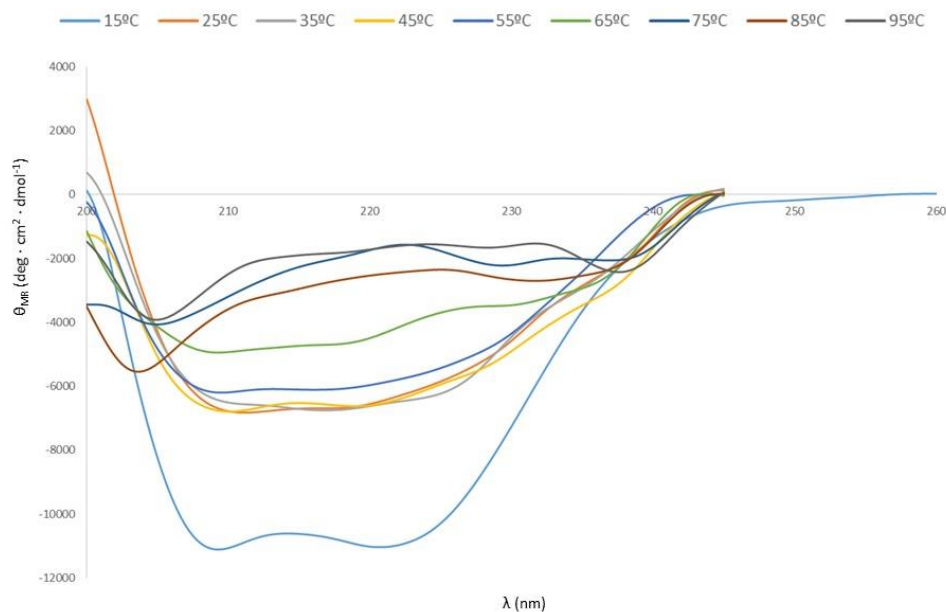
Figura xxv. Espectro de dicroísmo circular de p53TD nativa a diferentes temperaturas (15°C-95°C). 20μM en 25mM NaPi pH 7, 100mM NaCl. La elipticidad fue normalizada con el promedio de la concentración por residuo, θ$_{MR}$.
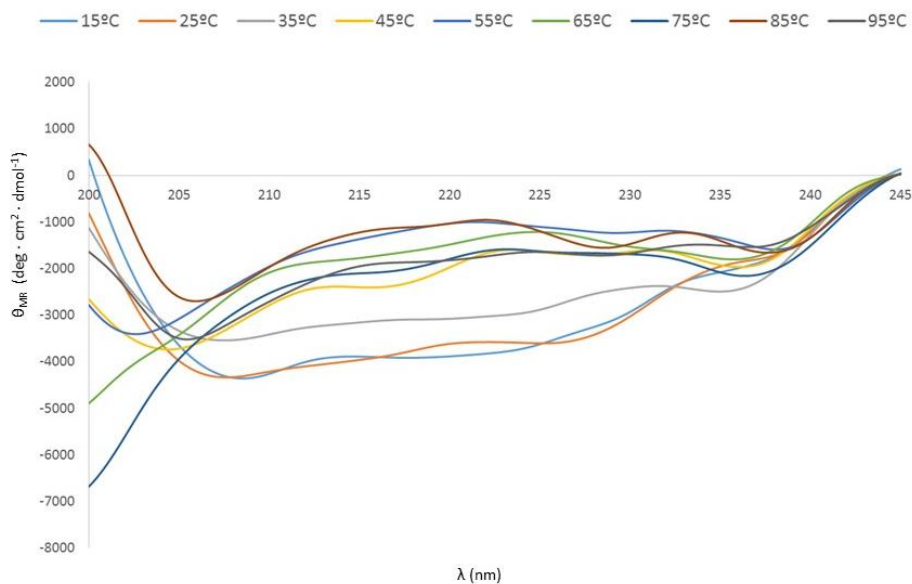

Figura xxvi. Espectro de dicroísmo circular de R337H a diferentes temperaturas (15°C-95°C). 20μM en 25mM NaPi pH 7, 100mM NaCl. La elipticidad fue normalizada con el promedio de la concentración por residuo, θ$_{MR}$.

Según la temperatura a la que tiene lugar el desplegamiento de cada una de las proteínas, es posible ver como el espectro evoluciona del característico de una estructura de α-hélice a un perfil desestructurado.

El efecto del pH sobre el mutante R337H, debido mayoritariamente a la presencia del puente salino, fue demostrado llevando a cabo ensayos de desplegamiento a diferentes pH (Figura xxvii).
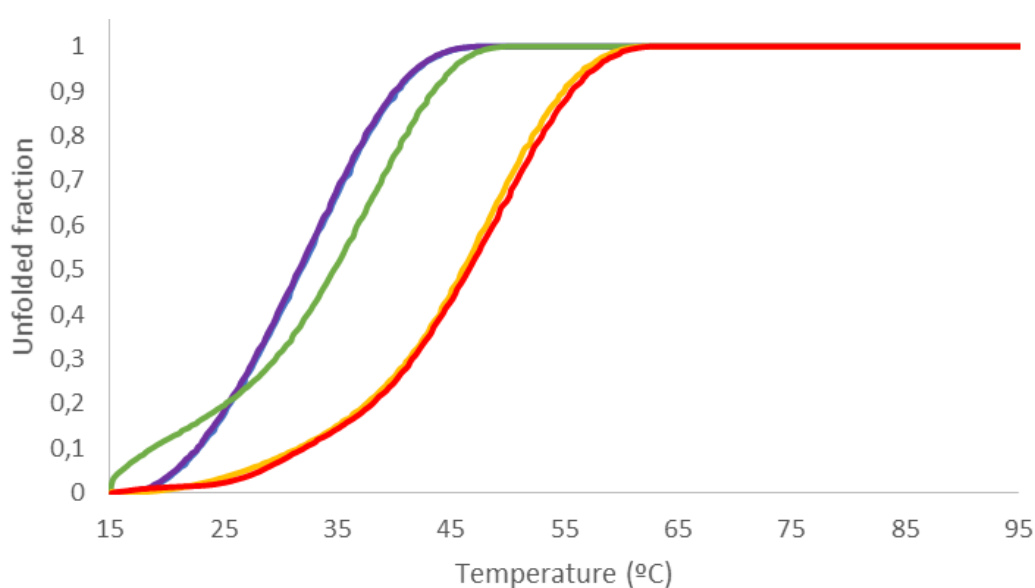
Figura xxvii. Curvas de desplegamiento de R337H (verde) a 20µM monómero en 25mM NaPi, 100mM NaCl. pH 5 rojo, pH 6 amarillo, pH 7 verde, pH 8 azul y pH 9 morado.

Es posible apreciar el incremento sustancial de estabilidad a mayores pH.

En cuanto a la fuerza iónica del medio, se demostró una mayor estabilidad cuanto menor fuera el contenido salino de éste.

Con el fin de rescatar la tetramerización de R337H, se evaluó el efecto de dos péptidos de la familia de arginina que fueron sintetizados en la tesis. Los compuestos evaluados fueron el péptido grapa (NH$_2$-Arg-(4&)Phe-Arg-(4&)Phe-DPro-COOH) y el péptido bicíclico (cyclo(-Arg-(4&)Phe-Arg-(4&)Phe-DPro-). Dichos péptidos se seleccionaron por presentar argininas. Estudios previos realizados en el grupo del Prof. Giralt,

demostraron que los grupos guanidinios presentes en calixarenos eran capaces de estabilizar la tetramerización del mutante R337H[156].

Se realizaron las curvas de desplegamiento a fin de comprobar si la presencia del ligando era capaz de estabilizar el tetrámero formado, incrementando la temperatura de transición (Figuras xviii y xxix).
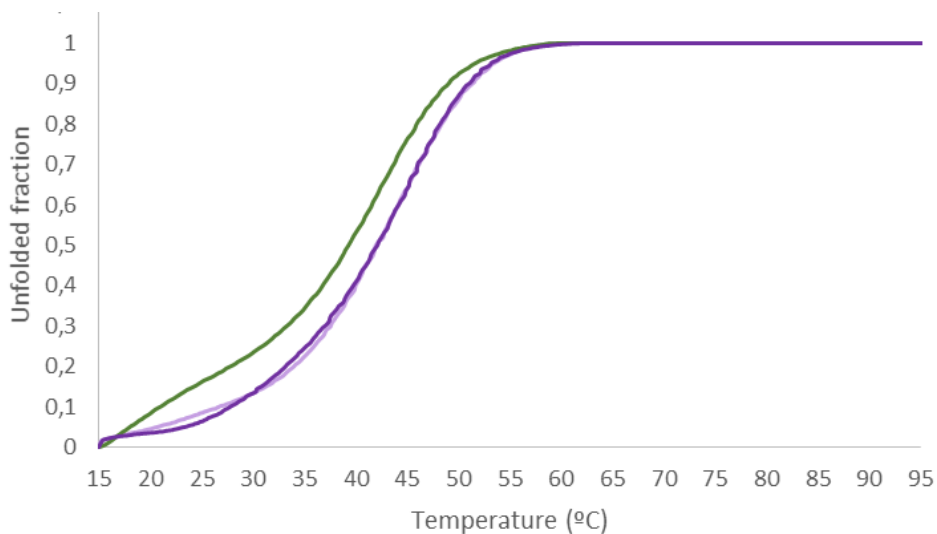
Figura xxviii. Curvas de desplegamiento de R337H a 20μM monómero en 25mM NaPi pH7, 100mM NaCl con 8 equivalentes de péptido bicíclico (morado claro) y con 16 equivalentes de péptido bicíclico (morado oscuro).
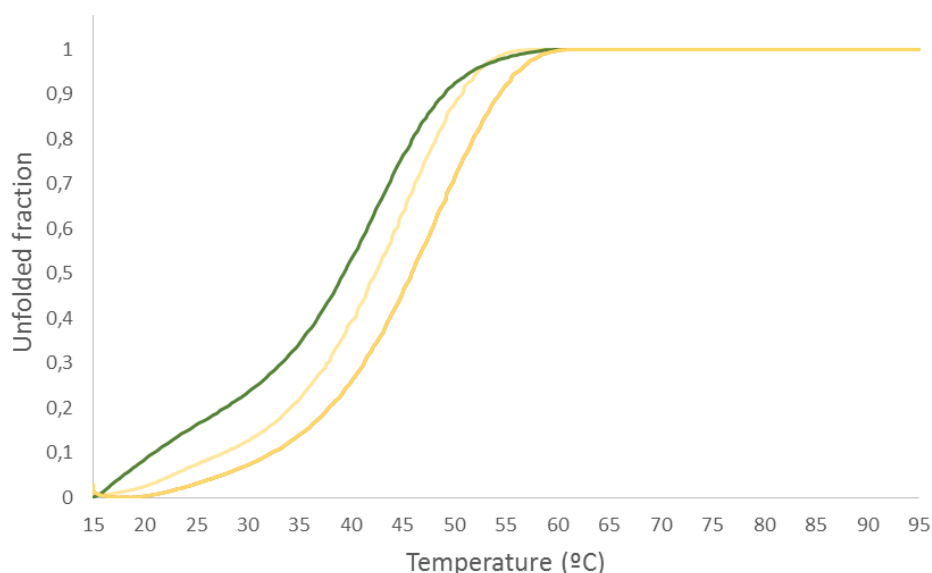
Figura xxix. Curvas de desplegamiento de R337H a 20µM monómero en 25mM NaPi pH7, 100mM NaCl con 8 equivalentes de péptido grapa (amarillo claro) y con 16 equivalentes de péptido grapa (amarillo oscuro).

Fue posible observar un ligero incremento de estabilidad, 3°C, con el ligando bicíciclo. No obstante, la incorporación de un mayor número de equivalentes no permitió mejorar dicho valor. En cuanto al péptido grapa, se consiguió un incremento de hasta 7°C incorporando 16 equivalentes del mismo. De modo que se obtuvo un ligando prometedor para conseguir estabilizar el autoensamblaje del mutante R337H.

Estudios *in silico* mostraron que la interacción tanto del ligando grapa como del ligando bicíclico tiene lugar con los residuos E336, E339, E343 y E346 presentes en la parte expuesta al solvente de la α-hélice de p53TD (Figura xxx).
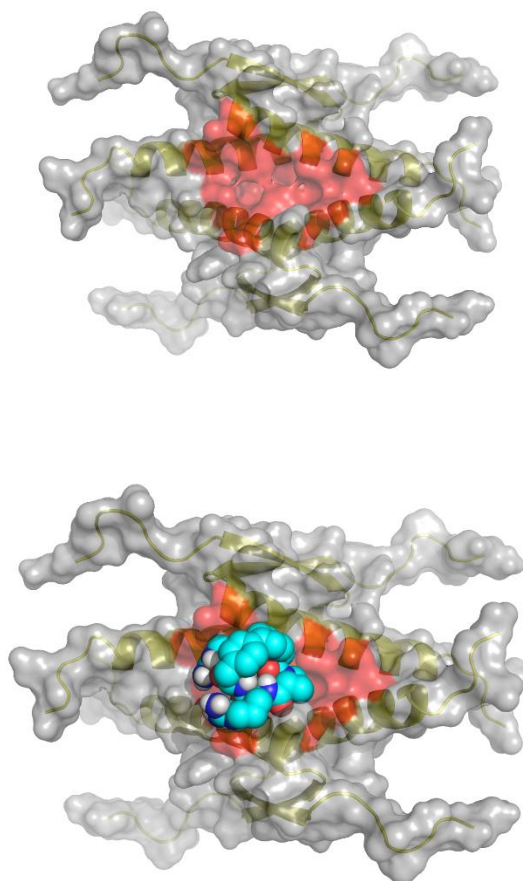
Figura xxx. Lugar de union de los péptidos con p53TD. En azul se representa, como ejemplo, el ligando de arginina biciclo.

FUTURAS DIRECCIONES

Una vez llevado a cabo el trabajo mostrado en la presente tesis, existen algunos experimentos de gran interés que permitirían mejorar su calidad así como sus futuras aplicaciones.

➢ Los compuestos ciclados cabeza-cola que contienen bromo presentan una potencial actividad como péptidos antimicrobianos. Por ello, creemos que sería útil realizar el pertinente estudio a fin de poder confirmar dicha hipótesis. En este contexto, su evaluación frente a proteasas permitiría también ampliar el conocimiento de sus propiedades farmacológicas.

➢ Los estudios de RMN de las proteínas marcadas con ^{15}N resultarían de gran interés a fin de permitir el estudio de las interacciones que tienen lugar con los ligandos analizados.

➢ La evaluación de otros compuestos sin motivos guanidinio ni los extremos libres frente al mutante R337H podría dar lugar un mayor conocimiento de la relevancia de los distintos grupos funcionales en el ligando prometedor.

➢ Finalmente, se podría continuar el estudio de dinámica molecular para obtener mayor información sobre el modo de interacción.

CONCLUSIONES

Las conclusiones extraídas se presentan a continuación:

Objetivo 1

i. Se ha conseguido optimizar la metodología para preparar los péptidos biaril bicíclicos. Los anillos biarilo se pueden sintetizar entre posiciones *meta* o *para* de la cadena lateral de fenilalanina.

ii. La ciclación en solución se ha estudiado en profundidad. Se han caracterizando las condiciones óptimas para la síntesis de los péptidos bicíclicos monoméricos. Los ciclodímeros no pueden ser obtenidos de forma excluyente, ni empleando fase sólida, por lo que se obtienen mediante un aislamiento del crudo en una etapa final de purificación.

iii. Los estudios conformacionales de los biciclos monoméricos demuestran que la torsión de biarilo atribuída a la posición del enlace entre fenialalninas afecta la conformación de la molécula.

iv. Los estudios por RMN, dinámica molecular y dicroísmo circular muestran conformaciones distintas para los dos ciclodímeros. Este hecho confirma que la posición del biarilo es muy importante.

v. Tres familias de compuestos (familia de lisina, familia de arginina y familia de serina) se han sintetizado.

Objetivo 2

i. El transporte por difusión pasiva se evaluó por PAMPA, mostrando la influencia positiva del biarilo, especialmente en combinación con la ciclación cabeza-col.

ii. La estabilidad en serum mostró que el anillo biarilo permite mejorar la resistencia a proteasas.

iii. No se pudo atribuir citotoxicidad a la introducción del biarilo. Mediante un ensayo de MTT con células HeLa, no se observó citotoxicidad para ninguno de los análogos de la familia de lisina.

Objetivo 3

i. Fue posible llevar a cabo la síntesis de péptidos bicíclicos con una grapa de Trp-Trp.

ii. Dichos péptidos mostraron una permeabilidad por difusión pasiva relevante, así como los péptidos cíclicos con bromo.

iii. La citoxicidad de los análogos bromados fue estudiada por XTT en células HeLa, sólamente el análogo 5-bromo mostró elevada mortalidad celular.

Objetivo 4

i. Se obtuvo por expresión en *E. coli*, el mutante R337H. Mediante síntesis química se obtuvieron la proteína nativa y el mutante R337H sin las colas, 37 residuos.

ii. Por dicroísmo circular se observó el perfil de α-hélice. Mediante las curvas de desplegamiento se vio la diferencia relevante entre ambas proteínas, siendo 30ºC menos estable el mutante R337H que la proteína nativa. Asimismo, también se observó su inestabilidad a pH ácido y a mayores fuerzas iónicas.

iii. El péptido de arginina bicíclico no permitió estabilizar de forma eficiente el mutante R337H. Sin embargo, el péptido grapa mostró un incremento en 7ºC la

estabilidad. Por ello, se considera un candidato interesante para rescatar la tetramerización de R337H.

iv. Los estudios de docking permitieron observan la interacción de las argininas de ambos péptidos, con los glutámicos E336, E339, E343 y E346 de las proteínas.